Les échanges entre le parasite et l'hôte dans l'infection par Echinococcus multilocularis : acteurs et conséquences dans le foie

Junhua Wang

Université de Franche-Comté, France/Université Médicale du Xinjiang, Chine

Thèse en co-tutelle pour le

Doctorat d'Université en Sciences de la Vie et de la Santé

Les échanges entre le parasite et l'hôte dans l'infection par Echinococcus multilocularis*: acteurs et conséquences dans le foie*

par

WANG Junhua

Née le 12 Octobre 1982 à Fugou, Henan, China

Directeur de thèse (UFC): Prof. Oleg BLAGOSKLONOV

Directeur de thèse (XMU) : Prof. Hao WEN

Membres du Jury :

Dr Peter Kern, Professeur émérite, Ulm Universität, Allemagne (Rapporteur)

Dr Yurong Yang, Professeur, Ningxia University, RP Chine (Rapporteur)

Dr Oleg Blagosklonov, Professeur, Université de Franche-Comté (co-Directeur)

Dr Hao Wen, Professeur, Xinjiang Medical University, Chine (co-Directeur)

Dr Bruno, Gottstein, Professeur, University of Bern, Suisse (Juge)

Dr Renyong LIN, Professeur, Xinjiang University, Chine (Juge)

Dr Dominique A. VUITTON, Professeur émérite, Université de Franche-Comté (Juge)

Acknowledgements

The research described in this thesis was carried out at UMR 6249 “Chrono-environnement”, and EA 4662 “Nanomédecine, imagerie, thérapeutique”, University of Franche-Comté (Besançon, France), at the Institute of Parasitology, University of Bern, with the financial support of the European Commission French-Swiss InterReg IV program ‘IsotopEchino’ project and of the Swiss National Science Foundation (31003A_141039/1), and at Xinjiang Key Laboratory on Echinococcosis and Institute for Clinical Medicine Research, First Affiliated Hospital of Xinjiang Medical University (Urumqi, China) with the financial support of a grant from the National Science Foundation of China (81060452).

I would like to thank my supervisors, Professor Oleg Blagosklonov (France) and Professor Hao Wen (China), for their support and guidance throughout this study.

Many thanks to the members of my thesis committee, Professor Bruno Gottstein, Professor Dominique A Vuitton, Professor Renyong Lin for their fruitful guidance, kind help and close collaboration during my whole study, and also for the caring and warmth they gave me during my stay in Besancon, Bern and Urumqi.

I would like to thank Professor Norbert Müller, Institute of parasitology, University of Bern, for his help on real-time PCR; Professor Laurance Millon, University of Franche-Comté, for her great help on the manuscript preparation; Professor Solang Bresson-Hadni, for her great help on the data analysis of AE patients; Professor Andrew Hemphil, Institute of parasitology, University of Bern, for his help on the manuscript preparation; Professor Xiaomei Lu, Director of the Institute for Clinical Medicine Research, First Affiliated Hospital of Xinjiang Medical University, for her valuable help in the pathological description of the mouse model and her fruitful advice; Professors Peter Kern and Yurong Yang for having accepted to serve as referees and jury members for this thesis in Besancon, and Cristina Huber and Liang Li for their excellent technical assistance. Ms Daniela Hayoz, Dr. Markus Spiliotis, Ms Cornelia Spercher, Ms Clemence Porte, Ms Jenny Knapp, Mr.Hai Li for their grateful support.

Many thanks to my colleagues at my home laboratory, Mr.Chuanshan Zhang and Mr.Guodong Lü for their substantial contributions to the animal experiments and excellent technical assistance.

I would also like to thank my mother and my brother for their encouragement and support throughout this PhD course.

Most importantly, I would like to thank my husband, Dongfeng Hao, not only for his grateful support, but also for his warm love to keep me encouraged and his warm hands to hold me when I was frustrated during experiments. I also thank my lovely son for his excellent growth during I was away from him.

Publications

Publications in international journals on the subject of the thesis

1. **Wang J,** Zhang C, Wei X, Blagosklonov O, Lü G, Lu X, Vuitton DA, Wen H and Lin R, TGF-β and TGF-β/Smad signaling in the interactions between *Echinococcus multilocularis* and its hosts, PLOS ONE, 2013, 8(2): e55379 (Wang, 2013)
2. **Wang J**, Lin R, Zhang W, Li L, Gottstein B, Blagosklonov O, Lü G, Zhang CS Lu X, Vuitton DA, and Wen H, Transcriptional profiles of cytokine/chemokine factors of immune cell-homing to the parasitic lesions: a comprehensive one-year course study in the liver of *E. multilocularis*-infected mice, PLOS ONE, 2014 (in press) (Wang, 2014 a)
3. **Wang J**, Huber C, Müller N, Vuitton DA, Blagosklonov O, Lin R, Wen H and Gottstein B, The Novel $CD4^+CD25^+$ Regulatory T Cell Effector Molecule Fibrinogen-like Protein 2 Contributes to the Outcome of Murine Alveolar Echinococcosis (submitted to PLOS Pathogens) (Wang, 2014 b)
4. **Wang J**, Blagosklonov O, Bresson-Hadni S, Richou C, Grenouillet F, Lin R, Wen H, Vuitton DA, Gottstein B. The novel $CD4^+CD25^+$ Treg effector molecule FGL2: A potential biomarker for viability of *E. mutilocularis* in relation to PET/CT imaging in human patients with alveolar echinococcosis (manuscript in preparation) (Wang, 2014 c)
5. Zhang C, **Wang J**, Lü G, Li J, Lu X, Mantion G, Vuitton DA, Wen H, Lin RY. Hepatocyte Proliferation/Growth Arrest Balance in the Liver of Mice during *E. multilocularis* Infection: A Coordinated 3-Stage Course. PLOS ONE, 2012: 7(1): e30127 (Zhang, 2012)

Publications in international journals on closely related subjects

1 Tuxun T, **Wang J (co-first author)**, Lin R, Shan J, Tai Q, Li T, Zhang J, Zhao J and Wen H. Th17/Treg imbalance in patients with liver cystic echinococcosis, Parasite Immunology, 2012, 34, 520–527

2 Zhang C, **Wang J,** Lü G, Li J, Lu X, Mantion G, Vuitton DA, Wen H, Lin RY Hepatocyte Proliferation/Growth Arrest Balance in the Liver of Mice during E. multilocularis Infection: A Coordinated 3-Stage Course, PLOS ONE,2012: 7(1): e30127.

3 **Wang J,** Lin R, Zhou Y, Jin Y, Tuxun X, Lü G, Zhang C, Lu X, Vuitton DA, Gottstein B and Wen H. $CD4^{+}CD25^{+}Foxp3^{+}$Tregs in the peripheral blood mononuclear cells (PBMCs) of patients with cystic Echinococcosis and in PBMCs after exposure to *Echinococcus granulosus* AgB *in vitro* (manuscript in preparation)

Communications

1. **Wang J,** Huber C, Müller N, Vuitton DA, Blagosklonov O, Grandgirard D, Leib SL, Lu X, Lin R, Wen H, Gottstein B, The Novel $CD4^+CD25^+$ Regulatory T Cell Effector Molecule Fibrinogen-like Protein 2 Contributes to the Outcome of Murine Alveolar Echinococcosis, Innovation for the Management of Echinococcosis Symposium-2014, Besancon, France, 2014.
2. **Wang J,** Huber C, Gottstein B, The Novel $CD4^+CD25^+$ Regulatory T Cell Effector Molecule Fibrinogen-like Protein 2 (FGL2) Contributes to the control of Murine Alveolar Echinococcosis, 25^{th} Meeting of the Swiss Immunology PhD students, Wolfsberg, Switzerland, 2013.
3. **Wang J,** Lü G, Zhang C, Zhang X, Lu X, Gottstein B,Wen H, Vuitton DA and Lin R, Course of the Th-1, Th-2 and Th-17 Cytokines and of Associated Chemokines Involved in the Periparasitic Recruitment of Cells in *Echinococcus multilocularis* Infection, 10^{th} joint Annual World Congress on Cytokines, Geneva, Switzerland, 2012.
4. **Wang J,** Lin R, Zhang C,Lü G, Wei X, Zhang X, Lu X, Vuitton DA, Wen H. Transforming Growth Factor-β1 (TGF- β) and Components of its Signaling Pathway in Liver of Patients with Alveolar Echinococcosis, 24^{th} world congress for echinococcosis, Urumqi, China, 2011.

Table of content

List of Figures and Tables

Figures

Tables

Abbreviations

Abbreviation	Denomination
AE	Alveolar echinococcosis
cDNA	complementary DNA
cRNA	complementary RNA
DEPC	Diethyl Pyrocarbonate
dNTP	deoxyribonucleoside triphosphate
DTT	Dithiothreitol
EB	ethidium bromide
EDTA	Ethylene diamine tetraacetic acid
E. *multilocularis*	*Echinococcu smultilocularis*
g	gram
GO	Gene Ontology
h	hour
HE	Hematoxylin and Eosin
HRP	horseradish peroxidase
IL	Interleukin
min	minute
MMLV	Molony Murine Leukemia Virus
PCR	polymerase chain reaction
rpm	Revolutions Per Minute
RNA	Ribonucleic acid
RT-PCR	reverse transcription polymerase chain reaction
SDS	Sodium Dodecyl Sulfate
TGF	Transforming growth factor
µl	microliter
µm	Micro meter

The cross-talk between the parasite and the host in **Echinococcus multilocularis** *infection: actors and consequences in the liver*

Résumé

L'échinococcose alvéolaire (EA) est une zoonose parasitaire rare mais qui, si elle n'est pas traitée ou si elle est traitée trop tardivement, peut se révéler extrêmement grave et même fatale. La maladie est en relation non seulement directement avec la destruction hépatique qui accompagne le développement du métacestode, le stade larvaire d'*Echinococcus multilocularis*, mais aussi avec la réponse immunitaire granulomateuse très importante qui entoure le tissu parasitaire ; tous deux sont responsables de la fibrose et de la nécrose hépatiques et de la cholestase chronique qui peuvent conduire à l'insuffisance hépatique terminale. Les lésions, qui se composent à la fois du métacestode, manifesté sous la forme de multiples vésicules, et des cellules qui ont migré des organes et tissus lymphoïdes périphériques pour coloniser le foie autour du métacestode, se comportent comme une tumeur maligne à marche lente qui envahit progressivement le foie, puis les organes et tissus de voisinage, et peut enfin métastaser à distance dans d'autres organes.

En dépit du rôle connu de la réponse granulomateuse de l'hôte dans les complications de l'EA, et de son rôle invoqué à la base de l'imagerie fonctionnelle des lésions hépatiques (comme celle obtenue par la Tomographie par émission de Positons utilisant le Fluoro-deoxy-glucose comme traceur), on connait peu de choses sur la réponse immune locale et sur les facteurs immuno-régulateurs qui influencent la migration des cellules de l'immunité dans le foie, de même que sur ceux qui seraient susceptibles d'influencer les principales caractéristiques de l'homéostasie hépatique comme la régénération/prolifération, dégénérescence, et dysfonction des hépatocytes. On sait depuis longtemps que le foie est le site privilégié du développement de l'infection par *E. multilocularis*. La croissance du métacestode induit de nombreuses voies de la réponse immunitaire et les mécanismes immunitaires impliqués dans les interactions hôte-parasite ont fait l'objet de nombreuses études. L'implication des voies d'orientation cytokinique T helper (Th)1 et Th2, et de plusieurs autres cytokines prises individuellement, ont été largement étudiées au cours des deux dernières décennies, que ce soit chez les patients atteints d'EA ou les rongeurs expérimentaux. Cependant, ces études n'ont été réalisées qu'à partir de prélèvements faits dans le système immunitaire périphérique: rate, ganglions lymphatiques chez les rongeurs expérimentaux, et cellules mononucléées du sang circulant chez l'homme ou cellules péritonéales chez la souris. Par ailleurs, des observations cliniques, chez les patients, comme l'importance de l'hépatomégalie du foie 'sain', non atteint par les lésions et la tolérance du foie vis-à-vis des résections hépatiques majeures, ainsi que des observations expérimentales, comme la diffusion de la fibrose à des zones hépatiques distantes de l'invasion par le métacestode et la réaction granulomateuse, suggèrent que

le métacestode et la réponse immunitaire locale pourraient influencer le parenchyme hépatique lui-même, y compris à distance des zones hépatiques atteintes. Cet aspect n'a jamais été étudié spécifiquement et de façon approfondie et les mécanismes potentiels en sont totalement inconnus. En particulier, l'étude des mécanismes impliqués dans les modifications de l'homéostasie hépatique aux différents stades de l'infection, mais aussi une analyse détaillée des profils de cytokines et chimiokines présents dans l'infiltrat cellulaire périparasitaire hépatique, de la présence du transforming growth factor-β (TGF-β) et des autres acteurs de sa voie d'activation, et de l'implication possible du Fibrinogen-like protein-2 (FGL2), une molécule effectrice des lymphocytes T-régulateurs ($CD25^{+}CD4^{+}$ Tregs) récemment identifiée, n'ont jamais été entrepris avec l'objectif de cerner de façon globale l'interaction de ces différents facteurs tout au long du développement de l'infection par *E. multilocularis*.

L'objectif de ce travail de thèse était donc d'explorer les acteurs-clés des échanges entre le métacestode et son hôte et les conséquences de leur mise en jeu sur le foie.

Méthodes. Pour les études in vivo, des souris BALB/c femelles exemptes de pathogènes ont reçu une injection de métacestode d'*E. multilocularis* dans le lobe antérieur du foie, pour le modèle d'infection secondaire intra-hépatique, ou dans le péritoine, pour le modèle d'infection secondaire intra-péritonéale. A chaque temps d'autopsie dans le modèle intrahépatique, 10 souris infectées expérimentalement ont été étudiées dans le groupe '*E. multilocularis'* et comparées à 5 souris du groupe 'témoin' qui avaient reçu une injection intra-hépatique de sérum physiologique, selon le même protocole chirurgical. Les souris ont été autopsiées à 2, 8, 30, 60, 90, 180, 270 et 360 jours après l'infection. Des échantillons de tissu hépatique prélevés à proximité et à distance des lésions parasitaires ou dans le lobe hépatique des souris témoins, ont été utilisés pour l'étude de la prolifération/croissance des hépatocytes, pour les analyses utilisant des puces à ADN, ou pour la détection des cytokines et chimiokines et des composants de la voie d'activation du TGF-β, à l'aide de techniques de Western-Blot, de qRT-PCR et d'immuno-histochimie. De plus, des échantillons de tissu prélevés à la périphérie des lésions, dans la zone de granulome, ont été étudiées avec les mêmes techniques pour la détection des cytokines et chimiokines et de leurs récepteurs. A chaque temps d'autopsie dans le modèle intra-péritonéal, six souris infectées par voie intra-péritonéale (souris Knock-Out $fgl2^{-/-}$ versus souris de type sauvage) ont été étudiées dans le groupe '*E. multilocularis'* et comparées à 6 souris témoins qui avaient reçu une injection intra-péritonéale de sérum physiologique, selon le même protocole. Les souris ont été autopsiées à 1 et 4 mois après l'infection. Les cellules spléniques et les cellules de l'exsudat péritonéal (PEC) ont été prélevées chez les souris infectées et les souris témoins et analysées pour détecter la réactivité lymphocytaire et la maturation des cellules dendritiques (DC).

Pour les études in vitro, 1) la co-culture des hépatocytes de rat avec le liquide vésiculaire d'*E. multilocularis* a été utilisée pour étudier TGF-β1 et les Smads de sa voie d'activation en Western-Blot ; 2) la co-culture de cellules spléniques primaires avec la concanavaline A (ConA) ou le liquide vésiculaire a été utilisée pour étudier la réactivité lymphocytaire T et la maturation des DC en cytométrie de flux ; 3) la co-culture de lymphocytes Tregs $CD4^+CD25^+$ et de lymphocytes T $CD4^+CD25^-$ a été utilisée pour étudier la fonction suppressive des Tregs en ELISA BrdU.

Résultats: 1) Les résultats obtenus par les études de prolifération/arrêt de croissance des hépatocytes ont montré qu'après l'infection par *E. multilocularis*, l'expression des gènes de la Cycline B1 et celle de la Cycline D1 augmentaient jusqu'au jour 30, puis revenaient au niveau des témoins après le jour 60 ; celles des gènes de Gadd45b, de la Cycline A et le PCNA augmentaient tout au long de la période; ERK1/ 2 était activée en permanence. Pendant ce temps, l'expression génique de p53, p21 et Gadd45c, et l'activation de la caspase 3 augmentaient graduellement en fonction du temps. Au stade terminal de l'infection (jours 180 à 360), l'expression génique de p53, p21 et Gadd45c était significativement plus élevée que chez les souris témoins ; JNK et la caspase 3 étaient activées. L'analyse par la technique TUNEL a aussi montré l'apoptose des hépatocytes à ce stade. Il n'y avait pas de modification pour la Cycline E, l'ARN messager de p53 et l'expression de p38 quel que soit le stade d'infection.

2) Les niveaux d'expression des ARN messagers dans les lésions parasitaires ont montré l'établissement très précoce (dès 2 jours après l'infection) d'une réponse immune mixte, Th1 et Th2, caractérisée par la présence concomitante d'IL-12α, IFN-γ et IL-4. Ensuite, le profil se complétait par l'apparition de cytokines tolérogènes, comme IL-5, IL-10 et TGF-β. IL-17 était exprimée de façon permanente dans le foie des souris infectées, essentiellement dans l'infiltrat périparasitaire ; ce fait été confirmé par l'augmentation des ARN messager d'IL-17A et d'IL-17B dès le stade très précoce, suivie d'une diminution de l'expression d'IL-17A. Les chimiokines de type Th1 et Th2 étaient également présentes pendant tous les stades de l'infection, généralement bien corrélées à la présence des cytokines correspondantes.

3) Les études de l'expression de TGF-β1, de ses récepteurs, et des Smads de sa voie métabolique ont confirmé qu'elle était très importante dans l'infiltrat périparasitaire, mais ont aussi montré qu'elle était présente dans les hépatocytes, à proximité et à distance des lésions d'EA. La fibrose était significative dès 180 jours après l'infection dans l'infiltrat périparasitaire, et également dans le parenchyme hépatique, même à distance des lésions. Sur l'ensemble de l'évolution de l'infection, l'expression de TGF-β1 était corrélée avec le rapport CD4/CD8 des lymphocytes T du granulome, depuis longtemps décrit comme caractéristique de la gravité de l'AE.

4) Les souris déficientes en FGL2 infectées par *E. multilocularis* avaient une charge parasitaire significativement moins élevée que les souris de type sauvage; cette

protection contre l'infection était associée à une prolifération augmentée des lymphocytes T en réponse à l'incubation avec la ConA et avec le liquide parasitaire, à une polarisation relative Th1, et à un nombre augmenté de lymphocytes B producteurs d'anticorps. Le nombre relatif et l'état de maturation des DC étaient plus élevés chez les souris fgl2$^{-/-}$; les marqueurs de co-stimulation CD80 and CD86 étaient aussi plus exprimés sur les DCs de ces souris, après stimulation par la ConA et le liquide vésiculaire. Des études complémentaires ont montré qu'IL-17A était impliquée dans la sécrétion de FGL2 dans ce modèle.

Conclusion : Le métacestode d'*E. multilocularis* exerce une influence profonde sur l'homéostasie du foie. Nos résultats soutiennent le concept d'activation séquentielle des voies métaboliques qui favoriseraient d'abord la prolifération des cellules de l'immunité et des cellules du foie, et donc la fertilité du métacestode et sa tolérance par l'hôte, puis favoriseraient ensuite la destruction hépatique, l'apoptose des hépatocytes, la diminution de la synthèse protéique et le métabolisme des xénobiotiques, et de façon concomitante le déficit immunitaire, et donc la dissémination des protoscolex après que la fertilité du métacestode ait été acquise. Certains de nos résultats donnent une explication rationnelle aux observations cliniques, comme l'hépatomégalie du foie non atteint et la survie parfois surprenante des patients atteints d'EA après résections hépatiques majeures, ou la fibrose, la nécrose et la défaillance hépatique aux stades avancés de la maladie, chez l'homme et chez l'animal expérimental.

Nos résultats suggèrent également que la réaction inflammatoire qui entoure le métacestode dans le foie contribue significativement à la sécrétion de cytokines et de chimiokines et aux mécanismes fonctionnels immunitaires de l'interaction hôte-parasite. En plus de donner une vue d'ensemble de l'évolution de la production des cytokines et chimiokines dans les lésions d'EA, ces résultats peuvent contribuer à identifier de nouvelles cibles pour une thérapeutique immunologique qui permettrait de pallier les conséquences pathologiques de l'infection par *E. multilocularis* et de complémenter l'action seulement parasitostatique des benzimidazoles. Nos résultats suggèrent qu'une régulation étroite de la production des divers isotypes d'IL-17, sous l'influence de TGF-β et de sa voie métabolique dépendant des Smads, également impliquée dans le développement de la fibrose hépatique, pourrait déterminer l'équilibre subtil entre tolérance vis-à-vis du parasite et protection de l'hôte. Le rôle du couple TGF-β/IL-17 pourrait être encore amplifié par l'effet exercé sur d'autres médiateurs de la tolérance comme le FGL2.

En effet, les données apportées par notre travail sur FGL2 donnent un nouvel éclairage aux processus de tolérance dans l'infection par *E. multilocularis*. Elles démontrent que ce facteur non-cytokinique contribue au devenir de l'infection par *E. multilocularis* en intervenant dans la maturation des DC et en favorisant les fonctions des cellules Tregs ; elles dévoilent pour la première fois le rôle d'IL-17 dans la régulation de FGL2 ; et elles

suggèrent que FGL2 pourrait servir de cible pour le développement de nouveaux traitements pour les maladies infectieuses, y compris l'EA.

Les études que nous avons développées dans notre travail de thèse n'ont pas permis de répondre à toutes les questions posées par les échanges complexes et réciproques entre la réponse immunitaire induite par le parasite et le foie de l'hôte. Elles représentent cependant une base de départ pour une meilleure compréhension des mécanismes moléculaires qui sous-tendent ces échanges localement, dans le foie, et apportent, au niveau de la biologie cellulaire, quelques explications mécanistiques à des faits d'observation clinique.

Summary in Chinese

研究背景：泡型包虫病（Alveolar Echinococcoisis, AE）是由多房棘球绦虫(*Echinococcus multilocularis*, Em)寄生于人体所致的一种罕见但致死性寄生虫病，几乎均原发于肝脏，如未经及时治疗，10年死亡率高达90%。泡球蚴在中间宿主肝内以出芽的方式生长或浸润式增殖，产生新囊泡，长入肝组织，囊壁外角皮层很薄且常不完整，囊体与周围组织间无明显界限，囊液持续渗漏可与肝组织接触，引起局部肝组织病变、增生、肝纤维化、萎缩、变性和坏死，晚期似肝癌一样转移或侵害周围脏器，临床有“虫癌”之称，预后极差。近年来出现的正电子发射断层显像CT（PET-CT）将CT与PET融为一体，由CT提供病灶的精确解剖定位，而PET根据病灶周围免疫细胞及肝细胞的代谢情况提供病灶详尽的功能与代谢等分子信息，具有灵敏、准确、特异及定位精确等特点，在包虫病诊断中，不仅可以精确定位病灶，还可以检查泡球蚴活性。

泡球蚴寄生于肝脏，最后形成占位性病变是一个渐进的过程，大量临床及基础研究证实泡球蚴感染早期引起的宿主免疫应答以Th1类为主，3个月后则转以Th2类为主，泡球蚴通过“免疫逃避”达到寄生宿主的目的，同时泡球蚴在宿主机体局部形成的肉芽肿使病灶周围浸润的细胞不能有效地参与细胞免疫应答的效应阶段，最终形成免疫抑制状态，使泡球蚴组织快速增殖而达到维持感染的目的。目前对泡球蚴引起的免疫反应的研究主要集中于外周淋巴器官（动物实验中主要集中于脾脏、淋巴结）或者特定的细胞（AE病人中主要集中于外周血单个核细胞，动物实验中主要集中于腹腔细胞）。肝泡型包虫病人病灶与正常肝脏组织之间存在周边增殖活跃浸润增殖区中大量存在的促炎性因子如TNF-α、IL-6和IL-1β以及抗炎性因子IL-10、TGF-β都会对其中的肝脏细胞造成损害，我们认为这些损害可能是由于泡球蚴会通过分泌有害物质至囊液或分泌至肝脏等直接方式以及通过宿主免疫细胞分泌大量的细胞因子、转化生长因子（TGF）-β等间接方式，对宿主的肝脏细胞造成损害，形成临床病理表征，但是目前对于泡球蚴感染引发的免疫反应对宿主肝脏细胞损害的分子致病机理的报道极少。关键免疫调节因子，如不同感染时期细胞因子和化学趋化因子、TGF-β、$CD4^+CD25^+$ Treg新型效应分子FGL2在宿主病理损伤中的作用及机制未见报道。本研究旨在阐明天然免疫和炎症相关细胞因子、T细胞免疫相关的细胞因子和化学趋化因子及$CD4^+CD25^+$ Treg新型效应分子FGL2在泡球蚴感染中作用及机制，及其在宿主病理损伤中作用及机制。

研究方法：

体内实验 肉眼直视下建立肝脏穿刺泡球蚴感染模型：8-10 周龄雌性 BALB/c 小鼠，随机分为实验组和对照组。乙醚麻醉，实验组开腹直视下肝左叶注射 0.1mL 泡球蚴混悬液，丝线缝合关闭腹腔。对照组相同部位注射等量生理盐水。感染 2、8、30、60、90、180、270、360 天处死小鼠，两组均在肝左叶相同部位采集标本；采用 36k 小鼠全基因组寡核苷酸芯片分析 BALB/c 小鼠肝泡球

蚴感染动物模型，肝脏基因 mRNA 转录本含量的改变；确定目标基因并联机检索 GeneBank 等整合数据库，按其生物功能进行分类。应用 Gene Cluster3.0 生物信息可视化分析软件进行等级聚类分析。筛选肝脏免疫相关基因；泡球蚴感染小鼠肝脏组织，福尔马林固定、石蜡包埋，4μm 连续切片。HE 染色观察病理变化，免疫组化方法、Western Blot 和实时荧光定量 RT-PCR 检测 TGF-β1、Smads、MAPK、肝细胞增殖和凋亡相关蛋白及 mRNA 的表达与分布，原位末端标记技术（TUNEL）检测病灶肝细胞凋亡；腹腔注射建立泡球蚴感染模型：8-10 周龄雌性 BALB/c 小鼠，随机分为实验组和对照组。实验组小鼠腹腔注射 0.1mL 泡球蚴混悬液，对照组小鼠注射等量生理盐水。感染 1、4 月处死小鼠，分别收集野生型和 fgl2 基因敲除小鼠腹腔细胞和脾细胞，流式细胞术检测和 qRT-PCR 检测 T 细胞活化及 DC 细胞成熟。

体外实验 ⑴原位肝脏灌注法分离大鼠肝细胞，与泡球蚴囊液共培养，15min、30min、1h、2h、24h 收集细胞，Western Blot 检测 TGF-β1、Smads、MAPK 相关蛋白的表达；⑵原代培养小鼠脾脏细胞与 ConA 或泡球蚴囊液共培养，48h 或 96h 后流式细胞术检测检测 T 细胞活化及 DC 细胞成熟；⑶$CD4^+CD25^+$ Tregs 与 $CD4^+CD25^-$ 效应 T 细胞共培养，BrdU ELISA 法检测细胞增殖。

实验**结果**：⑴在泡球蚴感染的早期，以 ERK1/2 信号通路被激活，促进肝细胞的增殖；在感染的中期，以 Gadd45β 高表达，调控肝细胞的抗凋亡；在感染的晚期，以细胞凋亡蛋白 p53、p21 高表达，肝细胞发生生长抑制或凋亡；

⑵泡球蚴感染早期以 Th1 免疫反应为主，感染中期呈现出混合的 Th1/Th2 免疫反应，感染晚期免疫反应降低，化学趋化因子在泡球蚴感染过程中发挥着重要的作用，病灶旁肝组织促进了细胞因子和化学趋化因子的产生和活性；在泡球蚴感染早期，IL-17A 和 IL-17F 在病灶炎性带组织和病灶旁肝组织中均高表达，感染晚期 IL-17A 表达低于对照组，而 IL-17F 表达有所降低，但仍高于对照组；

⑶随着泡球蚴感染时间的延长，肝损伤逐渐增加，肝纤维化程度增加，TGF-β1 及在 TGF-β/Smad 信号通路泡球蚴感染所致的肝纤维化中具有促进作用；⑷泡球蚴感染激活宿主肝细胞 TGF-β/Smad 信号通路，造成了肝纤维化；在泡球蚴感染进程中，TGF-β1 的表达与 CD4/CD8 比值呈现正相关；

⑸FGL2 基因敲除能促进 T 细胞增殖、减弱 Treg 的免疫抑制作用、促进 Th1 免疫反应、增加抗体生成 B 细胞的表达、并促进 DC 细胞成熟，从而显著的减少泡球蚴在宿主体内的生长与繁殖；体外实验表明 IL-17A 促进 FGL2 的生成。

结论：⑴在泡球蚴感染宿主肝脏的过程中，泡球蚴通过直接刺激（囊液中的有害成分、原头蚴本身分泌的某些成分）或间接（引起宿主免疫系统分泌的 TGF-β 及相关细胞因子）刺激，产生细胞毒性，造成宿主细胞应激反应，激活宿主肝细胞 MAPK 信号通路（ERK 和 JNK 信号通路）和细胞周期相关调控因子，影响宿主肝细胞周期、引起宿主肝细胞增殖、生长抑制、凋亡和肝细胞功能改变等，最终导致宿主“肝肿大（感染早、中期）”或肝脏萎缩、变性坏死（感染晚期）；

⑵泡球蚴感染早期以 Th1 免疫反应为主，感染中晚期呈现出混合的 Th1/Th2 免疫反应，化学趋化因子在泡球蚴感染过程中也发挥着重要的作用，病灶旁肝组织促进了细胞因子和化学趋化因子的产生和活性；
⑶首次证明细胞因子和化学趋化因子，尤其是 IL-17，在泡球蚴感染病灶旁炎性带和病灶旁肝组织发挥着重要的作用，结果提示 TGF-β 对 IL-17 不同的亚型表达及 Treg 具有调控作用，调节 T 细胞向特定方向分化，并诱导免疫细胞发生凋亡，从而介导泡球蚴的免疫逃避，同时造成宿主组织损伤；
⑷我们的研究结果的提示，在泡球蚴感染宿主肝脏过程中，泡球蚴感染引起宿主炎症反应或泡球蚴自身，分泌 TGF-β 及炎症/抗炎症细胞因子，激活下游 Smad 信号通路，引起机体免疫抑制状态的形成，造成泡球蚴的“免疫逃避”，同时导致宿主肝脏发生病理性损伤；
⑸我们对 Treg 新型效应分子 FGL2 的研究为阐明泡球蚴感染免疫耐受的机制提供了新的思路和方法，为包虫病的预后监测提供新的依据和思路。

对寄生虫感染免疫反应与宿主病理损伤之间的关系研究刚刚起步，有关机制尚不清楚。泡球蚴感染在宿主免疫应答过程中的信号转导，与宿主细胞增殖凋亡调控基因表达的关系，以及诱导凋亡特异的抗原等在宿主体内发挥的作用，均有待于进一步研究，其结果将有助于从分子水平认识泡球蚴感染诱导宿主细胞凋亡的调节机制，为肝泡型包虫病的临床治疗提供新的思路，从而为进一步提高肝泡型包虫病的整体疗效奠定基础。

关键词：转化生长因子-β；Th 类细胞因子；趋化因子；泡球蚴；肝纤维化；肝损伤

Summary in English

Background： Alveolar echinococcosis (AE) is a rare, but - if remaining untreated or treated too late- severe and fatal zoonotic helminthic disease, predominantly caused not only by the direct hepatic damage which follows the continuous tumor-like proliferation of the larval stage (metacestode) of *Echinococcus multilocularis (E.multilocularis),* but also indirectly by the intense local granulomatous immune response which surrounds the parasitic tissue; both are responsible for chronic liver injury, liver fibrosis, necrosis, chronic cholestasis and finally hepatic failure.
The lesions, composed both of the multiple vesicle-forming metacestode and of cells homing from lymphoid organs and permanently settling around the metacestode, behave like a slow-growing liver cancer, progressively invading the liver, then the neighboring tissues and also metastazing to other organs. Despite the alleged involvement of the granulomatous response in the functional imaging (e.g. through Fluoro-deoxy-glucose-Positron Emission Tomography) and in the complications of AE, very little is known on the local, hepatic, immune response and key immune-regulation factors to influence immune cell-homing to the liver as well as liver cell homeostasis: regeneration, degeneration and dysfunction.
It has long been known that the liver is the key organ in *E. multilocularis* infection. *E. multilocularis* growth induces the activation of numerous pathways of the immune response and the immune mechanisms involved in the interaction between the parasite and its host have been extensively studied. The involvement of Th1/Th2 and individual cytokines has been rather extensively studied within the past 2 decades both in humans and in experimental rodents. However, nearly all studies have been performed on peripheral lymphoid organs (spleen, lymph nodes in experimental animals) or cells (peripheral mononuclear cells in humans, peritoneal cells in experimental animals). On the other hand, clinical observations, such as the magnitude of hepatomegaly in AE patients and/or the tolerance of the liver to major resections at surgery, or the diffusion of fibrosis to parts of the liver which are not involved in the parasitic and immune periparasitic processes in experimental animals, have suggested that direct influence could be exerted by the metacestode-induced immune response on the liver parenchyma. However, this has never been studied in depth and the potential mechanisms are unknown. Especially, the study of the mechanisms involved in changes in liver homeostasis at different infection stages, a detailed cytokine and chemokine profile analysis of the periparasitic infiltrate in the liver, the presence of transforming growth factor-β (TGF-β) and other components of TGF-β/Smad pathway in the liver, and novel $CD4^+CD25^+$ Treg effector molecule fibronogen-like protein2 (FGL2) have, however, not yet been carried out in a comprehensive way all along the whole course of infection in *E. multilocularis* intermediate hosts. The aim of this thesis work was to explore the key actors (innate and proinflammation cytokines, Th-related cytokines and chemokines, major immune regulation cytokine TGF-β and $CD4^+CD25^+$ Treg effector molecule FGL2) and the consequence in the liver (hepatocyte proliferation/growth arrest) in the crosstalk between *E. multilocularis* and its hosts.

Methods: For *in vivo* studies, pathogen-free female BALB/c mice were injected by *E. multilocularis* metacestodes both in the anterior liver lobe (intra-hepatic infection mouse model) and in the peritoneum (intra-peritoneal infection mouse model). For each autopsy time-point in the intra-hepatic infection mouse model, ten experimentally infected mice were used in *E. multilocularis* group and compared with five control mice, which received an intra-hepatic injection of 0.1 mL of saline in the anterior liver lobe using the same surgical procedure. Mice were killed at 2, 8, 30, 60, 90, 180, 270 and 360 days, respectively.

Liver tissue samples taken close to or distant from the parasitic lesions or from the sham-injected liver lobe in control mice were used for hepatocyte proliferation/growth arrest or DNA microarray or TGF-β/Smad signaling pathway detection by using Western Blot, qRT-PCR and immunohistochemistry. In addition, to study cytokine and chemokine expression in the liver, samples were taken at the periphery of the lesions, in the granulomatous area. For each autopsy time-point in the intra-peritoneal infection mouse model, six experimentally infected mice ($fgl2^{-/-}$ Knock-Out mice versus wild type mice) were used in *E. multilocularis* group and compared with six control mice, which received an intra-peritoneal injection of 0.1 mL of saline using the same procedure. Mice were killed at 1 and 4 months, respectively. Spleen cells and peritoneal exudate cells (PEC) were taken from AE- $fgl2^{-/-}$ and AE-WT mice (and non-infected mice as control) and used for T cell reactivity and Dendritic Cells (DC) maturation detection.

For *in vitro* studies, 1) Co-culturing primary rat hepatocytes with *E. multilocularis* fluid was used to study TGF-β1, down-stream Smads activation by using Western Blot. 2) Co-culturing primary spleen cells with ConA or *E. multilocularis* fluid was used for T cell reactivity and DC maturation detection by using flow cytometry. 3) Co-culturing $CD4^+CD25^+$ Tregs with $CD4^+CD25^-$ T cells was used for Treg suppression function assay by using BrdU ELISA.

Results: 1) Results of hepatocyte proliferation/growth arrest studies showed that, after *E. multilocularis* infection, CyclinB1 and CyclinD1 gene expression increased up to day30 and then returned to control level after day60; Gadd45b, CyclinA and PCNA increased all over the period; ERK1/ 2 was permanently activated. Meanwhile, p53, p21 and Gadd45c gene expression, and caspase 3 activation, gradually increased in a time-dependent manner. In the late stage (day180–360), p53, p21 and Gadd45c gene expression were significantly higher in infected mice; JNK and caspase 3 were activated. TUNEL analysis showed apoptosis of hepatocytes. No significant change in CyclinE, p53 mRNA and p-p38 expression were observed at any time.

2) mRNA expression levels in the hepatic parasitic lesions showed that a mixed Th1/Th2 immune response, characterized by the concomitant presence of IL-12á, IFN-γ and IL-4, was established very early in the development of *E. multilocularis*.

Subsequently, the profile extended to a combined tolerogenic profile associating IL-5, IL-10 and TGF-β. IL-17 was permanently expressed in the liver, mostly in the periparasitic infiltrate; this was confirmed by the increased mRNA expression of both IL-17A and IL-17F from a very early stage, with a subsequent decrease of IL-17A after this first initial rise. All measured chemokines were significantly expressed at a given stage of infection; their expression paralleled that of the corresponding Th1, Th2 or Th17 cytokines

3) TGF-β1, its receptors, and down-stream Smads were markedly expressed in the periparasitic infiltrate and also in the hepatocytes, close to and distant from AE lesions. Fibrosis was significant at 180 days p.i. in the periparasitic infiltrate and was also present in the liver parenchyma, even distant from the lesions. Over the time course after infection TGF-β1 expression was correlated with CD4/CD8 T-cell ratio long described as a hallmark of AE severity.

4) FGL2-deficient mice infected with *E. multilocularis* exhibited a significantly decreased parasite load, associated with increased T cell proliferation in response to ConA, impaired Treg numbers and function, relative Th1 polarization, and increased numbers of antibody-producing B cells, as compared to infected WT mice. Both relative number and maturation status of dendritic cells were higher in $fgl2^{-/-}$ mice and CD80 and CD86 were more expressed in DCs following ConA and VF stimulation. Additional experiments confirmed that IL-17A contributes to FGL2 secretion in this model.

Conclusions: *E. multilocularis* metacestode definitely exerts a deep influence on liver homeostasis. Our data support the concept of a sequential activation of metabolic pathways which (1) would first favor parasitic, liver and immune cell proliferation and survival, and thus promote metacestode fertility and tolerance by the host, and (2) would then favor liver damage/apoptosis, impairment in protein synthesis and xenobiotic metabolism, as well as promote immune deficiency, and thus contribute to the dissemination of the protoscoleces after metacestode fertility has been acquired. These findings give a rational explanation to the clinical observations of hepatomegaly and of unexpected survival of AE patients after major hepatic resections, and of fibrosis, necrosis and hepatic failure at an advanced stage and in both human patients and experimental animals.

Our results also suggest that the surrounding inflammatory reaction in the liver contributes significantly to cytokine/chemokine secretion and functional immunological mechanisms within the host-parasite interactions. In addition to giving a comprehensive insight in the time course of cytokines and chemokines in *E. multilocularis* lesion, our results contribute to identify new targets for possible immune therapy to minimize *E. multilocularis*-related pathology and to complement the only parasitostatic effect of benzimidazoles in AE.

Our data suggest that TGF-β and downstream Smads signaling pathway are associated with fibrosis, while a TGF-β-related fine tuning of the various isotypes of IL-17 may determine the overall balance between tolerance towards the parasite and protection of the host. The fine tuning of IL-17 by TGF-β would then regulate other mediators of immune tolerance such as FGL2.

Our data on the novel $CD4^+CD25^+$ Treg effector molecule FGL2 give new insight into the tolerance process in *E. multilocularis* infection. They demonstrate that this non-cytokine factor contributes to the outcome of *E. multilocularis* infection by interfering in the maturation of DCs and in promoting Treg cell functions; they give evidence for a role of IL-17 in FGL2 regulation, and suggest that targeting FGL2 could be used for the development of novel treatment approaches in infectious diseases.

Our investigations have not answered all multiple questions raised by the complex and reciprocal interactions between the parasite-induced immune response and the host liver; however, they constitute an excellent starting point for an increased understanding of the molecular mechanisms underlying these interactions and give some mechanistic/cell biology-related explanations to clinical observations.

Key words: *Echinococcus multilocularis*; Alveolar echinococcosis; Hepatocyte proliferation/growth arrest; Cytokines; Chemokines; TGF-β; Liver Fibrosis; FGL2; $CD4^+CD25^+$ Treg

1. Introduction: *Echinococcus multilocularis* and Alveolar Echinococcosis

Echinococcus multilocularis (E.multilocularis) is a cyclophyllid tape worm present in the intestine of carnivores such as dogs, wolves, foxes. Along with some other members of the *Echinococcus* genus (especially *E. granulosus*), its larval form (metacestode) produces the disease known as echinococcosis in certain terrestrial mammals, including wolves, foxes, jackals, coyotes, domestic dogs and humans. Unlike *E. granulosus*, which usually produces a single large-sized cyst, *E. multilocularis* produces many small cysts (also referred to as *loculi*, in Latin language, hence the name) that spread throughout the liver, then invades other organs of the infected animal. Ingestion of these cysts, usually by a canid eating an infected rodent, results in a heavy infestation of the canid's gut by tapeworms.

1.1 Life cycle

The life cycle of *E. multilocularis* involves a primary or definitive host and a secondary or intermediate host, each harboring different life stages of the parasite. Foxes, domestic dogs and other canids are the definitive hosts for the adult stage of the parasite. The head of the tapeworm attaches to the intestinal mucosa by hooks and suckers. It then produces hundreds of microscopic eggs, which are dispersed through the feces (Vuitton *et al.* 2011). Wild rodents such as voles, mice, *Ochotona* spp. ('pikas') and small lagomorphs (on the Tibetan plateau, China) serve as the intermediate hosts. Eggs ingested by rodents develop in the liver, lungs and other organs to form multilocular cysts. Humans could also become an intermediate host by handling infected animals or ingesting contaminated food, vegetable, and water. The life cycle is completed after a fox or canine consumes a rodent infected with cysts. Larvae within the cyst develop into adult tapeworms in the intestinal tract of the definitive host (Vuitton, 2011; Zhang *et al.* 2011; Yang *et al.* 2012). Except in rare cases where infected humans are eaten by canines, humans are a dead-end or incidental host (an intermediate host that does not allow transmission to the definitive host) for *E. multilocularis*.

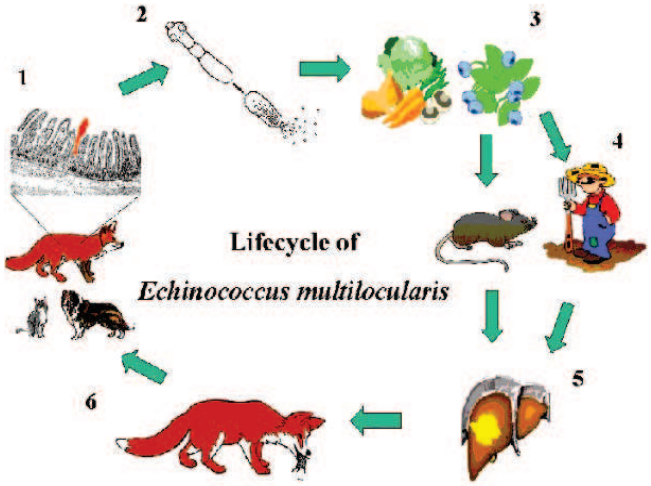

Figure1.1 Life cycle of *Echinococcus multilocularis*

1. adult worms are present in intestine of definitive host

2. eggs pass into feces, ingested by humans or intermediate host

3. onchospheres penetrate the intestinal wall, are carried via blood vessels to lodge in organs

4. echinococcosis vesicles (metacestode) develop in liver, lungs, brain, heart

5. protoscoleces (‘hydatid sand’ in cystic echinococcosis) ingested by definitive hosts attach to the small intestine and develops into adult worms

1.2 Epidemiology

The main endemic regions for human AE are Central Europe (southern Germany, Switzerland, western Austria, eastern France), Russia, Turkey, Japan (Hokkaido), China and North America (Alaska, northern Canada) (Kern *et al*. 2003; Vuitton *et al*. 2003). 573 cases were registered in the French registry between 1982 and December 2013, 200 cases (35%) from Franche comté Region, the region where Besançon University Hospital is located (Grenouillet *et al.* 2013; Said-Ali *et al.* 2013). AE is generally considered, compared to most of other infectious diseases, to be a “rare” disease. However, the disease has extended its range in Europe and USA in the last few decades (Kern *et al*. 2003; Vuitton *et al*. 2003, 2011). Between 1982 and 2000 a total of 559 cases were reported throughout Europe (Kern *et al*. 2003; Grenouillet *et al.* 2013). And the disease is spreading throughout the Midwestern United States, where it was previously rare or nonexistent (Torgerson *et al*. 2010). Besides, the

current estimates suggest an annual of 20000 new human cases worldwide with 91% of them occurring in the People's Republic of China (PRC) (Torgerson *et al*. 2010). New epidemiological trends are related to an unprecedented increase in the fox population in Europe, to the unexpected development of urban foxes in Japan and in Europe, and to changes in the environmental situation in many countries worldwide due to climatic or anthropic factors which might influence the host-predator relationship in the animal reservoir and/or the behavioral characteristics of the populations in the endemic areas (Torgerson *et al*. 2010).

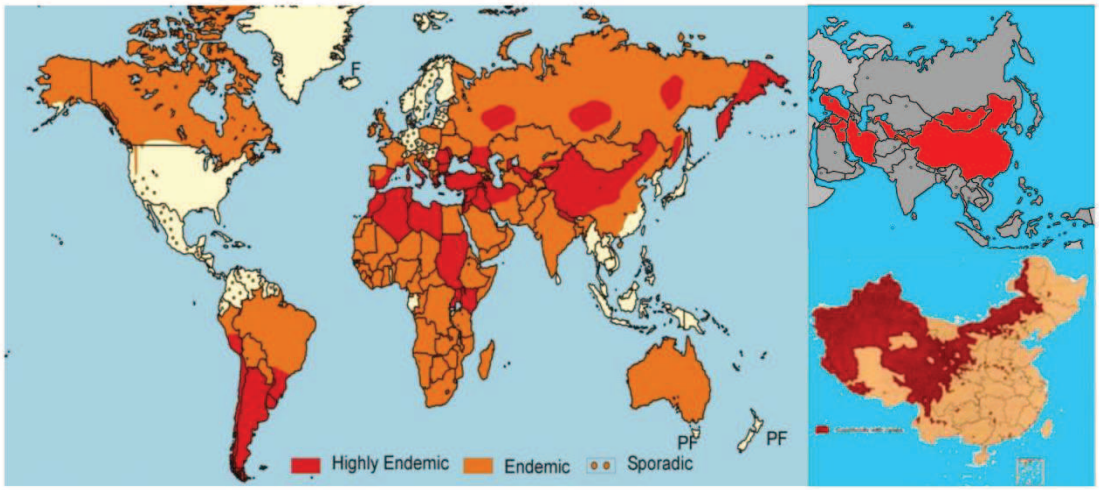

Figure 1.2 Endemic areas of alveolar echinococcosis

The incidence of human infection with *E. multilocularis* and AE is increasing in urban areas, as wild foxes (an important reservoir species of the sylvatic cycle) are migrating to urban and suburban areas and gaining closer contact with human populations (Vuitton *et al.* 2011). Also, restocking fox enclosures for fox hunting with infected animals spreads the disease. Children, health care workers and domestic animals are at risk of ingesting the cysts after coming into contact with the feces of infected wild foxes. Even with the improvement of health in developed/industrialized countries, the prevalence of alveolar echinococcosis (AE) did not decrease (Vuitton *et al.* 2011). On the contrary, incidence of AE has now also been registered in east-northern European countries, such as the Baltic States, and sporadic incidence was mentioned in other European countries (Vuitton *et al.* 2011).

1.3 Alveolar echinococcosis in humans and its diagnosis and treatment

The severity of AE in humans is related to a very long clinical latency and a progression in the liver comparable to a slow-growing cancer. The parasitic tissue is surrounded by an intense fibro- inflammatory reaction and both the biliary and

vascular walls may be involved in the parasitic process. Macroscopical examination indicates that the parasitic tissue has no clear limits with the adjacent liver parenchyma (Figure 1.3). At the periphery, the tissue is composed of numerous small irregular cavities corresponding to the parasitic vesicles, which is the active area of the parasitic mass. In the centre, the older part of the parasitic lesion is mainly made up of fibrous tissue that is sometimes calcified. Very often, particularly in huge AE lesions, necrosis develops in this central part due to poor vascularization of the lesion. This necrotic area favours superimposed bacterial infection leading to a clinical picture of liver abscess.

Figure 1.3 Macroscopical view of alveolar echinococcosis of the liver in a partial hepatectomy. The yellow parasitic mass (on the left) has no clear limits with the adjacent liver parenchyma (dark brown on the right). The periphery of this huge lesion is the ‘‘active’’ area, composed of fibro-inflammatory tissue and small parasitic vesicles (thin arrows). The center of the lesion is largely necrotic (thick arrow).

According to: Bresson-Hadni et al, Parasitology International, 2006 (55) S267 – S272

Microscopically, *E. multilocularis* larvae grow as tumorlike buds that transform into multiple vesicles filled with fluid and, in 15% of cases, with protoscoleces. The parasitic vesicles are lined with a germinal layer and a laminated layer, which are immediately surrounded by an exuberant granulomatous response generated by the host's immune system. This reaction has two main consequences, fibrosis and necrosis. Both reactions protect the host against larval growth but may also be deleterious (Vuitton *et al.* 2011).

The periparasitic granuloma is a major characteristic of AE pathology in humans, and pathological changes in AE are associated with an intense infiltration by immune cells, i.e. macrophages of various functional types (Vuitton & Gottstein, 2010), including the so-called “epithelioid cells” and “giant cells”, typical of granulomas and T lymphocytes (Bresson-Hadni *et al*. 1990). Experimental studies in infected mice and immunologic studies in humans have revealed the importance of cell-mediated

immunity in the control of larval growth. Immune responses, characterized by a helper T cell Th 1 profile of cytokine secretion, can kill the larvae, thus protecting the host. Conversely, the progressive forms of the disease are characterized by a Th 2 profile consisting of increased interleukin (IL)–10, transforming growth factor (TGF)–β, and IL-5 secretion (Mejri *et al.* 2010; Vuitton & Gottstein, 2011).

Directly or indirectly based on the immune response of the host, serological tests and imaging exams are commonly used to diagnose this disease (Kern, 2010). Currently, a range of imaging techniques can be used at the different stages of management of AE. For diagnosis, ultrasonography remains the first line examination. For a more accurate disease evaluation, aiming to guide the surgical strategy, computerized tomography (CT), Magnetic Resonance (MR) imaging, including cholangio-MR imaging are of importance, providing useful complementary information. More recently, Positive-Emission Tomography (PET) using [18F] fluoro-deoxyglucose (FDG) has been developed for the follow-up of inoperable AE patients under long-term benzimidazole therapy.

1.3.1 Serological diagnosis

Frequently used serological tests including antibody tests, ELISA, Western blot and indirect hemaglutination (IHA) are important not only for confirmation of AE cases, but also for epidemiological studies in endemic areas such as Germany (Jensen *et al*. 2001; Röming *et al*. 1999), France (Bresson-Hadni *et al*. 1994) and China (Bartholomot *et al*. 2002; Craig *et al*. 2000; Craig *et al*. 1992). The search for highly sensitive and specific antigens probably represents the greatest challenge in the immunodiagnosis of *E. multilocularis* infection. Thus, in the last three decades, a wide range of antigens from different developmental stages of the parasite have been assayed for their potential as candidate molecules for the sero-diagnosis of AE in humans. In particular, the use of partially purified and recombinant antigens has improved the sensitivities and specificities of the diagnostic tests considerably (Gottstein *et al.* 1983; Sako, 2002). Metacestode antigens used for diagnosis are as follows:

The native Em2 antigen (also termed Em2a), revealed by *in-vivo* and *in-vitro* studies, is a structural component found only in the metacestode laminated layer, and not in freshly hatched oncospheres, protoscolex or adult stages (Gottstein *et al.* 1983; Deplazes *et al*. 1991). The glycosylated antigen Em2 (G11) has been found to be the major antigenic component of Em2 (Deplazes *et al*. 1991). It induces non-specific *in-vitro* T-lymphocyte proliferation in B-cell-deficient μMT mice, and low-avidity

IgG isotypes *in vivo* in C57BL/6 mice (Dai *et al*. 2001). These findings seem to indicate that Em2 (G11) is a T-cell-independent antigen that could contribute to the tolerance towards proliferation of the parasite metacestode. Em492, an *E. multilocularis* metacestode component identified more recently by Walker et al. (Walker *et al*. 2004), shares with Em2 (G11) the galactose-a (1,4)- galactose epitope, suggesting that both antigens may be related immunologically. Em492, as well as Em2 (G11), is localized in the laminated layer of the metacestode, and seems also to be involved in the immunosuppressive events that occur at the host-parasite interface (Vuitton & Gottstein, 2010). With regard to metabolized proteins, an E. multilocularis protoscolex-associated antigen of 62 kDa (Auer *et al.* 1988), two 70- and 90 kDa- proteins (Korkmaz *et al*. 2004), and several recombinant *E. multilocularis*-proteins (such as antigen II/3 (Vogel et al. 1988) and its subfragments II/3-10 (Müller *et al.* 1989), EM10 (Frosch et al. 1991), and Em18 (Ito *et al*. 1995), have all been published and discussed in view of a potential biological role (Mejri *et al.* 2010). However, these antigens were mainly used to investigate respective immune responses with emphasis on immunodiagnosis of AE, and their biological functions have not been appropriately studied. $Em2^{plus}$- ELISA and Em18-Western Blot are currently widely used to distinguish between AE and CE with very high specificity (Helbig *et al*. 1993; Ma *et al*. 1996). EmAP (alkaline phosphatase), an antigen which was shown to induce the production of antibodies associated with disease severity and resistance to treatment in AE patients, was also shown to induce only Th2-type cytokine secretion (Lawton *et al*. 1997; Sarciron *et al*. 1997). The14-3-3-gene of *E. multilocularis* appears to play a key role in basic cellular events related to cellular proliferation, including signal transduction, cell-cycle control, cell differentiation, and cell survival (Siles-Lucas *et al*. 1998; Siles-Lucas & Gottstein *et al*. 2003). The recently identified Em P29, was shown to induce non-specific *in-vitro* T-lymphocyte proliferation and a Th1 immune response, suggesting that it is protective against secondary *E.multilocularis* infection (Gottstein, personal communication; unpublished data).

1.3.2 Ultrasonography and computerized tomography in AE

Ultrasonography (US) and computerized tomography (CT) remain the basic morphological imaging techniques in AE. Colour and pulsed doppler coupled with US is very useful in studying the relationship between the parasitic lesion and vessels (Vuitton *et al*. 2004; Bresson-Hadni *et al*. 2005; Reuter *et al*. 2001).

US is the current screening method of choice for diagnosis and regular follow-up imaging in AE. A typical US aspect is observed in 70% of the cases, when AE lesions

are generally large in size. The lesion is characterized by irregular limits and heterogeneous content with juxtaposition of hyperechogenic (fibrous tissue) and hypoechogenic (‘‘active’’ parasitic tissue) areas. Very often, the hyperechogenic fibrous tissue contains scattered calcifications, well identified by US, as hyperechogenic foci with characteristic dorsal shadowing. US can also provide information on biliary and vascular involvement: intra-hepatic bile duct dilatations can be easily disclosed, as well as infiltration of the inferior vena cava, hepatic or portal veins walls by the parasitic tissue (Bresson-Hadni *et al*. 2006). Recently, contrast-enhanced US has been evaluated in AE: results suggest that the typical enhancement at the periphery of the lesions may correspond to the periparasitic immune infiltrate/granuloma, due to its rich vascularization (Tao *et al.* 2011; Zeng *et al*. 2012).

The second imaging technique is CT that is always performed after US examination to confirm the morphological aspects of AE. CT helps to specify the number, size and localization of the lesions in the liver. It is the best technique to detect the typical calcifications inside the lesion (Reuter *et al*. 2001). In the case of very calcified lesions, US examination is of limited use and CT is mandatory to delineate precisely the parasitic mass, particularly the posterior border. CT also shows the extent of regeneration/hypertrophy in the liver lobe, which was not invaded by the metacestode pseudo-tumor, and its part taken in the hepatomegaly often found in AE patients.

1.3.3 Magnetic resonance (MR) imaging in AE

MR imaging may facilitate the diagnosis in uncertain cases with non-calcified lesions, by showing the small aggregated vesicles, thus the pathognomonic aspect of the disease: “honeycomb” or “bunch of grape” pictures, best see on T2 weighted images (Reuter *et al*. 2001; Claudon *et al*. 1990; Bartholomot *et al*. 1997; Kodama *et al*. 2003). MR imaging is the best technique to characterize the different components of the parasitic lesion and could become the reference radiological exam in case of a nodular homogeneous form detected by US, which seems to correspond to an early AE lesion, either primary or recurrent after surgery. Moreover, this technique is very useful in studying the extension of the parasitic tumor to adjacent structures, and, therefore, should be included in pre-operative evaluations, especially if a large resection or a liver transplantation is planned. The proximity of parasitic lesions to

blood vessels is sometimes better assessed with MR imaging than CT. It is particularly useful in the pre-operative evaluation to show inferior vena cava and hepatic vein invasion and the up- and downstream consequences. But MR imaging does not detect calcifications, considered as quite specific of AE lesions (Bresson-Hadni *et al*. 2006).

1.3.4 Positron emission tomography in AE

Conventional imaging techniques are unable to give information on parasite metabolic activity. Radio-labelled fluoro-deoxyglucose positron-emission tomography (FDG- PET) is a valuable technique in nuclear medicine for detecting tissue metabolic activity; it was initially proposed to assess parasite viability and seemed very promising to appreciate the efficacy of AE treatments (Reuter *et al*. 1999). Morpho-PET, which is a PET- scan combined with a CT-scan using image fusion, combines the advantages of both imaging exams. The results of the evaluation of 30 patients in France, using morpho-PET, totally agreed with those of the previous German studies on PET: in unresectable patients, PET-CT can evaluate the morpho-functional aspects of the disease and assess the efficacy of BZM treatment (Bresson-Hadni *et al*. 2006) (Figure 1.4).

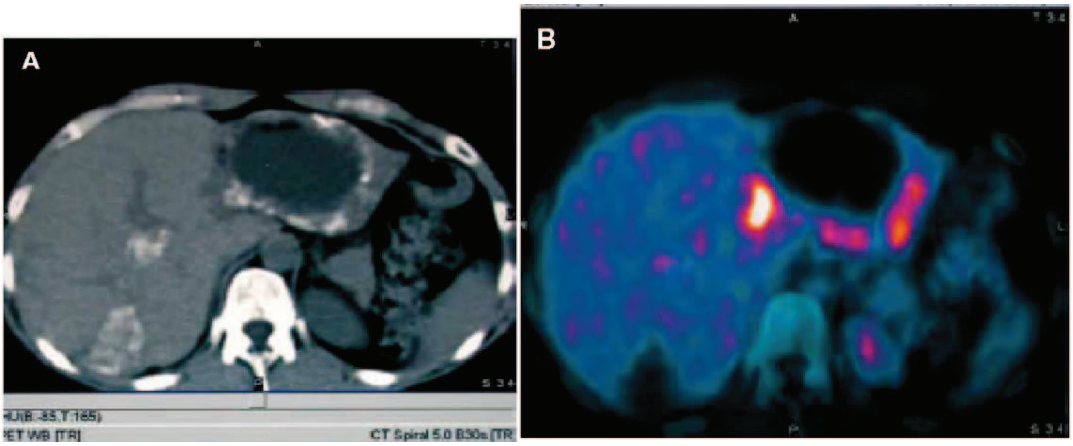

Figure1.4 FluoroDeoxyGlucose-Positron Emission Tomography (PET)/Computed Tomography (CT) imaging in alveolarechinococcosis of the liver (A, B)
CT-scan image (A): Bi-focal AE in a young woman under albendazole (ABZ) therapy for 14 years. PET image of the same lesions (B): Intense peri-lesional activity (“hot-spots”) around the huge left AE focus. The other AE lesion, located in the right lobe of the liver, became largely calcified during the follow-up and shows no peri-lesional enhancement, suggesting an efficacy of ABZ.

According to Bresson-Hadni et al, Parasitology International, 2006 (55) S267 – S272

With the assumption that PET accurately reflected the viability of the parasite, albendazole treatment withdrawal, based on PET images, was evaluated, and results were rather disappointing, since recurrence were observed several months after withdrawal, despite negative PET images in these patients (Reuter *et al.* 1999, 2001,2004; Bresson-Hadni *et al.* 2006; Ehrhardt *et al.* 2007; Crouzet *et al.* 2010; Bresson-Hadni *et al.* 2011). Recently, one study showed that delayed ^{18}F-FDG PET (images taken 3 hours after FDG injection) better differentiated between active and inactive liver lesions in AE patients (Caoduro *et al.* 2010); its value to serve as a basis for treatment withdrawal has still to be evaluated prospectively. However, all observations made from the clinical use of PET also raised the question of the cells actually responsible for FDG uptake, and thus PET images, in patients with AE, and it is currently widely accepted that PET images only reflect indirectly parasite viability. The accumulation of FDG may well reflect the metabolic activity of the immune cells; but the relationship between parasite viability and the nature, composition and activity of the periparasitic granulomatous infiltrate is far from being known, in humans as well as in the experimental models of AE. Such observations largely contributed to the initiation of my thesis project, in order to better understand the composition and dynamics of the periparasitic infiltrate, i.e. the profiles of cytokines/chemokines related to immune cell-homing to the parasitic lesions, the role of key cytokines and molecules on immune tolerance/protection, thus on parasite viability, and the mutual influence of the parasite and the liver.

1.3.5 Treatment of AE

If no specific therapy is initiated, in 94% of patients the disease is fatal within 10–20 years following diagnosis (Jura *et al.* 1998). Radical surgery is the basis of treatment for early AE, but patients not suitable for surgery and those who have had surgical resection of parasite lesions must be treated with benzimidazoles (albendazole, mebendazole) for several years (McManus, 2012). Benzimidazoles only halt parasite proliferation; they do not kill the parasites; despite the improvements in the chemotherapy of echinococcosis with benzimidazole derivatives, complete elimination of the parasitic mass cannot be achieved in most of the infected patients. In patients without complete resection of the lesions, they should thus be given life-long although they may have deleterious side effects such as liver damage (Kern, 2010; Vuitton & Bresson-Hadni, 2014). Several alternative drugs have been tested in vitro and in vivo against *E. multilocularis* metacestode (reviewed in Vuitton & Bresson-Hadni, 2014), but none has currently been tested in clinical trials. Results of observations in humans and experimental studies in animals also suggest that, in the

absence of fully effective anti-parasitic chemotherapy for AE, modulation of the host's immune response could be envisaged to fight against the parasite (Vuitton & Gottstein, 2010); to achieve this goal, the mechanisms involved in the host-parasite interplay in the liver should be better elucidated. On the other hand, to evaluate the progression/regression of the disease in benzimidazole treated patients, and decide of a possible treatment withdrawal after some years, markers of progression/regression, both imaging (i.e. PET or other functional imaging techniques), and biochemical/immunological, markers (i.e. serology, other markers, such as FGL2, a novel molecule possibly related to *E. multilocularis* tolerance) need to be further explored.

1.4 Experimental models to study *E. multilocularis* metacestode stage

In vivo methods of studying experimental echinococcosis in laboratory rodents include oral inoculation of eggs from adult cestodes (Yamashita *et al*. 1963) and subcutaneous (Ali-Khan *et al*. 1980; Kassis *et al*. 1976; Yamashita *et al*. 1956), intraperitoneal (Yamashita *et al*. 1968a) and intrahepatic (Yamashita *et al*. 1963) secondary infection. The method of oral inoculation with eggs has advantages in that primary lesions mimic those of a natural infection (Rausch, 1954; Ohbayashi, 1960; Veit *et al.* 1995; Bauder *et al.* 1998) and are usually located in the liver (Ohbayashi *et al*. 1960). However, the technique is hazardous in that eggs from the adult worm are infective to humans (Yamashita *et al*. 1968b). Moreover, until the recent development of techniques to grow adult *Echinococcus* to maturity in laboratory rodents (Kamiya *et al*. 1990), it necessitated keeping the definitive host (usually a dog) and harvesting its feces for eggs.

The secondary subcutaneous murine AE model is currently used for experimental treatment studies (Stettler *et al*. 2004). In this model, the parasite metacestodes are injected into the subcutaneous tissue of a mouse or a Mongolian jird (*Meriones unguiculatus*), where the parasites proliferate and develop tumor-like features such as progressive growth and invasion of neighboring tissues (Küster *et al*. 2013).

The secondary intra-hepatic murine AE mouse model (Liance *et al.* 1984) represents a combined model of infection (development of the *E. multilocularis* larva), immune response (granulomatous reaction leading to fibrosis) and tumor (occupying process in the liver with simultaneous induction of liver regeneration) (Vuitton *et al.* 2003). An intra-hepatic infection model can be used for a parallel cellular and molecular study of the parasite and of the liver in which it is growing; it may allow a

simultaneous approach of the crosstalk between the granuloma and the liver and of its consequences on liver fibrosis. In addition, as the liver has special properties regarding immune tolerance (Jenne & Kubes, 2013), reproducing the most usual location of the parasite, may allow conclusions closer to the clinical situation. However, as it requires surgical operation, for practical and ethical reasons, this model is more difficult to develop than the usual intra-peritoneal infection.

The secondary intra-peritoneal murine AE mouse model, i.e. injection of protoscoleces into the peritoneum, is the most widely used model of alveolar echinococcosis in rodents. It is an easy way for in vivo testing of anti-parasite drugs. For immunological research, this model allows the study of peritoneal macrophages and of mesenteric and/or para-aortic lymph nodes (Mejri *et al.* 2011). The intra-peritoneal infection model can give a comprehensive insight in the mechanisms of immune response with a therapeutic purpose.

However, using the in vivo models, the only one available for decades, it was difficult to draw definite conclusions from studies about the factors modulating *E. multilocularis* metacestode differentiation, and investigations into gene expression and regulation were hampered by the close and complex host–parasite interactions that exists (Hemphill *et al.* 2002). Several *in vitro* metacestode culture models have thus been developed to study the basic parameters of parasite proliferation and differentiation, to investigate the interactive role of heterologous cells, to localize several *E. multilocularis* antigens, and to dissect the ultrastructure and composition of the acellular laminated layer (the structure that is predominantly involved in the physical interaction between the parasite and host immune and non-immune cells and tissues) (Brehm & Spiliotis, 2008; Spiliotis & Brehm, 2009).

Spiliotis developed an *in vitro* system for the long-term cultivation of *E. multilocularis* larvae. In his system, the parasite was first grown in co-culture with Reuber cells (3-w), after which the parasite was cultured in the absence of host cells but in the presence of supernatant of these feeder cells. In the absence of feeder cells from the host, long-term survival of the parasite depended strictly on low oxygen conditions and the presence of reducing agents in the medium. Host serum supported survival of the parasite but the growth of metacestode vesicles and differentiation towards the protoscolex stage only occurred in the presence of culture medium that was preconditioned by hepatoma cells or several other immortal cell lines (Spiliotis *et al*. 2004).

In terms of beneficial effects of host cells on parasite development, it has been suggested that Caco2 and/or hepatocyte feeder cells and/or cell lines produce growth factors for metacestode vesicles (Hemphill & Gottstein, 1995; Jura *et al*. 1996; Spiliotis *et al*. 2004). Host cells may also remove compounds from the culture medium which are toxic for the parasite.

For immunological studies, the availability of cultured *E. multilocularis* germinal cells, isolated or structured in vesicles, has allowed a more precise study of the sensitivity of parasite cells to initiators/modulators of the immune response, and open new avenues in the research on the host-parasite cross-talk.

1.5 Host-parasite relationship and immune responses to the metacestode stage

Host-parasite interactions in the *E. multilocularis*-intermediate host model depend on a subtle balance between cellular immunity, which is responsible for host's resistance towards the metacestode, the larval stage of the parasite, and tolerance induction and maintenance. The pathological features of alveolar echinococcosis are related both to parasitic growth and to host's immune response, leading to fibrosis and necrosis. The disease spectrum is clearly dependent on the genetic background of the host as well as on acquired disturbances of Th1-related immunity, as mentioned above.

1.5.1 Susceptibility and Resistance to *E. multilocularis*

In the experimental animals, *E. multilocularis* exhibits different growth rates and maturation characteristics in various species of hosts, that is, species of rodents or lagomorphs for *E. multilocularis*, but also of multiple other animal species such as swine and primates (Vuitton & Gottstein, 2010). Extensive studies in the differences in host immune responses suggest that differences in susceptibility/resistance, is putatively related to respective immune responses in different murine models (Liance *et al*. 1984, 1990; Bresson-Hadni *et al*. 1990; Guerret *et al*. 1998; Gottstein *et al*. 1994). It was shown that impairment of cellular immunity (immune suppression) is followed by an increase in susceptibility to *E. multilocularis* in immunosuppressed mice (Baron & Tanner, 1976) and was further demonstrated in SCID mice (Playford *et al*. 1992) and in nude mice (Dai *et al*. 2004). A similar increase of susceptibility of experimental mice, associated with a decrease of delayed type hypersensitivity, was also observed in mice infected with *E. multilocularis* and treated with an immunosuppressive drug, cyclosporine, which interferes with IL-2 production in T-cells (Liance *et al*. 1992). Conversely, cellular immune response against parasitic antigens is stronger in infected resistant mice (Liance *et al*. 1990; Gottstein *et al*. 1994), and resistance is increased by stimulation of the cellular immune response (Rau *et al*. 1975).

In humans, increased susceptibility was evidenced by a rapid increase in size of lung metastases, the development of brain metastases, late re-invasion of the transplanted liver by parasitic cell remnants, and even early re-invasion of the

transplanted liver from a spleen metastasis in the transplanted patients (Bresson-Hadni *et al*. 1999; Koch *et al*. 2003); and by a rapid and irreversible growth of *E. multilocularis* larvae in the HIV-co-infected patients (Sailer *et al*. 1997; Zingg *et al*. 2004). It was shown an inhibition of specific lymphocyte proliferative responses in transplanted patients with recurrence of the disease, whereas transplanted patients considered as cured exhibited a very high proliferative response over a long time period (Bresson-Hadni *et al*. 1998). The persistence of a high proliferative response was also observed in Alaska patients with lesions containing dead parasites, and patients with severe AE had a depressed proliferation rate (Gottstein *et al*. 1991).

The genetic basis for either host resistance (no immunosuppression?) or susceptibility (immune suppression?) is clearer in humans than in the mouse model. Preliminary investigations showed that the frequency of certain HLA alleles (HLA-DR13) was increased in patients with a regressive course of disease after therapy compared to controls or patients with progressive alveolar echinococcosis (Gottstein & Bettens, 1994). A European study showed that HLA-DRB1*1 was associated with a reduced risk for disease development (Eiermann *et al*. 1998) and that there was a significant link between MHC polymorphism and clinical presentation of AE, such as association of HLA-DQB1*02 and disease severity, and the spontaneous and higher secretion of IL-10 in patients with a progressive AE and the HLA $DR3^{+}$, $DQ2^{+}$ haplotype (Godot *et al*. 2000). Clustering of cases in certain families, in communities otherwise exposed to similar risk factors, also points to immuno-genetic predisposition factors that may allow the larva to escape host immunity more easily (Vuitton *et al.* 2006). However, since inbred mice of the same H-2 haplotype differ significantly in their susceptibility to *E. multilocularis* there are obviously other, non-MHC-linked genes contributing to the disease susceptibility.

1.5.2 Pathological observations in AE

The pattern of growth and development of AE is different from that observed in cystic echinococcosis, due to *E. granulosus*. Structurally, the lesions are more complex (multivesicular), with infiltrative rather than expansive growth. These multiple cysts do not lead to the formation of a limiting fibrous layer (adventitial layer) or a host-tissue barrier. In susceptible animal hosts, fibrosis is present but may be limited (Guerret *et al.* 1998). In resistant animal hosts and in humans an intense fibrosis reaction develops from the center to the periphery of the parasitic mass, with concomitant degeneration of the parasite vesicles. In this mass of fibrous tissue, the germinal and laminated membranes appear disorganized and distorted among focal calcifications, and embedded in acellular fibrosis and/or necrosis (Vuitton *et al.* 1986; Guerret *et al.* 1998). The normal pattern of multiple small cysts seen in the natural

intermediate hosts, which can be also be seen at the very beginning of *E. multilocularis* development in humans, is only observed at the periphery of the lesions when the development of the parasitic pseudo-tumor has lasted for several years. The germinal cells infiltrate surrounding tissues, forming small exogenous and endogenous vesicles enmeshed in the dense cellular connective tissue. Most of the periparasitic immune infiltrate is thus found at the periphery of the lesions (in those areas where enhancement of contrast is observed at CT or contrast-enhanced US, and where FDG uptake is observed at PET imaging). If the germinal cells (or vesicle debris including viable germinal cells) enter blood or lymphatic vessels, metastatic growth may occur in distant organs, most commonly in the lungs and brain (Bresson-Hadni *et al.* 2006).

In humans, accidental intermediate hosts, the severity of AE results from both the continuous asexual proliferation of the metacestode and the intense inflammatory granulomatous infiltration around the parasite which causes pathological damages in the liver. Granuloma, extensive fibrosis, and necrosis are actually the characteristic pathological findings in *E. multilocularis* infection. The lesions, composed both of the multiple vesicle-forming metacestode and of cells homing from lymphoid organs and permanently settling around the metacestode, behave like a slow-growing liver cancer, progressively invading the liver. Fibrosis in AE is extremely active from the beginning of the infection. Irreversible acellular fibrosis composed of cross-linked collagens ensues and isolates the parasitic lesions from the host but also compresses and obstructs major vessels and bile ducts, destroys the liver parenchyma resulting in symptoms of biliary obstruction, portal hypertension and necrosis of the central portion of the cyst with abscess formation (Kern, 2010). Ascites, and esophageal, gastric and duodenal varices may develop at the terminal stages of the disease, because of portal hypertension due to vessel compression/obstruction, which may generate sometimes fatal clinical complications; irreversible liver failure is rare, usually due to secondary biliary cirrhosis (Kern, 2010).

1.5.3 The periparasitic immune cell infiltrate in AE

Pathological changes in AE are associated with an intense infiltration by immune cells, i.e. macrophages of various functional types, including the so-called “epithelioid cells” and “giant cells”, typical of granulomas and T lymphocytes (Manfras *et al*. 2002). At the time of initial encounter with its murine host, the metacestode might modulate the immune response. The changes that it induces are dynamic and depend on the stage of development, for example, ranging from oncosphere, to early stage vesicles up to a fully maturated and fertile metacestode. Dendritic cells (DCs) and

macrophages (MØs) are among the first cells encountered by the parasite, which, by secreting and expressing certain molecules, has evolved mechanisms to suppress the major inflammatory and thus immunopathological pathway. Besides, $CD4^+$ T lymphocytes are present from the early stage of parasite growth, and $CD8^+$ T lymphocytes were shown to home to the periparasitic infiltrate secondarily and to be associated with parasite tolerance and severity of the disease (Vuitton, 2003; Vuitton *et al*. 2006; Manfras *et al*. 2002; Manfras *et al*. 2004).

Dendritic cells and macrophages (MØ)

DCs, the most important antigen-presenting cells (APCs) in the initiation of a type 1 or type 2 immune response, depending on the nature of the antigen(s) (Foti *et al.* 2006), range among the first players in the elaboration of a specific immune response. In the frame of a Th1 immune orientation, it is largely accepted that DCs are activated mostly by bacterial or viral pathogens via Toll-like receptor (TLR) ligation to produce IL-12 and TNF-a, both pro-inflammatory cytokines inducing a Th1 oriented response (Boonstra *et al.* 2003; Takeda *et al.* 2003). Th1-associated DC activation by microbial products evokes rapid phenotypic changes, including up-regulation of MHC class II, CD80, CD86 and CD40 (Reis e Sousa *et al.* 1999; Romagnoli *et al.* 2004). Thereafter, DCs have the ability to fully activate effector T cells. There is no mirror-image signature of cytokine and surface ligands that DCs express to stimulate Th2 differentiation. However, exposure of DCs to some helminthic antigens, including the products of filarial *Acanthocheilonema viteae* (ES-62), *Schistosoma mansoni* soluble egg antigen (SEA), and the schistosome-associated glycan lacto- N-ficopentaose III (LNFPIII), was found to pulse DCs to prime CD4+ T cells into Th2 type cells, and this occurred in the absence of increased MHC class II expression and co-stimulation molecule up-regulation (Whelan *et al.* 2000; MacDonald *et al.* 2001; Thomas *et al.* 2003). Ingold *et al.* (2000) have revealed the presence of high molecular mass glycans that form the major structural elements on the laminated layer of the metacestode of *E. multilocularis.* Whether exposure of DCs to these AE-glycans would pulse them to prime naïve $CD4^+$ T into Th2 differentiated cells needs to be addressed.

Macrophages from AE-infected mice (AE-MØ) as APCs exhibited a reduced ability to present a conventional antigen (chicken ovalbumin, C-Ova) to specific responder lymph node T cells when compared to normal MØ from non-infected mice (Mejri & Gottstein, 2006). This obstructed activity in antigen presentation of AE-MØ appeared to trigger an unresponsiveness of T cells, which in turn led to the suppression of their clonal expansion during the chronic phase of AE infection. In a similar context it was shown that high periparasitic NO production by peritoneal

exudate cells, mainly AE-MØs, also contributed to periparasitic immunosuppression (Dai &Gottstein, 1999; Andrade *et al.* 2004). Parasite- derived molecules also interfered with antigen presentation and cell activation, leading to a mixed Th1/Th2-type response at the later stage of infection. This correlated with the marked depression of the cell mediated immune response that had been observed in chronic AE (Devouge & Ali-Khan, 1983; Kizaki *et al.* 1991, 1993).

T and other cells

Cells of the innate immune system are not the only targets of these immunomodulatory parasite-derived molecules. Endothelial cells (in the skin, lungs, intestine and liver) can also be induced to express and secrete anti-inflammatory mediators, such as IL-10 and prostaglandins (Zaccone *et al.* 2008). In this way, the parasite not only reduces its likelihood of elimination but can also minimize local host-tissue damage, with coincidental and paradoxical benefits for the host. By inducing functional changes in DCs and MØs, the metacestode can achieve important shifts in T cell subsets. From those data accumulated in the last 2 decades it has been concluded that, in *E. multilocularis* metacestode infection, an initial acute inflammatory Th1 response was subverted gradually to a mixed Th1/Th2 response during the chronic phase of AE (Vuitton, 2006; Vuitton & Gottstein, 2010).

In the past decade, the Th1–Th2 paradigm has been revisited continually and alternative T cell lineages have been proposed. $CD4^+$ $CD25^+$ $Foxp3^+$ regulatory T (Treg) cells and Th17 cells are as two distinct subsets from Th1 and Th2 cells. They play important role in human AE, as mentioned in details in 1.5.4.

Eosinophils

One of the striking features observed in experimental murine AE (and also in naturally acquired AE of humans) is the absence of any eosinophilia. The mobilization of eosinophils is known to be a crucial immunological event that plays an important role in the host defence against helminths (Yamaguchi et al. 1988), but its role remains controversial. In many examples of nematode infections, eosinophilia is a marked characteristic, and eosinophils directly cause profound damage to the worm tegument, such as in *Strongyloides ratti* and in *T. spiralis*, in which a marked reduction of fertility and longevity was observed (Machado *et al.* 2005). On the other hand, eosinophils had no detectable effects on the infection with *Mesocestoides corti*, *Hymenolepis diminuta* and *Fasciola hepatica* (Ovington & Behm, 1997). An extravasation of eosinophils causing eosinophilia in the peritoneal cavity has been demonstrated to be beneficial for the host by causing damage to the immigrant immature *Fasciola hepatica*, resulting in the erosion of the tegumental syncytium

(Burden et al. 1983). It was shown in experimental murine AE that metacestode antigens (VF and E/S) exhibit proteolytic activity on eotaxin *in vitro* (Mejri & Gottstein, 2009). Inhibition of eotaxin activity may suppress the mobilization of eosinophils into the peritoneal cavity of intraperitoneally AE- infected mice. In experimental murine AE, the detected eotaxin inactivation by VF and E/S products may contribute to explain the absence of eosinophils within the peritoneal cavity of AE-secondary infected mice. Absent eosinophils thus may be a part of a series of events that maintain a low level of inflammation displayed within the peritoneal cavity of experimentally infected mice.

1.5.4 Cytokine profile of AE

Th1/Th2 related Cytokines in AE

Cytokine profiles, due to the secretion of characteristic cytokines by (mostly but not only) T "helper"(Th) cells give an insight into immune mechanisms involved in host-infectious organism relationship and in the types of immune responses that are developed after the early stage of antigen and "pattern" recognition (Vuitton & Gottstein, 2010). In most previous studies, secretion and expression of cytokines, chemokines, and related factors that govern immune cell-homing to *E. multilocularis* infection site were studied in the peripheral blood of human AE patients (Hubner *et al*. 2006; Kocherscheidt *et al*. 2008; Dreweck *et al*. 1999; Godot *et al*. 2000; Jenne *et al*. 1997; Harraga *et al*. 2003) and and on spleen and lymph node cells in the experimental model (Dai *et al*. 2004; Bresson-Hadni *et al*. 1990; Dai & Gottstein1999). In the immune-competent but susceptible host, *E. multilocularis* induces skewed Th2-responses, with high production of IL-4, IL-5 and IL-10 (Dreweck *et al*. 1999). In chronic AE, Th2-cytokines are associated with increased susceptibility to disease, while Th1-cytokines induce a rather protective immunity which involves IFN-α (Godot *et al*. 2003) and IL-12 (Emery *et al*. 1998) as initiating cytokines, and IFN-γ (Liance, *et al*. 1999) and TNF-α (Shi *et al*. 2004; Amiot *et al*. 1999) as effector cytokines.

Th17 related Cytokines in AE

Recently, the discovery of the IL-17 cytokine family has added a new dimension to the balance of inflammation and tolerance during parasite infections. The presence of IL-17 secreting $CD4^+$ T (Th17) lymphocytes correlates with severe hepatic pathology in murine schistosomiasis (Rutitzky *et al*. 2005). A more recent study, published during the completion of our thesis, showed that different isotypes played different roles in *E. multilocularis* infection, e.g. IL-17A was rather protective, while IL-17F might contribute to both protection and pathogenesis, as reported in human AE patients (Lechner *et al*. 2012).

Cytokines leading to tolerance

$CD4^+$ $CD25^+$ Tregs expressing the fork head/winged helix transcription factor (Foxp3) inhibit IL-2 production (Hori *et al*. 2003; Ghiringhelli *et al*. 2005). It has been suggested to play important role in immune tolerance by a study in patients with AE (Hübner *et al*. 2006), and in the experimental AE mouse model (Mejri *et al*. 2010). It is widely accepted that Tregs regulate immune response during *E. multilocularis* infection through the regulatory cytokines IL-10 and TGF-β (Vuitton & Gottstein, 2010). In a previous study, by using a microarray-based approach, researchers from our team observed that mRNA levels of the Fibrinogen-like protein 2 (FGL2), a Treg novel effector molecule, were significantly up-regulated in the liver of mice perorally infected with *E.multilocularis* eggs (Gottstein *et al*. 2011); this prompted us to study this factor as an additional actor of Treg-induced tolerance in AE.

FGL2, a member of the fibrinogen-related superfamily of proteins known to be secreted by T cells, has recently been reported by a number of groups to be highly expressed by Tregs and has been proposed to have a role in Treg effector function (Levy *et al*. 2000). It has been shown that FGL2 could inhibit dendritic cell maturation and induce apoptosis of B cells through binding to low-affinity FcgammaRIIB receptor, and thus contribute to Treg activity (Liu *et al*. 2008). There is evidence that FGL2 exerts immunosuppressive effect on T cell proliferation. Thus it plays an important role both in innate and adaptive immunity, being expressed by activated $CD4^+$and $CD8^+$ T cells and reticulo-endothelial cells (macrophages and endothelial cells) (Ghanekar *et al*. 2004; Belyavsky *et al*. 1998; Fingerote *et al*. 1996; Liu *et al*. 2010; McGilvray *et al*. 1998; Ning *et al*. 1998). It has been implicated as a novel biomarker of cancer (Rabizadeh *et al*. 2012), and in the pathogenesis of inflammatory disorders such as allo- and xenograft rejection (Ghanekar *et al*. 2004; Mendicino *et al*. 2005; Ning *et al*. 2005; Wilczynski *et al*. 2006; Xie *et al*. 2011; Zhang *et al*. 2004), or cytokine-induced fetal loss (Clark *et al*. 2002). It was also shown to play a role in infectious diseases, such as viral hepatitis (Belyavsky *et al*. 1998; McGilvray *et al*. 1998). To our knowledge, it has until now been neglected as a key-player in parasite-induced tolerance. As the therapeutic tools in AE are very limited so far, and immune modulation might represent an alternative option, Tregs and their effector molecule FGL2 could become attractive targets, putatively allowing a modulation of the patient's immune response to yield protective immune reactions that will result in a dying-out of the parasite metacestode; it could also represent an interesting marker of the tolerance status of AE patients, thus of the progression of the metacestode.

As mentioned above, the main cytokines involved in immune tolerance are IL-10 and TGF-β, have been largely studied in the past 3 decades. The metacestode actively achieves a tolerance status through the induction of regulatory cytokines IL-10 and

TGF-β (Mejri *et al.* 2009). Most of the studies in AE as well as in the experimental models have first focused onto IL-10. Spontaneous secretion of IL-10 by the PBMCs is the immunological hallmark of patients with progressing lesions of AE (Godot *et al.* 1997). However, only very preliminary results showed the presence of TGF-β secreting cells in the periparasitic granuloma surrounding *E. multilocularis* vesicles in the liver of patients with AE (Zhang *et al.* 2008), and exploring TGF-β in its multiple functions in *E.multilocularis* infection is still an open field of research.

TGF-β in AE

TGF-β is a major regulator of the immune responses, inducing and maintaining T-regulatory cells, reducing cytotoxic effector immune response and balancing the tolerogenic and immunogenic forces at play in various physiological states and chronic diseases, such as fetus growth and survival during gestation (Ouellette *et al*. 1997), cancer (Cufi *et al*. 2010), chronic inflammatory diseases (Feng *et al*. 2011), or chronic and allergic respiratory diseases (Jetten *et al*. 1986). In these conditions, this polypeptide also regulates a variety of cell events involved in tissue regeneration and fibrosis. Similarly, its role has been recognized both to induce and maintain immune tolerance towards parasites and to induce fibrosis in several examples of helminth infection (Harraga *et al*. 2003). However, opposite to the recognized role of IL-10 (Harraga *et al*. 2003; Vuitton, 2003), little is known about TGF-β involvement in the pathophysiology of larval echinococcosis. Only preliminary studies are available in AE: TGF-β was shown to be expressed in most lymphocytes of the periparasitic infiltrate in liver biopsies from AE patients. It was suggested that TGF-β may play a role in maintaining host tolerance against *E. multilocularis* growth by preventing T-cell cytotoxicity against the parasite (Zhang *et al*. 2008). In cystic echinococcosis (CE), immunostaining of TGF-β has also been shown at the periphery of hydatid cysts in the liver of patients (Wu *et al*. 2004); and another study confirmed a progressive increase in the expression of mRNA of TGF-β in the liver of *E. granulosus*-infected BALB/c mice (Mondragon-de-la-Pena *et al*. 2002). There is abundant evidence that TGF-β1, besides its role in immune tolerance, is an extremely potent inducer of the synthesis of procollagen and other extra-cellular matrix (ECM) components (Bartram *et al*. 2004; Higashiyama *et al*. 2007), and has an essential role in the pathogenesis of liver fibrosis. The major signaling pathway for all TGF-β members is activated through ligand binding to a cell-surface receptor complex of type I and type II serine–threonine kinases receptors; and a group of intracellular signaling intermediates known as Smads is then phosphorylated. Phosphorylated Smads translocate to the nucleus where they function as transcription factors, initiating target gene transcription (Banas *et al*. 2007). However, although it may be crucial in the host-parasite interactions, the relationship between the TGF-β/Smad pathway, and especially the expression of Smad7 which may play a regulatory role in the system,

and clinical and/or pathological features of AE in experimental models as well as in humans has never been addressed.

1.5.5 Chemokine profile of AE

In addition to cytokines, granulomas are associated with a variety of chemokines (Sadek *et al*. 1998; Qiu *et al*. 2001), which represent a family of molecules whose presumed function is to direct cellular movement. Chemokines are involved during innate recognition stages of immunity and may help direct Th1 and Th2 cytokine-producing cells during the generation of adaptive immunity (Lu *et al*. 1998; Lo *et al*. 1999). In addition, chemokines may be inflammatory or homeostatic, and facilitate lymphocyte migration during inflammation and immune surveillance (Kroetz *et al*. 2011). Furthermore, there is also considerable *in vitro* evidence that immune-related cytokines further capitalize on these effector molecules by regulating their expression and secretion. Chemokine expression by a variety of cultured cell types has been demonstrated to display positive or negative regulatory responses to cytokine stimulation (Sherry *et al*. 1998; Teran *et al*. 1999; Gasperini *et al*. 1999; Pype *et al*. 1999; Lamkhioued *et al*. 2000; Fujisawa *et al*. 2000).

Kocherscheidt et al. studied chemokine responses in AE patients at different states of infection (progressive, stable and cured AE) (Kocherscheidt *et al*. 2008). The production of CC and CXC chemokines which are associated with inflammation (MIP-1 alpha/CCL3, MIP-1 beta/ CCL4, RANTES/CCL5 and GRO-alpha/CXCL1) was constitutively larger in all groups of AE patients than in controls (Kocherscheidt *et al*. 2008). A disparate cellular responsiveness was observed in all groups of AE patients to viable *E. multilocularis* vesicles; cluster 1 (GRO-alpha/CXCL1, MCP-3/CCL7, MCP-4/CCL13, TARC/CCL17, LARC/CCL20) and cluster 2 chemokines (PARC/CCL18, MDC/CCL22, MIG/CXCL9) were downregulated, while cluster 3 chemokines (MIP-1 alpha/CCL3, MIP-1 beta/CCL4, RANTES/CCL5) appeared up-regulated (Kocherscheidt *et al*. 2008). The fact that *E. multilocularis* metacestodes selectively suppressed cellular chemokine production in AE patients may constitute an immune escape mechanism, which reduces inflammatory host responses, prevents tissue destruction and organ damage, but may also facilitate parasite persistence (Mejri *et al*. 2009). However, little is known on the expression of chemokines in the liver, and on the dynamics of the expression of chemokines in the periparasitic infiltrate, perhaps because of the difficulties of such studies in humans. It was never studied in experimental animals either, although experimental models may allow us to better characterize the course of chemokine expression at the various stages of *E. multilocularis* development.

2. Working hypothesis, questions and objectives

We hypothesized that *E. multilocularis* metacestode exerted a deep influence on liver homeostasis. On the other hand, we anticipated that functional imaging of AE in humans could be better interpreted if the factors governing immune cell homing around the metacestode were better known. And finally, both to define new markers of AE progression and to target immune modulation as a therapeutic tool in AE, we addressed the respective roles of TGF-β and TGF-β/Smad signalling pathway, and of the $CD4^+CD25^+$ Treg-effector molecule FGL2. We proposed a concept of immune cell activation at early infection stage and immune tolerance at late infection stage which would 1) first favor parasitic, liver and immune cell proliferation and survival, and thus promote metacestode fertility and tolerance by the host, and 2) would then favor liver damage/apoptosis, as well as promote immune deficiency, and thus contribute to the dissemination of the protoscolex after metacestode fertility has been acquired (Figure 2.1).

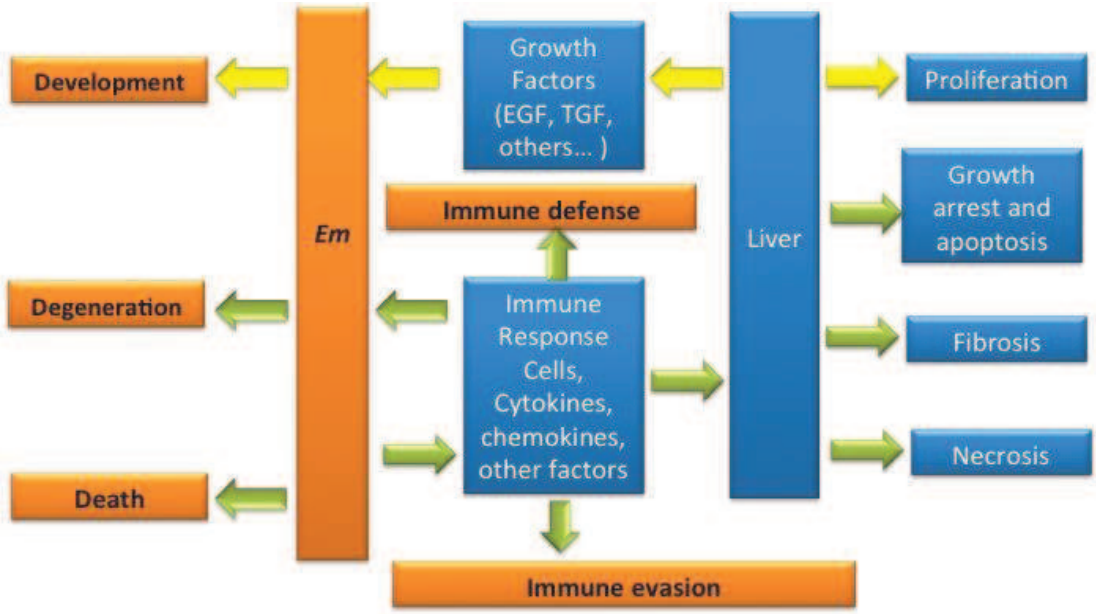

Figure2.1 Working hypothesis

Interactions between the parasite and the host are multiple and complex, and until now, most of the studies have focused on the parasite and the immune cells of the host; only some studies considered how the parasite-induced immune response interfere with the liver parenchyma, especially for the induction of fibrosis (Grenard *et al.* 2001). We thus focused part of our studies on the liver parenchyma. In addition, most of previous studies dealt with systemic immune response, in the spleen, lymph nodes, or peripheral blood; our aim was thus to study the immune response locally, in the liver, whenever possible.

The scientific questions and objectives of this thesis work were as follows:

Question 1. Has *E.multilocularis* any influence on host's liver homeostasis, and

especially on liver proliferation/apoptosis? The objectives are to explore the activation of proteins involved in proliferation and/or growth arrest/apoptosis metabolic pathways during the 3 stages of *E. multilocularis* infection; and to explore sequential activation of liver and immune cell proliferation and survival.

Question 2.What is the dynamics of cytokine/chemokine expression in the periparasitic immune infiltrate and adjacent liver? The objectives are to give a comprehensive appraisal of the various factors and pathways involved in immune cell homing around the *E. multilocularis* metacestode, at the various successive stages of disease; and to study the parasite and the host immune response in their usual context, the liver, in the experimental mouse model of hepatic secondary infection.

Question 3. How are TGF-β and TGF-β/Smad signaling involved in the interactions between *E. multilocularis* and its host? The objective is to explore the influence of TGF-β/Smad signaling pathways in liver fibrosis in AE and possible dysregulation promoting fibrosis and/or tolerance.

Question 4. Is FGL2 involved in the cross-talk between *E. multilocularis* and its host and how does it regulate immune tolerance? The objectives are to study the role of FGL2 on T and B cell reactivity and maturation of dendritic cells (DC) at the different stages of *E. multilocularis* infection, i.e. early and late stages; to study how parasite-origin components exert an effect on immune response in condition of fgl2 depletion due to *E. multilocularis* infection; and to explore how FGL2 is secreted due to *E. multilocularis* infection

3. Models and Methods used in the thesis work

3.1 *In vivo* and *in vitro* models used in this thesis work

Primary infection (peroral) mouse model

An established mouse model of primary alveolar echinococcosis was used as previously described (Siles-Lucas, 2003; Pater, 1998). Briefly, 8-weeks-old female C57BL6/J mice were infected (n = 10) at the age of 10 weeks by peroral inoculation with 100 mL sterile water containing 2×10^3 eggs of *E. multilocularis*, using appropriate biosafety level 3 laboratory conditions (Swiss biosafety approval number A990006/3A). The infecting organisms (parasite eggs) were initially isolated from a naturally infected fox. Egg viability and infection potential were pre-evaluated upon explorative titrated infection experiments carried out in mice preliminarily to the present studies (Gauci, 2002). Mock-infected control animals (n=5) were perorally inoculated with 100 mL of sterile water. Animals were sacrificed with an overdose of pentobarbital (100 mg/kg, intraperitoneally) for the mock-infected control group (n = 5) and for the group representing the chronic stage of primary AE (n = 10).

Intra-hepatic infection mouse model

Pathogen-free female BALB/c mice (8–10-week old) were housed in cages with a 12-h light/dark cycle and provided with rodent chow and water. BALB/c mice were infected by *E. multilocularis* and tissue samples were collected and detected as previously described (Lin *et al.* 2010; Zhang *et al*. 2011). For each autopsy time-point, ten experimentally infected mice were used in *E. multilocularis* group (n=10) and compared with five control mice (n=5), which received an intra-hepatic injection of 0.1 mL of saline in the anterior liver lobe using the same surgical procedure.

Intraperitoneal infection mouse model

The parasite used in this study was a cloned *E. multilocularis* (KF5) isolate maintained by serial passages (vegetative transfer) in C57BL/6 mice (Gottstein *et al.* 1992). Metacestode tissue was obtained from infected mice by aseptic removal from the peritoneal cavity. After grinding the tissue through a sterile 50 μm sieve, 100 freshly prepared acephalic vesicular cysts were suspended in 100 μL RPMI-1640 (Gibco, Basel, Switzerland) and injected intraperitoneally. Each experimental group included 6 animals unless otherwise stated. Control mice (mock-infection) received 100μL of RPMI-1640 only.

3.2 Laboratory methods used in this thesis work

Microarray data analyses and annotation of gene function

RNA extracts from both infected and control mice were selected for array hybridization after intra-hepatic infection. Total RNA was purified with NucleospinH RNA Clean-up Kit (Macherey-Nagel, Germany) and each purified RNA sample isolated from an individual sample was run on a single microarray. All microarray procedures were done according to a previously described procedure (Lin *et al.* 2011).

Quantitative real-time RT-PCR

qRT-PCR was run in a thermocycler (iQ5 Bio-Rad, Hercules, CA, USA) with the SYBR Green PCR premix (Qiagen, Hilden, Germany) following the manufacturer's instructions. To normalize for gene expression, mRNA expression of the housekeeping gene β-actin was measured in parallel. Fluorescence was measured in every cycle, and a melting curve was analyzed after the PCR by increasing the temperature from 55 to 95 °C (0.5 °C increments). A defined single peak was obtained for all amplicons, confirming the specificity of the amplification.

Immunohistochemistry analysis

Immunohistochemistry was performed on formalin-fixed, paraffin-embedded tissue. Briefly, 4 μm tissue sections were de-paraffinized in xylene and rehydrated in gradual dilutions of ethanol. Endogenous peroxidase was blocked with 3% hydrogen peroxide. Sections were pretreated by microwave heating for 15 min in antigen unmasking solution to increase staining, and were incubated with non-immune goat serum for 30 min to block non-specific background. Sections were then incubated overnight at 4℃ with the primary antibody and subsequently with horseradish peroxidase conjugated host-specific secondary antibodies, 3, 3'-diaminobenzidine was used as chromogen. Sections were counterstained with hematoxylin for 5 min, dehydrated, and covered with slips. For all samples, negative controls consisted of substitution of the isotype-matched primary antibody with PBS.

Western Blot analysis

Western Blot analysis of cell lysates was performed by SDS-PAGE using NuPAGE followed by transfer to nitrocellulose membrane. The appropriate antibodies and GAPDH were detected with Western Breeze Kit (Invitrogen, California, USA). The expression levels of respective proteins (in "relative units") were quantified using Quantity One software.

Flow cytometry

After blocking non-specific binding of antibodies to the FcγIII and FcγII receptors with 1 μg of purified anti-CD16/CD32 for 20 min in the dark, the cells were stained with surface maker separately for 15 min with 1 μg of primary antibodies. For intracellular staining, after surface maker staining, the cells were first fixed for 20mins at room temperature, and then stained with PE-labeled cytokine antibodies in Inside Perm for 15mins. The corresponding primary labeled isotype control antibodies were used for staining controls. Stained cells were analyzed in a flow cytometer (Becton Dickinson, Heidelberg, Germany) using the corresponding CELL QUEST software.

Sandwich Enzyme-Linked Immunosorbent Assay

After washing of pre-coated plates 3 times with Tris-Tween buffered saline, serum samples (50 μL) were added to each well, and after a 2-hour incubation at room

temperature and three washes with Tris-Tween buffered saline, the wells were incubated with mouse FGL2 detection antibody for 1 hour at room temperature. The plate was washed again for 3 times, and polyclonal anti-FGL2 binding was detected with a secondary horseradish peroxidase-conjugated anti-rabbit antibody. Tetramethlybenzidine was then added and absorbance was measured at 450 nm using an enzyme linked immunosorbent assay (ELISA) plate reader.

Luminex assay for cytokine expression in the serum

Cytokine levels in mouse serum samples were assessed undiluted using microsphere-based multiplex assays (MILLIPLEX® MAP Mouse Cytokine/Chemokine Multiplex Assays MPXMCYTO-70K, Merck Millipore, Zug, Switzerland) according to the manufacturer's instructions. Serum concentrations of selected cytokines were measured. A minimum of 50 beads per analyte was measured on a Bioplex-200 platform (Bio-Rad, Hercules, CA, USA). Calibration was performed using BioPlex Manager software version 4.1.1 by linear regression analysis using the four lowest standards provided by the manufacturer. When measured cytokine concentrations were below the detection limit, a value corresponding to the detection limit of the assay was used for statistical analysis (Table 3.1 and Figure 3.6).

Table 3.1 Laboratory methods used in the thesis work

Method	Aim	Reference
Microarray analyses	To screen the changed immune related genes	Wang, 2013
qRT-PCR	To further study the mRNA levels of target genes, i.e. key cell cycle genes, Th1/2/17/Treg related cytokines and chemokines, TGF-β and Smad genes	Zhang, 2012, Wang, 2013
Immunohistochemistry	To locate and semi-quantify the target proteins in the cells, i.e. key cell cycle and apoptosis proteins, TGF-β and Smads, liver fibrosis makers	Zhang, 2012, Wang, 2013
Western Blot	To semi-quantify the target protein in the cells, i.e. key cell cycle and apoptosis proteins, TGF-β and Smads	Zhang, 2012, Wang, 2013
Flow cytometry	Cell counting, target protein detection and cell sorting, i.e. different cytokine expression in $CD4^+$ T cells, maturation of DCs, $CD4^+CD25^+$ Treg isolation	Wang 2014

ELISA	To detect the serum level of FGL2	FGL2 paper
Luminex	To detect the serum levels of selected cytokines, i.e. IFN-γ, IL-4, IL-17A, IL-10, IL-1β, IL-6	FGL2 paper
Suppression assay	To study the suppression function of Treg on effector T cell proliferation, i.e. $CD4^+CD25^+$ Treg from WT mice and fgl2-/- mice co-cultured with effector T cells	FGL2 paper

3.3 Statistical analysis methods

All the data were analyzed by SPSS 17.0. The results were presented as means ± SD. One-way ANOVA and Student's *t*-test were used to compare the differences between groups, and Spearman's rho was used to analyze the correlation coefficient. $P<0.05$ was considered to indicate statistical significance.

Figure 3.6 *E. multilocularis* Infection models used in the thesis work

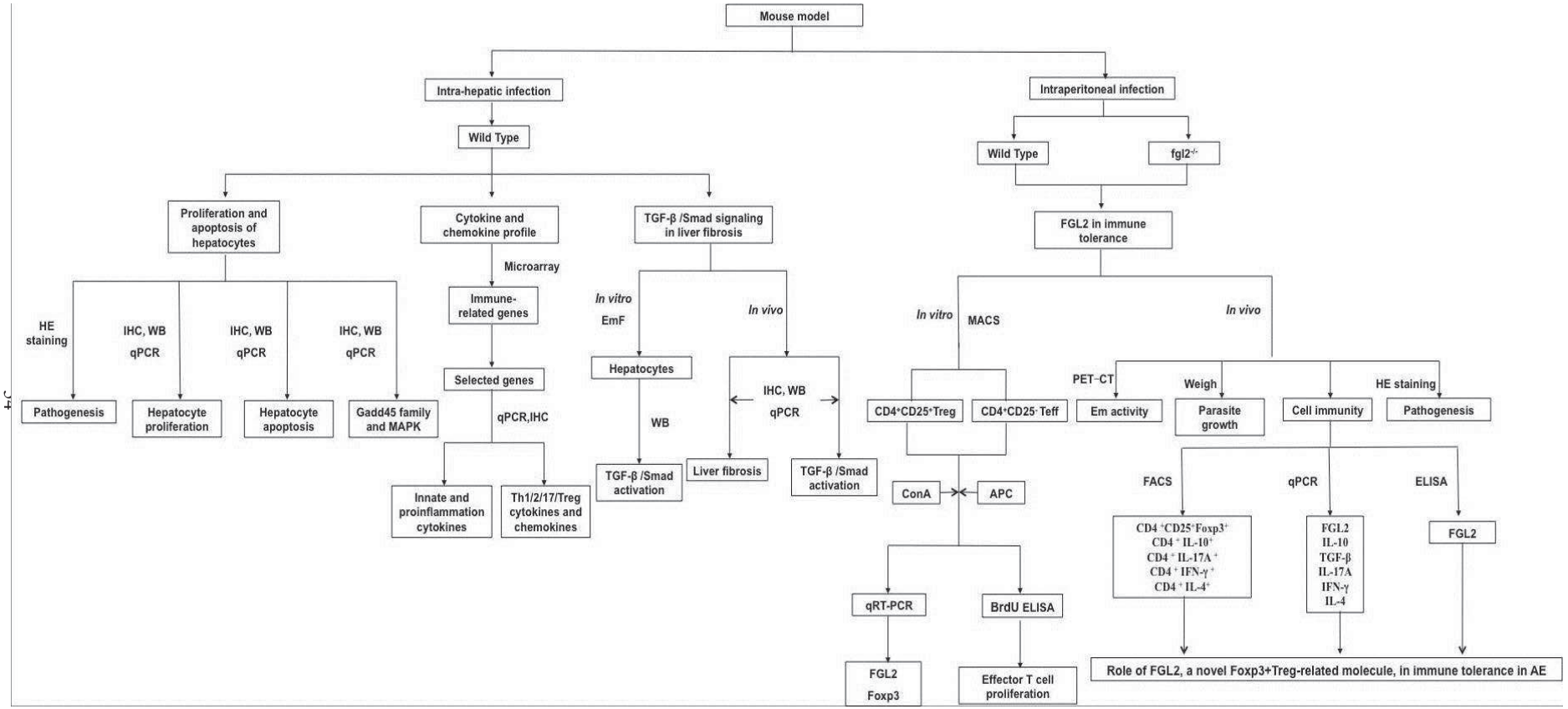

4. Has *E.multilocularis* any influence on host's liver homeostasis, and especially on liver proliferation/apoptosis?

To address this question, we employed the intra-hepatic AE mouse model and measured the levels of MAPKs activation, Cyclins, PCNA, Gadd45b, Gadd45c, p53 and p21 expression from day 2 to 360 post-infection by western blot and qPCR and, using immunohistochemistry we studied the same components in relation to the pathological changes in the liver, both in the infection site and in the neighboring liver parenchyma where proteins and mRNAs were measured.

Background and objectives:

AE is characterized by an infiltrative, destructive and tumor- like growth of the *E. multilocularis* metacestode, usually affecting the liver of natural intermediate hosts such as small rodents or the human liver. Clinical manifestations are results of both a slow but continuous asexual proliferation of the metacestode and an intense infiltration by macrophages, T lymphocytes, and fibroblasts/myofibroblasts around the parasite, eventually leading to fibrosis and necrosis. A striking clinical observation in AE patients is also the hepatomegaly observed in the liver lobe/segments that are not invaded by the parasite; such liver regeneration, which allows surgeons to perform extensive liver resections (Wen *et al.* 2011; Mantion & Vuitton, 2011), is partly explained by the portal vein obstruction; a direct influence of *E. multilocularis* and associated immune reaction has never been considered. Very little is known on the influence of helminth parasites which develop in the liver on the proliferation/growth arrest metabolic pathways in the hepatocytes of the infected liver over the various stages of infection. The aims of the present study were 1) to explore the influence of *E. multilocularis* metacestode on components of cell cycle regulation which characterize the host's hepatic proliferation in the liver of mice infected with *E. multilocularis*; 2) to simultaneously explore the activation of inhibitory proteins involved in growth arrest/apoptosis metabolic pathways during the 3 stages of infection.

OPEN ACCESS Freely available online

PLoS one

Hepatocyte Proliferation/Growth Arrest Balance in the Liver of Mice during *E. multilocularis* Infection: A Coordinated 3-Stage Course

Chuanshan Zhang[1], Junhua Wang[1], Guodong Lü[1], Jing Li[1], Xiaomei Lu[1], Georges Mantion[2], Dominique A. Vuitton[2,3], Hao Wen[1]*, Renyong Lin[1]*

1 State Key Laboratory Incubation Base of Major Diseases in Xinjiang and Xinjiang Key Laboratory of Echinococcosis, First Affiliated Hospital of Xinjiang Medical University, Urumqi, Xinjiang, China, **2** World Health Organization-Collaborating Centre for the Prevention and Treatment of Human Echinococcosis, Department of Digestive Surgery; Jean Minjoz Hospital, University of Franche-Comté and University Hospital, Besançon, France, **3** Research Unit EA 3181 "Epithelial Carcinogenesis: Predictive and Prognostic Factors," University of Franche-Comté, Besançon, France

Abstract

Background: Alveolar echinococcosis (AE) is characterized by the tumor-like growth of *Echinococcus* (*E.*) *multilocularis*. Very little is known on the influence of helminth parasites which develop in the liver on the proliferation/growth arrest metabolic pathways in the hepatocytes of the infected liver over the various stages of infection.

Methodology/Principal Findings: Using Western blot analysis, qPCR and immunohistochemistry, we measured the levels of MAPKs activation, Cyclins, PCNA, Gadd45β, Gadd45γ, p53 and p21 expression in the murine AE model, from day 2 to 360 post-infection. Within the early (day 2–60) and middle (day60–180) stages, CyclinB1 and CyclinD1 gene expression increased up to day30 and then returned to control level after day60; Gadd45β, CyclinA and PCNA increased all over the period; ERK1/2 was permanently activated. Meanwhile, p53, p21 and Gadd45γ gene expression, and caspase 3 activation, gradually increased in a time-dependent manner. In the late stage (day180–360), p53, p21 and Gadd45γ gene expression were significantly higher in infected mice; JNK and caspase 3 were activated. TUNEL analysis showed apoptosis of hepatocytes. No significant change in CyclinE, p53 mRNA and p-p38 expression were observed at any time.

Conclusions: Our data support the concept of a sequential activation of metabolic pathways which 1) would first favor parasitic, liver and immune cell proliferation and survival, and thus promote metacestode fertility and tolerance by the host, and 2) would then favor liver damage/apoptosis, impairment in protein synthesis and xenobiotic metabolism, as well as promote immune deficiency, and thus contribute to the dissemination of the protoscoleces after metacestode fertility has been acquired. These findings give a rational explanation to the clinical observations of hepatomegaly and of unexpected survival of AE patients after major hepatic resections, and of chronic liver injury, necrosis and of hepatic failure at an advanced stage and in experimental animals.

Citation: Zhang C, Wang J, Lü G, Li J, Lu X, et al. (2012) Hepatocyte Proliferation/Growth Arrest Balance in the Liver of Mice during *E. multilocularis* Infection: A Coordinated 3-Stage Course. PLoS ONE 7(1): e30127. doi:10.1371/journal.pone.0030127

Editor: David Joseph Diemert, The George Washington University Medical Center, United States of America

Received August 17, 2011; **Accepted** December 12, 2011; **Published** January 10, 2012

Funding: This work was supported by grants from the National Natural Science Foundation of China (30860253, 30960341) and Xinjiang Natural Science fund (201091154, 200810104). The funders had no role in study design, data collection and analysis, decision to publish, or preparation of the manuscript.

Competing Interests: The authors have declared that no competing interests exist.

* E-mail: renyongl@yahoo.com.cn (RL); Dr.wenhao@163.com (HW)

Introduction

The larval stage of the fox-tapeworm *Echinococcus* (*E.*) *multilocularis* is the causative agent of alveolar echinococcosis (AE), one of the most dangerous parasitic disease of the northern hemisphere [1]. AE is characterized by an infiltrative, destructive and tumor-like growth of the *E. multilocularis* metacestode, usually affecting the liver of natural intermediate hosts such as small rodents or the human liver [2]. Clinical manifestations are results of both a slow but continuous asexual proliferation of the metacestode and an intense infiltration by macrophages, T lymphocytes, and fibroblasts/myofibroblasts around the parasite, eventually leading to fibrosis and necrosis [3,4,5,6]. Clinical symptoms usually appear many years after the first contact with the parasite eggs (oncospheres); progression of the lesions is very slow and the observed complications and liver dysfunction are the result of a complex and often latent sequence of events. In the experimental model of secondary *E. multilocularis* metacestode infection, which well mimics the natural infection [7,8], according to its clinical course AE is divided into 1) an early stage with tumor-like growth of the metacestode and mild hepatic enlargement, 2) a middle stage with invasive parasitic lesions and progressive hepatomegaly and 3) an advanced/terminal stage (also called "late stage") associated with invasion of other organs and/or metastases, fibrosis of the lesions and cholestasis, which may cause secondary liver cirrhosis with subsequent portal hypertension and eventually impaired liver function [9]. We and others have shown in previous studies that these clinical changes were accompanied by a typical

course of cytokine production, with, sequentially 1) a Th1 profile followed by 2) a combined Th1 and Th2 profile, also characterized by a markedly increased production of IL-10 [10], and finally 3) a decrease in all types of cytokines associated with a deep impairment of the immune response [11,12]. Changes with time in a variety of other components/enzymes involved in the immune response such as chemokines [13], proteins of the acute inflammatory phase [14], and nitric oxide synthase [15] have also been shown. However, despite the presence of well-known clinical symptoms (hepatomegaly, liver necrosis) which evoked such influence in patients with AE, until recently, little was known on the influence of the metacestode on the hepatocytes of the surrounding liver parenchyma.

The orderly progression of cells through the phases of the cell cycle is governed by the sequential assembly and activation of holoenzyme complexes [16]. The Mitogen-Activated Protein Kinase (MAPK) pathway and cell cycle regulatory proteins, including Cyclins, Cyclin-dependent kinases (Cdks), Cyclin-dependent kinase inhibitor 1α (Cdkn1α or p21), growth arrest and DNA damage-inducible 45(Gadd45α, Gadd45β and Gadd45γ), participate in the regulation of cell cycle progression [17,18,19,20]. Importantly, CyclinD1, a regulator of cellular proliferation, is itself regulated by ERK1/2 [21,22]. The Cip/Kip family member, p21 was shown to inhibit cell proliferation and activities of several Cyclin-Cdk complexes *in vitro* [23,24]. Transcriptional regulation of the p21 gene is controlled by the tumor suppressor protein p53 acting on the p53 responsive element in the distal region of the p21 promoter in response to intracellular signals such as DNA damage [25,26]. Furthermore, Gadd45γ is also a p53-regulated human gene, which interacts with PCNA, a normal component of multiple quaternary complexes, including the Cycling Cdks and the Cdk inhibitor p21, which play a central role in DNA repair, growth suppression and apoptosis [27,28,29]. In addition, the JNK and p38 cascades appear to be pro-apoptotic. Their activation, via MTK1/MEKK4, is mediated by Gadd45γ as was shown in response to various external stresses including bacterial infection, hyperosmolarity, and UV irradiation; these cascades also appear to be closely related to cell death [30,31,32].

Our previous study, using western blot technique, has shown that metabolic pathways involved in liver proliferation and growth arrest and especially the MAPKs system were specifically induced by *E. multilocularis* growth. We observed that ERK1/2 and p38 were activated in the liver of AE patients and that ERK, JNK and p38 were activated in rat primary hepatocytes during exposure to *E. multilocularis* vesicle fluid (EmF) or *E. multilocularis* axenic culture supernatant (EmCM) *in vitro* [33]. Furthermore, using microarray and qPCR technique, we followed the time-course of *E. multilocularis* infection from day30 to 180 after intrahepatic injection of metacestode for the expression of genes involved in the inflammatory/immune response as well as numerous metabolic pathways specific to the liver. We found an increased expression of Gadd45β (2.19 fold at day90; 4.49 fold at day180), Gadd45γ (3.98 fold at day60; 4.92 fold at day90 and 21.94 fold at day180) and p21 (5.60 fold at day60; 4.42 fold at day180) in the middle and late stages of *E. multilocularis* infection in mice [34]. Gadd45β gene was originally characterized as a primary responder in myeloid differentiation induced by IL-6 [35]. More recent studies have shown that Gadd45β, unlike two other homologs (Gadd45α and γ), plays an anti-apoptotic role and is activated by TNF-α via NFκB [19]. Thus, induction of Gadd45β coincides with the entry into an active cell cycle; its action might be to protect hepatocytes from apoptosis in the middle stage. Then induction of p21 and Gadd45γ coincides with the entry into an inhibitory phase regarding cell proliferation; its action might be to promote hepatocyte growth arrest and/or apoptosis in the late stage. However, the underlying mechanisms for the involvement of the host liver MAPK signaling pathways, and of cell cycle regulated proteins such as Cyclins, Gadd45β, p53, p21 and Gadd45γ in the progression of *E. multilocularis*-infected mice *in vivo* are unknown to date. Their contribution to the hepatocyte proliferation and growth arrest process which appears to accompany *E. multilocularis* metacestode development is also ignored.

The aims of the present study were thus, in the secondary experimental murine model of AE, 1) to explore the influence of *E. multilocularis* metacestode on components of cell cycle regulation which characterize the host's hepatic proliferation in the liver of mice infected with *E. multilocularis* over a time period of 1yr, i.e. from the date of *E. multilocularis* inoculation to the very late stage of infection; 2) to simultaneously explore the activation of inhibitory proteins involved in growth arrest/apoptosis metabolic pathways during the 3 stages of infection. For these purposes, we measured the levels of ERK1/2, JNK, p38 activation, Cyclins, PCNA, Gadd45β, Gadd45γ, p53 and p21 by western blot and qPCR and, using immunohistochemistry we studied the same components in relation to the pathological changes in the liver, both in the infection site and in the neighboring liver parenchyma where proteins and mRNAs were measured.

Results

Hepatic injury induced by *E. multilocularis*

As shown in Figure 1, from day30 to 180 post-infection, the typical pathological changes which characterize *E. multilocularis* lesions were observed in the liver of the mice infected with *E. multilocularis*; at days 2 and 8, only infiltrating lymphocytes, surrounding *E. multilocularis* inoculum, could be observed; at days 270 and 360 post-infection, the pseudo-tumor parasitic mass included many vesicular and/or cystic structures embedded within thick fibrous tissue, the periparasitic area was composed of inflammatory fibrous tissue and necrotic areas and mixed with small granulomatous nodules [34]. The hepatic parenchyma close to the lesions was progressively invaded by fibrous connective tissue septa, and solitary islands of hepatic tissue were observed. At the same time points, no hepatic injury was observed in the mice of the control groups (Figure 1).

Activation of MAPKs in the liver of mice during *E. multilocularis* infection

As shown in Figure 2A and 2B, western blotting showed increased ERK1/2 phosphorylation (p-ERK1/2) from day2 (~1.40-fold) to 360(~2.78-fold); it peaked at day180 (~5.69-fold); there was a significant difference between *E. multilocularis* infected and non-infected mice at day90 post-infection ($P < 0.05$), and increased JNK phosphorylation (p-JNK) from day180 (~1.89-fold) to 360 (~1.85-fold); it peaked at day270 (~2.19-fold) post-infection; it was significantly different between *E. multilocularis*-infected and non-infected mice at all time points since day180 ($P < 0.05$). Interestingly, no phosphorylated-p38 (p-p38) was observed in liver during the course of infection. As shown in Figure 2C, in the lesion area, p-ERK1/2 was expressed in a few hepatocytes at days 2 and 8 while there was no positive staining in the inflammatory response zone. At days 30 and 60 the intensity of the immunostaining increased, showing p-ERK1/2 localization in infiltrating lymphocytes and fibroblast-like cells. At days 90, 180 and 270, the staining was more intense in the infiltrating lymphocytes, and then decreased at day360. Within the liver parenchyma close to the lesion and peri-parasitic infiltrate, p-

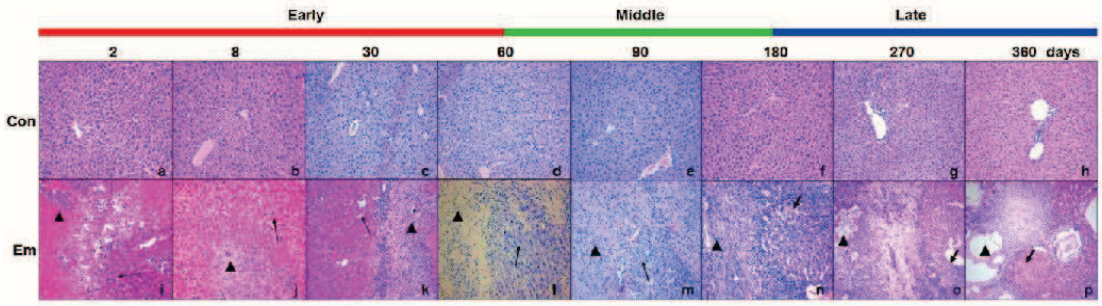

Figure 1. Representative histopathology of mice liver during *E. multilocularis* infection. (a–h): No morphological changes were observed in the liver of control mice. (i–p): Proliferating hepatocytes close to the parasitic lesions were observed from days 2 to 180 (*thin arrow*) and some coagulation necrosis areas (*thick arrow*) close to the parasitic lesions were observed from days 180 to 360 in the liver from *E. multilocularis* infected mice. The *arrowheads* indicate the parasitic lesions in the liver of infected mice ("lesion" row); the lesions had the typical aspect of *E. multilocularis* germinal layer and laminated layer, surrounded by a periparasitic cell infiltrate composed mostly, from the center to the periphery, of macrophages and fibroblasts/myofibroblasts, and lymphocytes. Final magnification, 200×. con, control, non-infected mice; Em, *E. multilocularis* infected mice.
doi:10.1371/journal.pone.0030127.g001

ERK1/2 was observed in hepatocytes from day2 to 60. At days 90 and 180, the number of hepatocytes which expressed p-ERK1/2 progressively increased, with staining intensities from "weak" to "moderate"; then p-ERK1/2 expression in hepatocytes decreased at day360. No liver cell positive for p-ERK1/2 immunostaining were observed in the liver of non-infected mice.

Expression of Gadd45β in the liver of mice during *E. multilocularis* infection

As shown in Figure 3A and 3B, western blotting showed increased Gadd45β expression from day60 (~1.75-fold) to 360 (~2.52-fold); it peaked at day180 (~62.64-fold) post-infection; there was a significant difference between *E. multilocularis*-infected and non-infected mice at days 60 and 180 ($P < 0.05$). Gadd45β mRNA expression was increased from day2 (~1.27-fold) to 360 (~1.81-fold); it peaked at day 90 (~3.28-fold) post-infection (Figure 3C). There was a significant difference between *E. multilocularis* infected and non-infected mice at days 60 and 90 ($P < 0.05$). At day8, Gadd45β expression was observed in infiltrating lymphocytes; it progressively increased in fibroblast-like cells and infiltrating lymphocytes from day30 to 180 (Figure 3D). Within the liver parenchyma close to the lesion and peri-parasitic infiltrate, Gadd45β expression was observed in hepatocytes around the portal and central veins at day30; it markedly increased at days 90 and 180 post-infection, with staining intensities from "moderate" to "strong"; then Gadd45β expression in hepatocytes mildly decreased at days 270 and 360. No liver cell positive for Gadd45β was observed in the livers of non-infected mice.

Expression of Cyclins A, B1, D1 and E in the liver of mice during *E. multilocularis* infection

As shown in Figure 4A and 4B, western blotting showed increased Cyclin A expression from day2 (~1.52-fold) to 270 (~1.63-fold); it peaked at day60 (~8.46-fold), and then decreased under the baseline at day360 (~0.86-fold) post-infection. There was a significant difference between *E. multilocularis* infected and non-infected mice at days 8, 30, 60, 90 and 180 ($P < 0.05$). Increased Cyclin B1 expression was observed at days 2 (~6.53-fold) and 8 (~3.71-fold); it then decreased to the baseline from day 30 to 360 post-infection. There was a significant difference between *E. multilocularis* infected and non-infected mice at days 2 and 8 ($P < 0.05$). Increased Cyclin D1 expression was observed at days 8 (~2.07-fold) and 30 (~1.41-fold); it then decreased under the baseline from day60 to 360 post-infection. There was a significant difference between *E. multilocularis* infected and non-infected mice at days 8 and 30 ($P < 0.05$). Mild increase in Cyclin E expression was observed from day 2 (~1.44-fold) to 180 (~1.30-fold), but no significant difference was found during the whole time-points ($P > 0.05$).

Cyclin A mRNA expression was increased from day2 (~1.62-fold) to 180 (~1.35-fold) and then decreased under the baseline at days 270 and 360; it peaked at day30 (~2.65-fold) post-infection (Figure 4C). There was a significant difference between *E. multilocularis* infected and non-infected mice at day30 ($P < 0.05$). Cyclin B1 mRNA expression was increased at day 2 (~2.17-fold); it then decreased to the baseline from day30 to 360 post-infection. However, there was no significant difference between *E. multilocularis* infected and non-infected mice ($P > 0.05$). Cyclin D1 mRNA expression was increased from day2 (~1.41-fold) to 30 (~2.34-fold); then it decreased under the baseline from day 60 to 360 post-infection. There was a significant difference between *E. multilocularis* infected and non-infected mice at day8 ($P < 0.05$). Cyclin E mRNA expression was mildly increased at days 2 (~1.30-fold), 8 (~1.25-fold) and 180 (~1.64-fold), but no significant difference was found during the whole course of infection ($P > 0.05$).

Expression of PCNA in the liver of mice during *E. multilocularis* infection

As shown in Figure 5A and 5B, western blotting showed increased PCNA expression from day8 (~1.49-fold) to 180 (~2.52-fold) which peaked at day90 (~2.54-fold) post-infection; it then decreased to the baseline at days 270 (~1.33-fold) and 360 (~1.19-fold). There was a significant difference between *E. multilocularis*-infected and non-infected mice at days 30, 60, 90 and 180 ($P < 0.05$). PCNA mRNA expression was increased from day8 (~2.06-fold) to day90 (~3.74-fold); it peaked at day90 (Figure 5C), then decreased to the baseline from day180 to 360. There was a significant difference between *E. multilocularis* infected and non-infected mice at days 8, 60 and 90 post-infection ($P < 0.05$). As shown in Figure 5D, immunohistochemistry showed an increased expression of PCNA in the hepatocytes of *E. multilocularis* infected and non-infected mice at days 2 and 8, then no PCNA expression was observed in the liver of non-infected mice; increased expression of PCNA was observed since day 8 until day180 in infected mice.

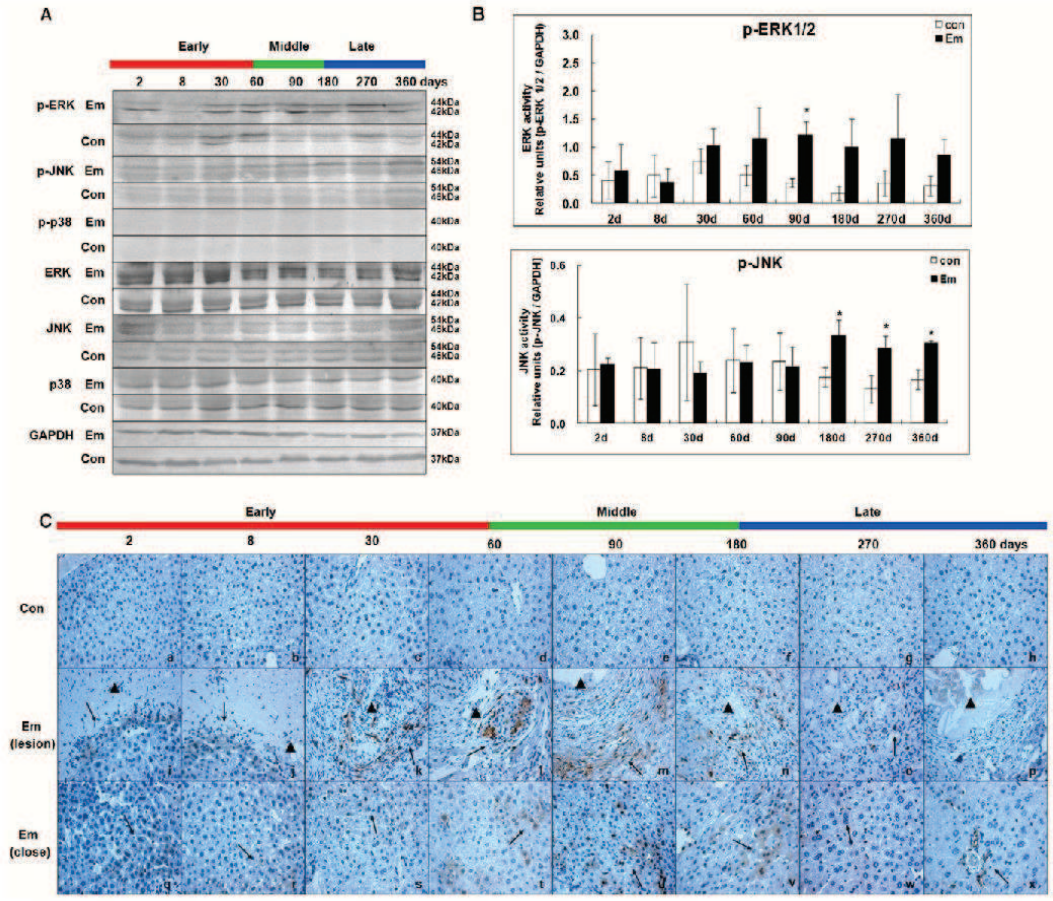

Figure 2. Activation of MAPKs in the liver of mice during *E. multilocularis* infection. Western blot analyses were performed on lysates from liver samples with antibodies that recognize phosphorylated (p-) and total ERK1/2, JNK and p38 respectively (A). Relative amount of phosphorylated and total ERK1/2, JNK and p38 was calculated from semi-quantitative analysis of the Western blots using densitometry (B). Histo-immunochemical analysis of p-ERK1/2 expression was performed on tissue samples: p-ERK1/2 expression was observed in infiltrating lymphocytes (lesion) and fibroblast-like cells (lesion) but also in hepatic cells (close to lesion) in the liver from *E. multilocularis* infected mice (*arrow*) (C). The *arrowheads* indicate the parasitic lesions in the liver of infected mice ("lesion" row). Final magnification, 400×. $^{*}P<0.05$ versus control. con, control, non-infected mice; Em, *E. multilocularis* infected mice; AU: arbitrary units; lesion: *E. multilocularis* metacestode and surrounding immune infiltrate; close: liver parenchyma close to *E. multilocularis* lesion.
doi:10.1371/journal.pone.0030127.g002

Expression of p53 in the liver of mice during *E. multilocularis* infection

As shown in Figure 6A and 6B, western blotting showed increased p53 expression at days 60 (~2.63-fold), 90 (~4.11-fold), 270 (~3.13-fold) and 360 (~2.77-fold); it peaked at day360 post-infection. There was a significant difference between *E. multilocularis*-infected and non-infected mice at days 90, 270 and 360 ($P < 0.05$). As shown in Figure 6C, no significant change of p53 mRNA expression was observed at any time-point.

Expression of p21 in the liver of mice during *E. multilocularis* infection

As shown in Figure 7A and 7B, western blotting showed increased p21 expression from day60 (~1.84-fold) to 360 (~8.15-fold); it peaked at day360 post-infection. The difference between *E. multilocularis*-infected and non-infected mice was significant at days 180, 270 and 360 ($P < 0.05$). As shown in Figure 7C, p21 mRNA expression, despite its increase from day30 (~3.21-fold) to 360 (~4.06-fold), was significantly different from that measured in non-infected mice when it peaked at day270 post-infection (~9.01-fold) ($P < 0.05$). As shown in Figure 7D, in the lesion area, p21 expression was observed in infiltrating lymphocytes and fibroblast-like cells at day180; it progressively increased from day270 to 360. Within the liver parenchyma close to the lesion and peri-parasitic infiltrate, p21 expression was observed in hepatocytes close to the lesion at day180. A marked increase in the liver cell expression of p21 was observed at days 270 and 360 post-infection, with staining intensities from "weak" to "moderate".

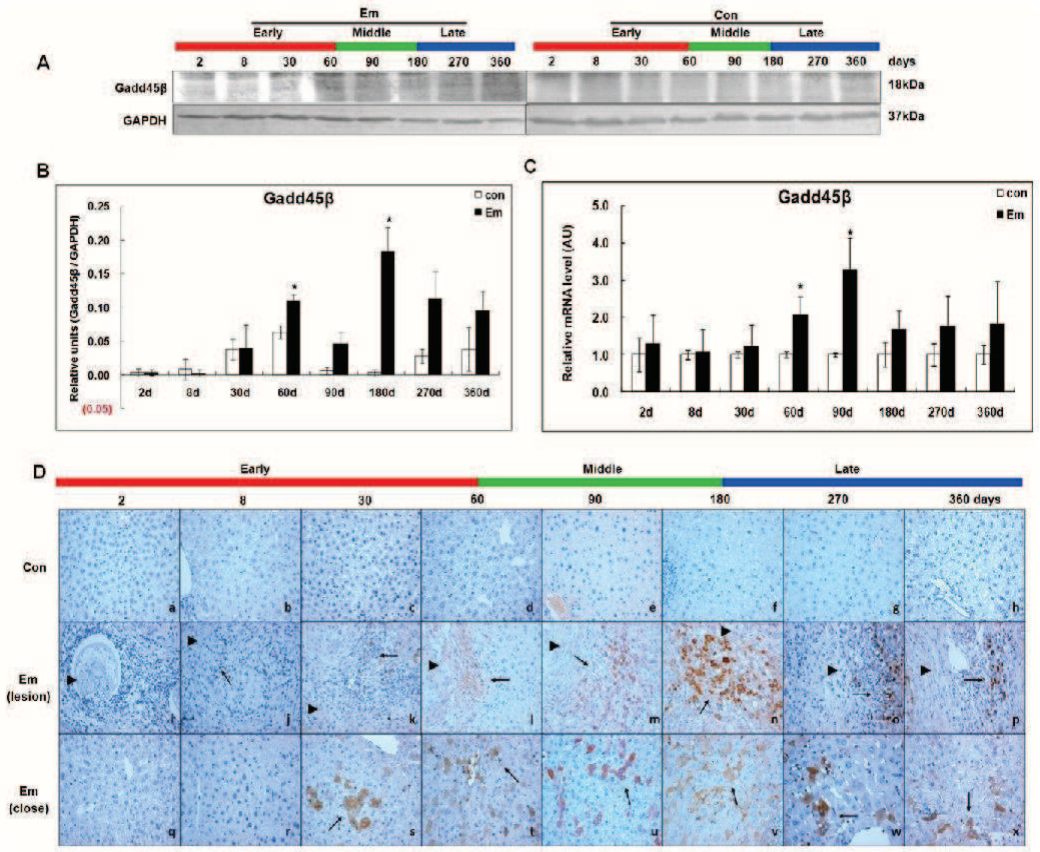

Figure 3. Gadd45β expression in the liver of mice during *E. multilocularis* infection. Western blot analyses were performed on lysates from liver samples with antibodies that recognize Gadd45β (A). Relative amount of Gadd45β expression was calculated from semi-quantitative analysis of the Western blots using densitometry (B). Gadd45β mRNA expression was measured by qPCR (C). Histo-immunochemical analysis of Gadd45β expression was performed on tissue samples: Gadd45β expression was observed in infiltrating lymphocytes (lesion) but also in hepatic cells (close to lesion) in the liver from *E. multilocularis* infected mice by histo-immunochemical analysis (*arrow*) (D). The *arrowheads* indicate the parasitic lesions in the liver of infected mice ("lesion" row). Final magnification, 400×. $^{*}P<0.05$ versus control. con, control, non-infected mice; Em, *E. multilocularis* infected mice; AU: arbitrary units; lesion: *E. multilocularis* metacestode and surrounding immune infiltrate; close: liver parenchyma close to *E. multilocularis* lesion.
doi:10.1371/journal.pone.0030127.g003

Expression of Gadd45γ in the liver of mice during *E. multilocularis* infection

As shown in Figure 8A, before day60, Gadd45γ mRNA expression was unchanged; it then increased from day60 (~3.23-fold) to 360 (~3.47-fold) and peaked at day180 (~7.86-fold) post-infection; it was significantly different between *E. multilocularis*-infected and non-infected mice at days 180 and 360 post-infection ($P < 0.05$). As shown in Figure 8B, Gadd45γ expression was observed in periparasitic infiltrating lymphocytes at day180; it increased inside the lesion at days 270 and 360. Within the liver parenchyma close to the lesion and periparasitic infiltrate, Gadd45γ expression was observed at day90 and markedly increased at days 180, 270 and 360 post-infection, with staining intensities from "moderate" to "strong". No liver cell positive for Gadd45γ was observed in the livers of non-infected mice.

Activation of caspase 3 in the liver of mice during *E. multilocularis* infection

Caspase 3 activation, a marker of the apoptotic protease cascade, was measured by western blotting, qPCR and immunohistochemistry. As shown in Figure 9A which shows immunoblotting with anti-caspase 3 (35kDα) and anti-cleaved caspase 3 (17 and 19kDα), cleaved caspase 3 was significantly increased at days 90, 270 and 360 post-infection. As shown in Figure 9B, before day60, caspase 3 mRNA level was unchanged; it then increased from day60 (~1.43-fold) to 270 (~2.98-fold), peaked at day90 (~3.70-fold), and decreased to the baseline at day360. There was a significant difference between *E. multilocularis*-infected and non-infected mice at day180 post-infection ($P < 0.01$). As shown in Figure 9C, in the periparasitic infiltrate, caspase 3 and cleaved-caspase 3 expression were observed in the lymphocytes at day90; it then increased inside the lesion from day180 to 360. Within the

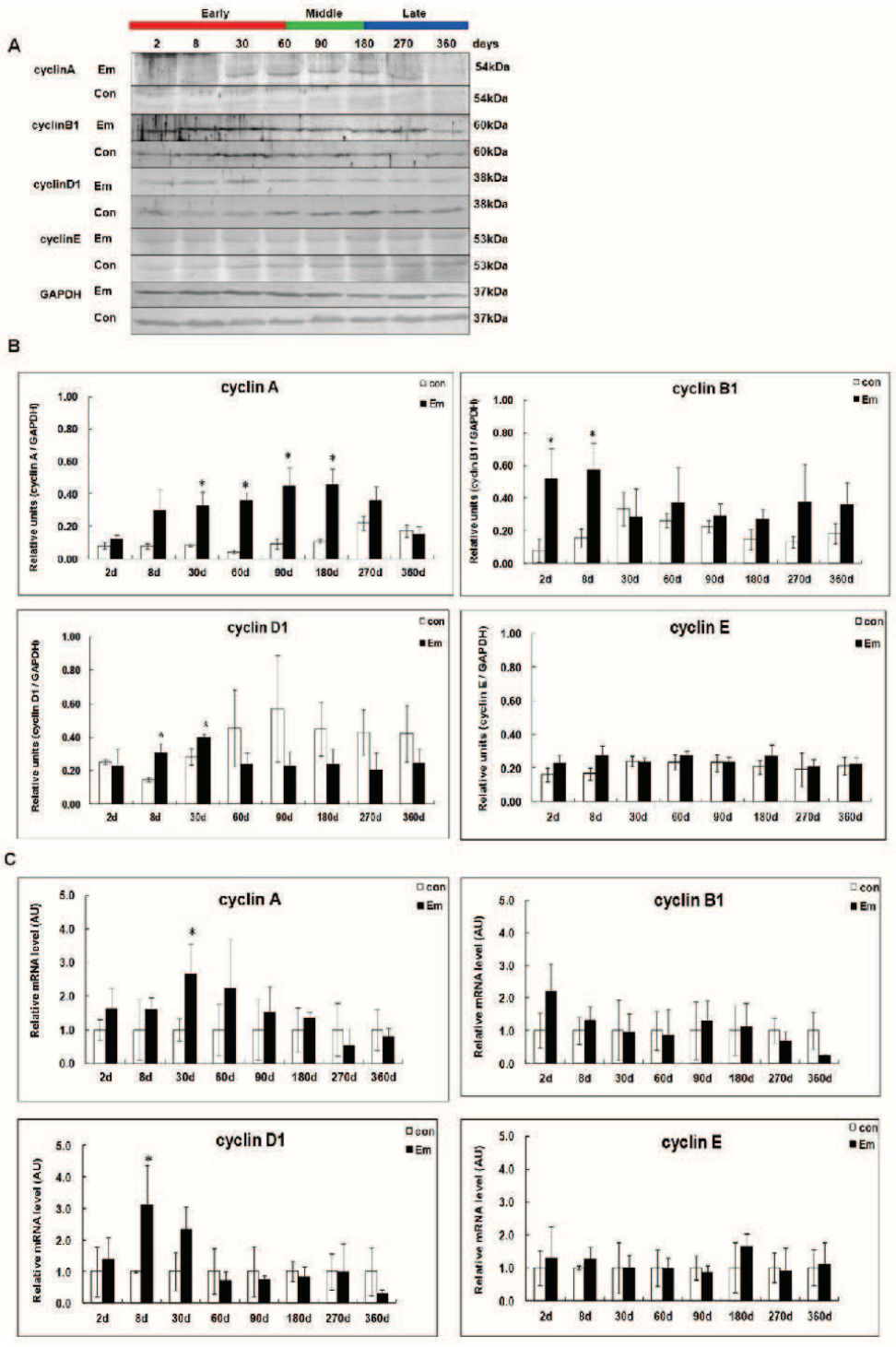
A
Early
Middle
Late
2 8 30 60 90 180 270 360 days
cyclinA Em 54kDa
Con 54kDa
cyclinB1 Em 60kDa
Con 60kDa
cyclinD1 Em 38kDa
Con 38kDa
cyclinE Em 53kDa
Con 53kDa
GAPDH Em 37kDa
Con 37kDa
B
cyclin A
cyclin B1
cyclin D1
cyclin E
Relative units (cyclin A / GAPDH)
Relative units (cyclin B1/ GAPDH)
Relative units (cyclin D1 / GAPDH)
Relative units (cyclin E / GAPDH)
con
Em
2d 8d 30d 60d 90d 180d 270d 360d
C
cyclin A
cyclin B1
cyclin D1
cyclin E
Relative mRNA level (AU)

Figure 4. Cyclins A, B1, D1 and E expression in the liver of mice during *E. multilocularis* infection. Western blot analyses were performed on lysates with antibodies that recognize cyclins A, B1, D1 and E (A). Relative amount of cyclins A, B1, D1 and E expression was calculated from semi-quantitative analysis of the Western blots using densitometry (B). Cyclins A, B1, D1 and E mRNA expression was measured in the liver from *E. multilocularis* infected or non-infected mice by qPCR(C). $^{*}P<0.05$ versus control. con, control, non-infected mice; Em, *E. multilocularis* infected mice; AU: arbitrary units.
doi:10.1371/journal.pone.0030127.g004

liver parenchyma close to the lesion and peri-parasitic infiltrate, caspase 3 and cleaved-caspase 3 expression was observed at days 60 and 90; it then markedly increased at days 270 and 360 post-infection, with staining intensities from "moderate" to "strong". Minimal immunostaining for caspase 3 and cleaved-caspase 3 was observed in the livers of non-infected mice.

TUNEL-positive cells in the liver of mice during *E. multilocularis* infection

To determine whether cells exhibited DNA strand breakage during *E.multilocularis* infection, and could thus be considered apoptotic, the TUNEL assay was applied to the liver sections. As shown in Figure 10, in the periparasitic infiltrate, some inflammatory cells with apoptosis were observed inside the lesion at days 180, 270 and 360. Within the liver parenchyma close to the lesion and peri-parasitic infiltrate, a few hepatocytes exhibiting apoptosis were observed at day180; the number of apoptotic hepatocytes significantly increased in a time-dependent manner up to day360 post-infection; during the late stage of infection, TUNEL staining intensities ranged from "weak" to "moderate". No apoptotic liver cells were observed in the livers of the non-infected mice.

Discussion

Changes in the metabolic pathways involved in the regulation of hepatic cell proliferation and growth arrest, and especially in the MAPKs system, have been extensively studied in infectious/inflammatory conditions, especially of viral origin [36,37,38]. Very little is known of the influence of helminth parasites which develop in the liver on the proliferation/growth arrest of the hepatocytes in the infected liver. Until recently, no study had ever specifically addressed the issue of liver proliferation/regeneration and growth

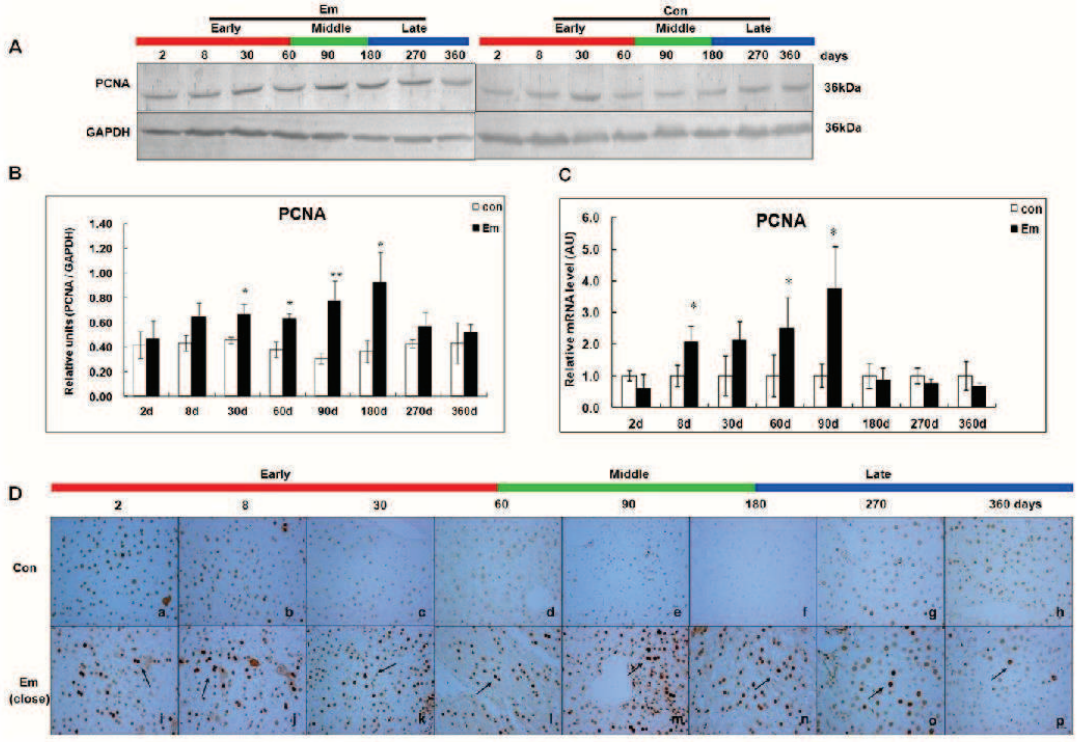

Figure 5. PCNA expression in the liver of mice during *E. multilocularis* infection. Western blot analyses were performed on lysates with antibodies that recognize PCNA (A). Relative amount of PCNA expression was calculated from semi-quantitative analysis of the Western blots using densitometry (B). PCNA mRNA expression was measured by qPCR (C) and PCNA expression by hepatic cells (close to lesion) in the liver from *E. multilocularis* infected or non-infected mice by histo-immunochemical analysis(*arrow*) (D). Final magnification, 400×. $^{*}P<0.05$ versus control. con, control, non-infected mice; Em, *E. multilocularis* infected mice; AU: arbitrary units.
doi:10.1371/journal.pone.0030127.g005

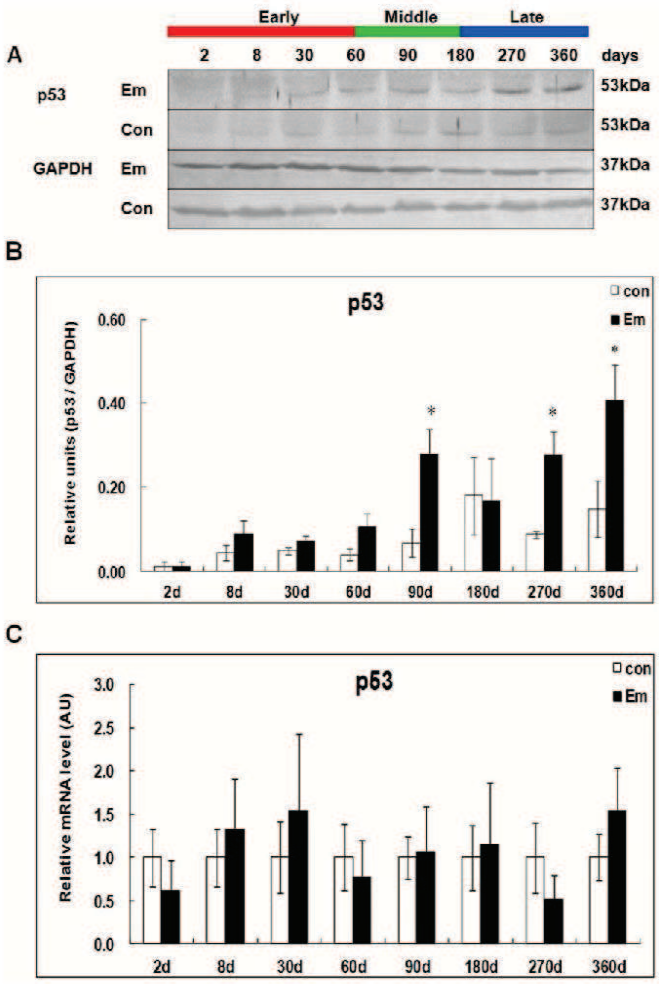

Figure 6. p53 expression in the liver of mice during *E. multilocularis* infection. Western blot analyses were performed on lysates from liver samples with antibodies that recognize p53 (A). Relative amount of p53 expression was calculated from semi-quantitative analysis of the Western blots using densitometry (B). p53 mRNA expression was measured in the liver from *E. multilocularis*-infected or non-infected mice by qPCR (C). $^{*}P<0.05$ *versus* control. con, control, non-infected mice; Em, *E. multilocularis* infected mice; AU: arbitrary units.
doi:10.1371/journal.pone.0030127.g006

arrest/apoptosis after *E. multilocularis* infection. In this longitudinal study using the murine experimental model of *E. multilocularis* infection, we could show that, opposite to those involved in cell proliferation and anti-apoptosis which were activated in the first half of the infection course, metabolic pathways involved in growth arrest and apoptosis were significantly activated in the liver of the infected mice in the second half of the infection course (Figure 11).

In the present study, we could confirm the induction of p-ERK1/2 and a parallel expression of Cyclin D1 and PCNA from the beginning of infection and their persistence during the progression of *E. multilocularis* growth in the liver during the first 2 stages of parasite development. This suggested that, as shown in other models, activation of the ERK1/2 pathway increased hepatocyte DNA synthesis and was involved in the activation of cell cycle [39,40,41]. Increased expression of PCNA in the hepatic cells under the influence of *E. multilocularis* was constantly found *in vivo*, in previous studies [33,34] and in this study as well. PCNA is a stable cell cycle-related 36 kDa nuclear protein which is increasingly expressed in late G1 and throughout S phase of the cell cycle. Its rate of synthesis is correlated with the proliferative rate of cells, and PCNA immunoblot and immunostaining can be used to reliably define and map proliferating cells in animal and human tissues [42,43]. Expression of PCNA in the liver hepatocytes of both infected and non-infected mice at days 2

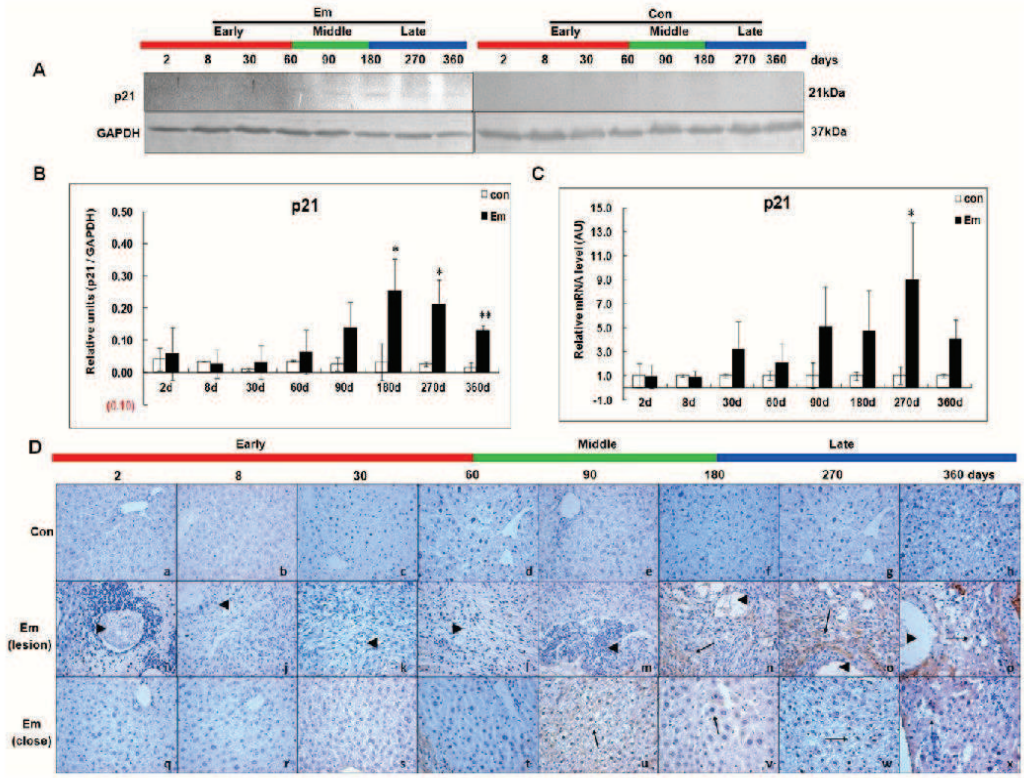

Figure 7. p21 expression in the liver of mice during *E. multilocularis* infection. Western blot analyses were performed on lysates from liver samples with antibodies that recognize p21 (A). Relative amount of p21 expression was calculated from semi-quantitative analysis of the Western blots using densitometry (B). p21 mRNA expression was measured by qPCR (C). Histo-immunochemical analysis of p21 expression was performed on tissue samples: p21 expression was observed in infiltrating lymphocytes (lesion) and fibroblast-like cells (lesion) but also in hepatic cells (close to lesion) in the liver from *E. multilocularis* infected mice (*arrow*) (D). The *arrowheads* indicate the parasitic lesions in the liver of infected mice ("lesion" row). Final magnification, 400×. $^{*}P<0.05$ *versus* control. con, control, non-infected mice; Em, *E. multilocularis* infected mice; AU: arbitrary units; lesion, *E. multilocularis* metacestode and surrounding immune infiltrate; close, liver parenchyma close to lesion.
doi:10.1371/journal.pone.0030127.g007

and 8 after infection clearly shows the regeneration process induced by the injection in the liver, which constitutes, per se, a liver injury. In our study, qPCR confirmed that intrahepatic PCNA synthesis was more increased in *E. multilocularis*-infected mice than in non-infected mice as early as day8, and that PCNA synthesis increase was also correlated with *E. multilocularis* development until day180. Then we also found that the induction of p-JNK induced by metacestode components we observed *in vitro* in a previous study [33] began at the end of the middle stage of infection and remained markedly increased at its late stage (up to 1 year). Such activation paralleled an up-regulation of p53, p21, Gadd45γ, an increased expression of cleaved-caspase 3, an increase in the number of TUNEL-positive (apoptotic) cells in the lesion and in the liver parenchyma, and a down-regulation of PCNA and Cyclin A. Activation of the metabolic pathways which govern growth arrest and apoptosis also paralleled the previously described decrease of lymphocyte proliferation and of cytokine production observed at the late stage of experimental infection [10,11,12].

Accumulated data have suggested that the stress- and cytokine-inducible Gadd45 family proteins (Gadd45α, Gadd45β, Gadd45γ) serve similar but not identical functions along various pro- or anti-apoptotic and growth-suppressive pathways [44]. Gadd45β, which interacts with critical cell cycle regulatory proteins, such as PCNA, Cdk1 and Cyclin B1, plays an active role in cell cycle adjustment [27,35,45]. From our previous microarray analysis, we could observe Gadd45β up-regulation at days 90 and 180 in the murine AE model [34], which highly suggested that up-regulated expression of Gadd45β gene might actually be a trigger for hepatic cell survival. Our present study showed that Gadd45β mRNA was significantly increased from day60 to 180. Both immunostaining and immunoblotting confirmed that Gadd45β protein was actually expressed in the liver during the same period, especially in the vicinity of the metacestode. Interestingly, Gadd45β is able to inhibit TNF-α-induced cytotoxicity and Fas-induced apoptosis [19,46,47], both of which were showed to be expressed at the periphery of the periparasitic granuloma, at the border of the liver parenchyma, in human AE [3,48]. A recent study has demonstrated that ERK and Gadd45β are closely related to NF-κB activity, forming a loop-like connection to increase cell survival after lethal damage induced by ionizing

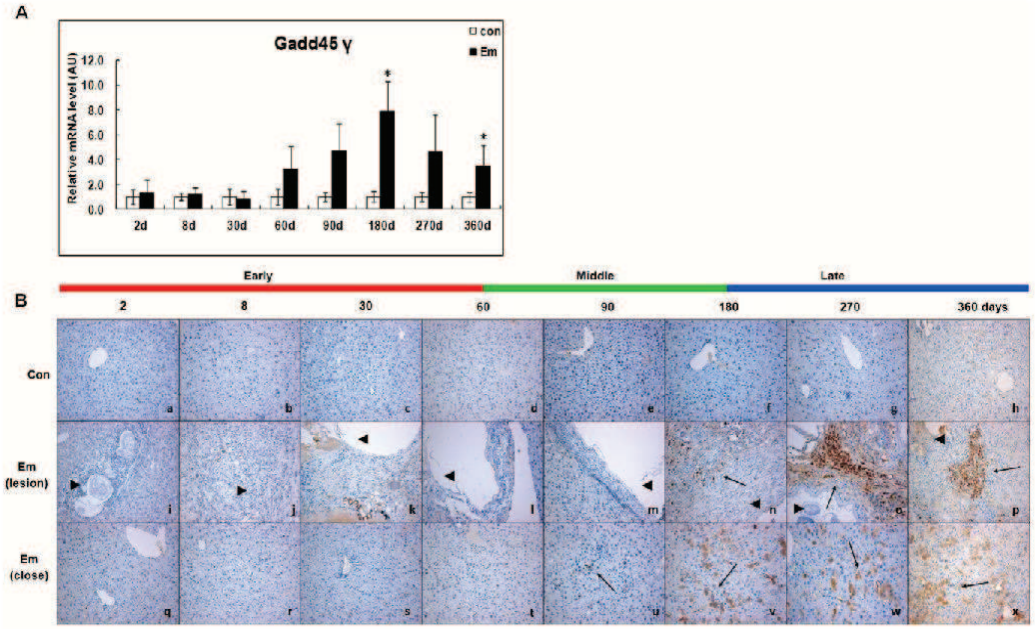

Figure 8. Gadd45γ expression in the liver of mice during *E. multilocularis* infection. Gadd45γ mRNA expression was measured by qPCR (A). Histo-immunochemical analysis of Gadd45γ expression was performed on tissue samples. Gadd45γ expression was observed in infiltrating lymphocytes (lesion) and hepatic cells (close to lesion) in the liver from *E. multilocularis*-infected or non-infected mice (*arrow*) (B). The *arrowheads* indicate the parasitic lesions in the liver of infected mice ("lesion" row). Final magnification, 200×. $^{*}P<0.05$ *versus* control. con, control, non-infected mice; Em, *E. multilocularis* infected mice; AU: arbitrary units; lesion, *E. multilocularis* metacestode and surrounding immune infiltrate; close, liver parenchyma close to *E. multilocularis* lesion.
doi:10.1371/journal.pone.0030127.g008

radiation [49]. Taken together, these observations suggest that activation of ERK1/2, Gadd45β and Cyclin A are able to interact and promote hepatocyte anti-apoptosis at the middle stage of infection. Gadd45γ is a critical and essential mediator of apoptosis induction among the three Gadd45 isoforms because Gadd45γ has strongly pro-apoptotic roles at all times [50]. Gadd45γ may interact with MTK1/MEKK4, which in turn activate both JNK and p38 leading to apoptosis in response to environmental stresses [51,52,53]. Our data obtained during the course of infection suggested a sequential activation of, first, Gadd45β in the first stages of infection, and, then, of Gadd45γ in the late stage of infection; however, the factors which are responsible for the shift to Gadd45γ expression after day180 of infection are unknown. Our present study showed that, like Gadd45γ expression, activation of JNK was observed from day180 to 360. Generally, JNK acts as a critical mediator of hypoxia/reoxygenation-induced apoptosis and also of TNF-induced apoptosis by glutathione depletion in hepatocytes [54,55]. Our data also suggest that p53-dependent mechanisms (p53-p21 and p53-Gadd45γ signaling pathways) may be involved following *E. multilocularis* infection to induce hepatocyte growth arrest/apoptosis. Our data regarding TUNEL-positive cells and elevation of cleaved-caspase 3 highly suggest that hepatocyte apoptosis is a significant event at the late stage of infection. These observations are consistent with the results of previous studies which showed that apoptosis-mediated damage was present in other parasitic diseases such as Chagas disease, toxoplasmosis, leishmaniasis, schistosomiasis due to *Schistosoma mansoni*, and cerebral malaria [56,57,58,59,60]. Hepatocyte apoptosis at the late stage of infection could result from either toxic by-products originating from the parasite or from parasite-induced inflammation. But unlike growth arrest/apoptosis, the activation of hepatocyte proliferation/anti-apoptosis processes we observed in the same experimental mice appears to be a less common phenomenon, which could represent one of the specificities of *E. multilocularis* infection at its early stages.

Hepatocytes suffering sublethal injury have the capacity to activate an internally-triggered cell regeneration mechanism and our previous studies as well as this one have brought evidence that, as it also occurs during viral infection or toxic injury [61], this regeneration mechanism was also operating in *E. multilocularis* infection [33,34], and was especially prominent at the first stages of infection, as was shown in experimental mice until day180 after infection. Liver regeneration is controlled by a wide array of signaling factors and plays a key role in recovery after acute and chronic liver injury. Hepatic cell proliferation is essential to enhance or restore hepatic function [62,63]. Although hepatocyte proliferation is often mediated by the injury/regeneration response, however, in other circumstances it is part of an adaptive response to stress stimuli which do not lead to cell death (direct hyperplasia). This proliferative response is regulated by cell cycle regulated proteins [64]. In AE, influence of the parasite on hepatocyte proliferation (and/or anti-apoptosis) is supported by the up-regulation of Cyclins A, B1, D1 and Gadd45β, which is summarized in Figure 10. Until day180, i.e. in the early and

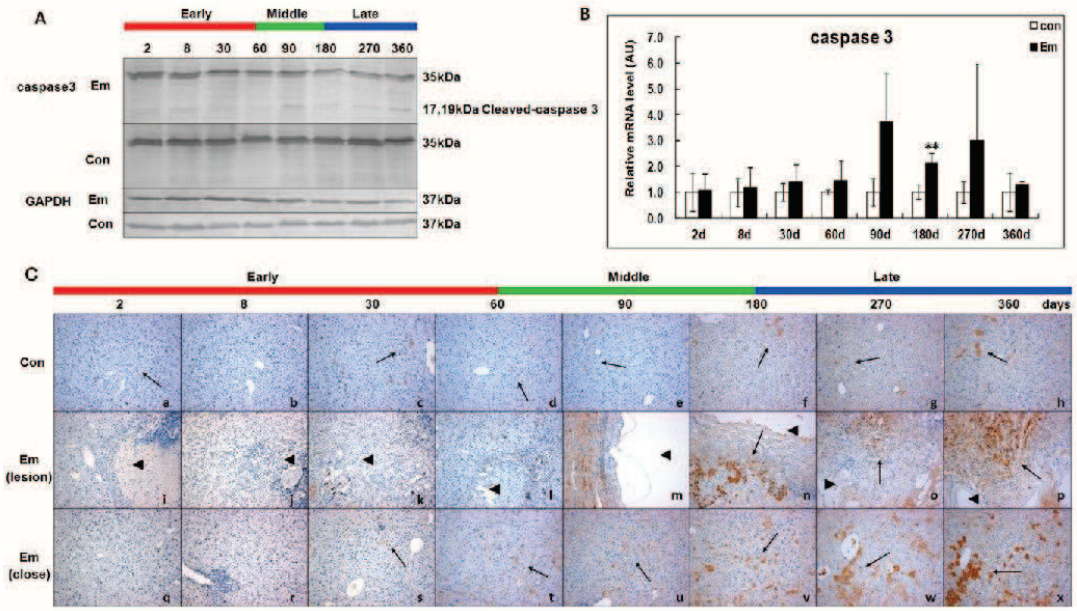

Figure 9. Activation of caspase 3 in the liver of mice during *E. multilocularis* infection. Western blot analyses were performed on lysates from liver samples with antibodies that recognize caspase 3 and cleaved-caspase 3 (A). Caspase 3 mRNA expression was measured by qPCR (B). Histo-immunochemical analysis of caspase 3 and cleaved-caspase 3 expression was performed on tissue samples. Caspase 3 and cleaved-caspase 3 expression was observed in infiltrating lymphocytes (lesion) and hepatic cells (close to lesion) in the liver from *E. multilocularis*-infected or non-infected mice (*arrow*) (C). The *arrowheads* indicate the parasitic lesions in the liver of infected mice ("lesion" row). Final magnification, 200×. $^{**}P<0.01$ *versus* control. con, control, non-infected mice; Em, *E. multilocularis* infected mice; AU: arbitrary units; lesion, *E. multilocularis* metacestode and surrounding immune infiltrate; close, liver parenchyma close to *E. multilocularis* lesion.
doi:10.1371/journal.pone.0030127.g009

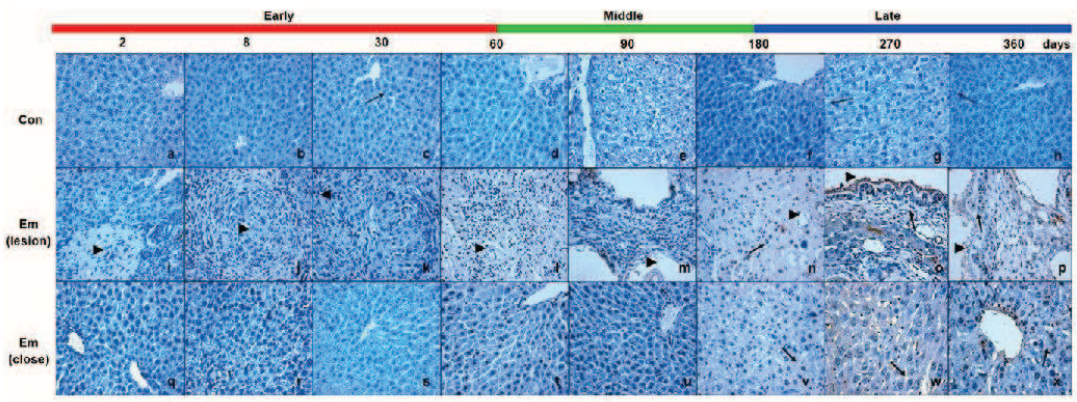

Figure 10. TUNEL assay in the liver during *E. multilocularis* infection. TUNEL assays were performed on the livers from *E. multilocularis*-infected and non-infected mice. Some TUNEL-positive infiltrating lymphocytes (lesion) and hepatic cells(close to lesion) were found in the liver of infected mice from day180 to 360; None was found at day60 and 90 (*arrows*). The *arrowheads* indicate the parasitic lesions in the liver of infected mice ("lesion" row). No TUNEL-positive cells were seen in the liver of non-infected mice. Final magnification, 400×. con, control, non-infected mice; Em, *E. multilocularis* infected mice; AU: arbitrary units; lesion: *E. multilocularis* metacestode and surrounding immune infiltrate; close: liver parenchyma close to *E. multilocularis* lesion.
doi:10.1371/journal.pone.0030127.g010

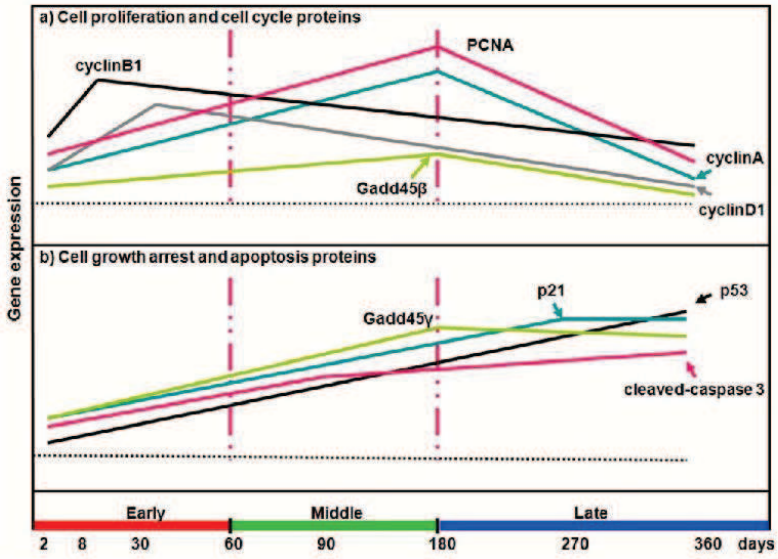

Figure 11. Overall changes in the gene expression of cell proliferation/cell cycle proteins (a) and cell growth arrest/apoptosis proteins (b) during the process of *E. multilocularis*-induced liver injury in mice.
doi:10.1371/journal.pone.0030127.g011

middle stages of infection, gene expression level of CyclinA was increased in a time-dependent manner, while gene expression levels of Cyclin B1 and CyclinD1 were increased up to day30 and then returned to the control level after day60. On the other hand, no significant change in the expression of Cyclin E was observed at any time during the period of observation. Up-regulation of PCNA, Cyclin D1, A and B1 is related to the regulation of the G1/S and G2/M phases [65,66], which were previously reported to increase biphasically after partial hepatectomy and other parasitic infection [67,68]. The "late stage" of infection, i.e. after day180 after infection, has rarely been studied in the murine model of secondary (or primary) *E. multilocularis* infection. In the most susceptible mice, impairment of vital functions due to *E. multilocularis* progression and metastases is fast and occurs between day180 and 270, which makes studies difficult to interpret. In addition, most of the studies addressed immunological mechanisms of immune tolerance; since they were just failing at that late stage [10,11,12], it was thus considered of less interest for that purpose. As the experimental mice we are working with, albeit quite susceptible to *E. multilocularis*, have a prolonged survival until day360, and because we observed activation of both proliferation and apoptosis pathways at day180, we decided to measure the expression and/or activation of the components of these pathways until day360. We were thus able to show the mirror image of growth arrest/apoptosis *versus* proliferation/anti-apoptosis during the natural course of metacestode progression in the liver (Figure 12). These results might suggest that the proliferative capability of hepatocytes was exhausted during continuously lasting hepatic damage, due to direct toxicity of parasitic components and/or cytotoxic attacks by the immune system. This exhaustion might also be due to the profound malnutrition (wasting disease/cachexia) observed in *E. multilocularis*-infected mice in the advanced stage of the disease, and the altered ability of liver cells to synthesize proteins, as suggested by the changes in the expression of many genes at this stage in the microarray analysis we recently performed [34]. However, during the early and middle stage of infection, despite the presence of the metacestode and its growth, very little necrosis is observed on the liver pathological sections in the experimental model; we could confirm such observations [69]. Necrosis of the liver lesion is not observed in all patients with AE: it has only been observed in more advanced/severe cases, and was associated with susceptibility markers and/or with expression of TNF-α by the periparasitic macrophages [48]. On the other hand, the immune tolerance generated by the presence of *E. multilocularis* metacestode in the liver is associated with a poor development of NK cytotoxicity and an inhibition of T-lymphocyte-dependent cytotoxicity, despite the high proliferation potential of T-lymphocytes, the presence of numerous CD8 T-lymphocytes in the liver within the parasitic lesion, and the expression of the appropriate ligands, such as MICA/B [70,71,72]. Such an inhibition is possibly due to the combined influence of IL-10 and TGF-β production [7,73,74]. In addition, hepatocytes do not die but do proliferate in response to parasite growth at the early and middle stages of infection, and we could observe a significant increase in the expression and/or activation of the components of the proliferation pathways by hepatic cells at that stage. Such observations at least partially rule out a direct influence of cytotoxic components, which would manifest itself at all stages of parasite development. Similar "exhaustion" at the late stage of the disease has also been observed for lymphocyte proliferation and cytokine secretion in susceptible experimental mice [10,11,12]. In patients with AE, incubation of peripheral blood mononuclear cells with parasitic antigens has been shown to induce significantly less proliferation in AE patients with severe disease than in patients with abortive or surgically cured cases [75]: taken together, these observations suggest a common negative influence of parasitic components on all types of cell

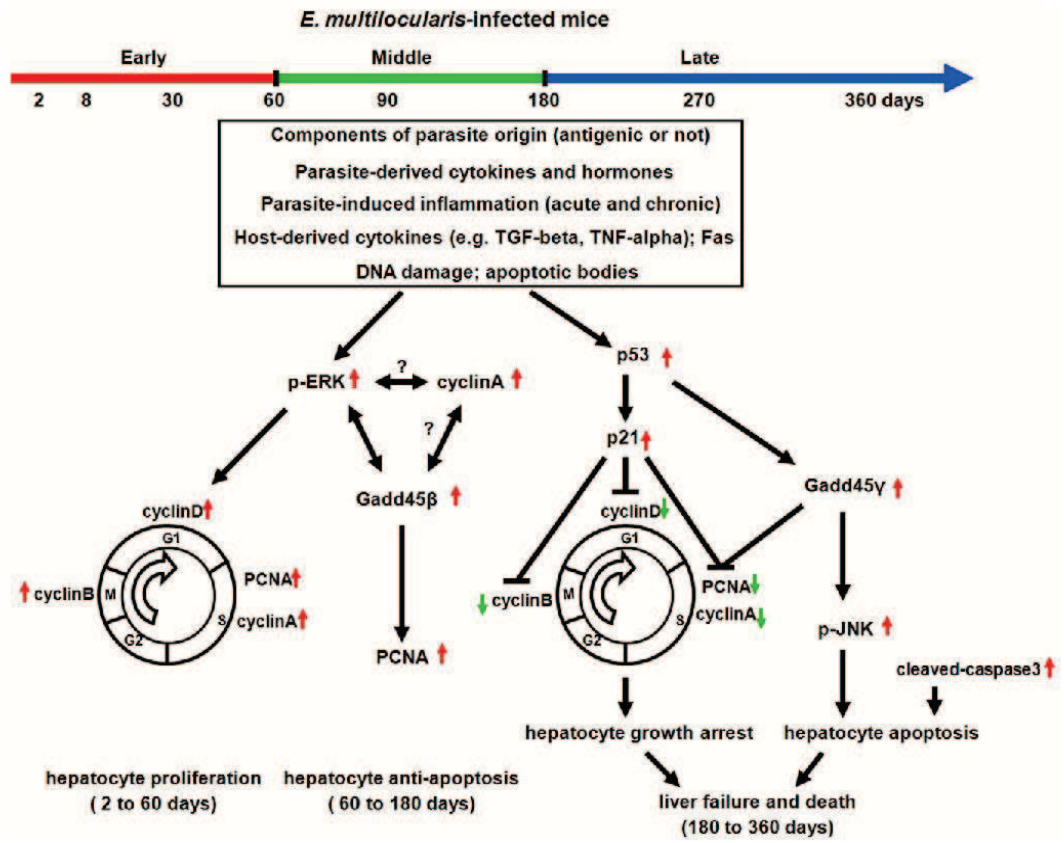

Figure 12. Schematic diagram summarizing the metabolic pathways involved in hepatocyte proliferation/anti-apoptosis and growth arrest/apoptosis in the liver of mice with *E. multilocularis* infection.
doi:10.1371/journal.pone.0030127.g012

proliferation, which would become patent only at an advanced stage of *E. multilocularis* development.

From day90 to 180 after infection, in the BALB/c mice, AE vesicles have become fully fertile and exhibit a number of protoscoleces; it might be hypothesized that this period represents the critical phase when the maturation of the metacestode has been achieved and after which the host is no longer required to promote parasite growth and fertility. In our experiments, day90 and 180 represented the critical steps when we still observed expression of the proliferation pathway components and peaks in the expression/activation of anti-apoptotic pathway components, as well as beginning of increase in the expression/activation of growth arrest/apoptotic pathway components. Then, growth arrest/apoptotic pathways clearly overcome proliferation/anti-apoptotic pathways. Our previous *in vitro* experiments showed that such sequential events were not associated with any non-specific "exhaustion", which could only be observed *in vivo*. They strongly suggested that they are governed by components of parasitic origin: activation of such pathways was observed in isolated hepatocytes under the influence of components present in the vesicle fluid and in the supernatants of metacestode axenic cultures [33]. Future work should elucidate the nature of these components which would act in a sequential manner: 1) at the early stage and beginning of the middle stage of *E. multilocularis* infection, they would favor parasitic cell, liver cell and immune cell proliferation and survival, and promote metacestode fertility and tolerance by the host, and 2) after fertility has been acquired, at the end of middle stage and all late stage of infection, they would contribute to the dissemination of the protoscoleces and next steps of the parasite cycle by favoring liver damage/apoptosis and subsequent major impairment in protein synthesis and xenobiotic metabolism [34], as well as immune deficiency [10,11,12,75], and eventually lead to the host's death.

In conclusion, this study is the first report which demonstrates a coordinated activation of the proliferation/anti-apoptosis and growth arrest/apoptosis mechanisms *in vivo* during the course of *E. multilocularis* infection. As suggested in a schematic diagram (Figure 12): 1) at the early stage of infection, activation of ERK1/2 and downstream targets such as CyclinD1, A, B1 and PCNA would favor hepatocyte proliferation, 2) at the middle stage of infection, permanent activation of ERK1/2 and Cyclin A and elevated Gadd45β expression may synergize to mediate an anti-apoptotic response to enhance liver cell survival and prevent lethal tissue damage induced both by the parasite itself and cytokines

such as TNF-α, and 3) at the late stage of infection, activation of JNK and the increased expression of p53, p21, Gadd45γ and cleaved-caspase 3 would induce hepatocyte growth arrest/apoptosis. These findings also give a rational explanation to the clinical observations: 1) hepatomegaly of unusual size is frequent at presentation; and an unexpected survival rate is observed after major hepatic resection in AE patients [76], and 2) chronic liver injury, necrosis, and hepatic failure in AE patients at an advanced stage and in experimental animals [6,9]. They provide a molecular basis for the balance between liver damage and repair in the progression of *E. multilocularis* infection.

Materials and Methods

Ethics Statement

All animals received humane care in compliance with the Medical Research Center's guidelines, and animal procedures were approved by the Animal Care and Use Committee and the Ethical Committee of First Affiliated Hospital of Xinjiang Medical University (20081205-2).

Experimental design

Pathogen-free female BALB/c mice (8–10 weeks old) were purchased from the Animal Center of Xinjiang Medical University and were maintained in an air-conditioned animal room with a 12-h light/dark cycle and provided with rodent chow and water. *E. multilocularis* metacestodes were obtained from intraperitoneal lesions maintained in *Meriones unguiculatus*, and 0.1 mL of pooled lesions (~1, 000 protoscoleces) was injected into the anterior liver lobe of infected mice as previously described [69]. For each autopsy time-point, ten experimentally infected mice were used in *E. multilocularis* group (n = 10) and compared with five control mice (n = 5), which received an intra-hepatic injection of 0.1 mL of saline in the anterior liver lobe using the same surgical procedure. Mice were killed at days 2, 8, 30, 60, 90, 180, 270 and 360.

Tissue sampling

In *E. multilocularis* infected mice, liver tissue samples were taken close to the parasitic lesions, i.e. 1–2mm from the macroscopic changes due to the metacestode/granuloma lesion (white-yellowish color), thus avoiding liver contamination with parasitic tissue and infiltrating immune cells; in control mice, liver tissue samples were taken from the same (anterior) liver lobe in the sham-injected area. Tissue fragments were separated into two parts and either deep-frozen in liquid nitrogen for western blot and qPCR or formalin-fixed for immunohistochemistry. In addition, liver tissue samples were also taken from the parasitic lesion (including periparasitic liver tissue adjacent by 1 mm to the macroscopically visible parasitic lesion) for histopathology and immunohistochemistry.

Pathology and parasitology

For histopathology livers were placed in 10% buffered formalin and then embedded in paraffin. Five micrometer thick microtome sections were prepared from each liver sample and stained with hematoxylin-eosin. The sections were examined for the pathological changes generated by *E. multilocularis* and for hepatotoxicity. The histological slides were evaluated blindly by two of the authors.

Western blot analysis

Western blot analysis of cell lysates was performed by SDS-PAGE using NuPAGE (Invitrogen, California, USA) followed by transfer to PVDF membrane. Using the appropriate antibodies: against total and p-ERK1/2, p-JNK, p-38 (dilution 1:500, Cell Signaling technology, Massachusetts, USA), Gadd45β (dilution 1:800), Cyclins A, B1, D1 and E (dilution 1:500), PCNA (dilution 1:1000), p53, p21 (dilution 1:500, Santa Cruz, California, USA), full length caspase 3 (35kDa) and large fragment of caspase 3 resulting from cleavage (17kDa) (dilution 1:500, Cell Signaling technology, Massachusetts, USA), and GAPDH (dilution 1:1000, Santa Cruz, California, USA) were detected using the WesternBreeze Kit (Invitrogen, California, USA). The expression levels of respective proteins (in "relative units") in non-infected mice and infected mice were quantified using Quantity One software (Bio-Rad, Hercules, CA), according to a previously described procedure [77].

Quantitative real-time PCR analysis (qPCR)

After removing contaminated DNA from the isolated RNA using DNaseI (Fermentas, Vilnius, Lithuania), 1 μg of total RNA was reverse transcribed into cDNA in 20 μL reaction mixtures containing 200U of Moloney murine leukemia virus reverse transcriptase (MMLV, Promega, Madison, USA); 100 ng per reaction of oligo (dT) primers; and 0.5mM each of dNTPs, dATP, dCTP, dGTP, and dTTP. The reaction mixture was then incubated at 42°C for 1 hour and at 95°C for 5 min to deactivate the reverse transcriptase.

The qPCR was run in a thermocycler (iQ5 Bio-Rad, Hercules, CA) with the SYBR Green PCR premix (TaKaRa, Dalian, China) following the manufacturer's instructions. Thermo-cycling was performed in a final volume of 20 μL containing 2 μL cDNA and 10 pmol of each primer (Table 1). To normalize for gene expression, mRNA expression of the housekeeping gene beta-actin was measured. For every sample, both the housekeeping and the target genes were amplified in triplicate using the following cycle scheme: after initial denaturation of the samples at 95°C for 1 min, 40 cycles of 95°C for 5 s and 60°C (or other) for 30 s were performed. Fluorescence was measured in every cycle, and a melting curve was analyzed after the PCR by increasing the temperature from 55 to 95°C (0.5°C increments). A defined single peak was obtained for all amplicons, confirming the specificity of the amplification.

Immunohistochemical staining

Paraffin-embedded liver tissue samples of control mice and infected mice were examined to determine the expression and distribution of p-ERK1/2, Gadd45β, PCNA, p21, Gadd45γ, caspase 3 and cleaved-caspase 3 protein at each time points. All sections were first deparaffinized and then incubated with 3% hydrogen peroxide for 10 min to block the endogenous peroxidase activity. After being washed with PBS and incubation for 1 hour with 5% normal goat serum to reduce non-specific background staining, the sections were incubated with the above mentioned primary antibodies against p-ERK1/2 (dilution 1:50), Gadd45β (dilution 1:100), PCNA (dilution 1:300), p21 (dilution 1:50), Gadd45γ (dilution 1:200), caspase 3 and cleaved-caspase 3(dilution 1:100) at 4°C overnight. Immunoreactive proteins were visualized using the appropriate anti-IgG secondary antibodies labeled with horseradish peroxidase (Santa Cruz, California, USA) and the chromogen 3′-diaminobenzidine (DAB, Zhongshan, Beijing, China) as a substrate[5]. Negative controls were incubated without primary antibodies but were otherwise subjected to all the immunohistochemical procedures. Sections were examined microscopically for specific staining and photographs were taken using a digital image-capture system (Leica, Solms, Germany); the intensity of positive hepatocyte staining was classified on an arbitrary scale including "negative", "weak", "moderate", and "strong" staining.

Table 1. Primers and cycling parameters of qRT-PCR.

Gene	Genbank accession	Primer Sequences	Annealing temperature	Expected Size
beta-actin	NM_007393	F: 5'-AACTCCATCATGAAGTGTGA-3' R: 5'-ACTCCTGCTTGCTGATCCAC-3'	56°C	248bp
PCNA	NM_0110045	F: 5'- GAGAGCTTGGCAATGGGAACA-3' R: 5'-GGGCACATCTGCAGACATACTGA-3'	60°C	185bp
CyclinA	NM_009828	F: 5'- AGCAGAAGAGACTCAGAAGAGG -3' R: 5'- GATAGTCAAGAGGTGTCAGTGG -3'	60°C	121bp
CyclinB1	NM_172301	F: 5'- AGGAAGAGCAGTCAGTTAGACC -3' R: 5'- CTGGAGGGTACATCTCCTCATA -3'	60°C	248bp
CyclinD1	NM_007631	F: 5'- GGGGACAACTCTTAAGTCTCAC -3' R: 5'- CCAATAAAAGACCAATCTCTC -3'	60°C	206bp
CyclinE	NM_007633	F: 5'- GAGCTTGAATACCCTAGGACTG -3' R: 5'-CGTCTCTCTGTGGAGCTTATAGAC -3'	60°C	245bp
Gadd45β	NM_008655	F: 5'- GAGGCGGCCAAACTGATGA-3' R: 5'-TCGCAGCAGAACGACTGGA-3'	60°C	128bp
p53	NM_001127233	F: 5'- ATTGGGACCATCCTGGCTGTAG -3' R: 5'- CGAGGCTGATATCCGACTGTGA -3'	60°C	148bp
p21	NM_007669	F: 5'-CTGTCTTGCACTCTGGTGTCTGA-3' R: 5'-CCAATCTGCGCTTGGAGTGA-3'	60°C	121bp
Gadd45γ	NM_011817	F: 5'- TGGATAACTTGCTGTTCGTGGA-3' R: 5'-CAGCAGAAGTTCGTGCAGTG-3'	60°C	122bp
Caspase 3	NM_009810	F: 5'- CTGCCGGAGTCTGACTGGAA-3' R: 5'-ATCAGTCCCACTGTCTGTCTCAATG-3'	60°C	97bp

doi:10.1371/journal.pone.0030127.t001

TUNEL analysis

Apoptosis in the livers of infected mice and non-infected mice was further analyzed using a commercial kit (Roche, Mannheim, Germany) based on the TdT-mediated dUTP-digoxigenin nick-end labeling (TUNEL) of apoptotic cells. Five micrometer sections of paraffin-embedded samples of liver were prepared as described above. Sections were examined microscopically for specific staining and photographs were taken using a digital image-capture system (Leica, Solms, Germany) (the intensity of TUNEL-positive hepatocyte staining was classed on an arbitrary scale from "negative" to "strong" staining).

Statistical analysis

All data were presented as the means with standard deviation and analyzed using SPSS version 11.0 software (SPSS, Chicago, IL, USA). Statistical significance was tested using the Student's *t* test; a *P* value of less than 0.05 was considered significant.

Acknowledgments

We would like to thank Xufa Wei, Tao Jiang and Chun Zhang for their excellent technical assistance.

Author Contributions

Conceived and designed the experiments: RL DV HW. Performed the experiments: CZ JW GL JL. Analyzed the data: RL DV CZ XL GM. Contributed reagents/materials/analysis tools: RL HW GM. Wrote the paper: RL DV HW CZ.

References

1. Eckert J, Deplazes P (2004) Biological, epidemiological, and clinical aspects of echinococcosis, a zoonosis of increasing concern. Clin Microbiol Rev 17: 107–135.
2. Bresson-Hadni S, Miguet JP, Mantion GA, Vuitton DA (2007) Echinococcosis of the liver. In: Rodes J, Benhamou JP, Blei AT, Reichen J, Rizzetto M, eds. Textbook of Hepatology, From basic science to clinical practice. 3rd ed: Oxford-Malden: Blackwell Publishing Inc. pp 1047–1057.
3. Vuitton DA, Guerret-Stocker S, Carbillet JP, Mantion G, Miguet JP, et al. (1986) Collagen immunotyping of the hepatic fibrosis in human alveolar echinococcosis. Z Parasitenkd 72: 97–104.
4. Ricard-Blum S, Bresson-Hadni S, Guerret S, Grenard P, Volle PJ, et al. (1996) Mechanism of collagen network stabilization in human irreversible granulomatous liver fibrosis. Gastroenterology 111: 172–182.
5. Grenard P, Bresson-Hadni S, El Alaoui S, Chevallier M, Vuitton DA, et al. (2001) Transglutaminase-mediated cross-linking is involved in the stabilization of extracellular matrix in human liver fibrosis. J Hepatol 35: 367–375.
6. Vuitton DA (2003) The ambiguous role of immunity in echinococcosis: protection of the host or of the parasite? Acta Trop 85: 119–132.
7. Bresson-Hadni S, Liance M, Meyer JP, Houin R, Bresson JL, et al. (1990) Cellular immunity in experimental Echinococcus multilocularis infection. II. Sequential and comparative phenotypic study of the periparasitic mononuclear cells in resistant and sensitive mice. Clin Exp Immunol 82: 378–383.
8. Guerret S, Vuitton DA, Liance M, Pater C, Carbillet JP (1990) Echinococcus multilocularis: relationship between susceptibility/resistance and liver fibrogenesis in experimental mice. Parasitol Res 84: 657–667.
9. Jiang CP, Don M, Jones M (2005) Liver alveolar echinococcosis in China: clinical aspect with relative basic research. World J Gastroenterol 11: 4611–4617.
10. Emery I, Liance M, Deriaud E, Vuitton DA, Houin R, et al. (1996) Characterization of T-cell immune responses of Echinococcus multilocularis-infected C57BL/6J mice. Parasite Immunol 18: 463–472.
11. Emery I, Liance M, Leclerc C (1997) Secondary Echinococcus multilocularis infection in A/J mice: delayed metacestode development is associated with Th1 cytokine production. Parasite Immunol 19: 493–503.
12. Gottstein B, Wunderlin E, Tanner I (1994) Echinococcus multilocularis: parasite-specific humoral and cellular immune response subsets in mouse strains susceptible (AKR, C57B1/6J) or 'resistant' (C57B1/10) to secondary alveolar echinococcosis. Clin Exp Immunol 96: 245–252.
13. Berres ML, Trautwein C, Zaldivar MM, Schmitz P, Pauels K, et al. (2009) The chemokine scavenging receptor D6 limits acute toxic liver injury in vivo. Biol Chem 390: 1039–1045.
14. Vuitton DA, Gottstein B (2010) Echinococcus multilocularis and its intermediate host: a model of parasite-host interplay. J Biomed Biotechnol 2010. pp 923–193.
15. Dai WJ, Gottstein B (1999) Nitric oxide-mediated immunosuppression following murine Echinococcus multilocularis infection. Immunology 97: 107–116.
16. Clark SP, Ryan TP, Searfoss GH, Davis MA, Hooser SB (2008) Chronic microcystin exposure induces hepatocyte proliferation with increased expression of mitotic and cyclin-associated genes in P53-deficient mice. Toxicol Pathol 36: 190–203.
17. Junttila MR, Li SP, Westermarck J (2008) Phosphatase-mediated crosstalk between MAPK signaling pathways in the regulation of cell survival. FASEB J 22: 954–965.
18. Ballif BA, Blenis J (2001) Molecular mechanisms mediating mammalian mitogen-activated protein kinase (MAPK) kinase (MEK)-MAPK cell survival signals. Cell Growth Differ 12: 397–408.
19. De Smaele E, Zazzeroni F, Papa S, Nguyen DU, Jin R, et al. (2001) Induction of gadd45beta by NF-kappaB downregulates pro-apoptotic JNK signalling. Nature 414: 308–313.
20. Brunt EM, Walsh SN, Hayashi PH, Labundy J, Di Bisceglie AM (2007) Hepatocyte senescence in end-stage chronic liver disease: a study of cyclin-dependent kinase inhibitor p21 in liver biopsies as a marker for progression to hepatocellular carcinoma. Liver Int 27: 662–671.
21. Raman M, Chen W, Cobb MH (2007) Differential regulation and properties of MAPKs. Oncogene 26: 3100–3112.
22. Marino M, Acconcia F, Bresciani F, Weisz A, Trentalance A (2002) Distinct nongenomic signal transduction pathways controlled by 17beta-estradiol

regulate DNA synthesis and cyclin D(1) gene transcription in HepG2 cells. Mol Biol Cell 13: 3720–3729.
23. Xiong Y, Hannon GJ, Zhang H, Casso D, Kobayashi R, et al. (1993) p21 is a universal inhibitor of cyclin kinases. Nature 366: 701–704.
24. Harper JW, Adami GR, Wei N, Keyomarsi K, Elledge SJ (1993) The p21 Cdk-interacting protein Cip1 is a potent inhibitor of G1 cyclin-dependent kinases. Cell 75: 805–816.
25. Waga S, Hannon GJ, Beach D, Stillman B (1994) The p21 inhibitor of cyclin-dependent kinases controls DNA replication by interaction with PCNA. Nature 369: 574–578.
26. Dulic V, Kaufmann WK, Wilson SJ, Tlsty TD, Lees E, et al. (1994) p53-dependent inhibition of cyclin-dependent kinase activities in human fibroblasts during radiation-induced G1 arrest. Cell 76: 1013–1023.
27. Smith ML, Chen IT, Zhan Q, Bae I, Chen CY, et al. (1994) Interaction of the p53-regulated protein Gadd45 with proliferating cell nuclear antigen. Science 266: 1376–1380.
28. Zhang W, Bae I, Krishnaraju K, Azam N, Fan W, et al. (1999) CR6: a third member in the MyD118 and GADD45 gene family which functions in negative growth control. Oncogene 18: 4899–4907.
29. Hall PA, Kearsey JM, Coates PJ, Norman DG, Warbrick E, et al. (1995) Characterisation of the interaction between PCNA and Gadd45. Oncogene 10: 2427–2433.
30. Xia Z, Dickens M, Raingeaud J, Davis RJ, Greenberg ME (1995) Opposing effects of ERK and JNK-p38 MAP kinases on apoptosis. Science 270: 1326–1331.
31. Mita H, Tsutsui J, Takekawa M, Witten EA, Saito H (2002) Regulation of MTK1/MEKK4 kinase activity by its N-terminal autoinhibitory domain and GADD45 binding. Mol Cell Biol 22: 4544–4555.
32. Zhu N, Shao Y, Xu L, Yu L, Sun L (2009) Gadd45-alpha and Gadd45-gamma utilize p38 and JNK signaling pathways to induce cell cycle G2/M arrest in Hep-G2 hepatoma cells. Mol Biol Rep 36: 2075–2085.
33. Lin RY, Wang JH, Lu XM, Zhou XT, Mantion G, et al. (2009) Components of the mitogen-activated protein kinase cascade are activated in hepatic cells by Echinococcus multilocularis metacestode. World J Gastroenterol 15: 2116–2124.
34. Lin R, Lü G, Wang J, Zhang C, Xie W, et al. (2011) Time course of gene expression profiling in the liver of experimental mice infected with Echinococcus multilocularis. PLoS ONE 6: e14557.
35. Jin S, Tong T, Fan W, Fan F, Antinore MJ, et al. (2002) GADD45-induced cell cycle G2-M arrest associates with altered subcellular distribution of cyclin B1 and is independent of p38 kinase activity. Oncogene 21: 8696–8704.
36. Alexia C, Lasfer M, Groyer A (2004) Role of constitutively activated and insulin-like growth factor-stimulated ERK1/2 signaling in human hepatoma cell proliferation and apoptosis: evidence for heterogeneity of tumor cell lines. Ann N Y Acad Sci 1030: 219–229.
37. Wu D, Cederbaum A (2008) Cytochrome P4502E1 sensitizes to tumor necrosis factor alpha-induced liver injury through activation of mitogen-activated protein kinases in mice. Hepatology 47: 1005–1017.
38. Ko KS, Tomasi ML, Iglesias-Ara A, French BA, French SW, et al. (2010) Liver-specific deletion of prohibitin 1 results in spontaneous liver injury, fibrosis, and hepatocellular carcinoma in mice. Hepatology 52: 2096–2108.
39. Kimata M, Michigami T, Tachikawa K, Okada T, Koshimizu T, et al. (2010) Signaling of extracellular inorganic phosphate up-regulates cyclin D1 expression in proliferating chondrocytes via the Na+/Pi cotransporter Pit-1 and Raf/MEK/ERK pathway. Bone 47: 938–947.
40. Ravenhall C, Guida E, Harris T, Koutsoubos V, Stewart A (2000) The importance of ERK activity in the regulation of cyclin D1 levels and DNA synthesis in human cultured airway smooth muscle. Br J Pharmacol 131: 17–28.
41. Kawanaka H, Tomikawa M, Baatar D, Jones MK, Pai R, et al. (2001) Despite activation of EGF-receptor-ERK signaling pathway, epithelial proliferation is impaired in portal hypertensive gastric mucosa: relevance of MKP-1, c-fos, c-myc, and cyclin D1 expression. Life Sci 69: 3019–3033.
42. Rudi J, Waldherr R, Raedsch R, Kommerell B (1995) Hepatocyte proliferation in primary biliary cirrhosis as assessed by proliferating cell nuclear antigen and Ki-67 antigen labelling. J Hepatol 22: 43–49.
43. Wolf HK, Michalopoulos GK (1992) Hepatocyte regeneration in acute fulminant and nonfulminant hepatitis: a study of proliferating cell nuclear antigen expression. Hepatology 15: 707–713.
44. Mak SK, Kultz D (2004) Gadd45 proteins induce G2/M arrest and modulate apoptosis in kidney cells exposed to hyperosmotic stress. J Biol Chem 279: 39075–39084.
45. Lu B, Ferrandino AF, Flavell RA (2004) Gadd45beta is important for perpetuating cognate and inflammatory signals in T cells. Nat Immunol 5: 38–44.
46. Zazzeroni F, Papa S, Algeciras-Schimnich A, Alvarez K, Melis T, et al. (2003) Gadd45 beta mediates the protective effects of CD40 costimulation against Fas-induced apoptosis. Blood 102: 3270–3279.
47. Columbano A, Ledda-Columbano GM, Pibiri M, Cossu C, Menegazzi M, et al. (2005) Gadd45beta is induced through a CAR-dependent, TNF-independent pathway in murine liver hyperplasia. Hepatology 42: 1118–1126.
48. Bresson-Hadni S, Petitjean O, Monnot-Jacquard B, Heyd B, Kantelip B, et al. (1994) Cellular localisations of interleukin-1 beta, interleukin-6 and tumor necrosis factor-alpha mRNA in a parasitic granulomatous disease of the liver, alveolar echinococcosis. Eur Cytokine Netw 5: 461–468.
49. Wang T, Hu YC, Dong S, Fan M, Tamae D, et al. (2005) Co-activation of ERK, NF-kappaB, and GADD45beta in response to ionizing radiation. J Biol Chem 280: 12593–12601.
50. Zerbini LF, Wang Y, Czibere A, Correa RG, Cho JY, et al. (2004) NF-kappa B-mediated repression of growth arrest- and DNA-damage-inducible proteins 45alpha and gamma is essential for cancer cell survival. Proc Natl Acad Sci U S A 101: 13618–13623.
51. Miyake Z, Takekawa M, Ge Q, Saito H (2007) Activation of MTK1/MEKK4 by GADD45 through induced N-C dissociation and dimerization-mediated trans autophosphorylation of the MTK1 kinase domain. Mol Cell Biol 27: 2765–2776.
52. Chi H, Lu B, Takekawa M, Davis RJ, Flavell RA (2004) GADD45beta/GADD45gamma and MEKK4 comprise a genetic pathway mediating STAT4-independent IFNgamma production in T cells. Embo J 23: 1576–1586.
53. Satomi Y, Nishino H (2009) Implication of mitogen-activated protein kinase in the induction of G1 cell cycle arrest and gadd45 expression by the carotenoid fucoxanthin in human cancer cells. Biochim Biophys Acta 1790: 260–266.
54. Matsumaru K, Ji C, Kaplowitz N (2003) Mechanisms for sensitization to TNF-induced apoptosis by acute glutathione depletion in murine hepatocytes. Hepatology 37: 1425–1434.
55. Crenesse D, Gugenheim J, Hornoy J, Tornieri K, Laurens M, et al. (2000) Protein kinase activation by warm and cold hypoxia- reoxygenation in primary-cultured rat hepatocytes-JNK(1)/SAPK(1) involvement in apoptosis. Hepatology 32: 1029–1036.
56. Gavrilescu LC, Denkers EY (2001) IFN-gamma overproduction and high level apoptosis are associated with high but not low virulence Toxoplasma gondii infection. J Immunol 167: 902–909.
57. Acosta Rodriguez EV, Zuniga E, Montes CL, Gruppi A (2003) Interleukin-4 biases differentiation of B cells from Trypanosoma cruzi-infected mice and restrains their fratricide: role of Fas ligand down-regulation and MHC class II-transactivator up-regulation. J Leukoc Biol 73: 127–136.
58. Stiles JK, Meade JC, Kucerova Z, Lyn D, Thompson W, et al. (2001) Trypanosoma brucei infection induces apoptosis and up-regulates neuroleukin expression in the cerebellum. Ann Trop Med Parasitol 95: 797–810.
59. Chen L, Rao KV, He YX, Ramaswamy K (2002) Skin-stage schistosomula of Schistosoma mansoni produce an apoptosis-inducing factor that can cause apoptosis of T cells. J Biol Chem 277: 34329–34335.
60. Wiese L, Kurtzhals JA, Penkowa M (2006) Neuronal apoptosis, metallothionein expression and proinflammatory responses during cerebral malaria in mice. Exp Neurol 200: 216–226.
61. Viebahn CS, Yeoh GC (2008) What fires prometheus? The link between inflammation and regeneration following chronic liver injury. Int J Biochem Cell Biol 40: 855–873.
62. Taub R (2004) Liver regeneration: from myth to mechanism. Nat Rev Mol Cell Biol 5: 836–847.
63. Fausto N, Campbell JS, Riehle KJ (2006) Liver regeneration. Hepatology 43: S45–53.
64. Svegliati-Baroni G, Ridolfi F, Caradonna Z, Alvaro D, Marzioni M, et al. (2003) Regulation of ERK/JNK/p70S6K in two rat models of liver injury and fibrosis. J Hepatol 39: 528–537.
65. Masaki T, Shiratori Y, Rengifo W, Igarashi K, Yamagata M, et al. (2003) Cyclins and cyclin-dependent kinases: comparative study of hepatocellular carcinoma versus cirrhosis. Hepatology 37: 534–543.
66. Neuwirt H, Puhr M, Santer FR, Susani M, Doppler W, et al. (2009) Suppressor of cytokine signaling (SOCS)-1 is expressed in human prostate cancer and exerts growth-inhibitory function through down-regulation of cyclins and cyclin-dependent kinases. Am J Pathol 174: 1921–1930.
67. Spiewak Rinaudo JA, Thorgeirsson SS (1997) Detection of a tyrosine-phosphorylated form of cyclin A during liver regeneration. Cell Growth Differ 8: 301–309.
68. Bouzahzah B, Nagajyothi F, Desruisseaux MS, Krishnamachary M, Factor SM, et al. (2006) Cell cycle regulatory proteins in the liver in murine Trypanosoma cruzi infection. Cell Cycle 5: 2396–2400.
69. Liance M, Vuitton DA, Guerret-Stocker S, Carbillet JP, Grimaud JA, et al. (1984) Experimental alveolar echinococcosis. Suitability of a murine model of intrahepatic infection by Echinococcus multilocularis for immunological studies. Experientia 40: 1436–1439.
70. Bresson-Hadni S, Monnot-Jacquard B, Racadot E, Lenys D, Miguet JP, et al. (1991) Soluble IL-2-receptor and CD8 in the serum and the periparasitic granuloma of patients with alveolar echinococcosis. Eur Cytokine Netw 2: 339–344.
71. Bresson-Hadni S, Vuitton DA, Lenys D, Liance M, Racadot E, et al. (1989) Cellular immune response in Echinococcus multilocularis infection in humans. I. Lymphocyte reactivity to Echinococcus antigens in patients with alveolar echinococcosis. Clin Exp Immunol 78: 61–66.
72. Nicod L, Bresson-Hadni S, Vuitton DA, Emery I, Gottstein B, et al. (1994) Specific cellular and humoral immune responses induced by different antigen preparations of Echinococcus multilocularis metacestodes in patients with alveolar echinococcosis. Parasite 1: 261–270.
73. Vuitton DA, Bresson-Hadni S, Laroche L, Kaiserlian D, Guerret-Stocker S, et al. (1989) Cellular immune response in Echinococcus multilocularis infection in humans. II. Natural killer cell activity and cell subpopulations in the blood and in the periparasitic granuloma of patients with alveolar echinococcosis. Clin Exp Immunol 78: 67–74.

74. Zhang S, Hue S, Sene D, Penfornis A, Bresson-Hadni S, et al. (2008) Expression of major histocompatibility complex class I chain-related molecule A, NKG2D, and transforming growth factor-beta in the liver of humans with alveolar echinococcosis: new actors in the tolerance to parasites? J Infect Dis 197: 1341–1349.
75. Gottstein B, Mesarina B, Tanner I, Ammann RW, Wilson JF, et al. (1991) Specific cellular and humoral immune responses in patients with different long-term courses of alveolar echinococcosis (infection with Echinococcus multilocularis). Am J Trop Med Hyg 45: 734–742.
76. Bresson-Hadni S, Vuitton DA, Bartholomot B, Heyd B, Godart D, et al. (2000) A twenty-year history of alveolar echinococcosis: analysis of a series of 117 patients from eastern France. Eur J Gastroenterol Hepatol 12: 327–336.
77. Fremin C, Ezan F, Boisselier P, Bessard A, Pages G, et al. (2007) ERK2 but not ERK1 plays a key role in hepatocyte replication: an RNAi-mediated ERK2 knockdown approach in wild-type and ERK1 null hepatocytes. Hepatology 45: 1035–1045.

Main conclusions and remarks:

1) Within the early (day 2–60) and middle (day60–180) stages, CyclinB1 and CyclinD1 gene expression increased up to day30 and then returned to control level after day60; Gadd45b, CyclinA and PCNA increased all over the period.

2) ERK1/ 2 was permanently activated.

3) Meanwhile, p53, p21 and Gadd45c gene expression, and caspase 3 activation, gradually increased in a time-dependent manner.

4) In the late stage (day180–360), p53, p21 and Gadd45c gene expression were significantly higher in infected mice; JNK and caspase 3 were activated. TUNEL analysis showed apoptosis of hepatocytes.

5) No significant change in Cyclin E, p53 mRNA and p-p38 expression were observed at any time.

5. What is the dynamics of cytokine/chemokine expression in the periparasitic immune infiltrate and adjacent liver?

To address this question, we employed the intra-hepatic AE mouse model and assessed the hepatic gene expression profiles of 18 selected cytokine and chemokine genes using qRT-PCR in the periparasitic immune reaction and the subsequent adjacent, not directly affected, liver tissue of mice from day 2 to day 360 post intra-hepatic injection of metacestode. DNA microarray analysis was also used to get a more complete picture of the transcriptional changes occurring in the liver surrounding the parasitic lesions.

Background and objectives:

The periparasitic granuloma is a major characteristic of AE pathology in humans and in experimentally infected mice. Despite the alleged responsibility of the granulomatous response in the images obtained by functional imaging techniques (e.g. through Fluoro-deoxy-glucose-Positron Emission Tomography) and their well-known role in the complications of AE, a comprehensive picture of the cytokine/chemokine immune response occurring in situ, in the periparasitic granuloma, had never been evidenced experimentally. And although their crucial role in cell homing to the inflammatory reaction sites is well known in other infection models, chemokines and IL-17 had received little attention in *E. multilocularis* infection. Our aims were to 1) give a comprehensive appraisal of the various components, especially cytokines and chemokines, involved in immune cell homing around the *E. multilocularis* metacestode, at the various successive stages of disease, and 2) to study the parasite and the host immune response in their usual context, the liver, in the experimental mouse model of hepatic secondary infection. Eighteen key-cytokines and -chemokines were measured both in the lesion, including the periparasitic infiltrate, and in the surrounding liver, close to the lesions, using qRT-PCR.

Transcriptional profiles of cytokine/chemokine factors of immune cell-homing to the parasitic lesions: a comprehensive one-year course study in the liver of *E. multilocularis*-infected mice

Running title: Cytokine/chemokine transcriptional profiles in AE

Junhua Wang[1,2,3#], Renyong Lin[1#], Wenbao Zhang[1], Liang Li[1], Bruno Gottstein[3], Oleg Blagosklonov[3], Guodong Lü[1], Chuangshan Zhang[1], Xiaomei Lu[1], Dominique A. Vuitton[4]*, Hao Wen[1]*

1. State Key Lab Incubation Base for Xinjiang Major Diseases Research and Xinjiang Key Laboratory of Echinococcosis, First Affiliated Hospital of Xinjiang Medical University, Urumqi, Xinjiang, China
2. Department of Nuclear Medicine, University of Franche-Comté and Jean Minjoz University Hospital, Besançon, Franche-Comté, France
3. Institute of Parasitology, University of Bern, Bern, Switzerland
4. WHO-Collaborating Centre for the Prevention and Treatment of Human Echinococcosis, University of Franche-Comté and University Hospital, Besançon, Franche-Comté, France

1. Correspondence to: Professor Hao Wen, State Key Lab Incubation Base of Xinjiang Major Diseases Research and Xinjiang Key Laboratory of Echinococcosis (2010DS890294), First Affiliated Hospital of Xinjiang Medical University, No.1 Liyushan Road, Urumqi 830054, P.R. China.
E-mail address: Dr.wenhao@163.com
Tel: +86 991 436 2844
Fax: +86 991 436 0051

2. Correspondence to: Professor Dominique A Vuitton, WHO-Collaborating Centre for the Prevention and Treatment of Human Echinococcosis, University of Franche-Comté, place Saint Jacques, 25030 Besancon, France.
E-mail address: dvuitton@univ-fcomte.fr
Tel/Fax: + 33 3 81 66 55 70

# The first two authors contributed equally to this work.

Funding: This work was supported by NSFC Grant Projects (81260452, 81260252), the Swiss National Science Foundation (31003A_141039/1), the Program for Changjiang Scholars and Innovative Research Team in Universities (IRT1181), and Xinjiang Key-Lab Projects (SKLIB-XJMDR-2012-Y1).The funders had no role in study design, data collection and analysis, decision to publish, or preparation of the manuscript.

Abstract

Pathogenesis of chronically developing alveolar echinococcosis (AE) is characterized by a continuous, granulomatous, periparasitic infiltration of immune cells surrounding the metacestode of *Echinococcus multilocularis (E.multilocularis)* in the affected liver. A detailed cytokine and chemokine profile analysis of the periparasitic infiltrate in the liver has, however, not yet been carried out in a comprehensive way all along the whole course of infection in *E. multilocularis* intermediate hosts. We thus assessed the hepatic gene expression profiles of 18 selected cytokine and chemokine genes using qRT-PCR in the periparasitic immune reaction and the subsequent adjacent, not directly affected, liver tissue of mice from day 2 to day 360 post intra-hepatic injection of metacestode. DNA microarray analysis was also used to get a more complete picture of the transcriptional changes occurring in the liver surrounding the parasitic lesions. Profiles of mRNA expression levels in the hepatic parasitic lesions showed that a mixed Th1/Th2 immune response, characterized by the concomitant presence of IL-12α, IFN-γ and IL-4, was established very early in the development of *E. multilocularis*. Subsequently, the profile extended to a combined tolerogenic profile associating IL-5, IL-10 and TGF-β. IL-17 was permanently expressed in the liver, mostly in the periparasitic infiltrate; this was confirmed by the increased mRNA expression of both IL-17A and IL-17F from a very early stage, with a subsequent decrease of IL-17A after this first initial rise. All measured chemokines were significantly expressed at a given stage of infection; their expression paralleled that of the corresponding Th1, Th2 or Th17 cytokines. In addition to giving a comprehensive insight in the time course of cytokines and chemokines in *E. multilocularis* lesion, this study contributes to identify new targets for possible immune therapy to minimize *E. multilocularis*-related pathology and to complement the only parasitostatic effect of benzimidazoles in AE.
Key words: Cytokines; Chemokines; IL-17; *E. multilocularis*

Author summary

Previous studies on peripheral lymphocytes showed that a specific time-dependent cytokine secretion evolved during the course of progressing AE in mice, with an initial Th1 profile, followed by a combined Th1-Th2 one. However, such a course had not yet been studied in the liver, in the periparasitic immune infiltrate surrounding the parasitic vesicles. Chemokines as well as IL-17 which are likely to be involved in the homing and persistence of inflammatory cells in the periparasitic area, had never been studied. Our data yield a dynamic and comprehensive picture of the immunological process characteristic of *E. multilocularis* infection. It shows that the combined cytokine profile associating IL-12α, IFN-γ but also the "starter-Th2 cytokine", IL-4, is established very early in the periparasitic infiltrate, and that subsequent decrease in IL-12α and TNF-α is accompanied by tolerogenic profile, IL-10, IL-5 and TGF-β. For the first time, it shows the major involvement of different chemokines and of IL-17. These results represent the basis of knowledge on which complementary studies focused onto individual components of the immune response to *E. multilocularis* may be designed. They will also serve as a basis to design immune manipulations that could be used for the treatment of AE in patients.

Introduction

Alveolar echinococcosis (AE) is a rare, but - if remaining untreated or treated too late- severe and fatal zoonotic helminthic disease, predominantly caused not only by the direct hepatic damage which follows the continuous tumor-like proliferation of the larval stage (metacestode) of *Echinococcus multilocularis (E.multilocularis),* but also indirectly by the intense local granulomatous immune response which surrounds the parasitic tissue [1]. Granuloma, extensive fibrosis, and necrosis are actually the characteristic pathological findings in *E. multilocularis* infection. The lesions, composed both of the multiple vesicle-forming metacestode and of cells homing from lymphoid organs and permanently settling around the metacestode, behave like a slow-growing liver cancer, progressively invading the liver, then the neighboring tissues and also metastazing to other organs [2]. Pathological changes in AE are associated with an intense infiltration by immune cells, i.e. macrophages of various functional types, including the so-called "epithelioid cells" and "giant cells", typical of granulomas [3] and T lymphocytes. $CD4^+$ T lymphocytes are present from the early stage of parasite growth and $CD8^+$ T lymphocytes are known to home to the periparasitic infiltrate secondarily and to be associated with parasite tolerance and severity of the disease [1,2,3,4]. Non-immune cells such as fibroblasts and myofibroblasts which are crucial for the development of fibrosis are also attracted by the host's immune response around the parasite.

It has been shown that *E. multilocularis* infection induced numerous pathways of the immune response; the involvement of individual cytokines has been rather extensively studied within the past 2 decades both in humans and in experimental rodents [1]. In the immune-competent but susceptible host, *E. multilocularis* induces skewed Th2-responses [5]. In chronic AE, Th2-dominated immunity is associated with increased susceptibility to disease, while Th1 cell activation induces a rather protective immunity which involves IFN-α [6] and IL-12 [7] as initiating cytokines, and IFN-γ [8] and TNF-α [9,10] as effector cytokines. During the course of *E. multilocularis* infection, as studied in mice, an initial acute stage Th1 response gradually switches to an increasingly dominating Th2 response; the thus mostly mixed Th1/Th2 profile of the chronic stage is associated with the expression of pro-inflammatory cytokines in the granuloma [11,12]. Th2 cytokines down-modulate the Th1 response which nevertheless decreasingly persists all along the infection until the late pre-mortem immune-suppressed stage of AE [11]. The metacestode actively achieves a tolerance status through the induction of regulatory cytokines, such as IL-10 and TGF-□β [11]. However, this bulk of information has mostly been obtained from studies on peripheral blood mononuclear cells (in humans), and on spleen and

lymph node cells in the experimental model [5,13,14]. In addition, nothing was known until very recently about role of IL-17 and Th17 cells [13,14] during *E. multilocularis* infection. Only two studies have given some insight into chemokine [15,16] and IL-17 [17] involvement in *E. multilocularis* infection, respectively; and this was done only in AE patients, and never in the infected liver tissue; the actual involvement of IL-17 and chemokines in the lesions is thus unknown. The time course of IL-17 expression is also unknown since human AE is usually discovered late, i.e. years after *E. multilocularis* infection of the patients, and findings in humans reflect only the late chronic stage of infection. Studies in the experimental mouse model are therefore necessary to dissect the various stages of *E. multilocularis* infection regarding the host's immune response.

In the present report, our objectives were to 1) give a comprehensive appraisal of the various components, especially cytokines and chemokines, involved in immune cell homing around the *E. multilocularis* metacestode, at the various successive stages of disease, i.e. early, middle and late stages as defined previously [18,19], and 2) to study the parasite and the host immune response in their usual context, the liver, in the experimental mouse model of hepatic secondary infection. Eighteen key-cytokines and -chemokines were measured both in the lesion, including the periparasitic infiltrate, and in the surrounding liver, close to the lesions, using qRT-PCR. To get a more complete picture of the influence of the parasite-induced host's immune response on the host's liver, a microarray technique was also used to study the surrounding liver tissue.

Materials and methods

Ethics Statement

The animal study was performed in strict accordance with the recommendations in the Guide for the Care and Use of Laboratory Animals. The protocol was approved by the Animal Care and Use Committee and the Ethical Committee of First Affiliated Hospital of Xinjiang Medical University (20081205-2). All surgery was performed under sodium pentobarbital anesthesia, and every effort was made to minimize suffering.

Mice and experimental design

Pathogen-free female BALB/c mice (8–10-week old) purchased from the Animal Center of Xinjiang Medical University (accredited by the ALLLAC) were housed in cages with a 12-h light/dark cycle and provided with conventional rodent chow and water ad libitum. All animals received human care in compliance with the Medical Research Center's guidelines, and animal procedures were approved by the Animal Care and Use Committee and the Ethical Committee of First Affiliated Hospital of

Xinjiang Medical University. *Echinococcus multilocularis* (*E. multilocularis*) metacestodes were obtained from intraperitoneal lesions maintained in *Meriones unguiculatus*, and 0.1 mL of pooled lesion suspension was injected into the anterior liver lobe of mice to be experimentally infected. For each autopsy time-point, eight experimentally infected mice were used in the *E. multilocularis* group (n=8) and compared with five control mice (n=5), which received an intra-hepatic injection of 0.1 mL sterile saline solution into the anterior liver lobe using the same surgical procedure. Mice were killed at 2, 8, 30, 60, 90, 180, 270 and 360 days p.i., respectively.

Tissue sampling of the parasitic lesion and surrounding granuloma, and of adjacent non-affected (periparasitic) liver tissue; and histological examination

In *E. multilocularis* infected mice, liver samples were taken both from (1) the parasitic lesion (including liver tissue directly adjacent by 1 mm to the macroscopically visible parasitic lesion, subsequently designated as "parasitic lesion tissue") for qRT-PCR, histopathology and immunohistochemistry (Zhang, 2012); and from (2) the liver tissue relatively close to the lesion (subsequently designated as "periparasitic liver tissue"), i.e. starting 2 mm from the macroscopic changes due to the metacestode/granuloma lesion, thus avoiding gross contamination of liver tissue by parasitic *E.multilocularis* tissue/cells and correspondingly involved infiltrating host immune cells, for both qRT-PCR and microarray analyses. Tissue fragments were directly deep-frozen in liquid nitrogen. Control samples were taken from the same (anterior) liver lobe from non-infected control mice.

RNA extraction and cDNA synthesis

'Lesion' and 'periparasitic liver' tissue samples of each mouse were processed and analyzed separately. Approximately 50 mm^3 –sized tissue samples from *E. multilocularis* infected mice or same size liver tissue samples from control mice were used to extract total RNA using TRIzol reagent (Invitrogen, Gaithersburg, MD, USA). The quality of RNA was confirmed by formaldehyde agarose gel electrophoresis, and the concentration of RNA was determined by reading the absorbance at 260/280nm. cDNA was synthesized from 1μg of RNA in the presence of ribonuclease inhibitor (Promega, Shanghai, China), dNTPs, Oligo(dT) 18 primers, and RevertAid™ M-Mulv reverse transcriptase in a total of 25 μL reaction mix.

Quantitative real-time RT-PCR

qRT-PCR was run in a thermocycler (iQ5 Bio-Rad, Hercules, CA, USA) with the SYBR Green PCR premix (Qiagen, Hilden, Germany) following the manufacturer's instructions. Thermocycling was performed in a final volume of 20 μL containing 2 μL cDNA and 10 pM of each primer (Table 5.1). To normalize for gene expression, mRNA expression of the housekeeping gene β-actin was measured in parallel. For every sample, both the housekeeping and the target genes were

amplified in triplicate using the following cycle scheme: after initial denaturation of the samples at 95 °C for 1 min, 40 cycles of 95 °C for 5 s and 60 °C (or other) for 30 s were performed. Fluorescence was measured in every cycle, and a melting curve was analyzed after the PCR by increasing the temperature from 55 to 95 °C (0.5 °C increments). A defined single peak was obtained for all amplicons, confirming the specificity of the amplification.

Table 5.1 Primers and cycling parameters of qRT-PCR

Gene	Gene bank accession	Primer Sequences	Annealing temperature	Expected Size
β-actin	NM_007393	F:5'-AACTCCATCATGAAGTGTGA-3' R:5'-ACTCCTGCTTGCTGATCCAC-3'	60.0 °C	248bp
TNF-α	NM_013693.2	F: 5'- TATGGCCCAGACCCTCACA-3' R: 5'-GGAGTAGACAAGGTACAACCCATC-3'	60.0 °C	199bp
IL-1β	NM_008361.3	F: 5'-ATCTCGCAGCAGCACATC-3' R: 5'-CCAGCAGGTTATCATCATCATC-3'	60.0°C	193bp
IL-6	NM_031168.1	F: 5'-TTCCATCCAGTTGCCTTCTTG-3' R: 5'-TCATTTCCACGATTTCCCAGAG-3'	60.0 °C	176bp
IFN-γ	K00083.1	F: 5'-ACTCAAGTGGCATAGATGTGGAAG-3' R: 5'-GACGCTTATGTTGTTGCTGATGG-3'	60.0°C	167bp
CXCL9	NM_008599.4	F: 5'-CTGGAGCAGTGTGGAGTTC-3' R: 5'-CCGTTCTTCAGTGTAGCAATG-3'	60.0°C	167bp
CXCL10	NM_021274.1	F: 5'-TTCTGCCTCATCCTGCTG-3' R: 5'-AGACATCTCTGCTCATCATTC-3'	60.0°C	200bp
CXCL12	NM_021704.3	F: 5'-CAGAGCCAACGTCAAGCATC-3' R: 5'-CGTCTTATCCAAGTGGTTTATGGAA-3'	60.0°C	152bp
IL-4	M25892.1	F: 5'-AGTTGTCATCCTGCTCTTC-3' R: 5'-GTGTTCTTCGTTGCTGTG-3'	55.0°C	165bp
IL-5	NM_010558.1	F:5'-TGAGGCTTCCTGTCCCTACTCATAA-3' R:5'-TTGGAATAGCATTTCCACAGTACCC-3'	60.0°C	119bp
CCL8	NM_021443.3	F: 5'-CTTTGCCTGCTGCTCATAG-3' R: 5'-GCACTGGATATTGTTGATTCTC-3'	60.0°C	150bp
CCL12	NM_011331.2	F: 5'-GCTACCACCATCAGTCCTC-3' R: 5'-CTGGCTGCTTGTGATTCTC-3'	60.0°C	135bp
CCL17	NM_011332.3	F: 5'-TCAGTGGAGTGTTCCAGGGATG-3' F: 5'-GGCGTCTCCAAATGCCTCA-3'	60.0°C	151bp
IL-17A	NM_010552.3	F: 5'-GTGTCTCTGATGCTGTTG-3' R: 5'-AACGGTTGAGGTAGTCTG-3'	60.0°C	193bp
IL-17F	NM_145856.2	F:5'-GTCGCCATTCAGCAAGAAAT-3' R: 5'-CAGCCAACTTTTAGGAGCATCT-3'	60.0°C	
Foxp3	NM_054039.1	F: 5'-GAGAGGCAGAGGACACTCAATG-3' R: 5'-GCTCAGGTTGTGGCGGATG-3'	60.0°C	108bp
TGF-β 1	NM_011577	F:5'-GTGTGGAGCAACATGTGGAACTCTA-3' R: 5'-TTGGTTCAGCCACTGCCGTA-3'	60.0°C	143bp

IL-10	NM_010548.2	F:5'-GCCAGAGCCACATGCTCCTA-3' R:5'-GATAAGGCTTGGCAACCCAAGTAA-3'	60.0°C	145bp

Microarray data analyses and annotation of gene function

RNA extracts from 3 infected and 3 control mice were selected for array hybridization, corresponding to 30 days, 60 days, 90 days and 180 days after infection. Total RNA was purified with NucleospinH RNA Clean-up Kit (Macherey-Nagel, Germany) and each purified RNA sample isolated from an individual sample was run on a single microarray. All microarray procedures were done according to a previously described procedure [22].

Immunohistochemical analyses

Immunohistochemistry was performed on formalin-fixed, paraffin-embedded tissue: 4μm tissue sections were de-paraffinized in xylene and rehydrated in gradual dilutions of ethanol. Endogenous peroxidase was blocked with 3% hydrogen peroxide. To increase staining, sections were pre-treated by microwave heating for 15 min in antigen unmasking solution (pH 6.8, 0.1 M citrate buffer, Zhongshan Jinqiao Biology Corporation, Beijing). To block non-specific background, the sections were incubated with non-immune goat serum for 30 min. Sections were then incubated overnight at $4^{o}C$ with the primary antibody diluted in pH 7.3 phosphate-buffered saline (PBS) (IL-17 1:100 (Santa Cruz Corporation, CA, USA). After 3 washes in PBS, the sections were subsequently incubated with horseradish peroxidase conjugated host-specific secondary antibodies and 3,3'-diaminobenzidine was used as chromogen. Sections were counterstained with hematoxylin for 5 min, dehydrated, and covered with slips. For all samples, negative controls consisted of substitution of the isotype-matched primary antibody with PBS.

Expression of the data and statistical analysis

Immunostaining for IL-17 was semi-quantified by calculating "expression scores" that consider both staining intensity and the percentage of cells stained at a specific range of intensities. A score of zero indicated the percentage of positive cells < 5%, 1+ = 5–25%, 2+ =25–50%, 3+ =50–75%, 4+ >75%. The staining intensity of each specimen was judged relative to the intensity of a control slide including an adjacent section stained with an irrelevant negative control antibody that was matched by species and isotype to the specimen. Staining of the section labelled with the negative reagent control was considered as background. A score of zero indicated no staining relative to background, 1 + = weak staining, 2 + = moderate staining, and 3 + =strong staining. According to standard pathology practices, staining intensity was reported at the highest level of intensity observed in all tissue elements, except the distinctive tissue element for which an expanded scoring scheme was reported. The

“expression scores” were calculated by multiplying the percentage of positive cells (0–4) and the staining intensity scores (0–3). For example: for a specimen with 30% of positive cells (3+), and a moderate staining intensity (2+), the “expression score”was3×2=6. Three pathologists read the sections and established the scores, and they were blinded to each other's results. Cells with a positive immunostaining were counted in five random visual fields of 0.95 square mm each, at initial magnification: x 20, for each sample.

All the data were analysed by SPSS 17.0. mRNA expression of the various cytokines, chemokines, and other components of the immune response of *E. multilocularis* infected mice were compared to the results obtained on the liver samples taken from control mice in the sham-infected liver lobe at the same time point. The results were presented as means ± SD. One-way ANOVA and Student’s *t*-test were used to compare the differences between groups, and Spearman’s rho was used to analyse the correlation coefficients. $P< 0.05$ was considered to indicate statistical significance.

Results

Hepatic histopathology during *E. multilocularis*-infection

From day 2 to day 360 post-infection (p.i.) with *E. multilocularis*, the hepatic parasitic lesions showed the various morphological patterns specific to the different stages of murine AE, as described in a previous study using the same experimental mice (data not shown) [18,19]. According to previous reports on the course of *E. multilocularis* secondary infection in experimental susceptible mice [18,19], the 3 main stages were defined as follows: early stage, from infection to day 60; middle stage from day 60 to day 180; and late stage from day 180 to day 360.

Innate immunity and pro-inflammatory cytokines

In *E. multilocularis* ‘parasitic lesions’ (i.e. including adjacent infiltrates, as defined in the Materials and Methods section), qRT-PCR showed that IL-12α mRNA expression was 6.3-fold higher at as early as day 2 p.i. than in control mice (Figure 5.1A). There was a significant difference between *E. multilocularis*-infected mice and control mice, at the early stage of infection, at time points of 2-, 8- and 30-day p.i. ($P< 0.05$). In the ‘periparasitic liver tissue’ (i.e. liver parenchyma close to the lesions, as defined in the Materials and Methods section), IL-12α mRNA expression was also higher than in control livers from day 8 to day 30 p.i.. There was a significant difference at 30-days p.i. ($P< 0.05$). Changes in IL-12α mRNA expression with time are shown in Figure 5.1A.

In *E. multilocularis* lesions, qRT-PCR showed that TNF-α mRNA expression

was increased at the early stage of infection, especially at days 2 and 8 p.i.; it remained high at 30 days p.i. but decreased subsequently (Figure 5.1B). There was a significant difference between *E. multilocularis* infected mice and control mice, at the time points of 2-, 8- and 30-day p.i. ($P< 0.05$). In the periparasitic liver tissue, TNF-α mRNA expression did not change from day 2 to day 360 (Figure 5.1B). In the lesions, there was an increase in IL-1β mRNA expression all over the infection course, from day 2 to day 360 p.i., with a peak at 60 days p.i.. IL-1β mRNA expression was 2.5-fold higher at day 2 and 7.6-fold higher at day 60 (Figure 5.1C), when compared to control mice. There was a significant difference between *E. multilocularis* infected mice and control mice, at the time points of 30-, 60-, 90-, 270- and 360-days p.i. ($P< 0.05$). In the liver tissue, IL-1β mRNA expression increased later, from 2.9-fold at day 30 to 4.7-fold at day 90 (Figure 5.1C), and was at its maximum at the middle stage of infection. There was a significant difference at the time points of 30-, 60- and 90-days p.i. ($P< 0.05$). In the lesions, IL-6 mRNA expression was markedly increased as early as 2 days; then it relatively decreased at day 30 p.i., then re-increased very significantly from day 90 p.i. (4.8-fold) (Figure 5.1D). There was a significant difference between *E. multilocularis* infected mice and control groups, at the time points of 2-, 60-, 90-, 180- and 360-days p.i. ($P< 0.05$). In the liver, IL-6 mRNA expression increased at the very early stage of infection, 1.8-fold at day 2 and1.9-fold at day 8 (Figure 5.1D); it returned back to normal at day 30, and re-increased from day 60 to day 90, then a high level was maintained until day 360.

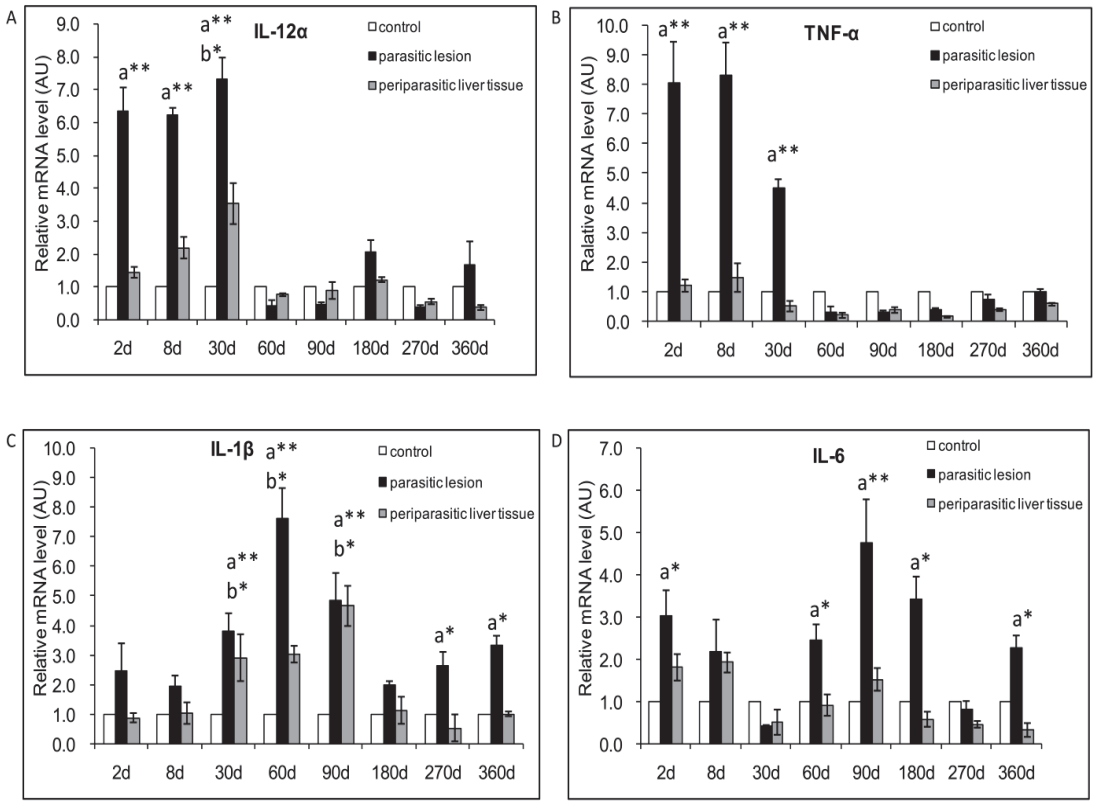

Figure 5.1 IL-12α and pro-inflammatory cytokine gene expressions in the liver of mice during *E. multilocularis* infection

Course of IL-12α mRNA expression measured by q RT-PCR (A).Course of TNF-α mRNA expression measured by qRT-PCR (B).Course of IL-1β mRNA expression measured by q RT-PCR (C).Course of IL-6 mRNA expression measured by qRT-PCR (D).

a: 'Parasitic lesion' versus 'Control'; b: 'Periparasitic liver tissue' versus 'Control'. *P< 0.05; **P< 0.01. 'Control', non-infected mice; 'Parasitic lesion': *E. multilocularis* metacestode and surrounding immune infiltrate; 'Periparasitic liver tissue: liver parenchyma close to the *E. multilocularis* lesion, but excluding macroscopically visible liver tissue alterations.

AU: arbitrary units.

Th1 cytokines and related chemokines

Th1 cytokines

In the lesions, an increase in IFN-γ mRNA expression was observed from day 2 to day 360 p.i., with a peak at 30 days p.i.. Except for an apparent decrease at day 8, IFN-γ mRNA-expression was especially increased at the early stage of infection, from 3.6-fold at day 2 to 4.8-fold at day 30 (Figure 5.2A). There was a significant difference between *E. multilocularis* infected mice and control mice, at the time points of 2-, 30-, and 60-day p.i., but also at the latest stage, 360- day p.i. (P< 0.05). In the liver, IFN-γ mRNA expression was increased from 2.4-fold at day 2 to 3.1-fold

at day 30 (Figure 5.2A), but became abrogated at the late stage of infection, from 0.5-fold at day 90 to 0.4 at day 360, compared to control mice. There was a significant difference at the time point of 30-day p.i. ($P< 0.05$).

Th1-related chemokines

Expression of CXCL9 mRNA was observed from day 2 to day 360 p.i.. In the lesions, CXCL9 mRNA expression was increased from day 90 to day 360, with a peak of 9.75-fold at day 180 (Figure 2B), compared to control mice. There was a significant difference between *E. multilocularis*-infected mice and control mice, at the time points of 2-, 8-, 90-, 180- and 270-days p.i., i.e. at the late stage of infection ($P< 0.05$). In the liver, CXCL9 mRNA expression was increased by 1.72-fold at day 2 and 2.78-fold at day 8 (Figure 2B); it was decreased by 0.30- fold at day 30 and by 0.21-fold at day 60, then expression re-increased by 3.5- fold at day 90 compared to control mice. There was a significant difference at the time points of 8- and 90-day p.i. ($P< 0.05$). In the lesions of *E. multilocularis*-infected mice, CXCL10 mRNA expression was increased by 1.6-fold at day 2; then levels progressively increased to a peak (7.8-fold the levels in control mice) at day 90 p.i. (Figure 5.2C). There was a significant difference between *E. multilocularis* infected mice and control mice, at the time points of 30-, 60- and 90-days p.i. ($P< 0.05$), i.e. at the middle stage of infection. In the liver, CXCL10 mRNA expression was increased at day 60 (2.1-fold) and at day 90 (2.2-fold) (Figure 5.2C), and was lower both at the early stage and the late stage of infection when compared to control mice. Expression of the mRNA of CXCL12, a chemotactic factor for lymphocytes, was observed from day 2 to day 360 p.i.. In the lesions, CXCL12 mRNA expression was markedly increased as early as day 2 post-infection, when it reached a peak (11.6-fold); it remained elevated until day 60 (Figure 5.2D). There was a significant difference between *E. multilocularis* infected mice and control groups, at the time points of 2-, 8- and 60-days p.i. ($P< 0.05$). In the liver, CXCL12 mRNA expression was increased early, from 1.1-fold at day 2 to 2.1-fold at day 8 (Figure 5.2D), and was lower than that observed in control mice at the late stage, from day 90 to day 360. There was a significant difference at the time points of 8- and 270-days p.i. ($P< 0.05$).

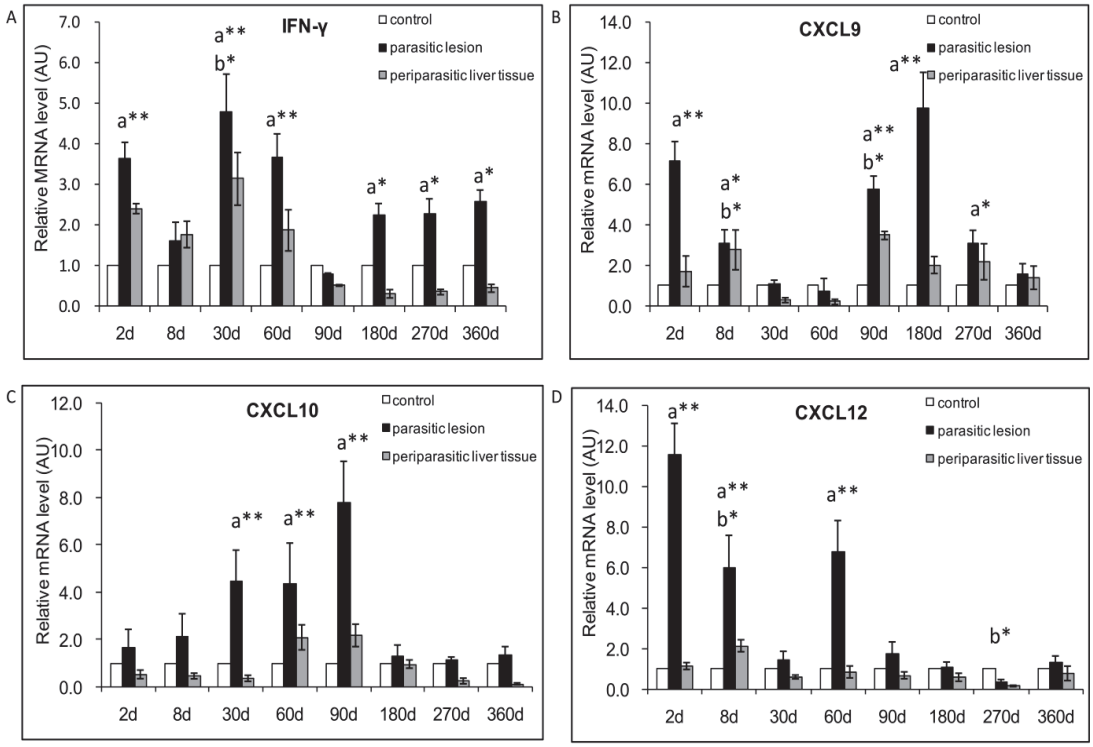

Figure 5.2 Th1-cytokine and related chemokine gene expressions in the liver of mice during *E. multilocularis* infection

Course of IFN-γ mRNA expression measured by qRT-PCR (A). Course of CXCL9 mRNA expression measured by qRT-PCR (B). Course of CXCL10mRNA expression measured by qRT-PCR (C). Course of CXCL12 mRNA expression was measured by qRT-PCR (D).

a: 'Parasitic lesion' versus 'Control'; b: 'Periparasitic liver tissue' versus 'Control'. **P*<0.05; ***P*<0.01. 'Control', non-infected mice; 'Parasitic lesion': *E. multilocularis* metacestode and surrounding immune infiltrate; 'Periparasitic liver tissue: liver parenchyma close to the *E. multilocularis* lesion, but excluding macroscopically visible liver tissue alterations.

AU: arbitrary units.

Th2 cytokines and related chemokines

Th2 cytokines

In *E. multilocularis* lesions, IL-4 mRNA expression followed a biphasic curve: it was increased early (3.8-fold at day 2), and was significantly different from that observed in control mice at 2 and 8 days; but it relatively decreased at 30 p.i.; it then re-increased and was still elevated at the late stage [4.2-fold at day 360; significantly different from control mice ($P< 0.05$). (Figure 5.3A)]. In the liver, IL-4 mRNA expression was increased compared to control mice [4.8-fold at day 8 and 3.2-fold at day 60, significantly different from control mice ($P< 0.05$) (Figure 5.3A)]. In *E. multilocularis* lesions, IL-5 mRNA expression was present from the early stage

(2.3-fold at day 2); however (Figure 5.3B), there was a peak of 13.6-fold at day 90, and a significant difference between *E. multilocularis* infected mice and control mice, all over the middle and late stages of infection, at the time points of 60-, 90-, 180- and 360-days p.i. ($P< 0.05$). In the liver, IL-5 mRNA expression was also markedly increased at the middle stage of infection: 3.5-fold at day 60 and 6.54-fold at day 90 (Figure 5.3B). There was a significant difference at the time points of 60- and 90-days p.i. ($P< 0.05$).

Th2-related chemokines

In the lesions, mRNA expression of CCL8, chemotactic for and activator of various immune cell types, including mast cells, eosinophils and basophils, monocytes, T cells, and NK cells [22], was increased from day 2 to day 360 p.i., with a peak at day 90 (Figure 5.3C). There was a significant difference between *E. multilocularis* infected mice and control mice, at the very early and at the middle stage of infection, at the time points of 8- and 90-days p.i. ($P< 0.05$). In the liver, there was no difference in CCL8 mRNA expression from day 2 to day 360 (Figure 5.3C) between infected and control mice. In the lesions, mRNA expression of CCL12, another Th2-related chemokine, which attracts eosinophils, monocytes and lymphocytes [25], increased early, from 2.0-fold at day 2 to 6.6-fold at day 8 p.i. when it became significantly different from control mice (Figure 5.3D); levels were also elevated at day 90 p.i. (3.5-fold; also significantly different from control mice). In the liver, CCL12 mRNA expression did not change from day 2 to day 360 (Figure 5.3D), compared to control mice. mRNA expression of CCL17, which induces T-cell chemotaxis and elicits its effects by interacting with the chemokine receptor CCR4, was observed in the lesions (1.7- fold increase at day 2 and 2.0-fold at day 180 p.i.), (Figure 5.3E). There was a significant difference between *E. multilocularis* infected mice and control groups, at the time points of 8-, 60- and 90-days p.i., when its expression peaked at 3.7 fold ($P< 0.05$). A slight decrease in CCL17 mRNA expression was observed at day 30 p.i., concomitant to the slight decrease also observed for the Th2-related cytokines IL-4 and IL-5. In the liver, CCL17 mRNA expression was higher than in control mice from day 2 to day 180 (Figure 5.3E). There was a significant difference at 90-days p.i. between infected and control mice ($P< 0.05$).

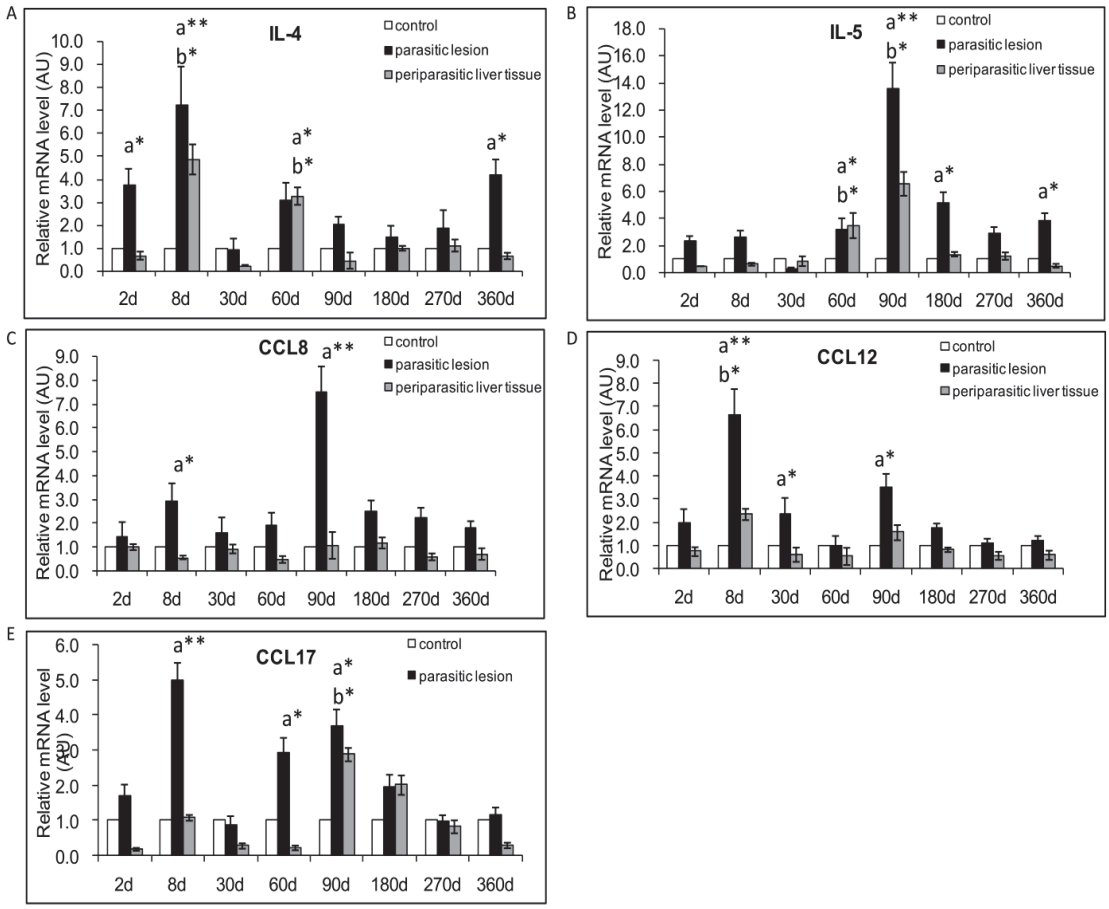

Figure 5.3 Th2-cytokine and related chemokine gene expressions in the liver of mice during *E. multilocularis* infection

Course of IL-4 mRNA expression measured by qRT-PCR (A). Course of IL-5 mRNA expression measured by qRT-PCR (B). Course of CCL8 mRNA expression measured by qRT-PCR (C).Course of CCL12 mRNA expression measured by qRT-PCR (D). Course of CCL17 mRNA expression was measured by qRT-PCR (E).

a: 'Parasitic lesion' versus 'Control'; b: 'Periparasitic Liver tissue' versus 'Control'. **P*<0.05; ***P*<0.01. 'Control', non-infected mice; 'Parasitic lesion': *E. multilocularis* metacestode and surrounding immune infiltrate; 'Periparasitic liver tissue: liver parenchyma close to the *E. multilocularis* lesion, but excluding macroscopically visible liver tissue alterations.

AU: arbitrary units.

Th17 cytokines

IL-17 and its isotypes

In the periparasitic infiltrate area, IL-17, disclosed by immunostaining (Figure 4A), was observed in most lymphocytes and macrophages in the periparasitic infiltrate, as well as in fibroblasts, and endothelial cells in hepatic sinusoids, especially around the granulomas, and in infiltrating immune cells of portal spaces,

from day 8 to day 360 p.i.. IL-17 positive scores ranged from 0.13 to 4.80 and reached the peak point at day 90p.i. (Figure 5.4B). In the liver close to the parasite lesions, moderate IL-17 expression was observed; there was a significant difference between AE-infected and sham-injected mice at day-8, -30, -90, 270 and 360p.i..

In *E. multilocularis* lesions, IL-17A mRNA expression was increased at the very early stage of infection, by 6.9-fold at day 2 and by 9.6-fold at day 8 p.i. (Figure 5.4C), and decreased at the late stage, from day 180 to day 360 p.i.. There was a significant difference between *E. multilocularis* infected mice and control groups, at the time points of 2-, 8- and 90-days p.i. ($P< 0.05$). In the liver, IL-17A mRNA expression was also increased at the very early stage: 6.7-fold at day 8; at this time point, the difference was significant (Figure 5.4C) ($P< 0.05$). In the lesion, IL-17F mRNA expression was present all over the infection course, from day 2 to day 360 p.i. (Figure 5.4D), with a peak of 5.63-fold at day 8 compared to control mice. There was a significant difference between *E. multilocularis* infected and control mice, at the time points of 8- and 60-days p.i. ($P< 0.05$). At the late stage, despite an apparent increase, compared to control mice, the difference was not significant. In the liver, IL-17F mRNA expression did not change significantly from day 2 to day 360 (Figure 5.4D).

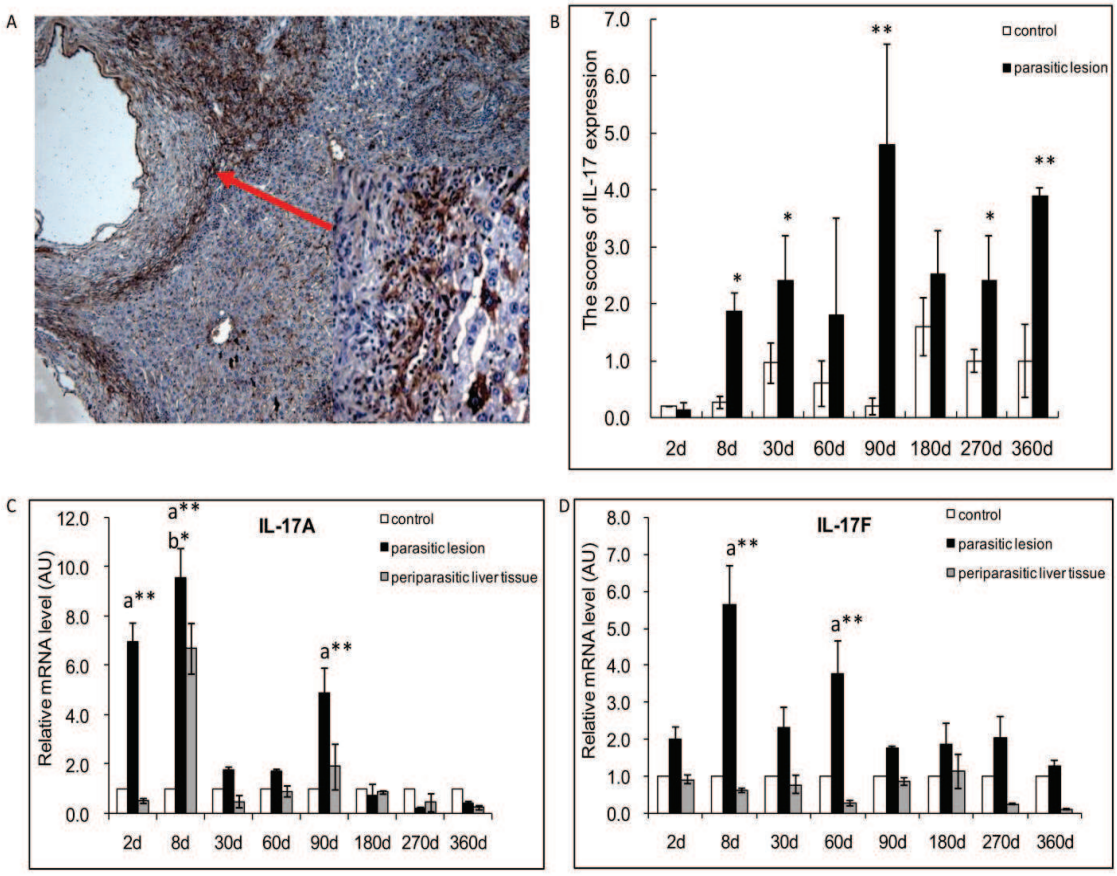

Figure 5.4 Th17-cytokine gene expression in the liver of mice during *E. multilocularis* infection

Course of IL-17AmRNA expression measured by qRT-PCR (A). Course of IL-17F mRNA expression measured by qRT-PCR (B). IL-17 expression at day 90, in most of the infiltrating lymphocytes of areas with inflammatory granulomas, in the cytoplasm of hepatocytes, endothelial cells of the hepatic sinusoids and fibroblasts (*arrow* indicates the area also shown at high magnification) (C). Expression scores of IL-17 was calculated from quantitative analysis of the histo-immunostaining using both staining intensity and the percentage of cells stained at a specific range of intensities (see Materials and Methods section)(D).

a: 'Parasitic lesion' versus 'Control'; b: 'Periparasitic liver tissue'versus 'Control'. *P<0.05; **P<0.01. 'Control', non-infected mice; 'Parasitic lesion': *E. multilocularis* metacestode and surrounding immune infiltrate; 'Periparasitic liver tissue: liver parenchyma close to the *E. multilocularis* lesion, but excluding macroscopically visible liver tissue alterations.

AU: arbitrary units.

Treg-related nuclear transcriptional factor and cytokines

Treg related nuclear transcriptional factor (Foxp3)

In *E. multilocularis* lesions, Foxp3 mRNA expression was increased by 2.4-fold at day 2 and by 3.0-fold at day 8 p.i. (Figure 5.5A); it then decreased from day 30 to

day 60 p.i., and re-increased, from 1.9-fold at day 90 to 2.3-fold at day 360 p.i., with a peak of 3.1-fold at day 180, at the late stage of infection (Figure 5A), thus following a biphasic curve in the course of infection. There was a significant difference between *E. multilocularis* infected mice and control mice, at the time points of 2-, 8-, 180- and 360-days p.i. ($P< 0.05$). In the liver, there was no significant change in Foxp3 mRNA expression (Figure 5.5A).

Treg-related cytokines

In *E. multilocularis* lesions, TGF-β1 mRNA expression also followed a biphasic curve, with a decrease at days 30 and 60 p.i.; it was increased by 3.6-fold at day 2 and 3.2-fold at day 270 p.i. (Figure 5.5B) with a peak of 5.7- fold at day 180 (Figure 5.5B). There was a significant difference between *E. multilocularis* infected mice and control mice, at the early and late stages of infection, at time points of 2-, 8-, 90-, 180-, 270- and 360-day p.i. ($P< 0.05$). In the liver, TGF-β1 mRNA expression was also increased from day 8 to day 360 p.i., with a peak at day 180 p.i.. Conversely to the expression of TGF-β1 mRNA in the lesions, in the liver, TGF-β1 mRNA was significantly elevated at the middle and late stages, at the time points of 90-, 180- and 270-days p.i. ($P< 0.05$). In *E. multilocularis* lesions, IL-10 mRNA expression was also biphasic, with a significant increase at the early and late stages of infection, but not at its middle stage (Figure 5.5C). There was a significant difference between *E. multilocularis* infected mice and control mice, at the time point of 8-day, then at 180-, 270- and 360-days p.i. ($P< 0.05$). In the liver, IL-10 mRNA expression did not change from day 2 to day 360 (Figure 5.5C) compared to control mice.

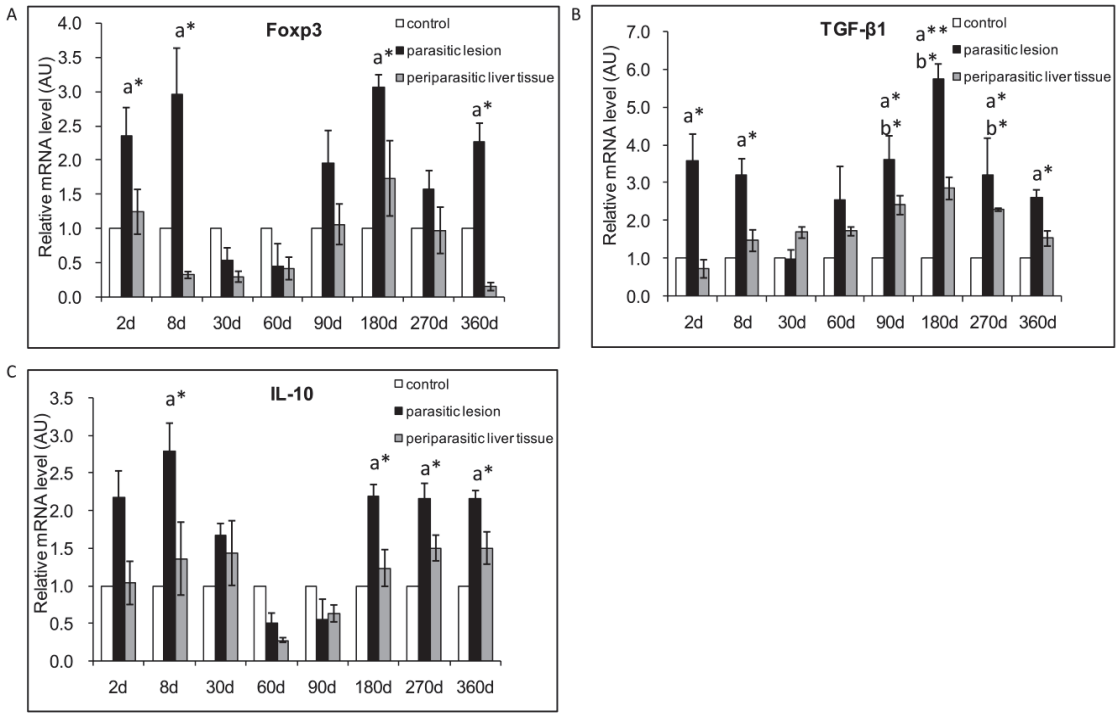

Figure 5.5 Treg transcription factor and Treg-cytokine gene expression in the liver of mice during *E. multilocularis* infection

Course of Foxp3 mRNA expression measured by q RT-PCR (A).Course of TGF-β1 mRNA expression measured by qRT-PCR (B).Course of IL-10 mRNA expression measured by qRT-PCR (C).

a: 'Parasitic lesion' versus 'Control'; b: 'Periparasitic liver tissue' versus 'Control'. **P*<0.05; ***P*<0.01. 'Control', non-infected mice; 'Parasitic lesion': *E. multilocularis* metacestode and surrounding immune infiltrate; 'Periparasitic liver tissue: liver parenchyma close to the *E. multilocularis* lesion, but excluding macroscopically visible liver tissue alterations.

AU: arbitrary units.

Immune response and inflammation gene expression in the liver of *E. multilocularis* infected mice

To further give a comprehensive picture of the immune response-related changes in the adjacent liver during *E. multilocularis* infection, and especially detect hyper-expression of the genes of cytokine/chemokine receptors, cDNA microarray technology was used. The individual genes associated with the gene ontology biological process "immune response", and "pathogen response" assessed at different time periods of infection, i.e. 30, 60, 90, 180 days p.i., are presented in Table 1. We used Gene Ontology (GO; www.geneontology.org) analysis which clusters the genes associated with immune response/defense (n=59) into functional subgroups including

macrophages, APCs, chemokines and chemokine receptors, lymphocytes, B-cells and eosinophils.

More precisely, at 30 days p.i., several biological processes relating to an active infection, as defined by GO cluster classification, were involved, including genes mostly associated with the response to external stimuli, response to wounding, immune response, response to stress, chemokine activity, defense response, MHC-related functions and inflammatory response. While several chemokine genes were found activated in the liver of AE mice by qRT-PCR, microarray analysis did not show any up-regulation of cytokine genes. Among genes of cytokine receptors, only those for IL-1 (IL-R1 like) and IL-7 (2.92 and 2.25 fold respectively) were up-regulated at day 30 (Table 1). Among genes encoding for chemokines, CCL5 (RANTES), a Th17-related chemokine that up-regulates IL-12 and IFN-γ, and is involved in Th1 cell-migration [16], was up-regulated 2.35-fold at day 30. Th2-related CCL8, CCL12 and CCL17 were up-regulated 29.58-fold, 5.64-fold and 3.36-fold at day 30, respectively. Among genes related to macrophage function, MGL1 and MGL2 (C-type macrophage galactose-type lectins) were up-regulated 2.56- and 4.64-fold respectively, compared to control mice.

At 60 days p.i., genes involved in the response to stress, response to external stimulus and response to biotic stimuli were added. There were few changes in the immune response gene expression, except for MPA2L (macrophage activation 2-like), which was down-regulated 2.33-fold and C4b (Complement component 4B), which was up-regulated 3.09-fold, respectively.

At 90 days p.i., among genes encoding for cytokine receptors, IL-13 Rα1 was up-regulated 2.39-fold (Table 1). Among the interferon-activated genes, Ifi202b, Ifi203 and Ifi204 were up-regulated 2.88-, 2.13-, and 2.47-fold, respectively. Among genes encoding for macrophage functions, MSR1 (macrophage type-I class-A scavenger receptors) and MPA2L (macrophage activation 2-like) were up-regulated 2.11- and 3.99-fold, respectively, when compared to control mice.

At 180 days p.i., hyper-expression of genes of the inflammatory response, response to stress, and response to external stimuli was maintained, and genes of antigen processing and presentation, complement activity and antigen processing via MHC class II were also hyper-expressed. Among genes of cytokine receptors, IL-17R was up-regulated 2.90-fold (Table 1). Among genes encoding for chemokines, CXCL9 was up-regulated 3.81-fold at day 180, and CXCL12 was down-regulated 2.11-fold at day 180.

Table 5.2 Gene ontology category: immune response and inflammatory response. Genes with up- or down-regulated transcriptions in the liver of *Echinococcus multilocularis* (*E.multilocularis*)-infected BALB/c mice are shown in comparison with non-infected sham-injected control animals (fold increase/decrease)

GeneBank accession number	Gene Symbol	Name	30 days	60 days	90 days	180 days
76074	5830443L24Rik	RIKEN CDNA 5830443L24 gene	*	*	2.84	*
11699	Ambp	Alpha 1 microglobulin/bikunin (Ambp)	-2.35	*	*	*
56298	Arl6ip2	ADP-ribosylation factor-like 6 interacting protein 2	*	*	2.05	*
236573	BC057170	cDNA sequence BC057170	*	*	3.41	*
12260	C1qb	Complement component 1, q subcomponent, beta polypeptide	*	*	*	2.12
12262	C1qc	Complement component 1, q subcomponent, C chain	*	*	*	3.58
12279	C1qg	Complement C1q subcomponent, C chainprecursor.	*	*	*	2.18
625018	C4b	Complement component 4B (Childo blood group)	*	3.09	*	*
230558	C8a	Complement component 8, alpha polypeptide	*	*	*	3.98
20304	Cc15	Chemokine (C-C motif) ligand 5	2.35	*	*	*
20307	Ccl8	chemokine (C-C motif) ligand 8	29.58	*	*	*
20293	Ccl12	chemokine (C-C motif) ligand 12	5.64	*	*	*
20295	Ccl17	chemokine (C-C motif) ligand 17	3.36	*	*	*
93671	Cd163	CD163 antigen	*	*	*	2.56
12500	Cd3d	CD3 antigen, delta polypeptide (Cd3d)	2.14	*	*	*
23833	Cd52	CD52 antigen	*	*	*	2.48
12516	Cd7	CD7 antigen (Cd7)	2.19	*	*	*
12525	Cd8a	CD8 antigen, alpha chain (Cd8a)	4.41	*	*	*
12526	Cd8b1	CD8 antigen, beta chain 1	3.13	*	*	*
12628	Cfhr1	Complement factor H-related 1	*	*	2.66	*
18636	Cfp	Complement factor properdin	*	*	*	2.19
17474	Clec4d	C-type lectin domain family 4, member d (Clec4d)	3.97	*	*	*
56619	Clec4e	C-type lectin domain family 4, member e (Clec4e)	5.08	*	*	*
17329	Cxcl9	Chemokine (C-X-C motif) ligand 9	*	*	*	2.81
20315	Cxcl12	chemokine (C-X-C motif) ligand 12	*	*	*	-2.21
14131	Fcgr3	Fc receptor, IgG, low affinity III	*	*	*	2.73
55932	Gbp3	Guanylate nucleotide binding	*	*	2.15	*

		protein 3				
15139	Hc	Hemolytic complement	*	*	*	2.03
15439	Hp	Haptoglobin	*	*	*	2.75
17082	I11r1	Interleukin 1 receptor-like 1 (Il1rl1), transcript variant 2	2.92	*	*	*
16197	I17r	Interleukin 7 receptor (Il7r)	2.25	*	*	*
16164	Il13ra1	interleukin 13 receptor, alpha 1	*	*	2.39	*
16172	Il17r	interleukin 17 receptor D	*	*	*	2.9
26388	Ifi202b	Interferon activated gene 202	*	*	2.88	*
15950	Ifi203	Interferon activated gene 203	*	*	2.13	*
15951	Ifi204	Interferon activated gene 204	*	*	2.47	*
16010	Igfbp4	Insulin-like growth factor bindingprotein 4	*	2.13	*	*
16797	Lat	Linker for activation of T cells (Lat)	2.12	*	*	*
17395	Mmp9	Matrix metallopeptidase 9 (Mmp9)	2.74	*	*	*
17312	Mgl1	macrophage galactose N-acetyl-galactosamine specific lectin 1	2.56	*	*	*
216864	Mgl2	macrophage galactose N-acetyl-galactosamine specific lectin 2	4.64	*	*	*
100702	Mpa2l	macrophage activation 2 like	*	-2.33	3.99	*
20288	Msr1	macrophage scavenger receptor 1	*	2.25	*	*
80891	Msr2	macrophage scavenger receptor 2	*	*	2.11	*
18405	Orm1	Orosomucoid 1	*	*	*	2.61
18406	Orm2	Orosomucoid 2	*	2.67	*	8.94
18514	Pbx1	Pre B-cell leukemia transcription factor 1	*	*	2.19	*
233489	Picalm	Phosphatidylinositol binding clathrin assembly protein	*	*	2.01	*
27226	Pla2g7	Phospholipase A2, group VII (platelet-activating factor acetylhydrolase, plasma)	*	*	*	2.57
18761	Prkcq	Protein kinase C, theta	*	*	-3.22	*
20208	Saa1	Serum amyloid A 1	*	*	*	11.63
20210	Saa3	Serum amyloid A 3	*	*	*	9.69
20211	Saa4	Serum amyloid A 4	*	*	*	2.32
20714	Serpina3k	Serine (or cysteine) peptidase inhibitor, clade A, member 3K (Serpina3k)	-3.38	*	*	*
20716	Serpina3n	Serine (or cysteine) peptidase inhibitor, clade A, member 3N	*	*	*	3.12

20750	Spp1	Secreted phosphoprotein 1	*	*	3.54	*
192187	Stab1	Stabilin 1	*	*	*	2.04
21822	Tgtp	T-cell specific GTPase	*	*	*	2.79
107568	Wwp1	WW domain containing E3 ubiquitin protein ligase 1	*	*	2.37	*

Correlations between mRNA levels of the various cytokines over the course of infection

Spearman correlation coefficients indicated a significant positive correlation between TGF-β1 mRNA expression in *E. multilocularis*'parasitic lesion', and that of Foxp3 (r=0.719, *P*=0.045), IL-10 (r=0.761, *P*=0.028) and CXCL9 (r=0.946, *P*< 0.01), but a significant negative correlation with IFN-γ (r=-0.743, *P*=0.035) (Table 5.3); it also showed a significant positive correlation between Foxp3 expression in *E. multilocularis* 'parasitic lesion', as measured by qRT-PCR, and IL-10 (r=0.761, P=0.028) and TNF-α (r=0.742, P=0.035), but a significant negative correlation with IL-1β (r=-0.754, *P*=0.033) (Table 5.4). There was a significant positive correlation between IL-17A expression in *E. multilocularis* 'parasitic lesion', as measured by qRT-PCR, and CCL12 (r=0.833, *P*=0.011), CCL17 (r=0.733, *P*=0.039), IL-4 (r=0.710, *P*=0.049) and TNF-α (r=0.804, *P*=0.016) (Table 5.5); there was also a significant positive correlation between IL-17F mRNA expression in *E. multilocularis* 'parasitic lesion' and CCL12 (r=0.708, *P*=0.049) and CCL17 (r=0.749, *P*=0.032)(Table 4). TNF-α mRNA expression in *E. multilocularis* 'parasitic lesion' was also significantly correlated to IL-12α (r=0.888, *P*=0.033) (Table 5.6).

Table 5.3 Correlations between mRNA of TGF-β1 and Foxp3, IL-10, IFN-γ and CXCL9

		Foxp3	IL-10	IFN-γ	CXCL9
TGF-β1	Spearman's rho	0.719*	0.761**	-0.743*	0.946**
	Sig.	0.045	0.028	0.035	0.000
	N	8	8	8	8

Note: * *P*< 0.05, ** *P*< 0.01.

Table 5.4 Correlations between mRNA of Foxp3 and TGF-β1, IL-10, IL-1β and TNF-α

		TGF-β1	IL-10	IL-1β	TNF-α
Foxp3	Spearman's rho	0.719*	0.761**	-0.754*	0.742*
	Sig.	0.045	0.028	0.033	0.035
	N	8	8	8	8

Note: * *P*< 0.05, ** *P*< 0.01.

Table 5.5 Correlations between mRNA of IL-17 and CCL12, CCL17, IL-4, and TNF-α

		CCL12	CCL17	IL-4	TNF-α
IL-17A	Spearman's rho	0.833*	0.733*	0.710*	0.804*
	Sig.	0.011	0.039	0.049	0.016
	N	8	8	8	8
IL-17F	Spearman's rho	0.708*	0.749*	0.695	0.497
	Sig.	0.049	0.032	0.056	0.210
	N	8	8	8	8

Note: * $P< 0.05$.

Table 5.6 Correlations between mRNA of TNF-α and IL-12α, as well as IL-17A

		IL-12α	IL-17A
TNF-α	Spearman's rho	0.888**	0.804*
	Sig.	0.003	0.016
	N	8	8

Note: * $P< 0.05$, ** $P< 0.01$.

Discussion

Despite the alleged causative involvement of the granulomatous response in the clinical development of AE and its role in functional imaging of the disease, since it is responsible for the Fluorodeoxyglucose (FDG) uptake in Positron Emission Tomography (PET) [20], a comprehensive picture of the cytokine/chemokine response that occurs in situ, i.e. in the periparasitic granuloma, had never been given. Chemokines and IL-17, which are crucial for immune cell homing, have so far received little attention in *E. multilocularis* infection. In the present longitudinal study of experimental *E. multilocularis* intra-hepatic infection model, we showed for the first time that 1) the mixed Th1/Th2/Treg response and the tri-phasic course of cytokines, suggested by previous studies on spleen cells from *E. multilocularis*-infected mice, was also documented in the periparasitic infiltrate, but nevertheless differed in some aspects, especially the marked and parallel expression of IL-12α and TNF-α but also IL-4 at a very early stage of the parasite/host interactions; 2) IL-17 was involved locally at the beginning of the immune response and remained so all along the course of infection, with a successive expression of different isotypes with possibly different roles; 3) a parallel course of cytokines and their related chemokines was highly in favor of their permanent role to maintain the homing of immune cells at close proximity of the parasitic vesicles; and 4) at least some of the components of the immune response were present in the surrounding liver

and were thus involved in a process which was long considered to be a localized "tumor-like" event (Figure 5.6 and 5.7).

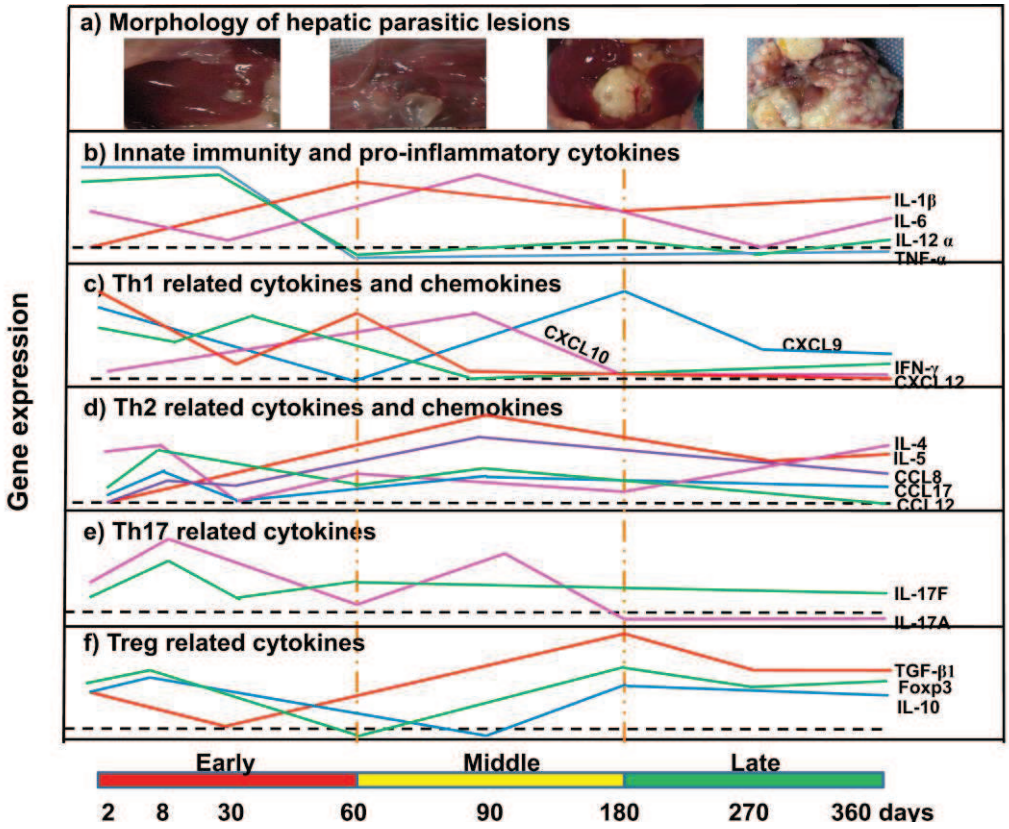

Figure 5.6 Course of the changes in the gene expression of innate immunity and proinflammtory cytokins (a), Th1 related cytokines and chemokines (b), Th1 related cytokines and chemokines (c), Th17 related cytokines (d), Foxp3 and Treg related cytokines (e) during the process of *E. multilocularis*-infection in mice

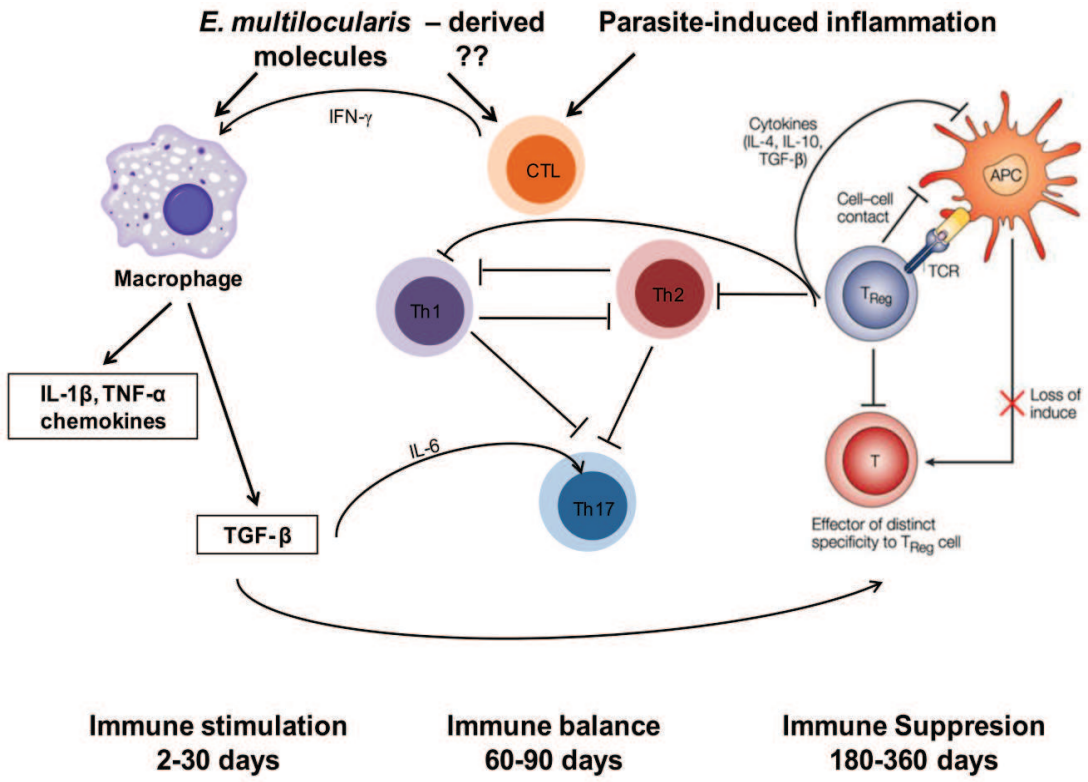

Figure 5.7 Schematic diagram summarizing the pathways of immune response involved in the host-parasite relationship in *E. multilocularis* infection

In the present study, we found that IL-12α and TNF-α were developing in parallel during the different stages of *E. multilocularis* infection. After an initial increase, IL-12α and TNF-α expression decreased dramatically after the 30th day of infection of mice. This fits well to previous findings, which had indicated a protective role against *E. multilocularis* by *in vivo* treatment with recombinant IL-12 in C57BL/6J mice [7], while mice KO for TNF-α [10], as well as patients with AE treated with a TNF-α inhibitor [20], had a faster and more severe course of disease. IL-1β and IL-6 were then showing up, presumably to sustain the inflammatory response, with a 'mirror' image of their respective increase all along infection. The initial peak of IL-6 as early as 2 days post-infection may be related to the early activation of the acute phase protein genes in the hepatocytes, disclosed by previous microarray studies [21,22]. Conversely, the absence of a significant increase of IL-6 at day 270 probably explains why, despite increased levels of haptoglobin, α-1 acid glycoprotein, C3 and C4, and ceruloplasmin in patients with AE, no increase of C-reactive protein (CRP) levels, typically associated with IL-6 stimulation, is usually observed, except in cases complicated by bacterial infection. Secretion of the pro-inflammatory cytokines IL-1β and IL-18 by PBMC of AE patients had been

shown to be reduced in response to *E. multilocularis* metacestode vesicles, compared to controls [12]. In our study in mice, although IL-1β was highly expressed at the early and middle stage, it subsequently decreased at the late stage and was not significantly different from control mice at day 180 post-infection and later, a time point which may approximately represent the disease stage of most patients at diagnosis of AE. Such selective dynamics of pro-inflammatory cytokine release may both install and maintain the periparasitic immune infiltrate from the very early stage of infection on, and also limit its activation and thus participate in the tolerance process.

In most previous studies, secretion and expression of cytokines, chemokines, and related factors that govern immune cell-homing to *E. multilocularis* infection site were studied in the peripheral blood of human AE patients [23], and in lymph node or spleen cells of experimentally infected mice [13,24,25]; in situ investigations focussing on the periparasitic infiltrate and the adjacent liver tissue are virtually lacking. Early expression of IFN-γ, as previously shown in studies on peripheral lymphocytes, was also confirmed in our longitudinal study of the periparasitic infiltrate; we hypothesize that it was very likely induced by the early expression of IL-12. The apparent decrease in IFN-γ at day 8 may be due either to a technical artefact or, more probably, to a temporary inhibition by IL-4, also markedly expressed at days 2 and 8 p.i.. Sustained IFN-γ expression together with the permanent expression of Th1 chemokines, and its negative correlation with TGF-β1 in the parasitic lesions all along the course of infection, although Th2 and T-reg cytokines are also permanently expressed, suggests that IFN-γ is very important for the persistence of the periparasitic infiltrate by permanent homing of immune cells and/or inhibition of their emigration. The decrease of IL-12 after the early stage of disease could be, at least partly, responsible for the lack of activation of CD8 T-cell or NK cell cytotoxicity despite the presence of IFN-γ [11,14,26].

Several concordant observations showed that the PBMCs of AE patients as well as spleen or lymph node cells of experimentally infected mice exhibit a markedly and steadily increasingTh2-oriented response characterized by high levels of IL-4, IL-5 andIL-10 expression [27]. The results from many studies have clearly identified IL-4/IL-5/IL-10 as important regulatory cytokines in parasitic infections, such as infection by *Schistosoma mansoni* in mice [28,29] and humans [30], *Schistosoma haematobium*[31], *Trichuris muris* [32], and *Trichinella spiralis*[33]. In *E. granulosus* infection, IL-4/IL-5/IL-10 had been found to be predominant in serum samples of infected individuals [34]; furthermore, in the peritoneal cells of experimental mice, i.e. at the site of *E. granulosus* establishment, IFN-γ was secreted first, at day 3, but as

early as day 5, a Th2-type response, including IL-4 and IL-13 was stimulated [35]. These results in CE suggest that a Th2-type response does not impair the establishment of *E. granulosus* metacestode, and does not prevent the development of the pericyst, a characteristic of CE pathology, which, conversely to AE, limits the progression of the metacestode [15]. In the parasitic lesions of *E. multilocularis*-infected mice, we observed a biphasic curve of IL-4 mRNA expression, with also a very early peak at 2-8 days. This early peak differed from what is usually reported in *E. multilocularis* infection upon investigation of peripheral lymphocytes stimulated by *E. multilocularis* antigens [5]. The early local expression of IL-4 mRNA might be crucial to prime naive $CD4^+$ T cells into differentiated Th2 type cells [35], and to prevent anti-parasite resistance, such as that occurring in most intermediate hosts, including humans. We hypothesize that early IL-4 mRNA expression is likely induced through the activation of innate immunity by specific metabolic components of the metacestode. Such an activation of IL-4 production has actually been described *in vitro* under the influence of *Echinococcus* components, both from *E. multilocularis* [23] and from *E. granulosus* [36]. In the present study, we also found a delayed increase of IL-5 and IL-10 in the middle/late stage of *E. multilocularis* infection. This delayed increase of IL-5 and IL-10 is matching previous observations made by others at the 'late stage' of infection, in human AE [37,38,39] and are in agreement with the data usually reported from the study of lymphocytes from experimentally infected mice [40]; this combined cytokine profile has been strongly linked to parasite evasion from the host immune response [27,41].

The discovery of the IL-17 cytokine family has added a new dimension to the balance of inflammation and tolerance during parasite infections. The presence of IL-17-secreting $CD4^+$ T (Th17) lymphocytes correlates with severe hepatic pathology in murine schistosomiasis [42]. In our study, IL-17, as detected by a monoclonal antibody directed against the common epitopes of the protein, was present in cells of the periparasitic infiltrate all along the course of infection; however, as far as the expression of mRNA isotypes of the cytokines is concerned, both IL-17A and IL-17F were increased at the early stage of *E. multilocularis* infection, and then decreased at the late stage; they were both positively correlated with CCL12 and CCL17; however, IL-17A exhibited a positive correlation with TNF-α, and appeared lower than even in controls, at the late stage of infection, while IL-17F was also expressed at low levels, but still higher than controls. This may indicate that IL-17A was rather protective but quickly inhibited, while IL-17F was less suppressed with time and may contribute to both protection and pathogenesis, as reported in human AE patients[17].

Chemokines are involved in the homing and persistence of immune cells in inflammatory reactions, especially to infectious agents [43,44]; they also participate in innate recognition stages of immunity and may help direct Th1 and Th2 cytokine-producing cells during the generation of adaptive immunity [18]. There is also considerable *in vitro* evidence that cytokines further capitalize on these molecules by regulating their expression and secretion and by using them to activate effector cells such as macrophages and fibroblasts [18]. Conversely, specific suppression of certain chemokine production and/or function by *E. multilocularis* metacestode in AE patients may constitute an additional immune escape mechanism [15]. We only measured the mRNA expression of 'key' chemokines, directly related to the main cytokine profiles, among the multiple components with chemokine activity. But all measured chemokines were significantly expressed at a given stage of infection. These results confirmed the importance of these compounds to maintain the granulomatous infiltrate at the proximity of the metacestode. The courseof Th1-related chemokines appeared "complementary"; CXCL 9 was more expressed when CXCL10 was less expressed, and vice versa, with a 'mirror' image, as previously described for IL-1 and IL-6. This may indicate some balance to ensure lymphocyte homing and persistence in the lesions. Th2-related chemokines were also permanently expressed: expression of CCL12 and CCL17 followed the course of IL-4, and CCL 8 followed the course of IL-5. Such changes in chemokine release may prevent pathogenic inflammation at the late stage. In addition, the microarray technique revealed a hyper-expression of RANTES (CCL5), chemotactic for Th1 cells, eosinophils, and basophils[11]. This finding suggests that this chemokine is also secreted by cells of the granuloma at the early stage (8-30 days) when IL-12, IFN-γ and IL-17 secretions are at their maximum. This should consequently also be explored more in detail in future studies.

The involvement of the adjacent, not directly affected liver tissue in the immune process of *E. multilocularis*/host interaction has received little attention. Recent studies have provided evidence that the adjacent liver was fully involved in the relationship between the parasite and its host; these studies have mostly focused on the proliferation/apoptosis balance [18] and the involvement of the TGF-β/Smad system [19]. Our study confirms that other mediators of the immune reaction and their receptors appear principally expressed in the liver tissue, thus also in areas not directly affected by the parasite and the periparasitic granuloma. In the adjacent periparasitic liver tissue, the expression of the various cytokines/chemokines was selective: not all cytokines/chemokines were expressed in the surrounding liver; some seemed to be specific for the immune cells of the periparasitic infiltrate, e.g. TNF-α, IL-17F and CCL8, which were not expressed at all in the liver. The contribution of the surrounding liver tissue, however, was quite significant for other ones, e.g. IL-12,

IFN-γ, IL-4 and IL-17A, at the early stage of infection; CXCL9, IL-4, IL-5, CCL17, at the middle stage; and IL-10 and TGF-β at the late stage of infection. From our study, which was performed on liver samples without cell identification, it is difficult to know if such expression was restricted to cells of the immune response present in the sinusoids/portal spaces after their homing to the liver, or was also present in autochthonous liver cells such as Kupffer cells, stellate cells, or hepatocytes. Precise identification and respective location will require appropriate studies. Among cytokine receptors, only those for IL-1 (IL-R1 like), IL-7, IL-13 (IL-13 Rα1), and IL-17 (IL-17 R) were up-regulated. This indirectly suggests that the liver was affected by at least one pro-inflammatory cytokine (IL-1) and one growth factor (IL-7), and by two types of Th-cytokines (Th2 and Th17). However, absence of up-regulation of IL-6 and TGF-β receptors in hepatic cells is puzzling and has to be further confirmed using other techniques in the same model.

References

1. Vuitton DA (2003) The ambiguous role of immunity in echinococcosis: protection of the host or of the parasite? Acta Trop 85: 119-132.
2. Vuitton DA, Zhang SL, Yang Y, Godot V, Beurton I, et al. (2006) Survival strategy of Echinococcus multilocularis in the human host. Parasitol Int 55 Suppl: S51-55.
3. Manfras BJ, Reuter S, Wendland T, Kern P (2002) Increased activation and oligoclonality of peripheral CD8(+) T cells in the chronic human helminth infection alveolar echinococcosis. Infect Immun 70: 1168-1174.
4. Manfras BJ, Reuter S, Wendland T, Boehm BO, Kern P (2004) Impeded Th1 CD4 memory T cell generation in chronic-persisting liver infection with Echinococcus multilocularis. Int Immunol 16: 43-50.
5. Emery I, Liance M, Deriaud E, Vuitton DA, Houin R, et al. (1996) Characterization of T-cell immune responses of Echinococcus multilocularis-infected C57BL/6J mice. Parasite Immunol 18: 463-472.
6. Godot V, Harraga S, Podoprigora G, Liance M, Bardonnet K, et al. (2003) IFN alpha-2a protects mice against a helminth infection of the liver and modulates immune responses. Gastroenterology 124: 1441-1450.
7. Emery I, Leclerc C, Sengphommachanh K, Vuitton DA, Liance M (1998) In vivo treatment with recombinant IL-12 protects C57BL/6J mice against secondary alveolar echinococcosis. Parasite Immunol 20: 81-91.
8. Liance M, Ricard-Blum S, Emery I, Houin R, Vuitton DA (1998) Echinococcus multilocularis infection in mice: in vivo treatment with a low dose of IFN-gamma decreases metacestode growth and liver fibrogenesis. Parasite 5: 231-237.
9. Shi DZ, Li FR, Bartholomot B, Vuitton DA, Craig PS (2004) Serum sIL-2R, TNF-alpha and IFN-gamma in alveolar echinococcosis. World J Gastroenterol 10: 3674-3676.
10. Amiot F, Vuong P, Defontaines M, Pater C, Dautry F, et al. (1999) Secondary alveolar echinococcosis in lymphotoxin-alpha and tumour necrosis factor-alpha deficient mice: exacerbation of Echinococcus multilocularis larval growth is associated with cellular changes in the periparasitic granuloma. Parasite Immunol 21: 475-483.
11. Mejri N, Hemphill A, Gottstein B (2009) Triggering and modulation of the host-parasite interplay by Echinococcus multilocularis: a review. Parasitology 137: 557-568.
12. Eger A, Kirch A, Manfras B, Kern P, Schulz-Key H, et al. (2003) Pro-inflammatory (IL-1beta, IL-18) cytokines and IL-8 chemokine release by PBMC in response to Echinococcus multilocularis metacestode vesicles. Parasite Immunol 25: 103-105.
13. Dai WJ, Waldvogel A, Siles-Lucas M, Gottstein B (2004) Echinococcus multilocularis proliferation in mice and respective parasite 14-3-3 gene expression is mainly controlled by an alphabeta CD4 T-cell-mediated immune response. Immunology 112: 481-488.

14. Mejri N, Muller N, Hemphill A, Gottstein B (2011) Intraperitoneal Echinococcus multilocularis infection in mice modulates peritoneal CD4+ and CD8+ regulatory T cell development. Parasitol Int 60: 45-53.
15. Hubner MP, Manfras BJ, Margos MC, Eiffler D, Hoffmann WH, et al. (2006) Echinococcus multilocularis metacestodes modulate cellular cytokine and chemokine release by peripheral blood mononuclear cells in alveolar echinococcosis patients. Clin Exp Immunol 145: 243-251.
16. Kocherscheidt L, Flakowski AK, Gruner B, Hamm DM, Dietz K, et al. (2008) Echinococcus multilocularis: inflammatory and regulatory chemokine responses in patients with progressive, stable and cured alveolar echinococcosis. Exp Parasitol 119: 467-474.
17. Lechner CJ, Gruner B, Huang X, Hoffmann WH, Kern P, et al. (2012) Parasite-specific IL-17-type cytokine responses and soluble IL-17 receptor levels in Alveolar Echinococcosis patients. Clin Dev Immunol 2012: 735342.
18. Zhang C, Wang J, Lu G, Li J, Lu X, et al. (2012) Hepatocyte proliferation/growth arrest balance in the liver of mice during E. multilocularis infection: a coordinated 3-stage course. PLoS One 7: e30127.
19. Wang J, Zhang C, Wei X, Blagosklonov O, Lv G, et al. (2013) TGF-beta and TGF-beta/Smad signaling in the interactions between Echinococcus multilocularis and its hosts. PLoS One 8: e55379.
20. Caoduro C, Porot C, Vuitton DA, Bresson-Hadni S, Grenouillet F, et al. (2013) The role of delayed 18F-FDG PET imaging in the follow-up of patients with alveolar echinococcosis. J Nucl Med 54: 358-363.
21. Gottstein B, Wittwer M, Schild M, Merli M, Leib SL, et al. (2011) Hepatic gene expression profile in mice perorally infected with Echinococcus multilocularis eggs. PLoS One 5: e9779.
22. Lin R, Lu G, Wang J, Zhang C, Xie W, et al. (2011) Time course of gene expression profiling in the liver of experimental mice infected with Echinococcus multilocularis. PLoS One 6: e14557.
23. Aumuller E, Schramm G, Gronow A, Brehm K, Gibbs BF, et al. (2004) Echinococcus multilocularis metacestode extract triggers human basophils to release interleukin-4. Parasite Immunol 26: 387-395.
24. Bresson-Hadni S, Liance M, Meyer JP, Houin R, Bresson JL, et al. (1990) Cellular immunity in experimental Echinococcus multilocularis infection. II. Sequential and comparative phenotypic study of the periparasitic mononuclear cells in resistant and sensitive mice. Clin Exp Immunol 82: 378-383.
25. Dai WJ, Gottstein B (1999) Nitric oxide-mediated immunosuppression following murine Echinococcus multilocularis infection. Immunology 97: 107-116.
26. Vuitton DA, Bresson-Hadni S, Laroche L, Kaiserlian D, Guerret-Stocker S, et al. (1989) Cellular immune response in Echinococcus multilocularis infection in humans. II. Natural killer cell activity and cell subpopulations in the blood and in the periparasitic granuloma of patients with alveolar echinococcosis. Clin Exp Immunol 78: 67-74.

27. Dreweck CM, Soboslay PT, Schulz-Key H, Gottstein B, Kern P (1999) Cytokine and chemokine secretion by human peripheral blood cells in response to viable Echinococcus multilocularis metacestode vesicles. Parasite Immunol 21: 433-438.
28. Sabin EA, Pearce EJ (1995) Early IL-4 production by non-CD4+ cells at the site of antigen deposition predicts the development of a T helper 2 cell response to Schistosoma mansoni eggs. J Immunol 155: 4844-4853.
29. Brunet LR, Kopf MA, Pearce EJ (1999) Schistosoma mansoni: IL-4 is necessary for concomitant immunity in mice. J Parasitol 85: 734-736.
30. Correa-Oliveira R, Malaquias LC, Falcao PL, Viana IR, Bahia-Oliveira LM, et al. (1998) Cytokines as determinants of resistance and pathology in human Schistosoma mansoni infection. Braz J Med Biol Res 31: 171-177.
31. Mutapi F, Winborn G, Midzi N, Taylor M, Mduluza T, et al. (2007) Cytokine responses to Schistosoma haematobium in a Zimbabwean population: contrasting profiles for IFN-gamma, IL-4, IL-5 and IL-10 with age. BMC Infect Dis 7: 139.
32. Schopf LR, Hoffmann KF, Cheever AW, Urban JF, Jr., Wynn TA (2002) IL-10 is critical for host resistance and survival during gastrointestinal helminth infection. J Immunol 168: 2383-2392.
33. Scales HE, Ierna MX, Lawrence CE (2007) The role of IL-4, IL-13 and IL-4Ralpha in the development of protective and pathological responses to Trichinella spiralis. Parasite Immunol 29: 81-91.
34. Amri M, Mezioug D, Touil-Boukoffa C (2009) Involvement of IL-10 and IL-4 in evasion strategies of Echinococcus granulosus to host immune response. Eur Cytokine Netw 20: 63-68.
35. Mourglia-Ettlin G, Marques JM, Chabalgoity JA, Dematteis S (2011) Early peritoneal immune response during Echinococcus granulosus establishment displays a biphasic behavior. PLoS Negl Trop Dis 5: e1293.
36. Rigano R, Profumo E, Bruschi F, Carulli G, Azzara A, et al. (2001) Modulation of human immune response by Echinococcus granulosus antigen B and its possible role in evading host defenses. Infect Immun 69: 288-296.
37. Godot V, Harraga S, Beurton I, Deschaseaux M, Sarciron E, et al. (2000) Resistance/susceptibility to Echinococcus multilocularis infection and cytokine profile in humans. I. Comparison of patients with progressive and abortive lesions. Clin Exp Immunol 121: 484-490.
38. Rigano R, Profumo E, Teggi A, Siracusano A (1996) Production of IL-5 and IL-6 by peripheral blood mononuclear cells (PBMC) from patients with Echinococcus granulosus infection. Clin Exp Immunol 105: 456-459.
39. Jenne L, Kilwinski J, Scheffold W, Kern P (1997) IL-5 expressed by CD4+ lymphocytes from Echinococcus multilocularis-infected patients. Clin Exp Immunol 109: 90-97.
40. Zhao H, Bai X, Nie XH, Wang JT, Wang XX, et al. (2012) [Dynamic change of IL-10 and TGF-beta1 in the liver of Echinococcus multilocularis-infected mice]. Zhongguo Ji Sheng Chong Xue Yu Ji Sheng Chong Bing Za Zhi 30: 32-35.

41. Harraga S, Godot V, Bresson-Hadni S, Mantion G, Vuitton DA (2003) Profile of cytokine production within the periparasitic granuloma in human alveolar echinococcosis. Acta Trop 85: 231-236.
42. Rutitzky LI, Lopes da Rosa JR, Stadecker MJ (2005) Severe CD4 T cell-mediated immunopathology in murine schistosomiasis is dependent on IL-12p40 and correlates with high levels of IL-17. J Immunol 175: 3920-3926.
43. Hicks DJ, Nunez A, Banyard AC, Williams A, Ortiz-Pelaez A, et al. (2013) Differential Chemokine Responses in the Murine Brain Following Lyssavirus Infection. J Comp Pathol.
44. Pak-Wittel MA, Yang L, Sojka DK, Rivenbark JG, Yokoyama WM (2012) Interferon-gamma mediates chemokine-dependent recruitment of natural killer cells during viral infection. Proc Natl Acad Sci U S A 110: E50-59.

Main conclusions and remarks:

Profiles of mRNA expression levels in the hepatic parasitic lesions showed that

1) IL-12α and TNF-α were developing in parallel during the different stages of *E. multilocularis* infection.

2) A mixed Th1/Th2 immune response, characterized by the concomitant presence of IL-12α, IFN-γ and IL-4, was established very early in the development of *E. multilocularis*.

3) At middle/late stage of *E. multilocularis* infection, the profile extended to a combined tolerogenic profile associating IL-5, IL-10 and TGF-β.

4) IL-17 was permanently expressed in the liver, mostly in the periparasitic infiltrate; both IL-17A and IL-17F were increased at the early stage of *E. multilocularis* infection, and then decreased at the late stage; they were both positively correlated with CCL12 and CCL17; however, IL-17A exhibited a positive correlation with TNF-α, and appeared lower than even in controls, at the late stage of infection, while IL-17F was also expressed at low levels, but still higher than controls.

5) The course of Th1-related chemokines appeared "complementary"; CXCL 9 was more expressed when CXCL10 was less expressed, and vice versa, with a 'mirror' image. Th2-related chemokines were also permanently expressed: expression of CCL12 and CCL17 followed the course of IL-4, and CCL 8 followed the course of IL-5.

6. How are TGF-β and TGF-β/Smad signaling involved in the interactions between *E. multilocularis* and its host?

To address this question, we measured the levels of TGF-β1, TGF-β receptors, and down-stream Smad2/3, Smad4 and Smad7 activation, as well as fibrosis marker α-SMA, Collagen I and III expression by using Western Blot, qRT-PCR and immunohistochemistry in an intra-hepatic mouse AE model from day 2 to 360 post-infection (p.i.).

Background and objectives:

TGF-β serves as a global regulator of immunity by controlling the initiation, maintenance, and resolution of inflammatory responses. After a preliminary study by researchers from our team had shown that TGF-β was abundantly expressed in the periparasitic infiltrate in patients with AE, our study of the sequential expression of cytokines and related chemokines in the liver confirmed that, among the factors essential to maintain the tolerance state (Treg-related cytokines), TGF-β was actually expressed in the periparasitic infiltrate all along the course of infection. This expression followed a biphasic curve, with a decrease at the middle stage and a re-increase at the end stage of infection (Wang, 2014 a). On the other hand, we also showed that the parasite and/or the periparasitic immune response were also involved in metabolic changes in the adjacent, not directly affected, liver tissue, and we suggested that TGF-β might be one of the actors of such changes (Zhang, 2012). In addition, fibrosis is among the hallmarks of AE, and TGF-β is well known to play a role in fibrogenesis. TGF-β might thus be a major regulator of the immune response in AE, and could also be involved in liver homeostasis and liver fibrosis. However, very little was known on the presence and course of the other components of the TGF-β/Smad pathway in the liver, and on their possible influence on fibrosis, over the various stages of infection. The aims of this study were 1) to delineate the location of TGF-β and components of the TGF-β pathway in the periparasitic immune cells and in hepatocytes, close to and distant from the lesions in the liver; 2) to better understand the functioning of the TGF-β/Smad pathway, and its possible relationship with the development of liver fibrosis in the parasite's hosts; 3) to further explore how TGF-β was secreted and regulated.

OPEN ACCESS Freely available online

PLOS ONE

TGF-β and TGF-β/Smad Signaling in the Interactions between *Echinococcus multilocularis* and Its Hosts

Junhua Wang[1,2☯], Chuanshan Zhang[1☯], Xufa Wei[1], Oleg Blagosklonov[2,3], Guodong Lv[1], Xiaomei Lu[1], Georges Mantion[3], Dominique A. Vuitton[3], Hao Wen[1]*, Renyong Lin[1]*

1 State Key Lab Incubation Base of Xinjiang Major Diseases Research (2010DS890294) and Xinjiang Key Laboratory of Echinococcosis, First Affiliated Hospital of Xinjiang Medical University, Urumqi, Xinjiang, China, **2** Department of Nuclear Medicine, University of Franche-Comté and Jean Minjoz University Hospital, Besançon, Franche-Comté, France, **3** WHO-Collaborating Centre for the Prevention and Treatment of Human Echinococcosis, University of Franche-Comté and University Hospital, Besançon, Franche-Comté, France

Abstract

Alveolar echinococcosis (AE) is characterized by the development of irreversible fibrosis and of immune tolerance towards *Echinococcus multilocularis (E. multilocularis)*. Very little is known on the presence of transforming growth factor-β (TGF-β) and other components of TGF-β/Smad pathway in the liver, and on their possible influence on fibrosis, over the various stages of infection. Using Western Blot, qRT-PCR and immunohistochemistry, we measured the levels of TGF-β1, TGF-β receptors, and down-stream Smads activation, as well as fibrosis marker expression in both a murine AE model from day 2 to 360 post-infection (p.i.) and in AE patients. TGF-β1, its receptors, and down-stream Smads were markedly expressed in the periparasitic infiltrate and also in the hepatocytes, close to and distant from AE lesions. Fibrosis was significant at 180 days p.i. in the periparasitic infiltrate and was also present in the liver parenchyma, even distant from the lesions. Over the time course after infection TGF-β1 expression was correlated with CD4/CD8 T-cell ratio long described as a hallmark of AE severity. The time course of the various actors of the TGF-β/Smad system in the *in vivo* mouse model as well as down-regulation of Smad7 in liver areas close to the lesions in human cases highly suggest that TGF-β plays an important role in AE both in immune tolerance against the parasite and in liver fibrosis.

Citation: Wang J, Zhang C, Wei X, Blagosklonov O, Lv G, et al. (2013) TGF-β and TGF-β/Smad Signaling in the Interactions between *Echinococcus multilocularis* and Its Hosts. PLoS ONE 8(2): e55379. doi:10.1371/journal.pone.0055379

Editor: Valli De Re, Centro di Riferimento Oncologico, IRCCS National Cancer Institute, Italy

Received October 1, 2012; **Accepted** December 21, 2012; **Published** February 6, 2013

Funding: This work was supported by the Xinjiang Young Scientist Foundation (2010211B19), the Program for Changjiang Scholars and Innovative Research Team in Universities (IRT1181), NSFC Grant Projects (30960342, 81260452, 81260252), and Xinjiang Key-Lab Projects (XJDX0202-2009-03). The funders had no role in study design, data collection and analysis, decision to publish, or preparation of the manuscript.

Competing Interests: The authors have declared that no competing interests exist.

* E-mail: renyongl@yahoo.com.cn (RL); Dr.wenhao@163.com (HW)

☯ These authors contributed equally to this work.

Introduction

Alveolar echinococcosis (AE) is a rare, but severe zoonotic helminthic disease due to the proliferation of the larval stage of cestode *Echinococcus multilocularis (E. multilocularis)* [1]. In humans, accidental intermediate hosts, the severity of this disease results from both a continuous asexual proliferation of the metacestode and an intense inflammatory granulomatous infiltration around the parasite which causes pathological damages in the liver. The lesions act like a slow-growing liver cancer, progressively invading the neighboring tissues and organs. Granulomas around the parasitic vesicles, extensive fibrosis, and necrosis are the characteristic pathological findings [2]. Studies performed in the 1980s–1990s showed that dense and irreversible fibrosis composed of thick concentric bundles of heavily cross-linked type I and type III collagens surrounded the parasitic vesicles, and that α-smooth muscle actin (α-SMA)-expressing myofibroblasts (MFB) derived from the hepatic stellate cells (HSC) could play an important role in fibrosis development [3–7]. The diffusion of the fibrotic process even far from the parasitic lesions strongly suggested that cytokines produced in the periparasitic area could be involved in collagen synthesis, locally in the lesions and also in the liver distant from the lesions; it was also suggested that cytokines might be involved in the cross-linking of the collagen bundles. Little evidence, however, has been given until now on how *E. multilocularis* metacestode interacts with its host to promote fibrosis and especially on the nature and role of cytokines in fibrosis development in AE.

TGF-β is a major regulator of the immune responses, inducing and maintaining T-regulatory cells, reducing cytotoxic effector immune response and balancing the tolerogenic and immunogenic forces at play in various physiological states and chronic diseases, such as fetus growth and survival during gestation [8], cancer [9], chronic inflammatory diseases [10], or chronic and allergic respiratory diseases [11]. In these conditions, this polypeptide also regulates a variety of cell events involved in tissue regeneration and fibrosis. Similarly, its role has been recognized both to induce and maintain immune tolerance towards parasites and to induce fibrosis in several examples of helminth infection [12]. However, opposite to the recognized role of Interleukin-10 [12,13], little is known about TGF-β involvement in the pathophysiology of larval echinococcosis. Only preliminary studies are available in AE: Zhang et al. [14] showed that TGF-β was expressed in most lymphocytes of the periparasitic infiltrate in liver biopsies from AE patients. It was suggested that TGF-β may play a role in

maintaining host tolerance against *E. multilocularis* growth by preventing T-cell cytotoxicity against the parasite [14]. In cystic echinococcosis (CE), immunostaining of TGF-β has also been shown at the periphery of hydatid cysts in the liver of patients [15]; and another study confirmed a progressive increase in the expression of mRNA of TGF-β in the liver of *E. granulosus*-infected BALB/c mice [16]. There is abundant evidence that TGF-β1, besides its role in immune tolerance, is an extremely potent inducer of the synthesis of procollagen and other extracellular matrix (ECM) components [17,18], and has an essential role in the pathogenesis of liver fibrosis. The major signaling pathway for all TGF-β members is activated through ligand binding to a cell-surface receptor complex of type I and type II serine–threonine kinases receptors; and a group of intracellular signaling intermediates known as Smads is then phosphorylated. Phosphorylated Smads translocate to the nucleus where they function as transcription factors, initiating target gene transcription [19]. Smad4 is apparently common to all ligand-specific Smad pathways, and is a central mediator in TGF-β superfamily signaling [20]. Smad7, which is induced by TGF-β itself, forms part of an inhibitory feedback loop by binding to the intracellular domain of the activated TGF-β RI [21–24]. Because Smad7 is responsible for the fine-tuning of TGF-β signals [25], an aberrant expression of Smad7 might disrupt the balanced activity of TGF-β under physiological and pathophysiological conditions. However, although it may be crucial in the host-parasite interactions (Fig. 1), the relationship between the TGF-β/Smad pathway, and especially Smad7 expression, and clinical and/or pathological features of AE in experimental models as well as in humans has never been addressed.

The aims of this study were 1) to delineate the location of TGF-β and components of the TGF-β pathway in the periparasitic immune cells and in hepatocytes, close to and distant from the lesions in the liver; 2) to better understand the functioning of the TGF-β/Smad pathway, and its possible relationship with the development of liver fibrosis in the parasite's hosts; 3) to further explore how TGF-β was secreted and regulated. For this purpose, and to get a comprehensive appraisal of TGF-β secretion and of its role in *E. multilocularis* infection, experimental AE in a mouse model of liver-targeted secondary AE [4] allowed us to study the time course of TGF-β expression as well as the dynamics of TGF-β signaling-related components, TGF-β RI, TGF-β RII, pSmad 2/3, Smad4 and Smad7, and to correlate them with the time course of the periparasitic infiltration by T-cell subpopulations, and to biochemical indicators of liver fibrosis, such as α-smooth muscle actin (α-SMA), and collagens I (COL I), and III (COL III). We also studied TGF-β and TGF-β signaling-related components in the liver of AE patients both at the protein and mRNA levels, in order to assess the situation at the late stage of infection in resistant hosts where immune tolerance and development of fibrosis are combined.

Results

Pathological Examination of the Livers Infected with *E. multilocularis*

In experimental mice, at the very early stage (2 and 8 days p.i.), in the surrounding of the metacestode injection site, lipid accumulation was observed in some hepatocytes (focal steatosis), and lymphocytes infiltrated the portal areas. No obvious change was found in the distant liver. From day 30 to day 90 after infection, at the periphery of the lesion, fibroblasts and inflammatory cells proliferated and an obvious increase of liver fibrosis was observed at the periphery of the lesion. There was no change

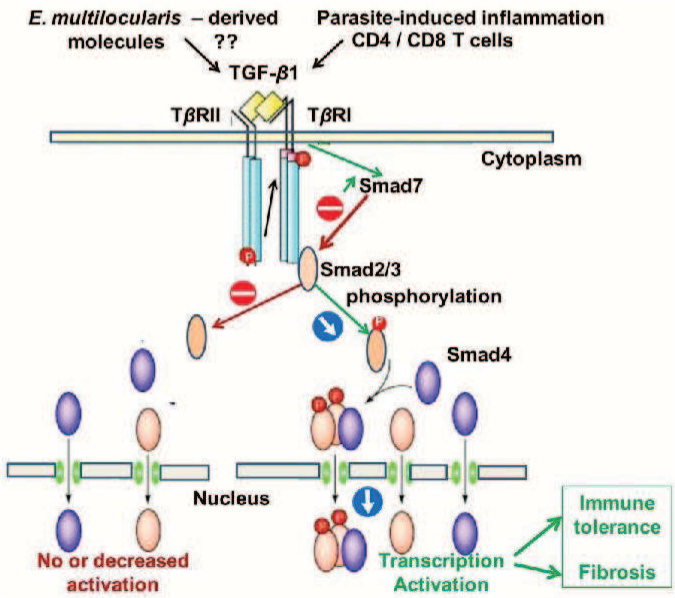

Figure 1. The TGF-β/Smad pathway; hypothesis for its involvement in the host-parasite relationship in *E. multilocularis* infection.
doi:10.1371/journal.pone.0055379.g001

in the areas distant from the lesion, except fibroblast and Kupffer cell proliferation, and an increased presence of lymphocytes in portal spaces. From day 180 to day 360, the typical granulomatous and fibrous periparasitic infiltrate of AE was fully established; in the liver, degenerating hepatocytes with atrophy and necrosis, as well as fibrous tissue development were observed in the areas immediately surrounding the granulomatous host response. Both fibroblasts and Kupffer cells proliferated in areas distant from the lesion. Mice in the control group at the same time-points showed normal hepatic histology (data not shown; available from reference [26]).

In AE patients, the liver lesions were similar to those observed in experimental mice at day 180 after infection, with the typical granulomatous and fibrous reaction surrounding parasite vesicles either active or degenerating. In the liver areas distant from the lesions, there was Kupffer cell proliferation, and lymphocytes infiltrated the portal areas. In the liver areas immediately surrounding the lesions, a few hepatocytes showed degeneration (data not shown).

Expression of α-SMA, and Collagen I, III in the Livers Infected with *E. multilocularis*

In experimental mice, in the liver of control animals α-SMA expression was present in the cytoplasm of smooth muscle cells, i.e. restricted to the walls of most of the portal and central veins while there was nearly no staining in the liver parenchyma (Fig. 2). 180 days after *E. multilocularis* infection, α-SMA positive score was higher in infected than in control mice; distribution of α-SMA positive cells was diffuse in the liver parenchyma, suggesting a myofibroblastic differentiation of stellate cells in the liver (Fig. 3A).

In AE patients, in the liver areas close to lesions, there was a strong α-SMA immunostaining present in the ECM and α-SMA expression scores were significantly higher in the areas close to lesions compared to those distant from lesions (Fig. 2 and 3F).

In experimental mice, there was a marked difference between *E. multilocularis*-infected mice and control mice with regard to the nature and location of collagens in the liver. At all time-points, strong staining for Collagen I and III was present in the periparasitic granuloma as concentric bundles extending from the laminated layer of the parasitic vesicles to the border of the normal liver (Fig. 2). Collagen III was also present as dotted lines between the cells at the outer part of the granulomatous infiltrate and, occasionally, in the cytoplasm of round cells in the sinusoids of the surrounding liver (Fig. 2).

In AE patients, in the liver areas close to lesions, there was a strong Collagen I and III immunostaining in the ECM. Expression scores of Collagen I and Collagen III were significantly higher in the areas close to lesions compared to those distant from lesions (Fig. 3F).

Infiltration by $CD4^+$ and $CD8^+$ T Cells in the Periparasitic Area in *E.multilocularis*-infected Mice

As the experimental model of AE allowed us to study the correlation, if any, between T lymphocyte infiltration in the liver and TGF-β expression over the time course of infection, CD4 and CD8 immunostaining was performed in the liver of mice; this was not performed in the liver of AE patients, since the time course could not be assessed. There was nearly no infiltration by $CD4^+$ T cells nor by $CD8^+$ T cells in the control groups whenever the time point after sham injection of saline in the liver (Fig. 2). In the periparasitic infiltrate surrounding the metacestode, in experimental infected mice, $CD4^+$ T cells were present from day 60 to day 360. CD4 positive scores ranged from 0.6 to 3.7 and reached the peak point at day 90 (Fig. 3D). Infiltration by $CD8^+$ T cells was expressed by scores which ranged from 2.3 to 5.4 and reached the peak point later than $CD4^+$ T cells, at day 360 (Fig. 3E).

Expression of TGF-β1 in the Livers Infected with *E. multilocularis*

Protein expression of TGF-β1. In experimental mice, a strong immunostaining for TGF-β1 was observed in the periparasitic infiltrate in most of areas with inflammatory granulomas from 30 days to 360 days p.i. In the liver area close to the parasitic lesions, a faint expression of TGF-β1 was observed in the endothelial cells at day 30; a marked expression was observed in endothelial cells of the hepatic sinusoids and in fibroblasts at day 60, as well as in endothelial cells of the hepatic sinusoids and in hepatocytes close to the parasitic lesions from 90 days to 360 days p.i. In the liver distant from the parasitic lesions, a faint staining for TGF-β1 was observed in the endothelial cells of hepatic sinusoids from 30 to 90 days p.i.; there was a moderate staining in endothelial cells of hepatic sinusoids from 180 to 360 days p.i., while a faint staining was observed in the hepatocytes from 90 and 360 days p.i. (Fig. 4 and 5A). An increased TGF-β1 expression measured using Western Blot in the liver of experimental infected mice was observed from day 2 (0.9-fold) to day 360 (3.2-fold); it peaked at day 180 (8.2-fold) after infection with *E. multilocularis*, then decreased to lower levels, albeit higher than in control mice until the end of follow-up; difference between experimental and control mice was significant at day 90, 180, 270 and 360 ($P<0.05$).

In AE patients, as observed in the mouse model, a strong immunostaining for TGF-β1 was observed in most lymphocytes and macrophages in the periparasitic infiltrate, as well as in Kupffer cells, fibroblasts, and endothelial cells in hepatic sinusoids, especially around the granulomas, and in infiltrating immune cells of portal spaces (Fig. 4). In the non-infiltrated liver, faint staining with anti-TGF-β1 antibodies was observed in hepatocytes, even in those observed in areas distant from the parasitic lesions (Fig. 4). Percentage of TGF-β1 positive cells was higher in areas close to than distant from lesions (Fig. 6A), with an intensity gradient from the periparasitic areas to the distant liver, since TGF-β1 staining appeared stronger close to the granulomatous reaction (Fig. 4). Western Blot measurements of TGF-β1 also showed that protein levels of the cytokine were significantly higher in the liver tissue close to lesions than in that distant from lesions (Fig. 6B and C) ($P<0.05$).

Correlation with T cell subpopulations and fibrosis markers. TGF-β1 expression in the periparasitic infiltrate was highly positively correlated with CD4/CD8 ratio ($r=0.818$) but not correlated with either $CD4^+$ or $CD8^+$ T cell scores, taken independently (Table 1).

Spearman correlation coefficients indicated a positive correlation between TGF-β1 expression and α-SMA, Collagen I, and Collagen III expression scores ($r=0.628$, $P=0.009$; $r=0.836$, $P<0.001$; $r=0.781$, $P<0.001$ respectively) in the livers from day 90 to day 360 p.i. in experimental mice under study (Table 2). There was also a positive correlation between TGF-β1 expression and α-SMA, Collagen I, and Collagen III expression scores ($r=0.620$, $P=0.001$; $r=0.498$, $P=0.013$; $r=0.655$, $P=0.001$ respectively) in the livers from the 16 patients with AE under study (Table 3).

RNA expression of TGF-β1. In experimental mice, real-time RT-PCR showed an increase in TGF-β1 mRNA expression from day 8 to the end of follow-up, with a peak at day 180 after infection. TGF-β1 mRNA expression increased from 0.57-fold at day 2 to 5.37-fold at day 180 (Fig. 5D) compared to control mice. There was a significant difference between *E. multilocularis* infected

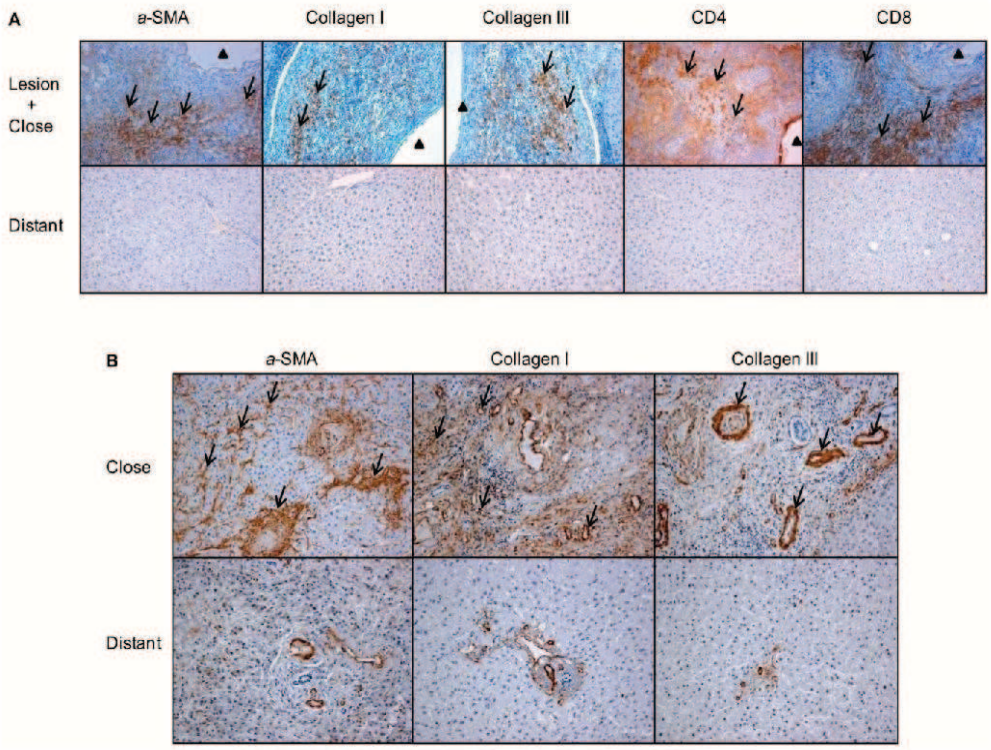

Figure 2. Immuno-histochemical expression of fibrosis markers in *E. multilocularis*-infected livers of experimental mice and AE patients, and of the periparasitic infiltration by $CD4^+$ T and $CD8^+$ T lymphocytes in the liver of experimental mice (arrow). A: In experimental mice. α-SMA: expression at day 8, in the cytoplasm of smooth muscle cells, hepatic stellate cells and myofibroblasts in the liver parenchyma; collagen I: expression at day 360, in the peri-parasitic granuloma as concentric bundles extending from the laminated layer of the parasitic vesicles to the border of the normal liver; collagen III: expression at day 360, in the peri-parasitic granuloma as concentric bundles extending from the laminated layer of the parasitic vesicles to the border of the normal liver, also present as dotted lines between the cells at the outer part of the granulomatous infiltrate and, occasionally, in the cytoplasm of round cells in the sinusoids of the surrounding liver; $CD4^+$ T cells: expression at day 90, in the periparasitic infiltrate surrounding the metacestode; $CD8^+$ T cells: expression at day 180, in the periparasitic infiltrate surrounding the metacestode. B: In AE patients. α-SMA: expressed in the extracellular matrix; collagen I expressed both in the extracellular matrix and hepatocytes; collagen III expressed in the extracellular matrix and hepatocytes. The arrowheads indicate the parasitic lesions in the liver of infected mice and human patients. Final magnification: 200×. 'Lesion': *E. multilocularis* metacestode and surrounding immune infiltrate; 'Close': liver parenchyma close to *E. multilocularis* lesion; 'Distant': liver parenchyma distant from *E. multilocularis* lesion.
doi:10.1371/journal.pone.0055379.g002

and control group at the time points of 60-, 90- and 180-days p.i. ($P<0.05$).

In AE patients, real-time RT-PCR showed that TGF-β1 mRNA expression was significantly higher in the liver tissue close to lesions compared to that distant from lesions (Fig. 6D) ($P<0.05$).

Expression of TGF-β RI and RII in the Livers Infected with *E. multilocularis*

Protein expression of TGF-β RI and RII. In experimental mice, TGF-β RI immunostaining was observed in the cytoplasm of lymphocytes and macrophages in the periparasitic infiltrate, and in most of the hepatocytes, fibroblasts, and endothelial cells in the liver close to the periparasitic infiltrate; no positive staining was observed in the control liver sections (Fig. 4). Positive cells ranged from 0.25% to 20.5% and reached a peak at day 60 p.i. In the liver distant from the parasitic lesions, a very faint staining for TGF-β RI was observed in the endothelial cells of hepatic sinusoids from 30 to 90 days p.i., a faint staining was observed in the hepatocytes from 60 to 360 days p.i. and in endothelial cells of hepatic sinusoids from 180 to 360 days p.i. (Fig. 7A). There was a significant difference between *E. multilocularis*-infected and control groups, close to lesion and distant from lesion at all time-points since day 30 ($P<0.05$, Fig. 7A). However, Western Blot results could not show a significant difference in the protein levels of TGF-β RI and TGF-β RII in infected versus control mice during the whole time course of *E. multilocularis* infection. TGF-β RII immunostaining was observed in the same cells as TGF-β RI in infected mice (Fig. 4). Positive cells ranged from 4.0% to 15.0% and reached a peak at day 60. There was a significant difference between *E. multilocularis* infected and control groups,

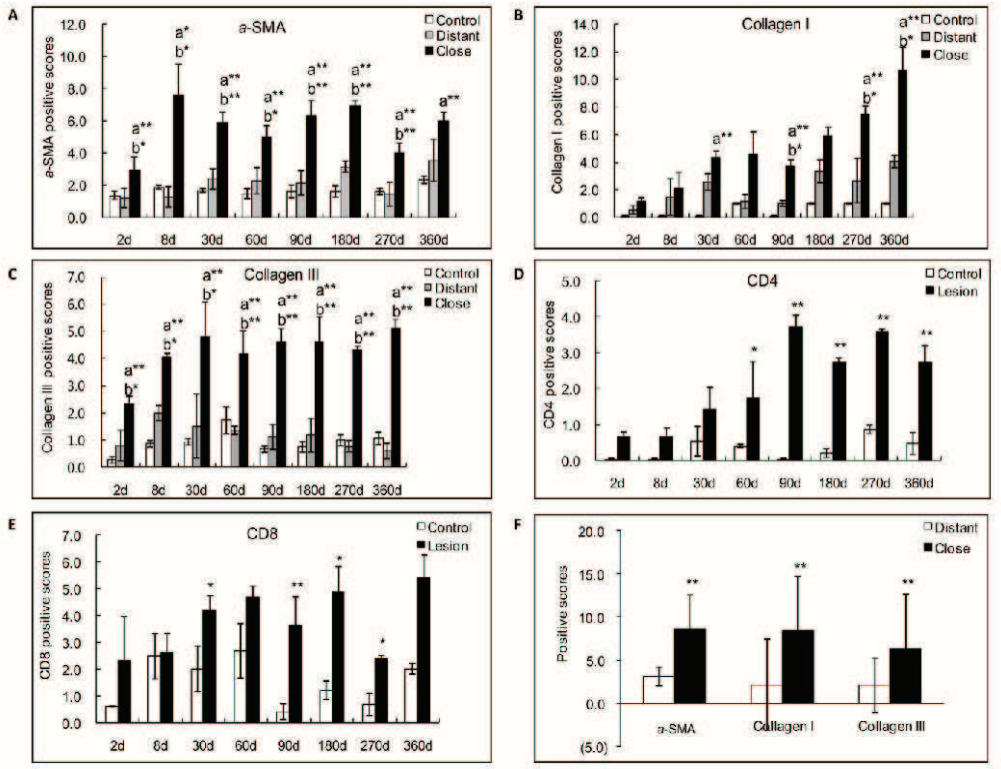

Figure 3. Semiquantitative expression of fibrosis markers in *E. multilocularis*-infected liver in experimental mice and in AE patients. Score for each marker expression was calculated from quantitative analysis of the histo-immunostaining using both staining intensity and the percentage of cells stained at a specific range of intensities (arrow) (see Materials and Methods section). A: Course of α-SMA expression in *E. multilocularis*-infected mice. B: Course of collagen I expression in *E. multilocularis*-infected mice; C: Course of collagen III expression in *E. multilocularis*-infected mice; D: Course of $CD4^+$ T cell infiltration in *E. multilocularis*-infected mice; E: Course of $CD8^+$ T cell infiltration in *E. multilocularis*-infected mice; F: Expression of fibrosis markers in the liver of AE patients. a: close versus control; b: close versus distant. *$P<0.05$; **$P<0.01$. 'Control', non-infected mice; 'Lesion': *E. multilocularis* metacestode and surrounding immune infiltrate; 'Close': liver parenchyma close to *E. multilocularis* lesion; 'Distant': liver parenchyma distant from *E. multilocularis* lesion.
doi:10.1371/journal.pone.0055379.g003

close to lesion and distant from lesion at all time-points ($P<0.05$, Fig. 7A).

In AE patients, expression of TGF-β RI differed markedly between patients and taking all 16 patients into account, there was no significant difference between the positive cells for TGF-β RI in areas close to and distant from lesions (Fig. 6A). Similarly, Western Blot results showed that TGF-β RI protein levels were not different in the liver tissue close to lesions compared to that distant from lesions (Fig. 6B and C). There was no significant difference either between the expression of TGF-β RII in areas close to and distant from lesions (Fig. 6B and C). However, compared with the areas distant from the parasitic lesions, the areas close to lesions displayed a stronger staining for TGF-β RII protein both at the cell membrane and in the cytoplasm (Fig. 4). Western Blot results showed that TGF-β RII protein levels were significantly elevated in the liver tissue close to lesions compared to that distant from lesions (Fig. 6B and C).

mRNA expression of TGF-β RI and RII. In experimental mice, an increased TGF-β RI mRNA expression was observed in infected mice at day 60 to day 180, which peaked at day180. *E.multilocularis* infection increased TGF-β RI mRNA expression from 0.43-fold at day 8 to 3.48-fold at day 180 (Fig. 7D). There was a significant difference between *E. multilocularis* infected and control groups at day 270 p.i. ($P<0.05$); however at that time, mRNA expression was lower in infected mice, despite a marked increase in the expression of the receptor as measured by immunostaining. Increased TGF-β RII mRNA expression was observed from day 30 to 90 and peaked at day 60 after infection. *E.multilocularis* infection increased TGF-β RII mRNA expression from 0.70-fold at 8 days to 2.52-fold at 60 days (Fig. 7D). The difference between *E. multilocularis*-infected and control mice was significant at day 60 and 90 ($P<0.05$).

In AE patients, there were no significant differences in TGF-β RI as well as TGF-β RII mRNA levels measured by real-time RT-PCR in the liver close to and distant from the lesions (Fig. 6D).

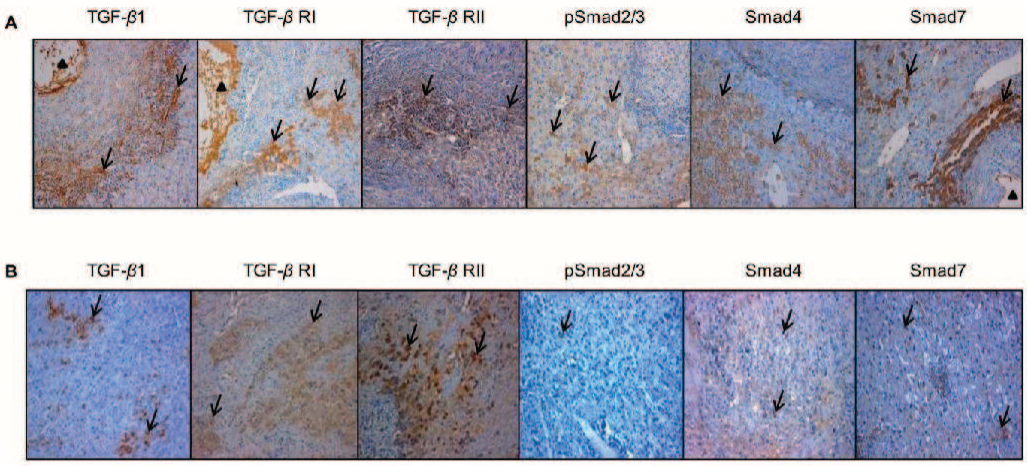

Figure 4. Immunohistochemical expression of the various components of the TGF-β/Smad pathway in the *E. multilocularis*-infected liver in experimental mice and in AE patients. A: In experimental mice. Expression of the various components of the TGF-β/Smad pathway at their peak of expression in the liver. TGF-β1: expression at day 90, in most of the immune cells in most of areas with inflammatory granulomas, in the cytoplasm of hepatocytes, endothelial cells of the hepatic sinusoids and fibroblasts; TGF-β RI and RII: expression at day 60, in the cytoplasm of lymphocytes and macrophages in the periparasitic infiltrate and in most of the hepatocytes, fibroblasts, and endothelial cells close to the periparasitic infiltrate; pSmad2/3: expression at day 30, in both the cytoplasm and nuclear of the hepatocytes; Smad4: expression at day 60, in both the cytoplasm and nuclear of the hepatocytes; Smad7: expression at day 90, in the cytoplasm of the hepatocytes. B: In AE patients. Specimen 'Close' was taken close to the parasitic lesions (0.5 cm from the macroscopic changes due to the metacestode/granuloma lesion), and Specimen 'Distant' was taken in the liver distant from the lesions (the non-diseased lobe of the liver whenever possible, or at least at 10 cm from the lesion). TGF-β1: expressed in most of the immune cells in most of areas with inflammatory granulomas, in the cytoplasm of hepatocytes, endothelial cells of the hepatic sinusoids and fibroblasts; TGF-β RI and RII: expressed in the cytoplasm of lymphocytes and macrophages in the periparasitic infiltrate and in most of the hepatocytes, fibroblasts, and endothelial cells close to the periparasitic infiltrate; pSmad2/3: expressed in both the cytoplasm and nuclear of the hepatocytes; Smad4: expressed in both the cytoplasm and nuclear of the hepatocytes; Smad7: expressed in the cytoplasm of the hepatocytes. The arrowheads indicate the parasitic lesions in the liver of infected mice and human patients. Final magnification: 200×.
doi:10.1371/journal.pone.0055379.g004

Phosphorylation of Smad2/3 and Expression of Smad4 in the Livers Infection with *E. multilocularis*

Protein expression of phosphorylated Smad 2/3. In experimental mice, pSmad2/3 was most usually expressed in the cytoplasm of the hepatocytes; very little nuclear expression was observed. In infected mice, immunostaining displayed a patchy distribution, and strong staining was observed in those hepatocytes which were close to the periparasitic infiltrate (Fig. 4). Conversely, no or a faint staining was observed in the liver distant from the parasitic lesions and in the liver from control mice. The positive cells of pSmad 2/3 ranged from 0.15% to 8.2% in the liver close to lesion, and reached a peak at day 30 and day 60 after infection. There was a significant difference between *E. multilocularis* infected and control groups, close to lesion and distant from lesion at day 30, 60, 90 and 180 ($P<0.05$, Fig. 8A). Western Blot measurements showed that there was no difference either in the phosphorylation of Smad2/3 protein in the areas close to lesions compared to those distant from lesions (Fig. 8B and C).

In AE patients, immunostaining of pSmad2/3 displayed a patchy distribution (Fig. 4), however non-related to the lobular structure of the liver and/or to the distance to the parasitic lesions. There was no significant difference between the positive cells of pSmad2/3 in areas close to and distant from lesions (Fig. 6A). Western Blot measurements showed that there was no difference either in the phosphorylation of Smad2/3 protein in the areas close to lesions compared to those distant from lesions (Fig. 6B and C).

mRNA expression of Smad2 and 3. In experimental mice, increased Smad2 and Smad3 mRNA expression was observed from day 30 to day 90. Smad2 mRNA expression peaked at day 90 and ranged from 0.8-fold at day 2 to 4.4-fold at day 90 (Fig. 8D). There was a significant difference between *E. multilocularis* infected and control groups at day 30 ($P<0.05$). Smad3 mRNA expression peaked at day 60 and ranged from 2.6-fold at day 60 days to 0.5-fold at day 360 (Fig. 8D). There was a significant difference of between *E. multilocularis* infected and control groups at day 60 ($P<0.05$).

In AE patients, there were no significant differences in Smad2 mRNA levels measured by real-time RT-PCR (Fig. 6D). However, mRNA levels of Smad3 were significantly higher in tissue samples close to lesions compared to those distant from lesions (Fig. 6D).

Protein expression of Smad4. In experimental mice, immunohistochemical study of Smad4 protein revealed higher cytoplasmic and nuclear staining of hepatocytes in areas close to lesions compared with areas distant from lesions. Distribution of Smad4 expression was similar to that of pSmad2/3 in its location, but more diffuse (Fig. 4). Positive cells for Smad4 ranged from 0.2% to 18.0% in the liver close to lesion, and reached a peak at day 60 p.i.There was a significant difference between *E. multilocularis*-infected and control groups, close to lesion and distant from lesion at day 30, 60, 90, 180, and 270 ($P<0.05$, Fig.9A). However, Western Blot analysis of Smad4 expression did not show any difference between infected and control mice, as well as

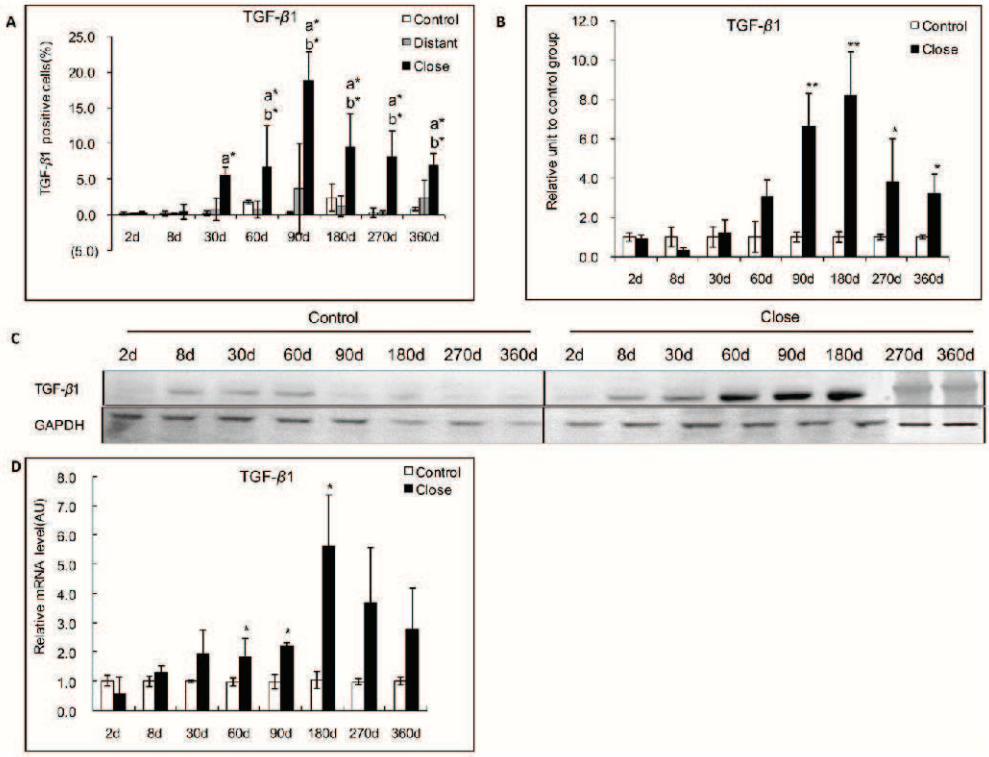

Figure 5. Course of TGF-β1 expression in the liver of experimental mice during *E. multilocularis* infection. A: Course of TGF-β1 expression observed by immune-staining in the liver from *E. multilocularis* infected mice, calculated as the percent of positive cells to the total number of counted cells (see Materials and Methods section). B: Relative amount of TGF-β1 calculated from semi-quantitative analysis of the Western Blot using densitometry. C: Representative example of the course of TGF-β1 protein measured by Western Blot. D: Course of TGF-β1 mRNA expression measured by real time RT-PCR. a: 'close' versus 'control'; b: 'close' versus 'distant'. *$P<0.05$; **$P<0.01$. 'Control', non-infected mice; 'Lesion': *E. multilocularis* metacestode and surrounding immune infiltrate; 'Close': liver parenchyma close to *E. multilocularis* lesion; 'Distant': liver parenchyma distant from *E. multilocularis* lesion. AU: arbitrary units; GAPDH: glyceraldehyde-3-phosphate dehydrogenase.
doi:10.1371/journal.pone.0055379.g005

between the liver close to and distant from the lesions, all over the time course (Fig. 9B and C).

In AE patients, immunohistochemical staining for Smad4 protein in the liver revealed cytoplasmic and nuclear staining of hepatocytes, with a homogenous distribution among cells; positive cells were higher in the areas close to lesions compared with those distant to lesions. Intensity of nuclear staining of Smad4 protein was noticeably higher in the areas close to the lesions (Fig. 4). Western Blot results also confirmed that Smad4 protein levels were significantly higher in the liver parenchyma close to lesions compared to that distant from lesions (Fig. 6B and C).

mRNA expression of Smad4. In experimental mice, increased Smad4 mRNA expression was observed from day 30 to day 90. Smad4 mRNA expression peaked at day 90 and ranged from 0.6-fold at day 8 to 1.9-fold at day 90 (Fig. 9D). There was a significant difference between *E. multilocularis* infected and control mice at day 90 ($P<0.05$).

In AE patients, the "lesions to periphery gradient" observed for the protein expression was also demonstrated at the mRNA level, as measured by real-time RT-PCR, with higher expression close to the lesions (Fig. 6D).

Expression of Smad 7 in the Livers Infected with *E. multilocularis*

Protein expression of Smad7. In experimental mice, Smad7 immunostaining was mostly present in the cytoplasm of the hepatocytes, with a varying intensity throughout the liver, higher in the areas close to the lesion than in those distant from the lesion (Fig. 4). A faint staining was observed in the hepatocytes from 30 to 360 days in the areas distant from the lesion and in the control group (Fig. 10A). Smad7 positive cells in the hepatic cells ranged from 0.40% to 9.45% and reached a peak at 90 days. There was a significant difference between *E. multilocularis* infected and control groups, close to lesion and distant from lesion at 60 days, 90 days, 180 days and 270 days p.i. ($P<0.05$, Fig. 10A). Western Blot results showed that there was no change in Smad7 expression between *E. multilocularis* infected and control mice

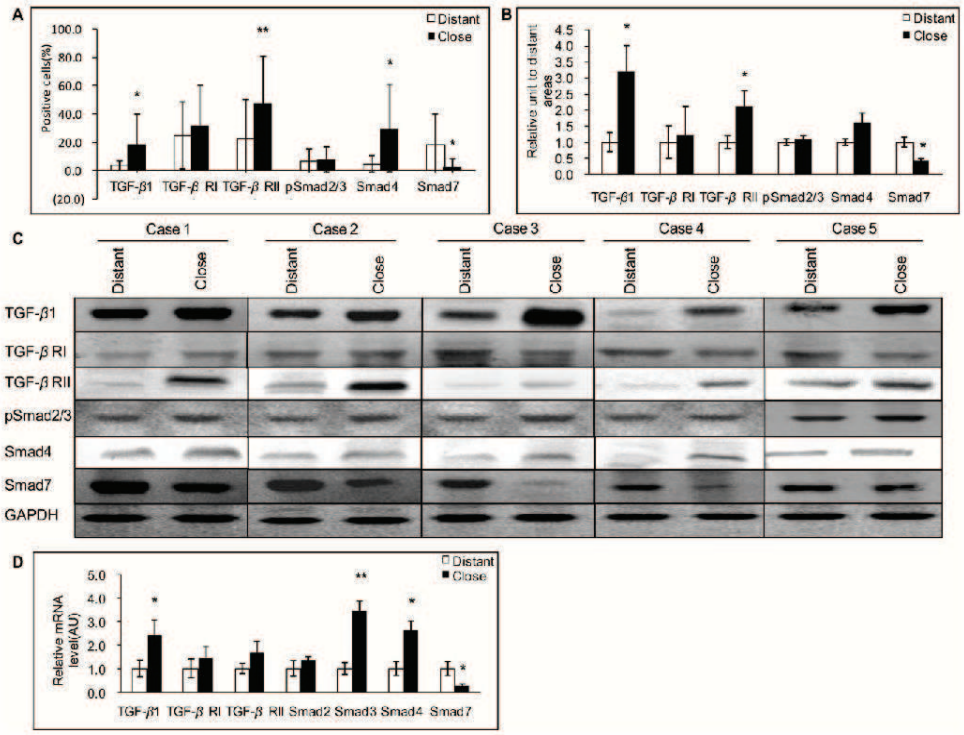

Figure 6. Expression of the various components of the TGF-β1/Smad pathway in the liver of AE patients. A: Expression of TGF-β1/Smads calculated as the percent of positive cells to the total number of counted cells after immunostaining (see Materials and Methods section). B: Relative amount of TGF-β1/Smads calculated from semi-quantitative analysis of the Western Blot using densitometry. C: Representative examples of Western Blot analyses performed on lysates from liver samples with antibodies that recognize TGF-β1, TGF-β RI, TGF-β RII, phosphorylated (p-) Smad2/3, Smad4 and Smad7. D: TGF-β1/Smads mRNA expression measured by real time RT-PCR. *$P<0.05$ versus control, **$P<0.01$ versus control. 'Distant': distant from lesion; 'Close': close to lesion; AU: arbitrary units; GAPH: glyceraldehyde-3-phosphate dehydrogenase.
doi:10.1371/journal.pone.0055379.g006

during the whole time course of *E. multilocularis* infection (Fig. 10B and C).

In AE patients, Smad7 immunostaining was mostly present in the cytoplasm of the hepatocytes, with a varying intensity throughout the liver. Opposite to the decreasing gradient from the lesions to the distant parenchyma observed with most of the other components, the expression scores of Smad7 expression were lower in the areas close to lesions than in those distant from the lesions (Fig. 4B). Western Blot results also showed that Smad7

Table 1. Results of the correlation analysis between TGF-β1 and CD4/CD8, CD4, CD8 positive cells in murine AE (from the histo-immunochemistry analysis).

		CD4/CD8	CD4	CD8
TGF-β1	Spearman's rho	0.818*	0.639	−0.118
	Sig.	0.013	0.088	0.780
	N	8	8	8

Note: *$P<0.05$.
doi:10.1371/journal.pone.0055379.t001

Table 2. Results of the correlation analysis between TGF-β1, Smad7 and liver fibrosis markers in murine AE (from the histo-immunochemistry analysis).

		α-SMA	Collagen I	Collagen III
TGF-β1	Spearman's rho	0.628**	0.836**	0.781**
	Sig.	0.009	$P<0.001$	$P<0.001$
	N	8	8	8
Smad7	Spearman's rho	−0.600	−0.853**	−0.316*
	Sig.	0.400	$P<0.001$	0.684
	N	8	8	8

Note: *$P<0.05$,
**$P<0.01$.
doi:10.1371/journal.pone.0055379.t002

Table 3. Results of the correlation analysis between TGF-β1, Smad7 and liver fibrosis markers in human AE (from the histo-immunochemistry analysis).

		α-SMA	Collagen I	Collagen III
TGF-β1	Spearman's rho	0.620**	0.498**	0.655**
	Sig.	0.001	0.013	0.001
	N	16	16	16
Smad7	Spearman's rho	−0.569**	−0.313	−0.463*
	Sig.	0.004	0.136	0.023
	N	16	16	16

Note: *$P<0.05$,
**$P<0.01$.
doi:10.1371/journal.pone.0055379.t003

protein levels were significantly lower in the liver parenchyma close to lesions compared to that distant from lesions (Fig. 6B and C).

Correlation with T cell subpopulations and fibrosis markers. Spearman correlation coefficients indicated a negative correlation between Smad7 expression and α-SMA, Collagen I, and Collagen III expression scores which was significant for Collagen I and Collagen III ($r=-0.853$, $P<0.01$; and $r=-0.316$, $P<0.05$ respectively) in the livers from day 90 to day 360 p.i. in experimental mice under study (Table 2). There was also a negative correlation between Smad7 expression and α-SMA, Collagen I, and Collagen III expression scores, which was significant for α-SMA and Collagen III ($r=-0.569$, $P=0.01$; and $r=-0.463$, $P=0.05$, respectively) in the livers from the 16 patients with AE under study (Table 3).

mRNA expression of Smad7. In experimental mice, Smad7 mRNA expression was significantly higher in *E. multilocularis*-infected than in control mice at day 30 ($P<0.01$) (Fig. 10D).

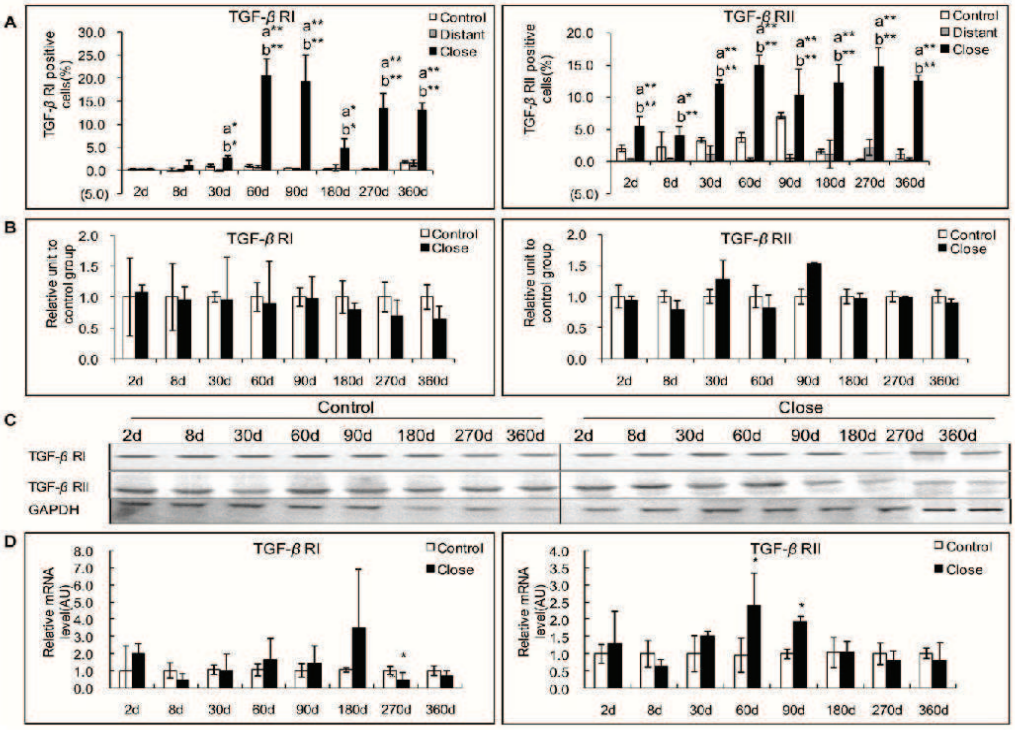

Figure 7. Course of TGF-β1 receptors (TGF-β RI and TGF-β RII) expression in the liver of mice during *E. multilocularis* infection in experimental mice. A: Course of TGF-β RI and RII expression observed by immune-staining in the liver from *E. multilocularis* infected mice compared to control mice, calculated as the percent of positive cells to the total number of counted cells (see Materials and Methods section). B: Relative amount of TGF-β RI and RII calculated from semi-quantitative analysis of the Western Blot using densitometry. C: Representative example of the course of TGF-β RI and RII protein measured by Western Blot in experimental mice. D: Course of TGF-β RI and RII mRNA expression measured by real time RT-PCR in experimental mice. a: 'close' versus 'control'; b: 'close' versus 'distant'. *$P<0.05$; **$P<0.01$. 'Control', non-infected mice; 'Lesion': *E. multilocularis* metacestode and surrounding immune infiltrate; 'Close': liver parenchyma close to *E. multilocularis* lesion; 'Distant': liver parenchyma distant from *E. multilocularis* lesion. AU: arbitrary units; GAPDH: glyceraldehyde-3-phosphate dehydrogenase.
doi:10.1371/journal.pone.0055379.g007

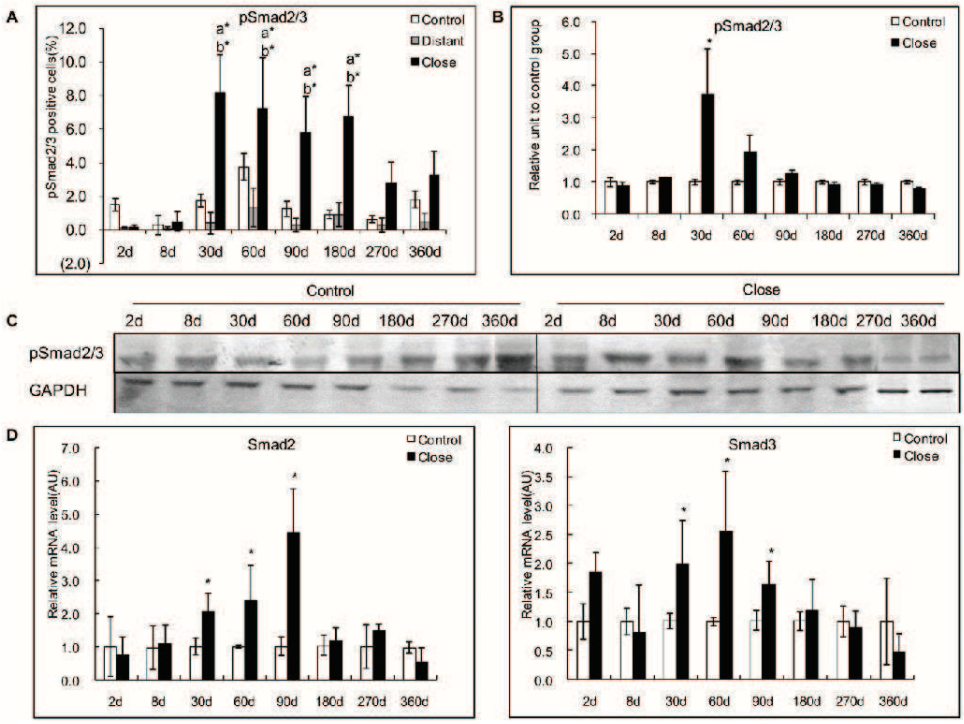

Figure 8. Course of pSmad2/3 expression in the liver of mice during *E. multilocularis* infection in experimental mice. A: Course of pSmad2/3 expression observed by immune-staining in the liver from *E. multilocularis* infected mice compared to control mice, calculated as the percent of positive cells to the total number of counted cells (see Materials and Methods section). B: Relative amount of pSmad2/3 calculated from semi-quantitative analysis of the Western blot using densitometry. C: Representative example of the course of pSmad2/3 protein measured by Western Blot in experimental mice. D: Course of Smad2 and Smad3 mRNA expression measured by real time RT-PCR in experimental mice. a: 'close' versus 'control'; b: 'close' versus 'distant'. *$P<0.05$; **$P<0.01$. 'Control', non-infected mice; 'Lesion': *E. multilocularis* metacestode and surrounding immune infiltrate; 'Close': liver parenchyma close to *E. multilocularis* lesion; 'Distant': liver parenchyma distant from *E. multilocularis* lesion. AU: arbitrary units; GAPDH: glyceraldehyde-3-phosphate dehydrogenase.
doi:10.1371/journal.pone.0055379.g008

In AE patients, lower Smad7 mRNA levels close to the lesions, as measured by real-time RT-PCR, further confirmed the reverse gradient from the lesions to the periphery observed at the protein level (Fig. 6D).

Correlation with fibrosis markers. There was a significant negative correlation between Smad7 and Collagen I expression scores in experimental mice under study ($r=-0.853$, $P<0.001$) (Table 2). There was also a significant negative correlation between Smad7 and α-SMA and Collagen III expression scores ($r=-0.569$, $P=0.004$; $r=-0.463$, $P=0.023$ respectively) (Table 3) in the liver of the 16 AE patients under study.

Discussion

Despite the major potential role attributed to TGF-β in the tolerance and the fibrosis processes in AE, only one study until now reported that TGF-β was expressed in the periparasitic infiltrate in liver biopsies from a patient with AE [14]; however, quantified expression of TGF-β protein and mRNA was never studied, and neither the presence of TGF-β receptors nor that of components of the TGF-β metabolic pathway were ever looked for in *E. multilocularis*-infected livers. In the present study, both in humans and in the longitudinal study of experimental *E. multilocularis* infection model, we confirmed that TGF-β and members of its pathway were actually present in *E. multilocularis*-infected livers (Fig. 11). We could show the expression of TGF-β in most lymphocytes and macrophages of the periparasitic infiltrate as well as in the liver parenchyma, even distant from the parasitic lesion. Phenotypic study of cells within the periparasitic granuloma also confirmed that $CD4^+$ T cells represented the major population of T cells at the beginning of the infection and that this sub-population was progressively replaced by $CD8^+$ T cells [9], and this change of CD4/CD8 ratios could contribute to maintain TGF-β1 secretion. TGF-β receptors were also expressed at the membrane of most cells in the periparasitic infiltrate and in the liver parenchyma from early to late stage post *E. multilocularis* infection. Expression of the receptors suggested that the markedly

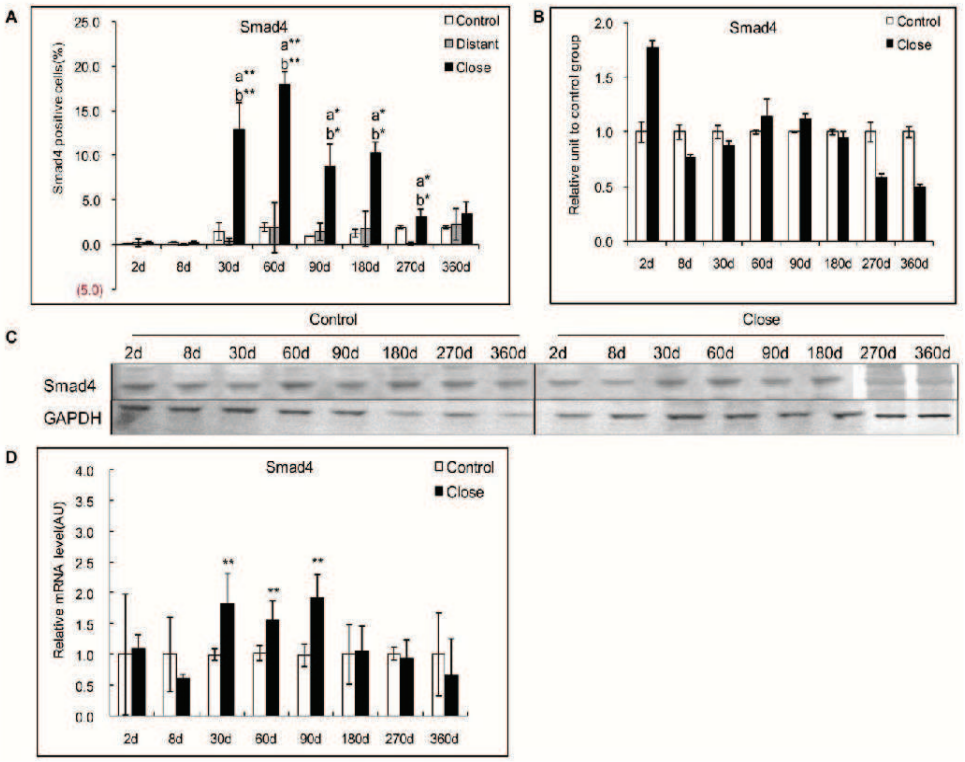

Figure 9. Course of Smad4 expression in the liver of mice during *E. multilocularis* infection in experimental mice. A: Course of Smad4 expression observed by immune-staining in the liver from *E. multilocularis* infected mice compared to control mice, calculated as the percent of positive cells to the total number of counted cells (see Materials and Methods section). B: Relative amount of Smad4 calculated from semi-quantitative analysis of the Western blot using densitometry. C: Representative example of the course of Smad4 protein measured by Western Blot in experimental mice. D: Course of Smad4 mRNA expression measured by real time RT-PCR in experimental mice. a: 'close' versus 'control'; b: 'close' versus 'distant'. *$P<0.05$; **$P<0.01$. 'Control', non-infected mice; 'Lesion': *E. multilocularis* metacestode and surrounding immune infiltrate; 'Close': liver parenchyma close to *E. multilocularis* lesion; 'Distant': liver parenchyma distant from *E. multilocularis* lesion.AU: arbitrary units; GAPDH: glyceraldehyde-3-phosphate dehydrogenase.
doi:10.1371/journal.pone.0055379.g009

elevated levels of TGF-β1 present in *E. multilocularis*-infected liver, were functional to regulate the activities of immune cells as well as hepatocytes and cells involved in fibrosis. This was confirmed by the changes also observed in various Smad components of the TGF-β pathway, with usually a marked increase since the middle stage of the chronic phase of the disease in *E. multilocularis* infected mice, which suggested an activation of the Smad cascade and thus an activation of the signal transduction of TGF-β1. Expression of the receptors and of Smads and phosphorylation of Smad 2/3 in the liver of human patients with hepatic AE, with various types of gradient in the liver depending on the cascade component, confirmed the significant activation of the system at the middle/late stage of *E. multilocularis* infection.

Fibrosis is a hallmark of AE, leading to a complete disappearance of the liver parenchyma in the periparasitic area, and to fibrosis in portal spaces. Fibrosis protects the host against the parasitic growth, but at the same time it distorts the liver parenchyma, contributes to bile duct and vessel obstruction and can lead to secondary biliary cirrhosis [5,7]. The irreversible acellular keloid scar-like fibrosis observed in AE is the ultimate result of cytotoxic and fibrogenetic events related to the immune response of the host which are taking place initially in the granulomatous area surrounding the young parasite larvae [13]. Previous observations in experimental models of AE have suggested that progression of fibrosis in AE involves an early deposition of type III collagen pro-peptide and type III collagen at the periphery of the granulomas, and a subsequent remodeling of fibrosis with bundles of type I collagen in the periparasitic central area [4]. Stellate cell–derived myofibroblasts have been observed in AE liver, both in humans [7] and in the experimental mouse model [4]. It was noted that in some regions of the liver where the parenchyma was totally replaced with dead parasitic lesions and fibrosis, HSC were the only cellular remnants present [7]. We confirmed that α-SMA, a specific cell marker for MFB, as well as type I and III collagens, were highly expressed in tissues surrounding AE lesions; the expression of collagen I increased

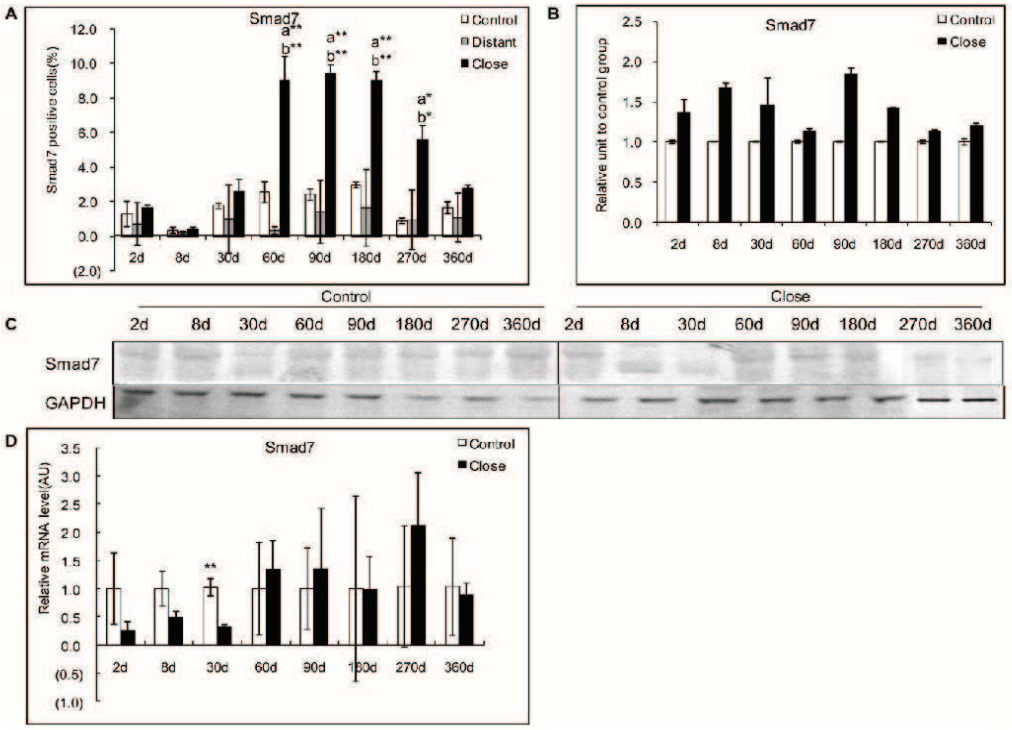

Figure 10. Course of Smad7 expression in the liver of mice during *E. multilocularis* infection in experimental mice. A: Course of Smad7 expression observed by immune-staining in the liver from *E. multilocularis* infected mice compared to control mice, calculated as the percent of positive cells to the total number of counted cells (see Materials and Methods section). B: Relative amount of Smad7 calculated from semi-quantitative analysis of the Western blot using densitometry. C: Representative example of the course of Smad7 protein measured by Western Blot in experimental mice. D: Course of Smad7 mRNA expression measured by real time RT-PCR in experimental mice. a: 'close' versus 'control'; b: 'close' versus 'distant'. *$P<0.05$; **$P<0.01$. 'Control', non-infected mice; 'Lesion': *E. multilocularis* metacestode and surrounding immune infiltrate; 'Close': liver parenchyma close to *E. multilocularis* lesion; 'Distant': liver parenchyma distant from *E. multilocularis* lesion. AU: arbitrary units; GAPDH: glyceraldehyde-3-phosphate dehydrogenase.
doi:10.1371/journal.pone.0055379.g010

steadily through the course of the infection, whereas collagen III rapidly reached its maximum level of expression at day 8; this sequence of events, which is usual in fibrotic processes (collagen III being produced quickly by fibroblasts before collagen I is synthesized) was already noticed in the first studies on AE fibrosis in the experimental model; in humans, as well as in mice at later stages, location of collagen III in areas of recent larval development supported this sequence [4,7].

The positive correlation we found between their expression and expression of TGF-β1, both in the experimental model and in human livers, is an indirect argument for a significant role of this cytokine in AE fibrosis. The major peak of TGF-β1 at the middle stage of infection in experimental animals, and its expression in AE patients who are diagnosed at a similar stage, suggest that although lower levels may initiate immune tolerance as early as the early stage, the cytokine becomes prominent later, when both maintenance of the tolerance state and development of fibrosis are at stake (Fig. 11). Several cytokines are involved in fibrosis development [27,28]. The role of pro-inflammatory cytokines, and especially tumor necrosis factor (TNF-α), in the protection of the host against *E. multilocularis* has been demonstrated, and it is likely that they act at least in part through the development of fibrosis [29]. In human livers with hepatic AE, the mRNAs of pro-inflammatory cytokines, interleukin (IL)-1β, IL-6, and TNF-α have been found in macrophages located at the periphery of granulomas, in those areas which were shown to be at the initiation of fibrogenesis [30]. IL-12, which inhibits the development of the parasitic vesicles after *E. multilocularis* infection, was also shown to induce a fast development of peri-vesicle fibrosis [31]. However, TGF-β is probably the most decisive cytokine and HSCs the most significant cells involved in liver fibrosis [32]; and the involvement of TGF-β and HSCs in the development of the fibrosis in other liver parasitic diseases, such as schistosomiasis, has been well documented [33,34]. During the development of chronic liver injury, including inflammation, fibrosis and regeneration, TGF-β1 plays a prominent role in stimulating liver fibrogenesis by MFBs derived from HSCs. TGF-β1 can be secreted by Kupffer cells, biliary cells, infiltrated inflammatory cells, and the HSC them-

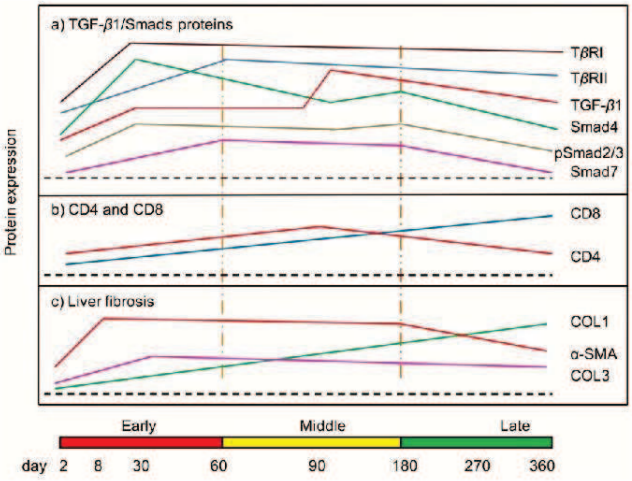

Figure 11. Course of the changes in the protein expression of TGF-β1/Smads (a), T cell subpopulation CDs (b) and liver fibrosis markers (c) during the process of *E. multilocularis*-induced liver injury in mice.
doi:10.1371/journal.pone.0055379.g011

selves; it inhibits hepatocyte proliferation, induces hepatocyte apoptosis, and activates HSC to differentiate into MFBs and secrete ECM components, including collagens, acting via both paracrine and autocrine pathways; TGF-β1 also inhibits ECM degradation and enhances accumulation of ECM in the liver [35]. Our results highly suggest that TGF-β and its signaling pathway are in the position to play this major role regarding fibrosis in AE.

The Smad family of proteins mediates signaling from the TGF-β R to the nucleus. In the current study, there was an increased expression of TGF-β R, Smad3 mRNA, and especially of Smad4 which is a central mediator in TGF-β superfamily signaling [20]. A few discrepancies between RNA expression and the amount of protein regarding TGF-β R and Smads may be explain by post-transcriptional events, and deserve further studies, since such events could be caused by parasite components. On the other hand, information given by immunostaining and Western Blot analysis is different, albeit complementary, since the type and microenvironment of the producing cells may compensate otherwise lower amounts of the protein. Our study showed that expression of Smad4 was higher in areas surrounding lesions than in distant liver in the patients with AE. Smad7, which is induced by TGF-β itself, is responsible for the fine-tuning of TGF-β signals [36]. It prevents the phosphorylation of Smad proteins, associates with ubiquitin ligases involved in TGF-β R-degradation, and acts as a transcriptional repressor inhibiting Smad-dependent promoter activation [37]. In physiological situations, its increase decreases the phosphorylation of Smad2/3, and thus decreases TGF-β functions. In chronic hepatic injury, the expression of Smad7 is paradoxically decreased [38]; as a result, TGF-β signal transduction cannot be effectively inhibited, and TGF-β functions are enhanced. An aberrant expression of Smad7 may thus disrupt the balanced activity of TGF-β under pathophysiological conditions. The low expression of Smad7 in the areas surrounding the lesions and its negative correlation with α-SMA and Collagen III highly suggest that in AE too the normal feed-back loop might not work properly, and that fibrosis might be permanently activated through

Table 4. Primers and cycling parameters of real time RT-PCR detection of TGF-β1 signaling pathway (mouse).

Gene	Genbank Accession	Primer Sequences	Annealing Temperature	Expected Size
TGF-β1	NM_011577	F:5′-GTGTGGAGCAACATGTGGAACTCTA-3′ R:5′-TTGGTTCAGCCACTGCCGTA-3′	52.1°C	143 bp
TGF-β RI	NM_009370.2	F: 5′-TGCAATCAGGACCACTGCAATAA-3′ R: 5′-GTGCAATGCAGACGAAGCAGA-3′	60.0°C	133 bp
TGF-β RII	NM_009371.2	F: 5′-AAATTCCCAGCTTCTGGCTCAAC-3′ R: 5′-TGTGCTGTGAGACGGGCTTC-3′	60.0°C	100 bp
Smad2	NM_010754	F: 5′-AACCCGAATGTGCACCATAAGAA-3′ R: 5′-GCGAGTCTTTGATGGGTTTACGA-3′	60.0°C	198 bp
Smad3	NM_016769	F: 5′-GTCAACAAGTGGTGGCGTGTG-3′ R: 5′-GCAGCAAAGGCTTCTGGGATAA-3′	60.0°C	150 bp
Smad4	NM_008540	F: 5′-TGACGCCCTAACCATTTCCAG-3′ R: 5′-CTGCTAAGAGCAAGGCAGCAAA-3′	60.0°C	136 bp
Smad7	NM_001042660	F: 5′-AGAGGCTGTGTTGCTGTGAATC-3′ R: 5′-CCATTGGGTATCTGGAGTAAGGA-3′	60.0°C	126 bp
β-actin	NM_007393	F: 5′-AACTCCATCATGAAGTGTGA-3′ R: 5′-ACTCCTGCTTGCTGATCCAC-3′	56.0°C	248 bp

doi:10.1371/journal.pone.0055379.t004

Table 5. Primers and cycling parameters of real time RT-PCR detection of TGF-β1 signaling pathway (Human).

Gene	Genbank Accession	Primer Sequences	Annealing Temperature	Expected Size
TGF'-β1	A23751.1	F:5'-ACACCAACTATTGCTTCAG-3' R:5'-TGTCCAGGCTCCAAATG-3'	55.7°C	159 bp
TGF-β RI	NM_001130916	F: 5'-AATTCCTCGAGATAGGCCGT-3' R: 5'-TGCGGTTGTGGCAGATATAG-3'	60.0°C	244 bp
TGF-β RII	NM_003242.5	F: 5'-AACAACATCAACCACAACACAG-3' R: 5'-CCGTCTTCCGCTCCTCAG-3'	56.2°C	250 bp
Smad2	NM_005901.4	F: 5'-GTCTCTTGATGGTCGTCTC-3' R: 5'-GGCGGAAGTTCTGTTAGG-3'	53.3°C	249 bp
Smad3	NM_001145104.1	F: 5'-GTGCTCCATCTCCTACTAC-3' R: 5'-CCTCTTCCGATGTGTCTC-3'	56.5°C	183 bp
Smad4	BC002379.2	F: 5'-CAGGACAGCAGCAGAATG-3' R: 5'-CAATACTCAGGAGCAGGATG-3'	55.6°C	232 bp
Smad7	NM_001190823.1	F: 5'-TTTGTGTATTTATTTCTTTCTCTC-3' R: 5'-CACTCTCGTCTTCTCCTC-3'	54.5°C	194 bp
β-actin	NM_002046.3	F: 5'-GCACCGTCAAGGCTGAGAAC-3' R: 5'-TGGTGAAGACGCCAGTGGA-3'	50.8°C	138 bp

doi:10.1371/journal.pone.0055379.t005

that mechanism. As TGF-β is likely to be crucial to maintain the immune tolerance state and T-reg generation/function essential to the parasite, *E. multilocularis* could be responsible for the paradoxical decrease of Smad7 in the periparasitic granuloma and nearby liver; this might be one of the mechanisms for the early induction of immune tolerance and for the progression from chronic hepatic injury to hepatic fibrosis during *E. multilocularis* infection. All results obtained in the mouse model however do not fully support an essential role for the inhibitory Smad7 feed-back loop: Smad7 was indeed high in the middle stage of *E. multilocularis* infection, and Smad7 expression negatively correlated globally with expression of collagen I and III in infected mice, but this elevation did not seem to markedly decrease pSmad2/3, and Smad4 expression; the light decrease of these components at day 90, could be an indication of its partial intervention; other mechanisms of regulation of the TGF-β pathway at that crucial stage of the disease, to maintain a high level of activity of the pathway are thus likely. In fact, TGF-β also induces other non-SMAD signaling pathways, which include activation of several MKKs (MAP kinase Kinase) and MEKs (MAPK/ERK Kinase) pathways (including JNK/SPAK, p38, and ERK1/2) through upstream mediators RhoA, Ras, TAK1 (TGF-βActivated Kinase), TAB1 (TAK1 Binding Protein); and the proteins XIAP (Xenopus Inhibitor of Apoptosis), HPK1 (Haematopoietic Progenitor Kinase-1) are also involved in this link [39]. Thus, TGF-β itself or its receptors, more than down-stream Smads, represent an attractive target for the development of therapeutics that simultaneously attack the pathogen and its micro-environment, the pleiotropic nature of TGF-β signaling, its role in tissue homeostasis and its dual role in pathogenesis present unique challenges that must be considered in pre-clinical and clinical drug development programs.

In preliminary *in vitro* studies (data not shown) we observed a secretion of TGF- β1 and an activation of the TGF-β pathway in rat hepatocyte cultures incubated with vesicle fluid of parasitic origin, in the absence of inflammatory cells, thus of immune cell-related cytokines. This is an intriguing finding which reinforces the hypothesis of a "cross-talk" between the parasitic larva and its host, already provided by a number of observations which suggested that the larval development of *E. multilocularis* is triggered by cell signaling originating from the intermediate host [40,41] and that *E. multilocularis* metacestode was thus able to "sense" host factors, which may result in an activation of the parasite metabolic pathway cascades [42]. Conversely, the parasite might also influence signaling mechanisms of host cells through the secretion of various molecules which might bind to host cell surface receptors or to the temporary storage of host-derived molecules in the vesicle fluid. Such interactions could contribute to immunomodulatory activities of *E. multilocularis*, to pathological consequences on the host's tissues, and/or be involved in mechanisms of organotropism [14]. In our previous study, a significant influence of *E. multilocularis* metacestode on the activation of MAPKs signalling pathways was found in the liver cells both in vivo in infected patients and in vitro in cultured rat hepatocytes [43]. A recent study has also provided evidence for the induction of apoptosis in host DC through *Echinococcus* E/S-products of early infectious stages of *E. multilocularis* [44]. These observations suggest that parasitic components, and not only factors from host origin, are actually acting on the host [44]. Further studies are, however, necessary to determine the parasite and/or host components actually involved in the activation of the TGF-β/Smad pathway.

Materials and Methods

Ethics Statement

The clinical investigation has been conducted according to the principles expressed in the Declaration of Helsinki. For research involving human participants, informed written consent has been obtained from the patients, as part of a research project approved by the Ethical Committee of First Affiliated Hospital of Xinjiang Medical University (20080812-5). The animal study was performed in strict accordance with the recommendations in the Guide for the Care and Use of Laboratory Animals. The protocol was approved by the Animal Care and Use Committee and the Ethical Committee of First Affiliated Hospital of Xinjiang Medical University (20081205-2). All surgery was performed under sodium pentobarbital anesthesia, and every effort was made to minimize suffering.

Experimental Design, Tissue Sampling and Histological Examination

Experimental animals. One hundred and twenty pathogen-free female BALB/c mice (8–10-week old) were housed in cages with a 12-h light/dark cycle and provided with rodent chow and water. BALB/c mice were infected by *E. multilocularis* and tissue samples were collected and detected as previously described [26,45]. For each autopsy time-point, ten experimentally infected mice were used in *E. multilocularis* group (n = 10) and compared with five control mice (n = 5), which received an intra-hepatic injection of 0.1 mL of saline in the anterior liver lobe using the same surgical procedure. Mice were killed at 2, 8, 30, 60, 90, 180, 270 and 360 days, respectively. Tissue samples from *E. multi-*

locularis lesions were taken and processed for histopathological examination and immunostaining. In addition, liver tissue samples were taken 1) close to the parasitic lesions, i.e. 1–2 mm from the macroscopic changes due to the metacestode/granuloma lesion, thus avoiding liver contamination with infiltrating immune cells and parasitic tissue, and 2) distant from the parasitic lesion, in another lobe of the liver, in *E. multilocularis* infected mice; in control mice, samples were taken in the injected lobe and in a non-injected lobe of the liver.

Patients. In humans, the diagnosis of *E. multilocularis* infection (AE) was based on positive serology with ELISA using crude *E. multilocularis* antigen, Antigen B, Em2 and Em18 (Xinjiang Bei Si Ming, Urumqi, China) and characteristic liver lesions observed on ultrasound- and CT scans. All diagnoses were confirmed by histological examination of the lesions [35]; tissue samples taken for diagnosis were also used for immunostaining. In addition, to measure proteins in the liver using Western Blot and mRNA using real time RT-PCR, paired liver specimens (0.5 cm3 each) were obtained at surgery by an experienced surgeon from 16 patients with AE at the First Affiliated Hospital of Xinjiang Medical University, Urumqi, China. From each patient, one specimen was taken close to the parasitic lesions (0.5 cm from the macroscopic changes due to the metacestode/granuloma lesion), and one was taken in the liver distant from the lesions (the non-diseased lobe of the liver whenever possible, or at least at 10 cm from the lesion), according to a previously described procedure [35].

Processing of tissue samples. Liver samples were separated into two parts and either deep-frozen in liquid nitrogen for RNA isolation or formalin-fixed for histopathological examination. For histological and immunohistochemical studies, the liver samples were fixed in 4% paraformaldehyde in neutral buffered formalin for a minimum of 24 h, embedded in paraffin, and cut into 4 µm serial sections. Paraffin-embedded liver tissue samples of experimental mice and AE patients were stained by Hematoxylin and Eosin (H&E) and Masson's trichrome for pathological observations.

Immunohistochemistry Analysis

Immunohistochemistry was performed on formalin-fixed, paraffin-embedded tissue. Briefly, 4 µm tissue sections were deparaffinized in xylene and rehydrated in gradual dilutions of ethanol. Endogenous peroxidase was blocked with 3% hydrogen peroxide. To increase staining, sections were pretreated by microwave heating for 15 min in antigen unmasking solution (pH 6.8, 0.1 M citrate buffer, Zhongshan Jinqiao Biology Corporation, Beijing). To block non-specific background, the sections were incubated with non-immune goat serum for 30 min. Sections were then incubated overnight at 4°C with the primary antibody diluted in pH 7.3 phosphate-buffered saline (PBS) (α-SMA 1:200, Collagen 1 (COL 1) 1:200, Collagen 3 (COL3) 1:200, CD4 1:100, CD8 1:100, TGF-β1 1:100, TGF-β receptor I (TGF-β RI) 1:200, TGF-β receptor II (TGF-β RII) 1:200, pSmad2/3 1:200, Smad4 1:200, and Smad7 1:100) (Santa Cruz Corporation, CA, USA). After 3 washes in PBS, the sections were subsequently incubated with horseradish peroxidase conjugated host-specific secondary antibodies and 3, 3′-diaminobenzidine was used as chromogen. Sections were counterstained with hematoxylin for 5 min, dehydrated, and covered with slips. For all samples, negative controls consisted of substitution of the isotype-matched primary antibody with PBS.

Western Blot Analysis

Western Blot analysis of cell lysates was performed by SDS-PAGE using NuPAGE (Invitrogen, California, USA) followed by transfer to nitrocellulose membrane (Invitrogen, California, USA). Ponceau S (Sigma, Missouri, USA) staining was used to ensure equal protein loading and electrophoretic transfer. Using the appropriate antibodies, TGF-β1, TGF-β RI, and RII, pSmad2/3, Smad4 and Smad7 (Cell Signaling Technology, Massachusetts, USA) and GAPDH (Santa Cruz Biotechnology, California, USA) were detected with WesternBreeze Kit (Invitrogen, California, USA). The expression levels of respective proteins (in "relative units") in the liver of control mice and *E. multilocularis* infected mice, as well as in the liver of AE patients, were quantified using Quantity One software (Bio-Rad, Hercules, USA).

Quantitative Real-time RT- PCR Analysis

After removing contaminated DNA from the isolated RNA using DNaseI (Fermentas, Vilnius, Lithuania), 1 µg of total RNA was reverse transcribed into cDNA in 20 mL reaction mixtures containing 200 U of Moloney murine leukemia virus reverse transcriptase (MMLV, Promega, Madison, USA); 100 ng per reaction of oligo (dT) primers; and 0.5 mM each of dNTPs, dATP, dCTP, dGTP, and dTTP. The reaction mixture was then incubated at 42°C for 1 hour and at 95°C for 5 min to deactivate the reverse transcriptase.

The real time RT-PCR was run in a thermocycler (iQ5 Bio-Rad, Hercules, CA, USA) with the SYBR Green PCR premix (TaKaRa, Dalian, China) following the manufacturer's instructions. Thermocycling was performed in a final volume of 20 µL containing 2 µL cDNA and 10 pM of each primer (Table 4 and 5). To normalize for gene expression, mRNA expression of the housekeeping gene GAPDH was measured. For every sample, both the housekeeping and the target genes were amplified in triplicate using the following cycle scheme: after initial denaturation of the samples at 95°C for 1 min, 40 cycles of 95°C for 5 s and 60°C (or other) for 30 s were performed. Fluorescence was measured in every cycle, and a melting curve was analyzed after the PCR by increasing the temperature from 55 to 95°C (0.5°C increments). A defined single peak was obtained for all amplicons, confirming the specificity of the amplification.

Expression of the Data and Statistical Analysis

Immunostaining of α-SMA, Collagen I, Collagen III, CD4 and CD8 was semi-quantified by calculating "expression scores" that consider both staining intensity and the percentage of cells stained at a specific range of intensities. A score of zero indicated the percentage of positive cells <5%, 1+ = 5–25%, 2+ = 25–50%, 3+ = 50–75%, 4+ >75%. The staining intensity of each specimen was judged relative to the intensity of a control slide including an adjacent section stained with an irrelevant negative control antibody that was matched by species and isotype to the specimen. Staining of the section labeled with the negative reagent control was considered as background. A score of zero indicated no staining relative to background, 1+ = weak staining, 2+ = moderate staining, and 3+ = strong staining. According to standard pathology practice, staining intensity was reported at the highest level of intensity observed in all tissue elements, except the distinctive tissue element for which an expanded scoring scheme was reported. The "expression scores" were calculated by multiplying the percent of positive cells (0–4) and the staining intensity scores (0–3). For example: for a specimen with 30% of positive cells (3+), and a moderate staining intensity (2+), the "expression score" was 3×2 = 6. Three pathologists read the sections and established the scores, and they were blinded to each other results. Immunostaining of TGF-β1/Smads was quantified by calculating "positive cells". Cells with a positive immunostaining were counted in five random visual fields of 0.95 square mm each, at initial

magnification: ×20, for each sample, and the result was expressed as the percent of positive cells to the total number of cells counted.

All the data were analyzed by SPSS 17.0. The results were presented as means ± SD. One-way ANOVA and Student's *t*-test were used to compare the differences between groups, and Spearman's rho was used to analyze the correlation coefficient. $P<0.05$ was considered to indicate statistical significance.

Acknowledgments

We would like to thank Hui Liu, Tao Jiang and Chun Zhang for their excellent technical assistance.

Author Contributions

Conceived and designed the experiments: RL DV HW. Performed the experiments: JW CZ XW GL. Analyzed the data: RL JW DV. Contributed reagents/materials/analysis tools: OB GM XL. Wrote the paper: RL JW DV HW.

References

1. Vuitton DA, Zhou H, Bresson-Hadni S, Wang Q, Piarroux M, et al. (2003) Epidemiology of alveolar echinococcosis with particular reference to China and Europe. Parasitology 127 Suppl: S87–107.
2. Vuitton DA, Zhang SL, Yang Y, Godot V, Beurton I, et al. (2006) Survival strategy of Echinococcus multilocularis in the human host. Parasitol Int 55 Suppl: S51–55.
3. Grenard P, Bresson-Hadni S, El Alaoui S, Chevallier M, Vuitton DA, et al. (2001) Transglutaminase-mediated cross-linking is involved in the stabilization of extracellular matrix in human liver fibrosis. J Hepatol 35: 367–375.
4. Guerret S, Vuitton DA, Liance M, Pater C, Carbillet JP (1998) Echinococcus multilocularis: relationship between susceptibility/resistance and liver fibrogenesis in experimental mice. Parasitol Res 84: 657–667.
5. Ricard-Blum S, Bresson-Hadni S, Guerret S, Grenard P, Volle PJ, et al. (1996) Mechanism of collagen network stabilization in human irreversible granulomatous liver fibrosis. Gastroenterology 111: 172–182.
6. Ricard-Blum S, Bresson-Hadni S, Vuitton DA, Ville G, Grimaud JA (1992) Hydroxypyridinium collagen cross-links in human liver fibrosis: study of alveolar echinococcosis. Hepatology 15: 599–602.
7. Vuitton DA, Guerret-Stocker S, Carbillet JP, Mantion G, Miguet JP, et al. (1986) Collagen immunotyping of the hepatic fibrosis in human alveolar echinococcosis. Z Parasitenkd 72: 97–104.
8. Ouellette MJ, Dubois CM, Bergeron D, Roy R, Lambert RD (1997) TGF beta 2 in rabbit blastocoelic fluid regulates CD4 membrane expression: possible role in the success of gestation. Am J Reprod Immunol 37: 125–136.
9. Cufi S, Vazquez-Martin A, Oliveras-Ferraros C, Martin-Castillo B, Joven J, et al. (2010) Metformin against TGFbeta-induced epithelial-to-mesenchymal transition (EMT): from cancer stem cells to aging-associated fibrosis. Cell Cycle 9: 4461–4468.
10. Feng M, Wang Q, Zhang F, Lu L (2011) Ex vivo induced regulatory T cells regulate inflammatory response of Kupffer cells by TGF-beta and attenuate liver ischemia reperfusion injury. Int Immunopharmacol 12: 189–196.
11. Jetten AM, Shirley JE, Stoner G (1986) Regulation of proliferation and differentiation of respiratory tract epithelial cells by TGF beta. Exp Cell Res 167: 539–549.
12. Harraga S, Godot V, Bresson-Hadni S, Mantion G, Vuitton DA (2003) Profile of cytokine production within the periparasitic granuloma in human alveolar echinococcosis. Acta Trop 85: 231–236.
13. Vuitton DA (2003) The ambiguous role of immunity in echinococcosis: protection of the host or of the parasite? Acta Trop 85: 119–132.
14. Zhang S, Hue S, Sene D, Penfornis A, Bresson-Hadni S, et al. (2008) Expression of major histocompatibility complex class I chain-related molecule A, NKG2D, and transforming growth factor-beta in the liver of humans with alveolar echinococcosis: new actors in the tolerance to parasites? J Infect Dis 197: 1341–1349.
15. Wu XW, Peng XY, Zhang SJ, Niu JH, Sun H, et al. (2004) [Formation mechanisms of the fibrous capsule around hepatic and splenic hydatid cyst]. Zhongguo Ji Sheng Chong Xue Yu Ji Sheng Chong Bing Za Zhi 22: 1–4.
16. Mondragon-de-la-Pena C, Ramos-Solis S, Barbosa-Cisneros O, Rodriguez-Padilla C, Tavizon-Garcia P, et al. (2002) Echinococcus granulosus down regulates the hepatic expression of inflammatory cytokines IL-6 and TNF alpha in BALB/c mice. Parasite 9: 351–356.
17. Bartram U, Speer CP (2004) The role of transforming growth factor beta in lung development and disease. Chest 125: 754–765.
18. Higashiyama H, Yoshimoto D, Okamoto Y, Kikkawa H, Asano S, et al. (2007) Receptor-activated Smad localisation in bleomycin-induced pulmonary fibrosis. J Clin Pathol 60: 283–289.
19. Banas MC, Parks WT, Hudkins KL, Banas B, Holdren M, et al. (2007) Localization of TGF-beta signaling intermediates Smad2, 3, 4, and 7 in developing and mature human and mouse kidney. J Histochem Cytochem 55: 275–285.
20. Heldin CH, Miyazono K, ten Dijke P (1997) TGF-beta signalling from cell membrane to nucleus through SMAD proteins. Nature 390: 465–471.
21. Zhou L, McMahon C, Bhagat T, Alencar C, Yu Y, et al. (2010) Reduced SMAD7 leads to overactivation of TGF-beta signaling in MDS that can be reversed by a specific inhibitor of TGF-beta receptor I kinase. Cancer Res 71: 955–963.
22. Sobral LM, Montan PF, Zecchin KG, Martelli-Junior H, Vargas PA, et al. (2010) Smad7 blocks transforming growth factor-beta1-induced gingival fibroblast-myofibroblast transition via inhibitory regulation of Smad2 and connective tissue growth factor. J Periodontol 82: 642–651.
23. Kamiya Y, Miyazono K, Miyazawa K (2010) Smad7 inhibits transforming growth factor-beta family type i receptors through two distinct modes of interaction. J Biol Chem 285: 30804–30813.
24. Chen HY, Huang XR, Wang W, Li JH, Heuchel RL, et al. (2010) The protective role of Smad7 in diabetic kidney disease: mechanism and therapeutic potential. Diabetes 60: 590–601.
25. Singh P, Wig JD, Srinivasan R (2011) The Smad family and its role in pancreatic cancer. Indian J Cancer 48: 351–360.
26. Zhang C, Wang J, Lu G, Li J, Lu X, et al. (2012) Hepatocyte proliferation/growth arrest balance in the liver of mice during E. multilocularis infection: a coordinated 3-stage course. PLoS One 7: e30127.
27. Przybyszewska M, Miloszewska J, Rzonca S, Trembacz H, Pysniak K, et al. (2011) Soluble TNF-alpha receptor I encoded on plasmid vector and its application in experimental gene therapy of radiation-induced lung fibrosis. Arch Immunol Ther Exp (Warsz) 59: 315–326.
28. Maille E, Trinh NT, Prive A, Bilodeau C, Bissonnette E, et al. (2011) Regulation of normal and cystic fibrosis airway epithelial repair processes by TNF-alpha after injury. Am J Physiol Lung Cell Mol Physiol 301: L945–955.
29. Amiot F, Vuong P, Defontaines M, Pater C, Dautry F, et al. (1999) Secondary alveolar echinococcosis in lymphotoxin-alpha and tumour necrosis factor-alpha deficient mice: exacerbation of Echinococcus multilocularis larval growth is associated with cellular changes in the periparasitic granuloma. Parasite Immunol 21: 475–483.
30. Bresson-Hadni S, Petitjean O, Monnot-Jacquard B, Heyd B, Kantelip B, et al. (1994) Cellular localisations of interleukin-1 beta, interleukin-6 and tumor necrosis factor-alpha mRNA in a parasitic granulomatous disease of the liver, alveolar echinococcosis. Eur Cytokine Netw 5: 461–468.
31. Emery I, Liance M, Deriaud E, Vuitton DA, Houin R, et al. (1996) Characterization of T-cell immune responses of Echinococcus multilocularis-infected C57BL/6J mice. Parasite Immunol 18: 463–472.
32. Wallace K, Burt AD, Wright MC (2008) Liver fibrosis. Biochem J 411: 1–18.
33. Allen JT, Spiteri MA (2002) Growth factors in idiopathic pulmonary fibrosis: relative roles. Respir Res 3: 13.
34. Anthony B, Mathieson W, de Castro-Borges W, Allen J (2010) Schistosoma mansoni: egg-induced downregulation of hepatic stellate cell activation and fibrogenesis. Exp Parasitol 124: 409–420.
35. Acharya SS, Dimichele DM (2008) Rare inherited disorders of fibrinogen. Haemophilia 14: 1151–1158.
36. Itoh S, Taketomi A, Tanaka S, Harimoto N, Yamashita Y, et al. (2007) Role of growth factor receptor bound protein 7 in hepatocellular carcinoma. Mol Cancer Res 5: 667–673.
37. Schmierer B, Hill CS (2007) TGF beta-SMAD signal transduction: molecular specificity and functional flexibility. Nat Rev Mol Cell Biol 8: 970–982.
38. Del Pilar Alatorre-Carranza M, Miranda-Diaz A, Yanez-Sanchez I, Pizano-Martinez O, Hermosillo-Sandoval JM, et al. (2009) Liver fibrosis secondary to bile duct injury: correlation of Smad7 with TGF-beta and extracellular matrix proteins. BMC Gastroenterol 9: 81.
39. Moustakas A, Pardali K, Gaal A, Heldin CH (2002) Mechanisms of TGF-beta signaling in regulation of cell growth and differentiation. Immunol Lett 82: 85–91.
40. Spiliotis M, Konrad C, Gelmedin V, Tappe D, Bruckner S, et al. (2006) Characterisation of EmMPK1, an ERK-like MAP kinase from Echinococcus multilocularis which is activated in response to human epidermal growth factor. Int J Parasitol 36: 1097–1112.
41. Gelmedin V, Caballero-Gamiz R, Brehm K (2008) Characterization and inhibition of a p38-like mitogen-activated protein kinase (MAPK) from Echinococcus multilocularis: antiparasitic activities of p38 MAPK inhibitors. Biochem Pharmacol 76: 1068–1081.
42. Brehm K, Spiliotis M, Zavala-Gongora R, Konrad C, Frosch M (2006) The molecular mechanisms of larval cestode development: first steps into an unknown world. Parasitol Int 55 Suppl: S15–21.
43. Lin RY, Wang JH, Lu XM, Zhou XT, Mantion G, et al. (2009) Components of the mitogen-activated protein kinase cascade are activated in hepatic cells by Echinococcus multilocularis metacestode. World J Gastroenterol 15: 2116–2124.

44. Nono JK, Pletinckx K, Lutz MB, Brehm K (2012) Excretory/secretory-products of Echinococcus multilocularis larvae induce apoptosis and tolerogenic properties in dendritic cells in vitro. PLoS Negl Trop Dis 6: e1516.

45. Liance M, Vuitton DA, Guerret-Stocker S, Carbillet JP, Grimaud JA, et al. (1984) Experimental alveolar echinococcosis. Suitability of a murine model of intrahepatic infection by Echinococcus multilocularis for immunological studies. Experientia 40: 1436–1439.

Main conclusions and remarks:

1) TGF-β1 was expressed in most lymphocytes and macrophages of the periparasitic infiltrate as well as in the liver parenchyma, even distant from the parasitic lesion.
2) $CD4^+$ T cells represented the major population of T cells at the beginning of the infection and that this sub-population was progressively replaced by $CD8^+$ T cells, and this change of CD4/CD8 ratios could contribute to maintain TGF-β1 secretion.
3) TGF-β receptors were also expressed at the membrane of most cells in the periparasitic infiltrate and in the liver parenchyma from early to late stage post *E. multilocularis* infection.
4) Various down-stream Smad components of the TGF-β pathway were marked increased at the middle stage of the chronic phase of the disease in *E. multilocularis* infected mice.
5) Fibrosis was significant at 180 days p.i. in the periparasitic infiltrate and was also present in the liver parenchyma, even distant from the lesions.

7. Is FGL2 involved in the cross-talk between *E. multilocularis* and its host and how does it regulate immune tolerance?

To address this question, and study *E. multilocularis* growth in the absence of FGL2, we employed intra-peritoneally infected FGL2$^{-/-}$ Knock-Out mice. As a key parameter for outcome, parasite load was measured by wet weight determination of the metacestode tumor-like tissue, and serum FGL2 levels were measured by sandwich ELISA. Spleen cells were firstly analyzed ex-vivo and secondly after being cultured with ConA stimulation for 48h or with *E.multilocularis* Vesicle Fluid (VF) antigenic stimulation for 96h. Spleen cells from non-infected WT mice were cultured with rFGL2/anti-FGL2 or rIL-17A/anti-IL-17A for further functional studies. For the Treg immune suppression assay, high purity of CD4$^+$CD25$^+$Tregs (N>99%) was incubated, together with CD4$^+$ effector T cells and irradiated spleen cells as APCs, with ConA for 48h. Flow cytometry and real time RT-PCR were used to determine T cell subpopulations including Treg numbers and phenotypes, Th17-, Th1-, Th2-type immune responses, and maturation of dendritic cells and B cells.

Background and objectives:

We previously showed that CD4$^+$ CD25$^+$ regulatory T (Treg) cells played a critical role in human echinococcosis by blunting immune responses to specific antigens, or by suppressing the secretion of proinflammatory cytokines, especially through interleukin (IL)-10 and transforming growth factor (TGF-β1). Moreover, increased CD4$^+$ CD25$^+$ Treg had also been observed in peritoneal cells in mice infected intraperitoneally (i.p.) with *E. multilocularis,* a finding that was concordant with other findings that *E. multilocularis* antigens promote T cell differentiation into Treg cells. Besides regulatory cytokines, among those factors which mediate immune regulation/tolerance by CD4$^+$ CD25$^+$ Tregs, Fibrinogen-like protein 2 (FGL2) has recently been recognised. In a previous study, by using a microarray-based approach, researchers from our team observed that mRNA levels of FGL2 were significantly up-regulated in the liver of mice perorally infected with *E.multilocularis* eggs. The aims of this work were thus: 1) to study the role of FGL2 on T and B cell reactivity as well as on the maturation of dendritic cells (DC) at two different stages of *E. multilocularis* infection, i.e. early and late stages, by using an original model of flg2$^{-/-}$ mice 2) to study how components of parasite origin, i.e. metabolites, such as those present in the vesicle fluid (VF) in *E. multilocularis* infection exert an effect on immune response in flg2$^{-/-}$ mice, 3) to explore how FGL2 is secreted during the course of *E. multilocularis* infection; and 4) to give a comprehensive picture of the various cell and molecular components involved in immune regulation in the peritoneal cells surrounding *E. multilocularis* metacestode (periparasitic infiltrate) and in the spleen. To achieve this goal, Th1/Th2-related and Treg/Th17 related cytokines, maturation of

dendritic cells (DC), B cell response, and Treg generation/functions were studied at the different stages of disease, in various experimental models which allowed or suppressed the influence of FGL2.

The Novel $CD4^+CD25^+$ Regulatory T Cell Effector Molecule Fibrinogen-like Protein 2 Contributes to the Outcome of Murine Alveolar Echinococcosis

Junhua Wang[1,2,3], Cristina Huber[1], Norbert Müller[1], Dominique A Vuitton[4], Oleg Blagosklonov[3] , Denis Grandgirard[5], Stephen L. Leib[5,6], Xiaomei Lu[2], Renyong Lin[2], Hao Wen[2], Bruno Gottstein[1]

1. Institute of Parasitology, University of Bern, Bern, Switzerland.
2. State Key Lab Incubation Base of Xinjiang Major Diseases Research (2010DS890294) and Xinjiang Key Laboratory of Echinococcosis, First Affiliated Hospital of Xinjiang Medical University, Urumqi, Xinjiang, China.
3. Department of Nuclear Medicine, University of Franche-Comté and Jean Minjoz University Hospital, Besançon, Franche-Comté, France.
4.WHO-Collaborating Centre for the Prevention and Treatment of Human Echinococcosis, University of Franche-Comté and University Hospital, Besançon, Franche-Comté, France.
5. Neuroinfection Laboratory, Institute for Infectious Diseases, University of Bern, Friedbühlstrasse 52, 3010 Bern, Switzerland.
6. Biology Division, Spiez Laboratory, Federal Office for Civil Protection FOCP, 3700 Spiez, Switzerland.

1. Correspondence to: Professor Bruno Gottstein, MD, PhD, Institute of Parasitology, University of Bern, Länggassstrasse 122, Bern 3012, Switzerland.
E-mail: bruno.gottstein@vetsuisse.unibe.ch
Tel : +41 31 631 24 18
Fax: +41 31 631 26 22

2. Correspondence to: Professor Professor Hao Wen and Professor Renyong Lin, PhD, State Key Lab Incubation Base of Xinjiang Major Diseases Research (2010DS890294) and Xinjiang Key Laboratory of Echinococcosis, First Affiliated Hospital of Xinjiang Medical University, No.1 Liyushan Road, Urumqi 830054, China.
E-mail: Dr.Wenhao@163.com; renyong_lin@sina.com
Tel: +86 991 436 6448
Fax: +86 991 436 2844

Funding: This work was supported by the Swiss National Science Foundation (31003A_141039/1), NSFC Grant Projects (81260452, 81260252, U1303222), the European Commission French-Swiss InterReg IV program ‘IsotopEchino’ project, the Program for Changjiang Scholars and Innovative Research Team in Universities (IRT1181) and Xinjiang Key-Lab Projects (SKLIB-XJMDR-2012-Y1). The funders had no role in study design, data collection and analysis, decision to publish, or preparation of the manuscript.

Abstract

Background: The immunology of murine alveolar echinococcosis (AE) is characterized by the development of immune tolerance against the *Echinococcus multilocularis (E.multilocularis)* metacestode allowing the parasitic tumor-like tissue to continuously proliferate and metastasize. The velocity of proliferation is dependent on the nature of the periparasitic inflammatory and other immune-mediated processes. In a previous explorative study, fibrinogen-like protein 2 (FGL2) was found to be up-regulated in AE-infected *versus* non-infected control animals. So far, nothing is known on the contribution of this novel $CD4^+$ $CD25^+$ regulatory T cell (Treg) effector molecule to the control of a helminth infection.Methods: $fgl2^{-/-}$ mice were experimentally infected with *E. multilocularis,* and age-and-gender-matching wild type (WT) animals were used as controls. Mice were sacrificed at 1 and 4 month(s) post-infection (p.i.). As a key parameter for infection outcome, parasite load was measured by wet weight determination of the metacestode tumor-like tissue, and serum FGL2 levels were measured by sandwich enzyme-linked immunosorbent assay. Spleen cells were firstly analyzed ex-vivo and secondly after being cultured with ConA stimulation for 48h or with *E. multilocularis* Vesicle Fluid (VF) antigenic stimulation for 96h. Spleen cells from non-infected WT mice were cultured with rFGL2/anti-FGL2 or rIL-17A/anti-IL-17A for further functional studies. For the Treg immune suppression assay, high purity of $CD4^+$ $CD25^+$ Tregs (N>99%) was achieved by first MACS and subsequently FACS. These purified cells were incubated, together with $CD4^+$ effector T cells and irradiated spleen cells as APCs, with ConA for 48h. Flow cytometry and real time RT-PCR were used to determine T cell subpopulations including Treg numbers and phenotypes, Th17-, Th1-, Th2-type immune responses, and maturation of dendritic cells and B cells. **Results:** FGL2-deficient mice infected with *E. multilocularis* exhibited a significantly decreased parasite load, associated with increased T cell proliferation in response to ConA, impaired Treg numbers and function, relative Th1 polarization, and increased numbers of antibody-producing B cells, as compared to infected WT mice. Both relative number and maturation status of dendritic cells were higher in $fgl2^{-/-}$ mice, and CD80 and CD86 were more expressed in DCs following ConA and VF stimulation. Additional experiments confirmed that IL-17A contributes to FGL2 secretion in this model.
Conclusions: Our data demonstrate that FGL2, together with IL-17 and by promoting Treg cell activity, appears as a key-player in the orchestration of the outcome of *E. multilocularis* infection; this study gives evidence for a role of IL-17 in FGL2 regulation, and suggests that targeting FGL2 could be used for the development of novel treatment approaches in infectious diseases.

Introduction

Alveolar echinococcosis (AE) is one of the clinically most severe zoonotic helminthic disease, characterized by a chronic and progressive hepatic damage occurring during the continuous proliferation of the larval stage (metacestode) of *Echinococcus multilocularis (E. multilocularis)* [1], with a fatal outcome if remaining untreated. AE is thus a neglected "malignant" parasitic disease deserving clinically the same attention as cancer. If the currently limited prevention and medical treatment options remain unchanged, increasing numbers of AE patients (emergence is presently affecting mainly Europe and China) will not receive appropriate care with foreseeable consequences on human distress, cost and economic losses [2]. Humans, as accidental intermediate hosts in the life cycle of the parasite, suffer from severe conditions in the late stage of the disease not only because of the continuous space-occupying metacestode proliferation in the liver and subsequent metastasis formation predominantly in the lungs and the brain, but also mainly because of the intense inflammatory granulomatous periparasitic infiltration resulting in a marked periparasitic tissue reconstruction of the affected organs. The parasitic lesions together with the periparasitic tissue reactions behave like a slow-growing liver cancer, progressively invading the neighboring tissues and organs directly or via metastases [3]. Pathological changes in AE are associated with an intense periparasitic infiltration by macrophages of various functional types, including the so-called "epithelioid cells" and "giant cells", typical of granulomas [2, 3] and by T lymphocytes. $CD4^+$ T lymphocytes are present from the early stage of parasite growth and $CD8^+$ T lymphocytes are known to home to the periparasitic infiltrate secondarily and to be associated with parasite tolerance and severity of the disease [1,3,4,5].

It has been previously shown that *E. multilocularis* infection induces an immune response that can select numerous pathways; the involvement of individual cytokines has been rather extensively studied within the past 2 decades [1]. A rather Th2-dominated immunity associates with an increased susceptibility to disease, which leads to chronic AE, while Th1 cell activation induces protective immunity, which may lead to aborted forms of infection [1, 2]. During the conventional course of *E. multilocularis* infection in susceptible experimental hosts, an initial Th1 response gradually switches to a more dominating Th2 response during the chronic phase of AE; this mostly mixed Th1/Th2 profile is nevertheless associated with the expression of pro-inflammatory cytokines in the periparasitic granuloma and partially protective immunity through fibrosis and necrosis [6]. We previously showed that $CD4^+$ $CD25^+$ regulatory T (Treg) cells played a critical role in human echinococcosis by blunting immune responses to specific antigens, or by suppressing the secretion of

proinflammatory cytokines, especially through interleukin (IL)-10 and transforming growth factor (TGF-β1) [7]. Moreover, increased $CD4^+$ $CD25^+$ Treg was also observed in peritoneal cells in mice infected intraperitoneally (i.p.) with *E. multilocularis,* a finding that was concordant with other findings that *E. multilocularis* antigens promote T cell differentiation into Treg cells (unpublished data).

In a previous explorative study, by using a microarray-based approach, we observed that mRNA levels of the fibrinogen-like protein 2 (FGL2) were significantly up-regulated in the liver of mice perorally infected with *E.multilocularis* eggs [8]. Fibrinogen-like protein 2 (FGL2), a member of the fibrinogen-related superfamily of proteins known to be secreted by T cells, has recently been reported by a number of groups to be highly expressed by Tregs and has been proposed to have a role in Treg effector function [9]. It has been shown that FGL2 could inhibit dendritic cell maturation and induce apoptosis of B cells through binding to low-affinity FcgammaRIIB receptor, and thus contribute to Treg activity [10]. There is evidence that FGL2 exerts immunosuppressive effect on T cell proliferation. Thus it plays an important role both in innate and adaptive immunity, being expressed by activated $CD4^+$a nd $CD8^+$ T cells and reticulo-endothelial cells (macrophages and endothelial cells) [11,12,13,14,15,16]. It has been implicated as a novel biomarker of cancer, and in the pathogenesis of inflammatory disorders such as allo- and xenograft rejection [11,17,18,19,20,21], or cytokine-induced fetal loss [22]. It was also shown to play a role in infectious diseases, such as viral hepatitis [11,14]. To our knowledge, it has until now been neglected as a key-player in parasite-induced tolerance. As the therapeutic tools in AE are very limited so far, and immune modulation might represent an alternative option, Tregs and their effector molecule FGL2 could become attractive targets, putatively allowing a modulation of the patient's immune response to yield protective immune reactions that will result in a dying-out of the parasite metacestode.

The major aims of this work were thus: 1) to study the role of FGL2 on T and B cell reactivity as well as on the maturation of dendritic cells (DC) at two different stages of *E. multilocularis* infection, i.e. early and late stages, by using an original model of $flg2^{-/-}$ knockout mice; 2) to study how parasite components, i.e. metabolites, such as those expressed in the vesicle fluid (VF) of the *E. multilocularis* metacestode, affect the immune response in $flg2^{-/-}$ knockout mice, 3) to explore how FGL2 is secreted during the course of *E. multilocularis* infection; and 4) to give a comprehensive picture of the various cell and molecular components involved in immune regulation of the peritoneal cells that are in direct contact with *E. multilocularis* metacestode (periparasitic infiltrate), and in the spleen as a key immune organ. To achieve this goal, Th1/Th2-related and Treg/Th17 related cytokines, maturation of dendritic cells (DC), B cell response, and Treg generation/functions

were studied at the different stages of disease, in an experimental model with active or abrogated FGL2-expression.

Results

Significantly decreased parasite load in fgl2$^{-/-}$ mice after *E. multilocularis* infection

Parasite load, gross morphology and histology of tissues and organs were compared between *E. multilocularis*-infected fgl2$^{-/-}$ (AE- fgl2$^{-/-}$) and wild type (WT) infected mice (AE-WT). At the early stage (1mo p.i.), there was no significant difference yet in parasite load between AE-fgl2$^{-/-}$ and AE-WT mice (0.45±0.53g vs 0.66±0.83 g). However, at the late stage (4mo p.i.), the parasite load became significantly lower in AE-fgl2$^{-/-}$ mice when compared to AE-WT mice (8.75±2.35 g vs 16.26±8.06) g (Figure 7.1). At the late stage of *E. multilocularis* infection, the parasite invaded the liver (a marker of pathogenicity) much less in AE-fgl2$^{-/-}$ mice than in AE-WT mice (33.3% vs 94.4%). At the periphery of the lesion, numbers of fibroblasts and inflammatory cells were similar in AE-fgl2$^{-/-}$ mice and AE-WT mice.

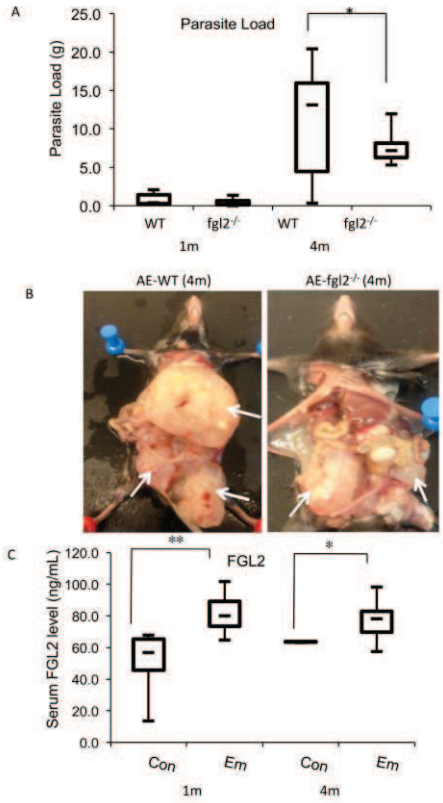

Figure 7.1 Parasite load and serum FGL2 levels after *E. multilocularis* infection.
(A) Parasite load in both *E. multilocularis*-infected wild type (WT) and *E. multilocularis*-infected fgl2$^{-/-}$ (KO) mice assessed by using wet weighing at different stages of *E. multilocularis* infection. (B) Representative example of *E. multilocularis* infection from both AE-WT and AE-fgl2$^{-/-}$ mice (KO) 4 month post infection (p.i.); arrows point at intraperitoneal metacestode tissue/lesions. (C) Serum FGL2 levels in AE-WT mice (Em) at different stages of *E. multilocularis* infection, as compared to non-infected control mice (Con). Data represent mean±SD of three independent experiments of five to six mice in each group. Comparison between groups was performed using a one-way ANOVA for statistical analysis. *P<0.05; **P<0.01.
'WT', wild type mice; KO, fgl2 knock out mice; 'Con', Control, non-infected mice; 'Em', *E. multilocularis* infected mice (= AE-mice).

Serum FGL2, TNF-α, and Th-related cytokine levels after *E. multilocularis* infection in fgl2$^{-/-}$ and WT control mice

Serum level of FGL2 was significantly higher in AE-WT mice both at the early and at the late stage of *E. multilocularis* infection when compared to non-infected WT controls (Figure 7.1), but there was no difference between 1 and 4 mo p.i.-levels. As expected, FGL2 was not detectable in any of the fgl2$^{-/-}$ mice (AE-infected and non-infected controls) (data not shown).

1mo after infection, TNF-α was significantly higher in AE-fgl2$^{-/-}$ mice when compared to AE-WT mice (P= 0.037); IFN-γ and IL-17A were also higher at 1mo p.i. in AE-fgl2$^{-/-}$ mice, but the difference between fgl2$^{-/-}$ and WT mice was statistically not significant (Figure 7.2).

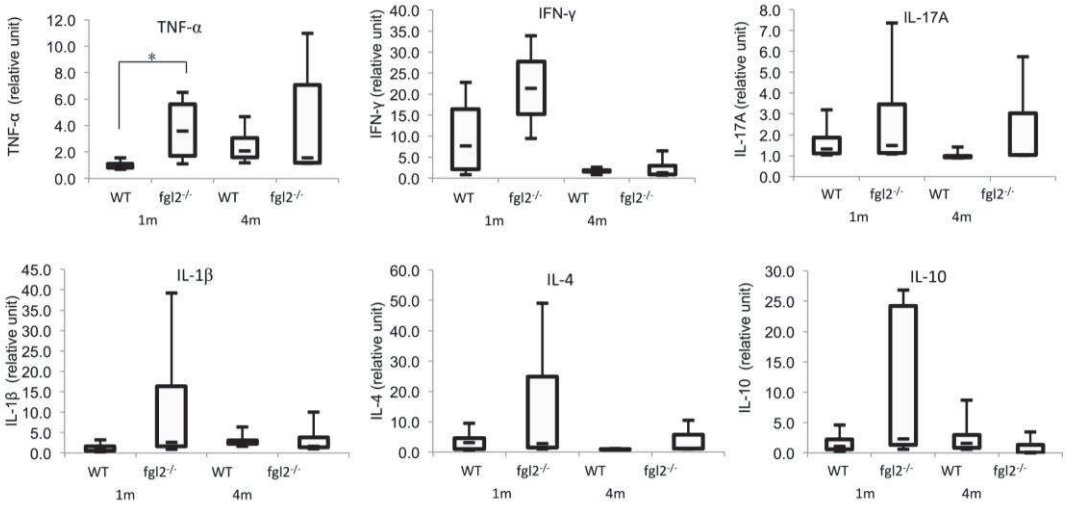

Figure 7.2 Proinflammtory and Th-related cytokine serum levels assessed in *E. multilocularis*-infected (AE) mice by Luminex technology.

Data represent mean±SD of three independent experiments of five to six mice in each group. Comparison between groups was performed using a one-way ANOVA for statistical analysis. *P<0.05.

'WT', AE-infected wild type mice; KO, AE-infected fgl2 knock out mice.

Spearman correlation coefficients indicated a positive correlation between IL-4 and FGL2 levels (r=0.363, P=0.023), as well as between IL-17A and FGL2 levels in the serum of AE-WT mice at 1mo and 4mo p.i. (Table 7.1).

Table 7.1 Correlations between serum level of FGL2 and IL-4, IL-17A

		IL-4	IL-17A
FGL2	Spearman's rho	0.363*	0.435*
	Sig.	0.023	0.045
	N	21	21

Note: * P< 0.05, ** P< 0.01.

Relationship between FGL2 and Treg function

Previous studies [23,24,25,26,27,28] have reported increased expression of fgl2-mRNA transcripts in Treg cells and proved a role for FGL2 as a putative Treg cell effector molecule. Thus this was not repeated anymore in this study. To determine whether FGL2 was important for the generation and maintenance of Treg cells in our murine AE-model, we analyzed both the expression of Treg cell markers

and of one of its related cytokines, IL-10, in peritoneal and spleen cells from AE-fgl2$^{-/-}$ mice and AE-WT mice during *E. multilocularis* infection. Compared to non-infected mice, there was no change in the expression of $CD4^+$ $CD25^+$ $Foxp3^+$ both in peritoneal and in spleen cells from AE-fgl2$^{-/-}$ mice, both at early and late stage of *E. multilocularis* infection. At 4mo p.i., expression of $CD4^+$ $CD25^+$ $Foxp3^+$ in peritoneal as well as spleen cells from AE-WT mice was elevated, and was significantly higher than that observed in fgl2$^{-/-}$ mice ($P<0.05$) (Figure 7.3). Expression of IL-10 in peritoneal and spleen cells from AE-fgl2$^{-/-}$ mice at 1mo p.i. was unchanged when compared to non-infected fgl2$^{-/-}$ mice, but was significantly lower than in AE-WT mice ($P<0.05$) (data not shown).

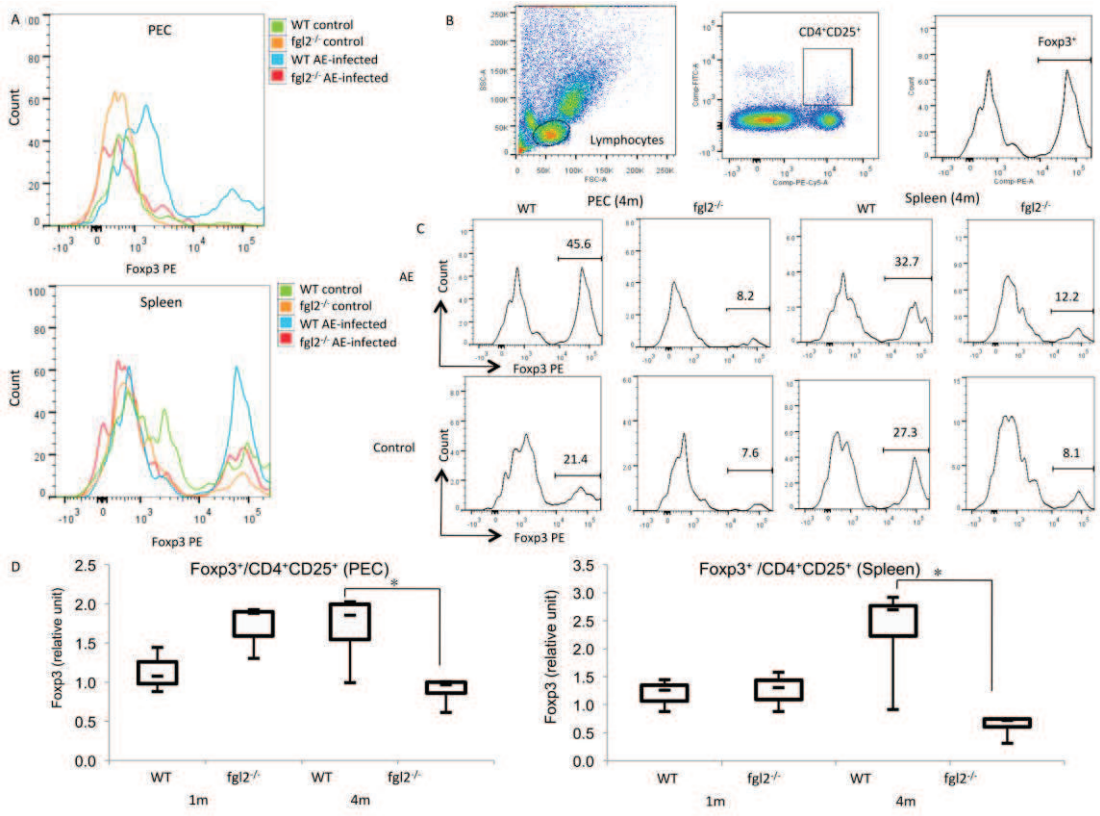

Figure 7.3 Fork head box protein 3 (Foxp3) expression in $CD4^+CD25^+$ T cells after *E. multilocularis* infection, assessed by flow cytometry.

(A) Foxp3 mean Fluorescence intensity (MFI) from AE-WT and AE-KO ($fgl2^{-/-}$) mice, and non-infected mice as controls. (B) Gating strategy of the determination of Foxp3-expressing $CD4^+CD25^+$ T cells in both peritoneal exudate cells (PEC) and spleen cells (Spleen). A gate was positioned around lymphocytes, and cells within this gate were used for identifying $CD4^+CD25^+$T cells. Foxp3 histogram plots overlaid with the isotype control plot were used to determine the number of $Fxop3^+$ cells. (C) Representative flow cytometry histogram plots of $Foxp3^+$ T cells within $CD4^+CD25^+$T cells in freshly isolated peritoneal cells and spleen cells from both AE-WT and AE-KO ($fgl2^{-/-}$) mice at different stages of *E. multilocularis* infection. (D) Expression of $Foxp3^+$ T cells within $CD4^+CD25^+$T cells in freshly isolated peritoneal cells and spleen cells from AE-WT and AE-KO ($fgl2^{-/-}$) mice, normalized using non-infected controls, at different stages of *E. multilocularis* infection. Graphs show the mean±SD of relative numbers of Tregs in PECs and spleen cells of infected AE-WT and AE-KO ($fgl2^{-/-}$) mice. Data were collected from three independent experiments of five to six mice in each group. Comparison between groups was performed using a one-way ANOVA for statistical analysis. *P<0.05.

'WT', wild type mice; KO, fgl2 knock out mice; 'PEC', peritoneal exudate cells; 'Spleen', spleen cells.

We then assessed the effect of targeted deletion of fgl2 on the ability of Treg cells to suppress the proliferation of normal $CD4^+$ $CD25^-$ T cells. Treg cells from $fgl2^{-/-}$ mice, either non-infected or *E. multilocularis*-infected, were less efficient in suppressing normal $CD4^+$ T cell proliferation when compared with Treg cells from WT mice at all Treg-cells-to-effector-T-cells ratios. At all ratios investigated, actually, there was no inhibition of $CD4^+$ T cell proliferation in cultures to which Treg cells from non-infected $fgl2^{-/-}$ mice had been added. However, at ratios 1:1 and 1:2 of Treg cells to effector T cells, we observed partial inhibition of normal $CD4^+$ T cell proliferation in cultures to which Treg cells from AE-$fgl2^{-/-}$ mice had been added (Figure 7.4).

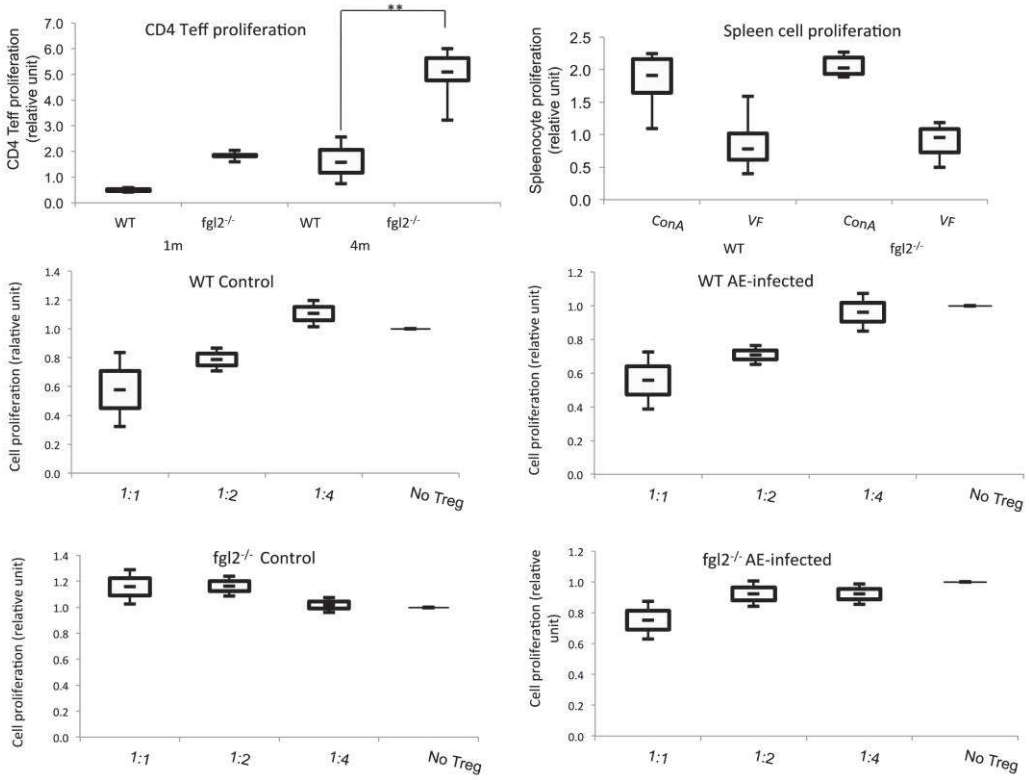

Figure 7.4 Treg suppression assay using cells from both AE-WT and AE-KO (fgl2$^{-/-}$) mice after *E. multilocularis* infection.

CD4^{+}CD25^{+} Tregs (suppressor cells) were isolated from spleen cells of both non-infected and infected WT mice and KO (fgl2$^{-/-}$) mice by using MACS and a following cell sorting by FACS. CD4^{+}CD25^{-}-T cells (responder) were isolated from spleen cells of non-infected WT mice by using MACS and a following cell sorting (FACS). CD4^{+}CD25^{+} Tregs (suppressor cells) and CD4^{+}CD25^{-} T cells (responder cells) were co-cultured at different suppressor : responder ratios in the presence of syngeneic APCs and anti-CD3 antibody (0.5 µg/mL); suppression of proliferation was measured using BrdU ELISA. Data represent mean±SD of two independent experiments. A two-way ANOVA with a Bonferroni test for post hoc analysis were used to compare means. *P<0.05.

Functions of T and B cells from AE-fgl2$^{-/-}$and AE-WT mice

To further explore the effects of FGL2 on the immune response during *E. multilocularis* infection, we examined the numbers and percentage of T and B cells, as well as their function, after *E. multilocularis* infection, both in WT and fgl2$^{-/-}$ mice. Although the percentages of CD4^{+} and CD8^{+} T cells within total lymphocytes, both in spleen cells and peritoneal cells, were not significantly different in AE-fgl2$^{-/-}$ and AE-WT mice, CD4/CD8 ratio and percentage of B cells were significantly higher in AE-fgl2$^{-/-}$ mice at 4mo p.i. as compared to AE-WT mice (Figures 7.4 and7. 5). Purified splenic CD4^{+} T cells from AE-fgl2$^{-/-}$mice exhibited an increased proliferation in response to ConA, as compared to splenic CD4 T cells from AE-WT mice (P<0.01) (Figure 7.6). Compared to cells from AE-WT mice, T helper (Th) cells from AE-fgl2$^{-/-}$ mice appeared oriented towards a Th1-response at early stage of infection; and at late stage of infection (4mo p.i.) towards a combined Th1/Th17-response, with a simultaneously lower Th2 response (Figure 7.6,7,8). Such polarization was confirmed at the mRNA level for IFN-γ and IL-4 by qRT-PCR in peritoneal cells but not in spleen cells (data not shown).

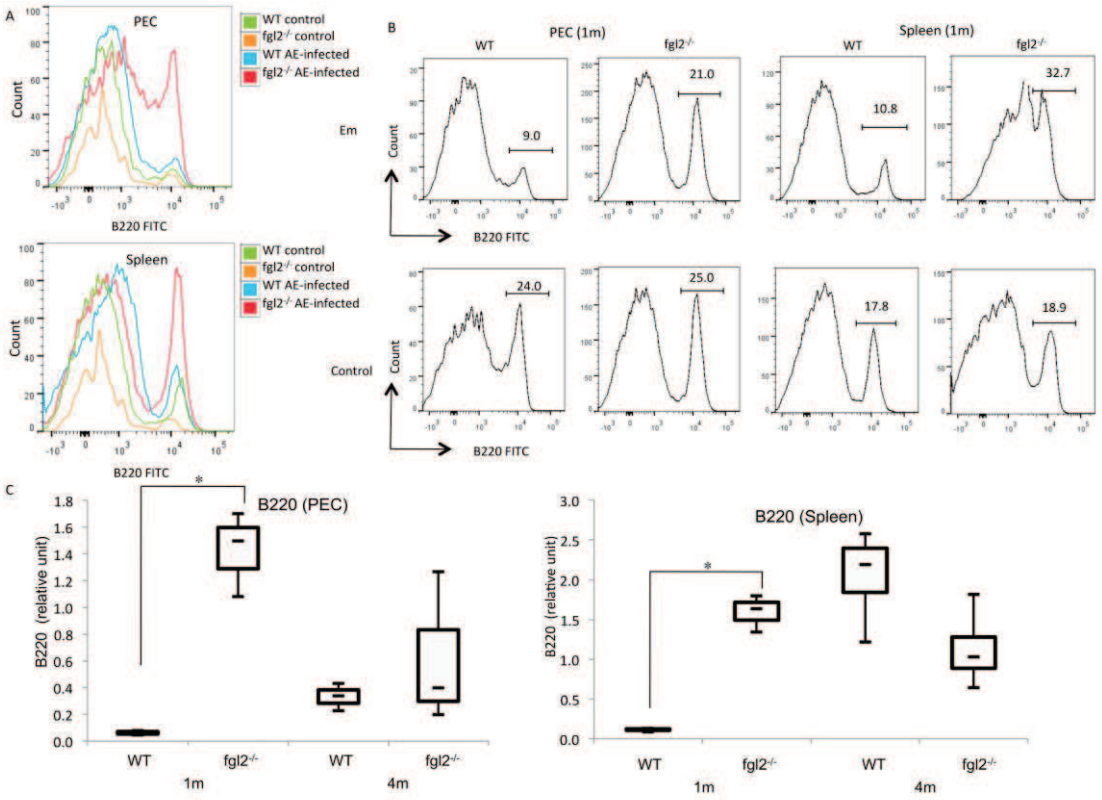

Figure 7.5 B220 expression after *E. multilocularis* infection by using flow cytometry. (A) B220 mean fluorescence intensity (MFI) in cells from AE-WT and AE-KO (fgl2$^{-/-}$) mice, and non-infected mice as controls. (B) Percentage of B220 within total lymphocytes in freshly isolated peritoneal and spleen cells from both AE-WT and AE-KO (fgl2$^{-/-}$) mice at different stages of *E. multilocularis* infection. (C) Representative flow cytometry histogram plots of B220 within total lymphocytes in freshly isolated peritoneal exudate cells and spleen cells from AE-WT and AE-KO (fgl2$^{-/-}$) mice, normalized using cells from non-infected controls, at different stages of *E. multilocularis* infection. Graphs show the mean±SD of relative numbers of B cells in PECs and spleens of AE-WT and AE-KO (fgl2$^{-/-}$) mice. Data were collected from three independent experiments of five to six mice in each group. Comparison between groups was performed using a one-way ANOVA for statistical analysis. *P<0.05.
'WT', wild type mice; KO, fgl2 knock out mice; 'PEC', peritoneal exudate cells; 'Spleen', spleen cells.

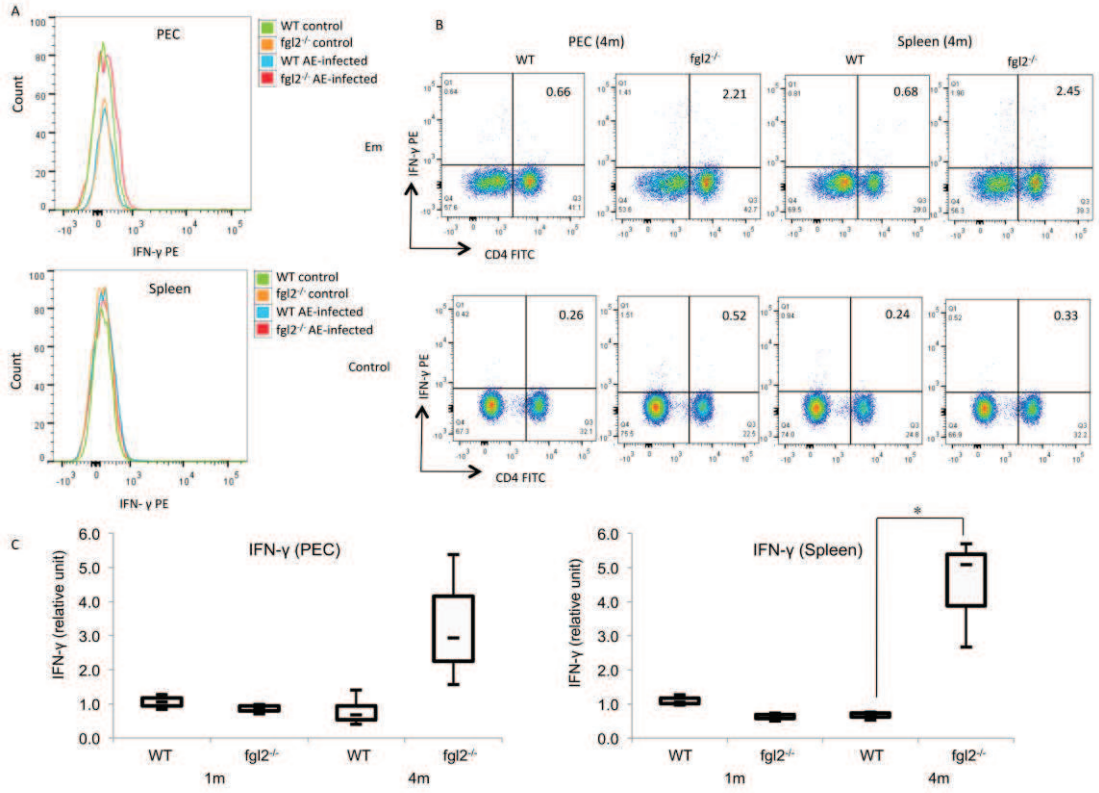

Figure 7.6 IFN-γ expression in $CD4^+$ T cells after *E. multilocularis* infection by using flow cytometry.

(A) IFN-γ mean fluorescence intensity (MFI) in cells from AE-WT and AE-KO ($fgl2^{-/-}$) mice, and non-infected mice as controls. (B) Representative flow cytometry histogram plots of IFN-γ^+ T cells within $CD4^+$ T cells in freshly isolated peritoneal and spleen cells from both AE-WT and AE-KO ($fgl2^{-/-}$) mice at different stages of *E. multilocularis* infection. (C) Expression of IFN-γ^+ T cells within $CD4^+$ T cells in freshly isolated peritoneal and spleen cells from AE-WT and AE-KO ($fgl2^{-/-}$) mice, normalized using cells from non-infected controls, at different stages of *E. multilocularis* infection. Graphs show the mean±SD of relative numbers of Tregs in peritoneal and spleen cells of AE-WT and AE-KO ($fgl2^{-/-}$) mice. Data were collected from three independent experiments of five to six mice in each group. Comparison between groups was performed using a one-way ANOVA for statistical analysis. *P<0.05.

'WT', wild type mice; KO, fgl2 knock out mice; 'PEC', peritoneal exudate cells; 'Spleen', spleen cells.

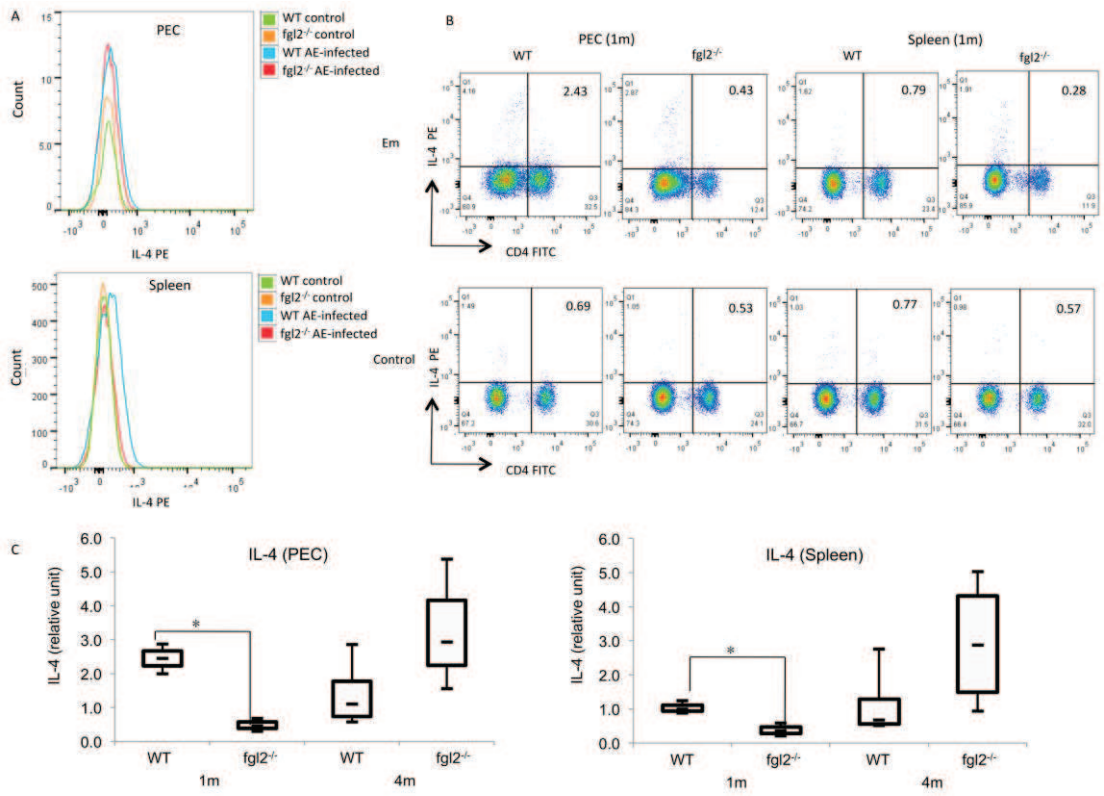

Figure 7.7 IL-4 expression in $CD4^+$ T cells after *E. multilocularis* infection by using flow cytometry.

(A) IL-4 mean fluorescence intensity (MFI) in cells from AE-WT and AE-KO ($fgl2^{-/-}$) mice, and non-infected mice as controls. (B) Representative flow cytometry histogram plots of $IL\text{-}4^+$ T cells within $CD4^+$ T cells in freshly isolated peritoneal and spleen cells from both AE-WT and AE-KO ($fgl2^{-/-}$) mice at different stages of *E. multilocularis* infection. (C) Expression of $IL\text{-}4^+$ T cells within $CD4^+$ T cells in freshly isolated peritoneal and spleen cells from AE-WT and AE-KO ($fgl2^{-/-}$) mice, normalized using cells from non-infected controls, at different stages of *E. multilocularis* infection. Graphs show the mean±SD of relative numbers of Tregs in peritoneal and spleen cells of AE-WT and AE-KO ($fgl2^{-/-}$) mice. Data were collected from three independent experiments of five to six mice in each group. Comparison between groups was performed using a one-way ANOVA for statistical analysis. **P*<0.05. 'WT', wild type mice; 'KO', fgl2 knock out mice; 'PEC', peritoneal exudate cells; 'Spleen', spleen cells.

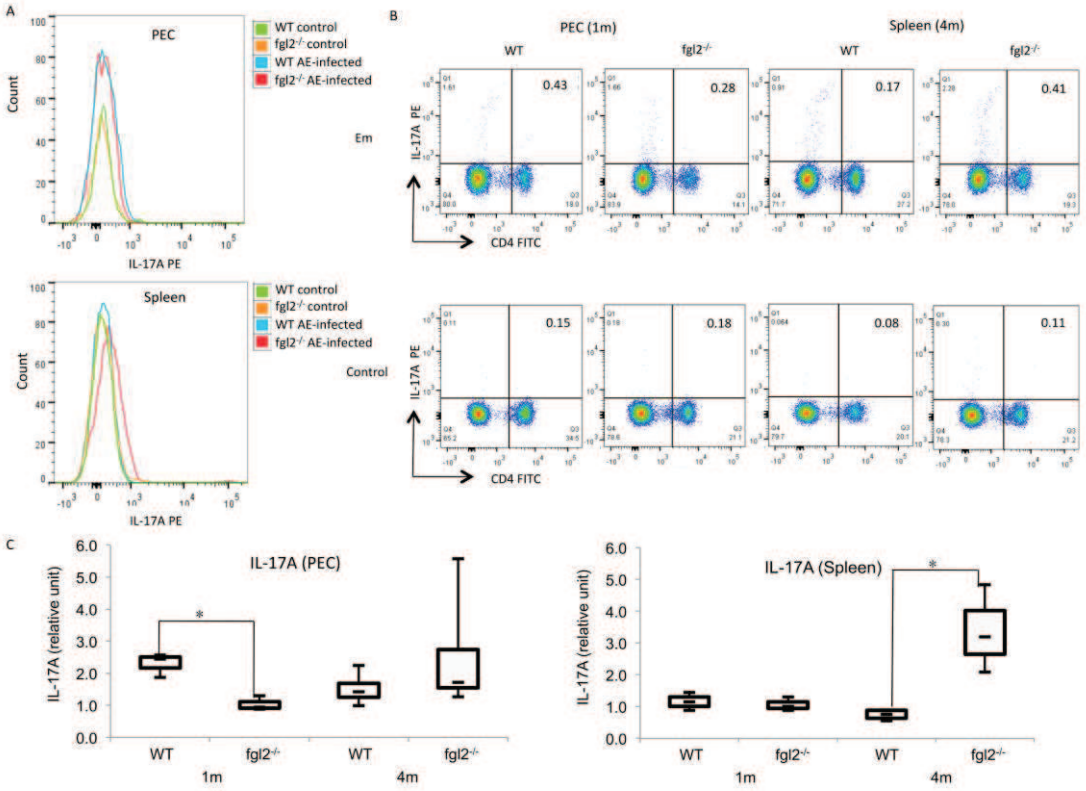

Figure 7.8 IL-17A expression in $CD4^+$ T cells after *E. multilocularis* infection by using flow cytometry.

(A) IL-17A mean Fluorescence intensity (MFI) in cells from AE-WT and AE-KO ($fgl2^{-/-}$) mice, and non-infected mice as controls. (B) Representative flow cytometry histogram plots of IL-17A $^+$ T cells within $CD4^+$ T cells in freshly isolated peritoneal and spleen cells from both AE-WT and AE-KO ($fgl2^{-/-}$) mice at different stages of *E. multilocularis* infection. (C) Expression of IL-17A $^+$ T cells within $CD4^+$ T cells in freshly isolated peritoneal and spleen cells from AE-WT and AE-KO ($fgl2^{-/-}$) mice, normalized using cells from non-infected controls, at different stages of *E. multilocularis* infection. Graphs show the mean±SD of relative numbers of Tregs in peritoneal and spleen cells of AE-WT and AE-KO ($fgl2^{-/-}$) mice. Data were collected from three independent experiments of five to six mice in each group. Comparison between groups was performed using a one-way ANOVA for statistical analysis. *P<0.05.

'WT', wild type mice; 'KO', fgl2 knock out mice; 'PEC', peritoneal exudate cells; 'Spleen', spleen cells.

Maturation of DCs from AE-fgl2$^{-/-}$and AE-WT mice

To study the role of FGL2 on different subsets of DCs, namely CD11b^{+} and CD11c^{+} DCs, we *ex vivo* assessed the maturation level both in peritoneal cells and in spleen cells from infected AE-fgl2$^{-/-}$ and AE-WT mice, and in non-infected mice as controls. Among CD11b^{+} DCs, expression of maturation markers, i.e. CD80^{+} in the peritoneal cells and CD86^{+} in spleen cells, was higher at 4mo p.i. in AE-fgl2$^{-/-}$ mice than in AE-WT mice (Figures 7.9 and 10). Among CD11c^{+} DCs, expression of the maturation marker CD86, but not of CD80, was higher both in the peritoneal and spleen cells from AE-fgl2$^{-/-}$ mice at 4mo p.i. (Figure 7.11). Taken together, these observations suggested that FGL2 may impair maturation of the 2 subpopulations of DCs at the late stage of *E. multilocularis* infection.

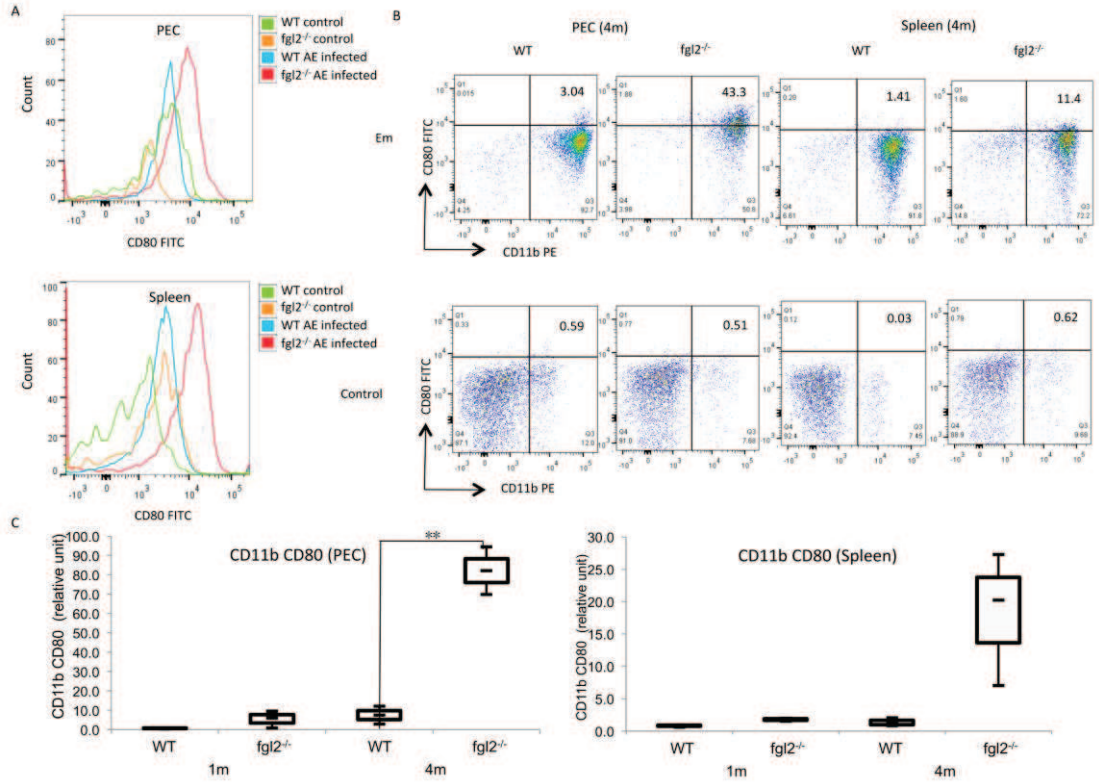

Figure 7.9 CD80 expression in CD11b^{+}DCs after *E. multilocularis* infection by using flow cytometry.

(A) CD80 mean fluorescence intensity (MFI) in cells from AE-WT and AE-KO (fgl2$^{-/-}$) mice, and non-infected mice as controls. (B) Representative flow cytometry histogram plots of CD80^{+}cells within CD11b^{+}DCs in freshly isolated peritoneal cells and spleen cells from both AE-WT and AE-KO (fgl2$^{-/-}$) mice at different stages of *E. multilocularis* infection. (C) Expression of CD80^{+} cells within CD11b^{+} DCs in freshly isolated peritoneal and spleen cells AE-WT and AE-KO (fgl2$^{-/-}$) mice, normalized using cells from non-infected controls, at different stages of *E. multilocularis* infection. Graphs show the mean±SD of relative numbers of Tregs in peritoneal and spleen cells of AE-WT and AE-KO (fgl2$^{-/-}$) mice. Data were collected from three independent experiments of five to six mice in each group. Comparison between groups was performed using a one-way ANOVA for statistical analysis. *P<0.05. 'WT', wild type mice; KO, fgl2 knock out mice; 'PEC', peritoneal exudate cells; 'Spleen', spleen cells.

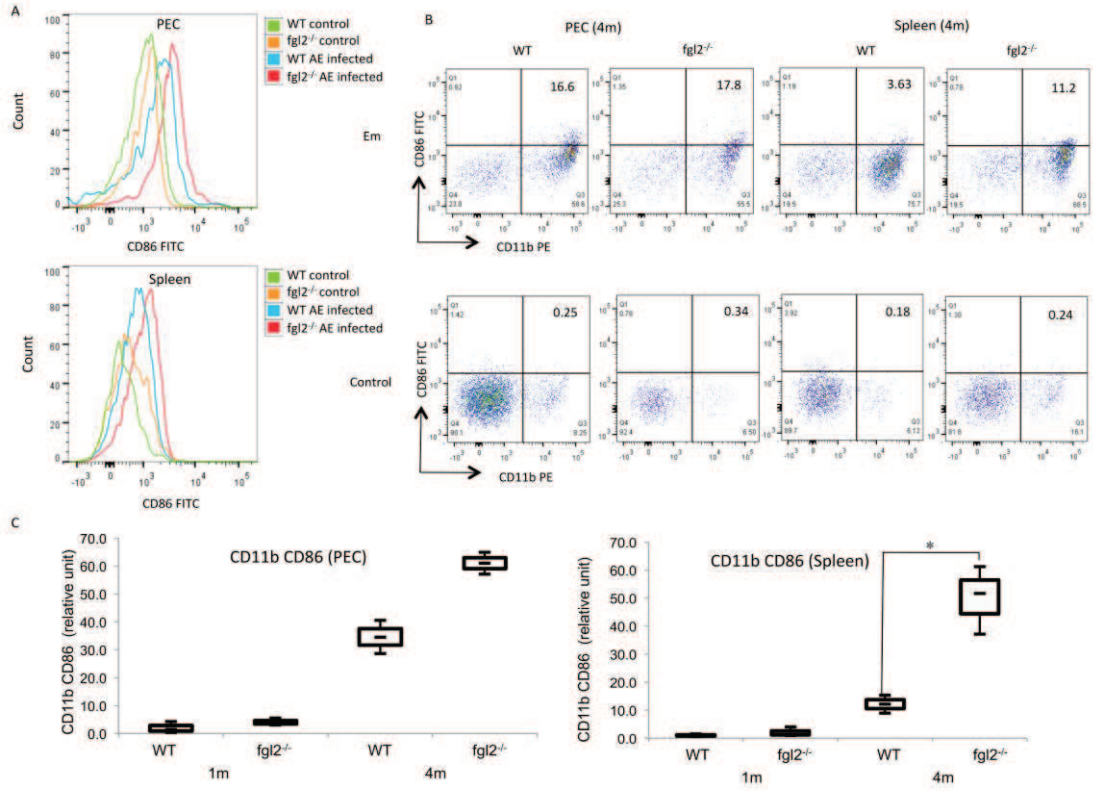

Figure 7.10 CD86 expression in CD11b^{+} DCs after *E. multilocularis* infection by using flow cytometry.

(A) CD86 mean fluorescence intensity (MFI) in cells from AE-WT and AE-KO (fgl2$^{-/-}$) mice, and non-infected mice as controls. (B) Representative flow cytometry histogram plots of CD86^{+} cells within CD11b^{+} DCs in freshly isolated peritoneal and spleen cells from both AE-WT and AE-KO (fgl2$^{-/-}$) mice at different stages of *E. multilocularis* infection . (C) Expression of CD86^{+} cells within CD11b^{+} DCs in freshly isolated peritoneal cells and spleen cells from AE-WT and AE-KO (fgl2$^{-/-}$) mice, normalized using cells from non-infected controls, at different stages of *E. multilocularis* infection. Graphs show the mean±SD of relative numbers of Tregs in peritoneal and spleen cells of AE-WT and AE-KO (fgl2$^{-/-}$) mice. Data were collected from three independent experiments of five to six mice in each group. Comparison between groups was performed using a one-way ANOVA for statistical analysis. *P<0.05.

'WT', wild type mice; KO, fgl2 knock out mice; 'PEC', peritoneal exudate cells; 'Spleen', spleen cells.

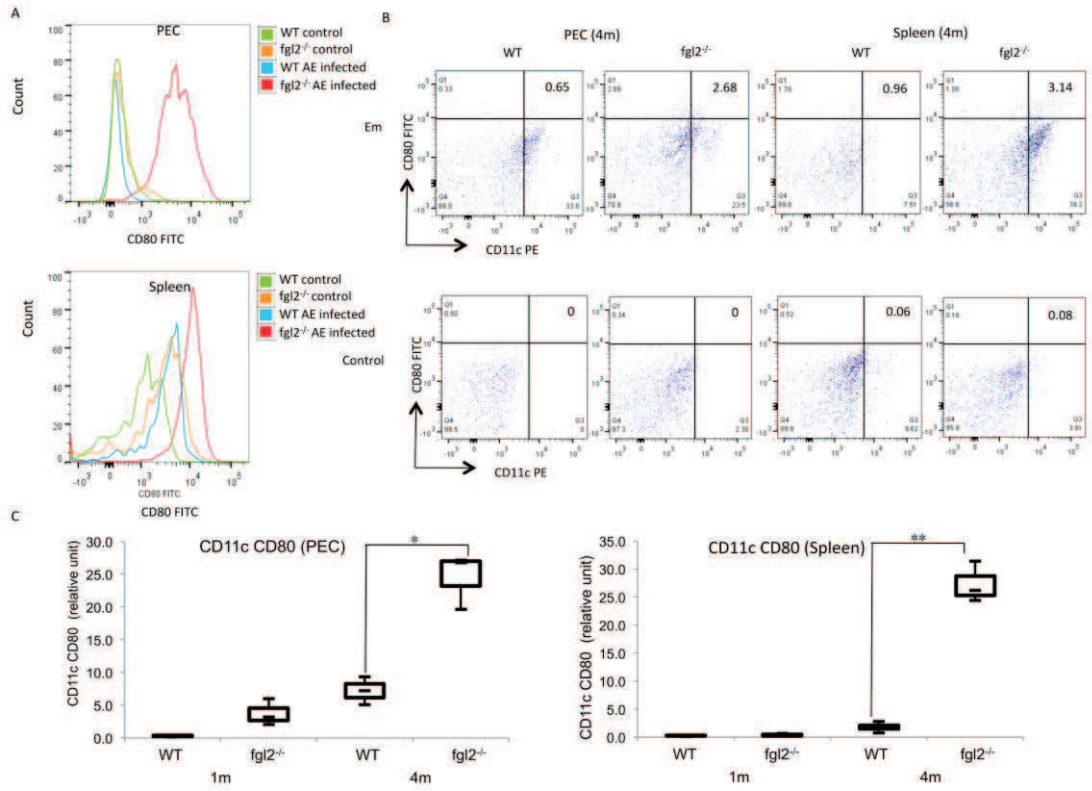

Figure 7.11 CD80 expression in CD11c^{+} DCs after *E. multilocularis* infection by using flow cytometry.

(A) CD80 mean fluorescence intensity (MFI) in cells from AE-WT and AE-KO (fgl2$^{-/-}$) mice, and non-infected mice as controls. Representative flow cytometry histogram plots of CD80^{+} cells within CD11c^{+} DCs in freshly isolated peritoneal and spleen cells from both AE-WT and AE-KO (fgl2$^{-/-}$) mice at different stages of *E. multilocularis* infection. (C) Expression of CD80^{+} cells within CD11c^{+} DCs in freshly isolated peritoneal and spleen cells from AE-WT and AE-KO (fgl2$^{-/-}$) mice, normalized using cells from non-infected control, at different stages of *E. multilocularis* infection. Graphs show the mean±SD of relative numbers of Tregs in peritoneal and spleen cells of AE-WT and AE-KO (fgl2$^{-/-}$) mice. Data were collected from three independent experiments of five to six mice in each group. Comparison between groups was performed using a one-way ANOVA for statistical analysis. *P<0.05, ** P<0.01. 'WT', wild type mice; KO, fgl2 knock out mice; 'PEC', peritoneal exudate cells; 'Spleen', spleen cells.

T cell functions and maturation of DCs in primary spleen cells from AE-fgl2$^{-/-}$and AE-WT mice, after ConA stimulation

Flow cytometric analyses showed that both expression of CD4^{+} IFN-γ^{+} and CD4^{+} IL-17A^{+} were significantly higher in spleen cells from AE-fgl2$^{-/-}$ mice at 4mo p.i., 48h after exposure to ConA, compared to AE-WT mice. There was no difference in expression of IL-4 between spleen cells from AE-fgl2$^{-/-}$ mice and AE-WT mice. CD4^{+} IL-2^{+} expression was significantly up-regulated in spleen cells from AE-fgl2$^{-/-}$ mice at 4mo p.i. (Figure 7.12A).

48h after exposure to ConA, surface expression of CD80 in CD11b^{+}DCs from AE-fgl2$^{-/-}$ mice at 4mo p.i. was significantly higher, than in CD11b^{+}DCs from AE-WT mice. Both CD80 and CD86 expression in CD11c^{+}DCs from AE-fgl2$^{-/-}$ mice at 4mo p.i. was higher than in CD11c^{+} DCs from AE-WT mice (Figure 7.12B).

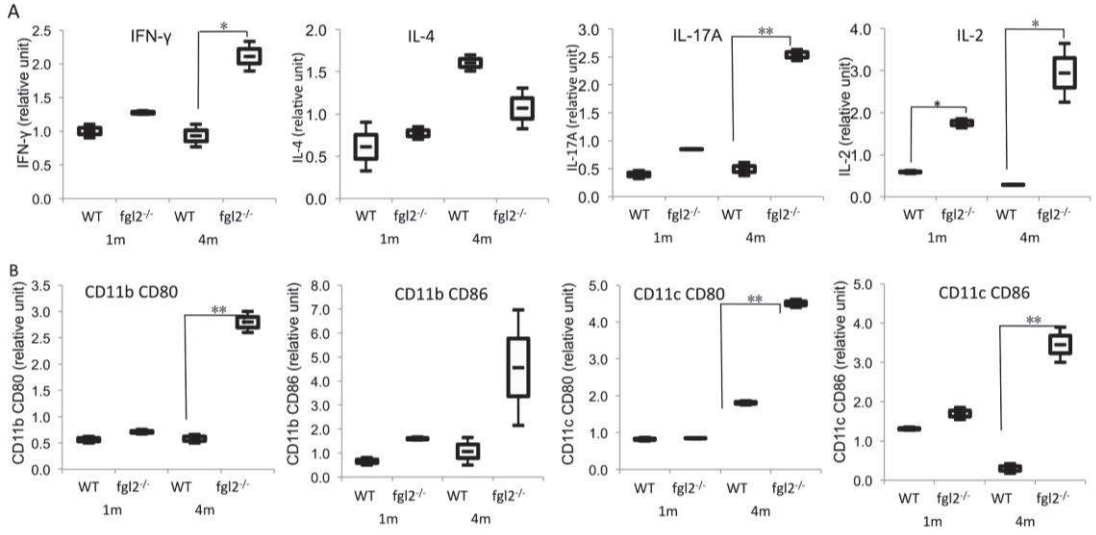

Figure 7.12 T cell reactivity and DC maturation in response to Concanavalin (Con) A stimulation after *E. multilocularis* infection.

(A) Expression of T cell reactivity markers in freshly isolated spleen cells from AE-WT and AE-KO (fgl2$^{-/-}$) mice, co-cultured with ConA, normalized using cells non-infected controls, at different stages of *E. multilocularis* infection. (B) Expression of DC maturation markers in freshly isolated spleen cells from AE-WT and AE-KO (fgl2$^{-/-}$) mice, co-cultured with ConA, normalized using cells from non-infected controls, at different stages of *E. multilocularis* infection. Data were collected from three independent experiments of five to six mice in each group. Comparison between groups was performed using a one-way ANOVA for statistical analysis. *P<0.05, ** P<0.01.

T cell functions and maturation of DCs in primary spleen cells from *AE*-fgl2$^{-/-}$and AE-WT mice, after exposure to *E. multilocularis* vesicle fluid (VF)

Flow cytometric analyses showed that, 96h after exposure to VF, expression of IL-4 was significantly higher in spleen cells from AE-WT mice at 4mo p.i. than in cells from AE-WT mice. However, there was no difference in expression of either IFN-γ or IL-17A between cells from AE-fgl2$^{-/-}$ mice and AE-WT mice. Expression of IL-2 was significantly up-regulated in cells AE-fgl2$^{-/-}$ mice at 4mo p.i., 4 days after exposure to VF, as compared to cells from AE-WT mice (Figure 7.13A).

Surface expression of CD80 both in CD11b^{+} and CD11c^{+} DCs from AE-fgl2$^{-/-}$ mice at 4mo p.i. was significantly higher, 96h after exposure to VF, than in DCs from AE-WT mice. However, there was no difference in CD86 expression in both subpopulations of DCs from AE-fgl2$^{-/-}$ mice after exposure to VF, compared to DCs from AE-WT mice (Figure 7.13B).

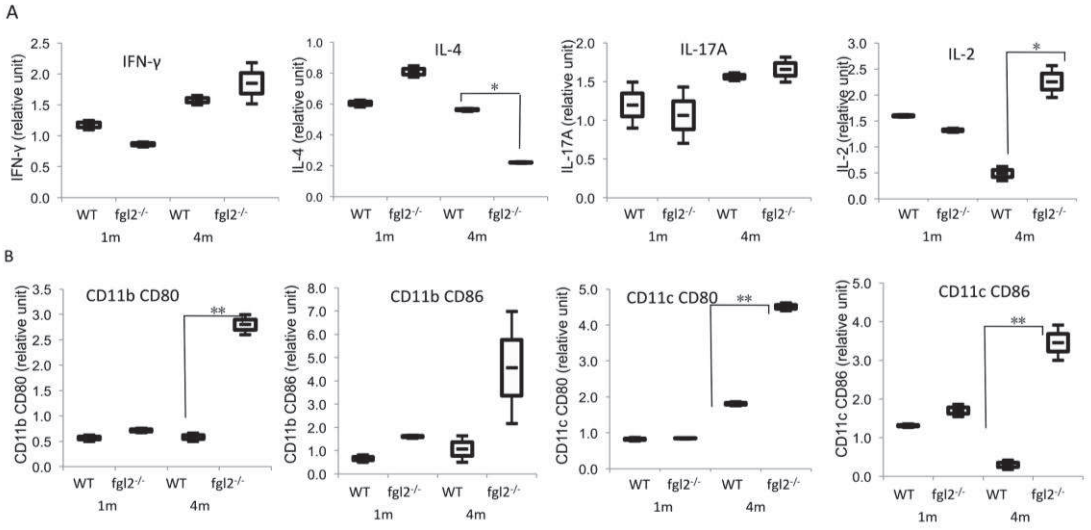

Figure 7.13 T cell reactivity and DC maturation in response to Vesicle fluid (VF) stimulation after *E. multilocularis* infection.

(A) Expression of T cell reactivity markers in freshly isolated spleen cells from AE-WT and AE-KO ($fgl2^{-/-}$) mice, co-cultured with VF, normalized with non-infected controls, at different stages of *E. multilocularis* infection. (B) Expression of DC maturation markers in freshly isolated spleen cells from AE-WT and AE-KO ($fgl2^{-/-}$) mice, co-cultured with VF, normalized using cells from non-infected controls, at different stages of *E. multilocularis* infection. Data were collected from three independent experiments of five to six mice in each group. Comparison between groups was performed using a one-way ANOVA for statistical analysis. *P<0.05, ** P<0.01.

T cell functions, maturation of DCs, and co-stimulation in spleen cells from non-infected WT mice, after exposure to recombinant FGL2 and anti-FGL2 monoclonal antibodies

To further assess the role of FGL2 in T cell functions and DC maturation in our mouse model, we cultured spleen cells from non-infected WT mice with/without recombinant FGL2 and anti-FGL2-MAbs. Flow cytometric analyses showed that the expression of both Foxp3 and IL-10 on CD4 T cells was increased in response to recombinant FGL2 in a dose-dependent manner (Figure 7.14). $CD4^+$ $Foxp3^+$ expression was decreased in the presence of anti-FGL2 in response to VF, which indicated that *E. multilocularis* metabolic components may exert immune-modulatory activity. Conversely, $CD4^+$ $IL\text{-}17A^+$ expression was decreased in the presence of high concentration of recombinant FGL2 (5μg/mL), but increased in a non-specific manner in response to ConA; there was no influence of VF on IL-17A expression (Figure 7.14). Like $CD4^+$ $Foxp3^+$, $CD4^+$ IFN-γ^+ expression was specifically increased in response to VF. For DCs, expression of CD86 on $CD11c^+$ DCs was decreased in the

presence of recombinant FGL2, but increased in an antigen-specific manner in response to VF. However, expression of CD86 and MHCII on $CD11b^+$ DCs showed the opposite. Expression of CD40 on $CD11c^+$ DCs and CD80 on $CD11b^+$ DCs was increased in the presence of anti-FGL2 (Figure 7.14). CD62L, a cell adhesion molecule which is highly expressed on naïve lymphocytes, but not expressed on effector memory T-lymphocytes [29], was found to be increased in the presence of recombinant FGL2 (1μg/mL), but decreased in the presence of anti-FGL2 on both CD4 T cells and total lymphocytes (Figure 7.14), which indicated that FGL2 may play an important role in down-regulating lymphocyte co-stimulation and effector cell production.

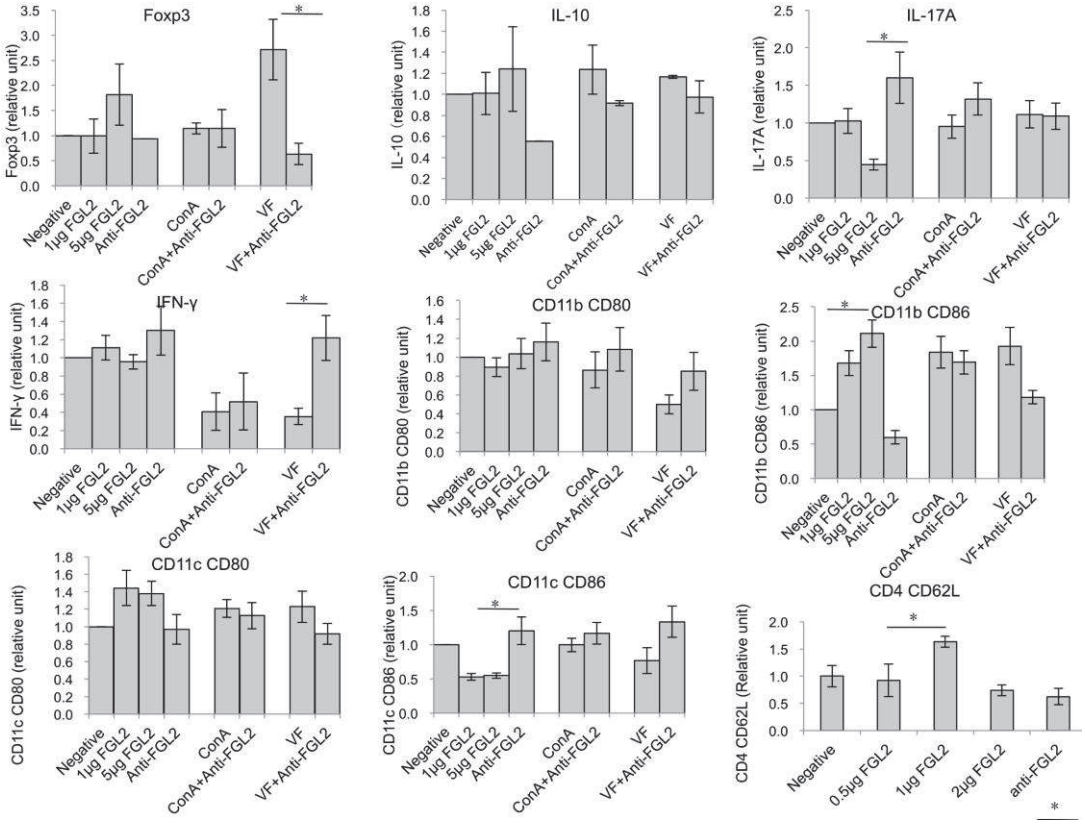

Figure 7.14 Recombinant FGL2 down-regulates T cell reactivity and DC maturation *in vitro*.

Different concentrations of recombinant FGL2 (0, 1, 5 μg/mL) and anti-FGL2 mAb (10 μg/mL) were added to primary spleen cells which were isolated from non-infected WT mice. Expression of T cell reactivity and DC maturation markers were determined by flow cytometry. Data were collected from three independent experiments of five mice in each group. Comparison between groups was performed using a one-way ANOVA for statistical analysis. *P<0.05, ** P<0.01.

IL-17A contributes to FGL2 secretion *in vitro*

Spearman correlation coefficients indicated a positive correlation between serum IL-17A level and FGL2 expression (r=0.435, *P*=0.045) in the serum from WT mice 1mo to 4mo p.i. in experimental mice under study (Table 7.1). To examine whether IL-17A contributes to FGL2 secretion, we employed "up and down experiments" as follows: spleen cells from non-infected WT mice were co-cultured either with recombinant IL-17A as an external stimulus, or with anti-IL-17A for blocking purpose, followed by a subsequent detection of FGL2 expression in the supernatant. Respective quantitative analyses by ELISA showed that recombinant IL-17A increased FGL2 secretion in a dose-dependent manner, while anti-IL-17A completely blocked FGL2 secretion (Figure 7.15).

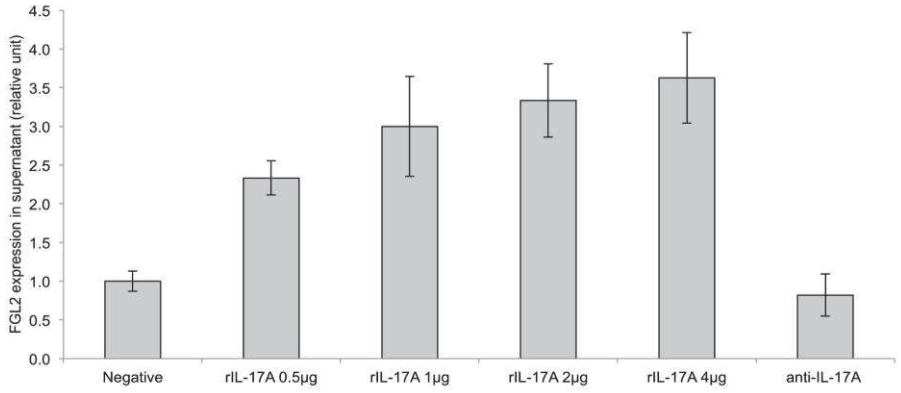

Figure 7.15 Recombinant IL-17A contributes to FGL2 secretion *in vitro*.
Different concentrations of recombinant FGL2 (0, 0.5, 1, 2 μg/mL) and anti-IL-17A mAbs (1 μg/mL) were added to primary spleen cells isolated from non-infected WT mice. FGL2 expression in the supernatant of cell cultures was determined by ELISA. Data were collected from three independent experiments of five mice in each group. Comparison between groups was performed using a one-way ANOVA for statistical analysis. **P*<0.05, ** *P*<0.01.

Discussion

In larval *E. multilocularis* infection, immune tolerance and/or down-regulation of immunity is a marked characteristic increasingly observed towards the late stage of infection in both humans [30] and in experimentally infected mice [6]. In this context, preliminary findings have shown that Tregs play an important role in the orchestration that controls inflammatory/immune response in AE and finally allows long-term parasite survival, proliferation and maturation [7]. No assessment of the contribution of the Treg-linked effector molecule FGL2 had so far ever been studied in parasite-host tolerance processes. *E. multilocularis* infection appeared to be a good model to study its intervention and allowed us to show for the first time that, in *E.*

multilocularis infection 1) FGL2 contributes to the outcome of infection by the metacestode; 2) FGL2 partly contributes to Treg functions; 3) FGL2 can down-regulate the maturation of DCs, suppress Th1 and Th17 immune responses, and support Th2 and Treg immune responses, 4) FGL2 contribute to the induction of B cell death; and finally 5) IL-17A contributes to FGL2 secretion.

One of the first and major aims of our experiments was to study the role of Treg-expressed FGL2 in the outcome of *E. multilocularis* infection. Using $fgl2^{-/-}$ infected mice, the respective findings were clear: infected AE-WT mice had significantly more parasite load at the late stage of infection, as compared to AE-$fgl2^{-/-}$ mice. This was accompanied by increased serum FGL2 levels while, as expected, no serum FGL2 could be determined in $fgl2^{-/-}$ mice; respective fgl2 mRNA expression levels in both peritoneal and spleen cells were also increased in AE-WT mice and there was a significant increase in Tregs. Taken together, these results support the hypothesis that Treg-expressed FGL2 contributes to the course and outcome of *E. multilocularis* infection. Such an effect of FGL2 has been shown in other models of infection, such as viral infection: antibodies directed against the C terminal domain of FGL2, which is known to account for its immunosuppressive activity, protected mice from the lethality of MHV-3 infection. Transfer of $fgl2^{+/+}$ Tregs to $fgl2^{-/-}$ mice increased mortality to MHV-3 infection, further supporting a role for Treg-expressed FGL2 in the outcome of the infection [42]. However, FGL2-deficient and control mice exhibit similar degrees of T cell expansion, immunopathology, and/or pathogen burdens during protozoan (*Toxoplasma gondii*), bacterial (*Yersinia enterocolitica*, *Listeria monocytogenes*, and *Mycobacterium tuberculosis*), and viral (murine gamma-herpesvirus-68 and Sendai) infections [31].

How FGL2 influences or modulates the outcome of experimental AE can, so far, only be discussed speculatively. In *E. multilocularis* infection, as reported in previous studies [6,32,33], cellular immunity that includes a rather Th1-oriented cytokine secretion profile can provide some control over metacestode development and/or proliferation at the early/initial stage of infection, while a progressively Th2-oriented immune response, which becomes marked at the later stage of infection, yields a now much more rapid metacestode growth. The control of metacestode proliferation appears to be predominantly T cell-dependent, as revealed by the use of different immune-compromised mouse models [34,35,36], and by observations in human AE-patients with immune suppression-associated conditions [37,38,39,40]. It is therefore conceivable that the proliferating metacestode itself specifically activates and concurrently modulates the immune response to its own advantage. Tregs, which over-express a subset of regulatory cytokine genes including IL-10 and TGF-β, resulting in the relative suppression of Th1 responses and endorsement of Th2 polarization, play a very important role in promoting immune tolerance in various

models of parasitic diseases [41]: they were up-regulated in our study; a previous study strongly suggested that they are also up-regulated in human AE-patients [42]; and, finally, elevated IL-10 as well as TGF-β synthesis/secretion has been repeatedly shown in experimental murine and human AE [43].

Various molecular and cellular events have been proposed to explain the mechanism by which Tregs suppress immune responses. These include cell-to-cell contact-dependent suppression, cytotoxicity, and immunosuppressive cytokine secretion [44]. It is generally accepted that anti-inflammatory cytokines, such as IL-10 and TGF-β, are important co-mediators of Treg activity *in vivo* [44]. However, the importance of these cytokines remains controversial, as several reports have demonstrated that antibodies against IL-10 and TGF-β fail to block Treg suppressive function. Also, Tregs from TGF-β–deficient mice have normal suppressive activity *in vitro* and can prevent development of autoimmune disease [44]. In addition, the ambiguous role of TGF-β, which is both a strong inducer of immune tolerance and an activator of the pro-inflammatory IL-17 cytokine system, remains puzzling [45,46]. Recently, it was reported that in BALB/cJ mice, Tregs demonstrate a constitutively high expression of FGL2 encoding mRNA, which even increased after MHV-3 infection, and it was suggested by adoptive transfer of wild-type Tregs into resistant $fgl2^{-/-}$ mice that FGL2 might be an important Treg effector molecule [47]. In a previous explorative study, we found that *fgl2* gene expression was significantly increased in the periparasitic liver tissue of mice perorally infected with *E.multilocularis* eggs [8]. Our resulting working hypothesis was thus that FGL2, playing important roles in both innate and adaptive immunity, similar to other members of the fibrinogen-like family of proteins that include tenascin and angiopoietin, could be another key-actor in *E. multilocularis*-host interactions, unknown until now. We were postulating that, using the present murine AE-model, we could elucidate new modes of action promoting and maintaining immune tolerance [48] that favors metacestode survival. In this study, we could for the first time experimentally demonstrate that recombinant FGL2 suppresses T cell proliferation in response to Con A and to *E. multilocularis* antigenic metabolites present in the VF. FGL2 also inhibited maturation of dendritic cells (DCs), suppressed Th1 and Th17 immune responses, and polarized an allogeneic immune response towards a Th2-oriented cytokine profile, both *in vivo* and *in vitro*. Conversely, in $fgl2^{-/-}$ mice, Th1 cytokine levels and activity of DCs, B- and T cells were all increased. FGL2 serum levels correlated with IL-4 expression in wild type mice before and after *E.multilocularis* infection, suggesting a close relationship between FGL2 and Th2-related immune response. The temporally increasing development of a Th2 immune response in wild type mice after *E.multilocularis* infection corroborated the generally known effect of FGL2 to promote a Th2 cytokine production, with a

concomitant inhibition of Th1- and Th17-oriented immunity. Furthermore, serum levels of IL-17A showed a positive correlation with FGL2 serum expression, suggesting for the first time that IL-17A could contribute to FGL2 secretion. This was confirmed *in vitro*, in that recombinant IL-17A promoted the production of FGL2 in spleen cells, while anti-IL-17A blocked respective FGL2 secretion.

We also investigated the importance of FGL2 for the function of Tregs, by directly assessing the effect of recombinant FGL2 and of an anti-FGL2 MAb on Treg activity *in vitro*. Recombinant FGL2 promoted Treg function, while anti-FGL2 completely abrogated Treg function, thus providing experimental support for our hypothesis. Further evidence for the role of FGL2 in Treg function was provided by the observation that fgl2-deficient mice had both decreased Treg numbers and impaired Treg function. The mechanism by which FGL2 mediates its immunosuppressive activity is currently under intense investigation. Recent data have indicated that FGL2 binds to the inhibitory FcγRIIB receptor (CD32) expressed primarily on APCs. This FGL2-FcγRIIB interaction was shown to induce B cell apoptosis and inhibit DC maturation [10]. In *E. multilocularis* infection, several cell types may express inhibitory FcγRIIB, such as macrophages (including the 'epithelioid cells' that line the 'immuno-modulating' laminated layer), and also the numerous $CD8^+$ T cells present in the periparasitic infiltrate; $CD8^+$ T cells have actually been shown to express this receptor in a murine model of *Trypanosoma cruzi* [49]. Taken together, and combined with our recent data on the course of cytokine expression by the periparasitic immune infiltrate in *E.multilocularis* infection [50], our data suggest that, under the influence of *E. multilocularis* metabolites (a) IL-6, TNF-α, IFN-γ and IL-17 are released; (b) these, especially IFN-γ as demonstrated previously [31], but also IL-17A as we showed in this study, contribute to FGL2 secretion by Tregs and other cells; and (c) once FGL2 is released, it can bind to FcγRIIB receptor, down-regulate the maturation of DCs, decrease co-stimulation of effector T cells, suppress Th1 and Th17 immune response, accelerate Th2 immune responses, induce apoptosis of B cells, and thus overall lead to an immune suppressed status that favors the continuous "tumor-like" progression of the parasitic metacestode tissue (Figure 16). Direct inhibition of macrophage and/or mast cell functions could also be induced by such a binding [51][50].

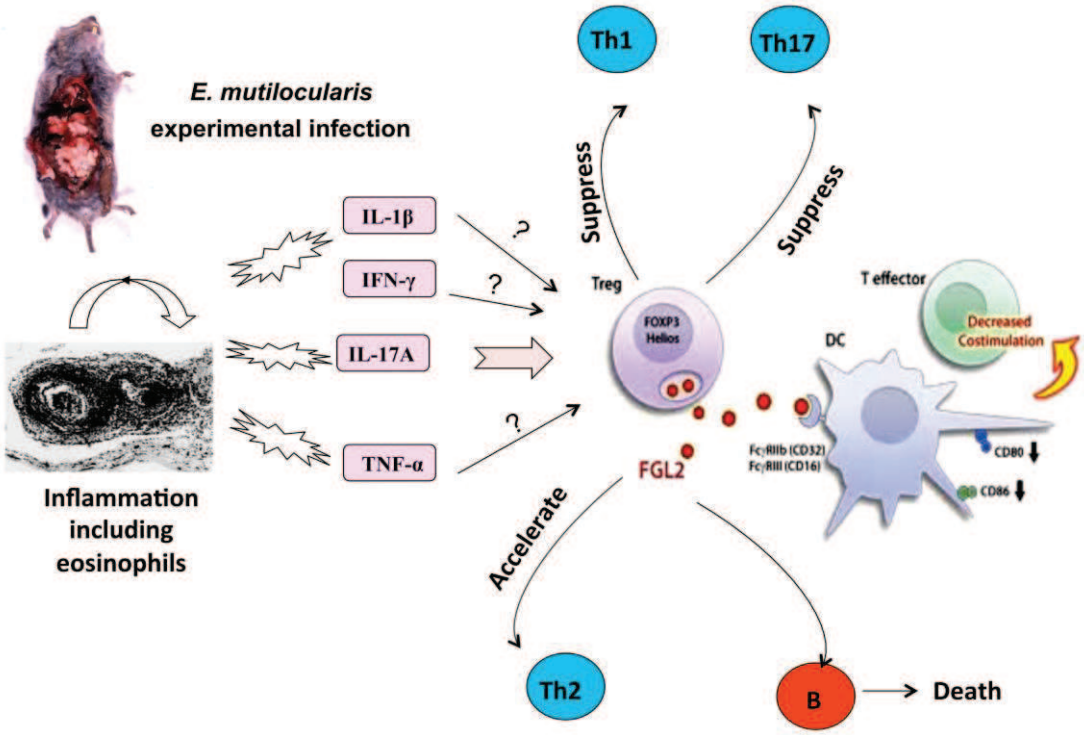

Figure 7.16 Schematic diagram summarizing the hypothesized mechanism of FGL2-related regulation of immune response involved in the host-parasite relationship in murine *E. multilocularis* infection.

Based on the present findings in experimental rodents, FGL2 may be proposed as a marker of progression of parasitic lesions, thus of the clinical status of AE patients with *E. multilocularis* infection. This is currently under investigation. We may also anticipate that FGL2 serum levels could be useful in predicting the course and outcome and/or parasite activity in human AE. Furthermore, our findings may provide a rationale for studying FGL2 as a target for immunomodulatory treatment option in patients with progressive AE. Our data demonstrate that FGL2, together with IL-17 and by promoting Treg cell activity, appears as a key-player in the orchestration of the outcome of *E. multilocularis* infection; this study gives evidence for a role of IL-17 in FGL2 regulation, and suggest that targeting FGL2 could be used for (a) the assessment of a present clinical status of AE-patients, (b) for the monitoring of conventionally treated AE patients, and (c) for the speculative development of novel treatment approaches in infectious diseases, including AE.

Materials and Methods

Ethics Statement

The animal study was performed in strict accordance with the recommendations of the Swiss Guidelines for the Care and Use of Laboratory Animals. The protocol was approved by the Commission for Animal Experimentation of the Canton of Bern (approval no. BE_103/11). Every effort was made to minimize suffering.

Experimental design, parasite sampling and histological examinations

Mice. fgl2$^{-/-}$ mice were generated by the Multi Organ Transplant Program, University of Toronto, and the methodology for their production has been described elsewhere [52]. In brief, *fgl2*$^{-/-}$ mice were obtained by transfecting 129Sv embryonic stem cells with the knockout construct (also derived from 129Sv). These stem cells were then injected into C57BL/6 blastocysts and the resulting chimeras were backcrossed for 10 generations into a C57BL/6 background [52]. Female *fgl2*$^{-/-}$ mice and respective WT animals, aged between 8-10 weeks, were used for intraperitoneal infection with *E. multilocularis* as previously described [37,38], and age and gender matched littermates were used for mock-infected control groups. From experimentally infected mice, all macroscopically visible parasite tissues were carefully collected upon necropsy as previously described [35,53].

Parasite and experimental infection. The parasite used in this study was a cloned *E. multilocularis* (KF5) isolate maintained by serial passages (vegetative transfer) in C57BL/6 mice [53]. In order to prepare the infection material for mice, metacestode tissue was obtained from previously infected mice by aseptic removal from the peritoneal cavity. After grinding the tissue through a sterile 50 µm sieve, approximatively 100 freshly prepared acephalic vesicular cysts were suspended in 100 µL RPMI-1640 (Gibco, Basel,Switzerland) and injected intraperitoneally. Each experimental group included 6 animals unless otherwise stated. Control mice (mock-infection) received 100µL of RPMI-1640 only.

Tissue mass and quantification. Mice were sacrificed by CO_2 euthanasia at 1mo (corresponding to an early stage of chronic infection) and 4mo(corresponding to a middle/late stage of disease) post-infection. Blood was collected by cardiac puncture, and serum samples were stored at -80°C. Parasite tissues were dissected and, if present, fat and connective tissues were removed carefully for subsequent wet-weighing of the parasite mass.

Cell preparations and Treg isolation. Peritoneal exudate cells (PEC) and splenic cells from naïve (control) and *E. multilocularis* infected (AE) fgl2$^{-/-}$ and WT mice were collected by peritoneal rinsing, or grinding separately with 5 mL RPMI-1640. Cells were subsequently washed twice with HBSS and resuspended in RPMI-1640

(Gibco) for cell staining or cell culture separately. Macrophages were removed from each group of mice after incubation of PEC or spleen cell suspension in 5 mL RPMI-1640+20% FCS in a Petridish for 2 h at 37 °C, in an atmosphere containing 5% CO_2 as follows: non-adherent cells were separated from macrophage-enriched adherent cells and were positively selected by MACS (magnetic cell separation) using the mouse $CD4^+$ $CD25^+$ T cell Isolation Kit (Miltenyi Biotec, Germany) according to the manufacturer's instructions. Highly (N99%) enriched iTreg cells were obtained by additional cell sorting after the MACS procedure, and finally washed and resuspended in complete RPMI-1640.

Tissue fixation and sectioning. Parasite samples were fixed in 4% paraformaldehyde in neutral buffered formalin for a minimum of 24 h, embedded in paraffin, and cut into 4μm serial sections. Paraffin-embedded parasite samples of experimental mice were HE and PAS-stained for pathological observations.

Con A or Vesicle fluid (VF) stimulation

Spleen cells were plated at a concentration of 2×10^5 cells/well in 200 μL of RPMI-1640 complete medium (Gibico, Basel, Switzerland) and stimulated with 2 μg/mL Con A (Sigma-Aldrich, Basel, Switzerland) for 48h, or 10μg/mL VF for 96h at 37 °C and 5% CO_2. The same cell reactions performed without ConA and VF were used as negative controls.

rFGL2 and anti-FGL2 stimulation

Spleen cells were plated at a concentration of 2×10^5 cells/well in 200 μL of RPMI-1640 complete medium (Gibico, Basel, Switzerland) and stimulated with 1μg/mL and 5μg/mL rFGL2 or 1μg/mL anti-FGL2 (Sigma-Aldrich, Basel, Switzerland) for 48h at 37 °C and 5% CO_2. The same cell reactions performed without rFGL2 or anti-FGL2 were considered as negative controls.

rIL-17A and anti-IL-17A stimulation

Spleen cells were plated at a concentration of 2×10^5 cells/well in 200 μL of RPMI-1640 complete medium (Gibico, Basel, Switzerland) and stimulated with 0.5, 1, 2 and 4μg/mL rIL-17A or 1μg/mL anti-IL-17A (Sigma-Aldrich, Basel, Switzerland) for 48h at 37 °C and 5% CO_2. The same cell reactions performed without rIL-17A or anti-IL-17A were considered as negative controls.

Cell proliferation assay

Cell proliferation was assayed using the colorimetric BrdU cell proliferation ELISA kit (Calbiochem, Merck chemicals, Switzerland). Around either 48h after ConA stimulation or 96h after VF stimulation after seeding of the cells, BrdU was added to a final concentration of 1 μM. After incubation for a further 16 h, BrdU incorporation was measured using a spectrophotometric plate reader at 450-540 nm and at 450-595 nm for a repeated reading.

Flow cytometry

Aliquots of 10^5 cells/100 µL of staining buffer per well were incubated each with 1 µg of purified anti-CD16/CD32 for 20 min in the dark in order to block non-specific binding of antibodies to the FcγIII and FcγII receptors. Subsequently these cells were stained with surface marker separately for 15 min with 1 µg of primary antibodies: FITC-labeled anti-CD4, anti-CD80, anti-CD86; PE-labeled anti-CD8, anti-CD11b, anti-CD11c, anti-B220, and PECy 5.5-labeled anti-CD4, FITC-labeled anti-CD25. All antibodies were from BD Pharmingen (Heidelberg, Germany). For intracellular staining, PEC or splenocytess were first incubated with Inside Fix for 20mins at room temperature, then stained with PE-labeled anti-IFN-r, anti-IL-4, anti-IL-17A, anti-IL-2, anti-IL-10 and anti-Foxp3 (BD Pharmingen, Palo. Alto, CA, USA) in Inside Perm for 15min. The corresponding primary labeled isotype control antibodies were used for staining controls. Cells resuspended in 300 µL of buffer (0.15 M NaCl, 1 mM NaH_2PO_4 H_2O, 10 mM Na_2HPO_4 $2H_2O$ and 3 mM NaN3) were analyzed in a flow cytometer (Becton Dickinson, Heidelberg, Germany) using the corresponding CELL QUEST software.

RNA extraction and cDNA synthesis

Approximately 5×10^6 of cells were prepared from non-infected and from *E.multilocularis*- infected -fgl2-/- (AE- $fgl2^{-/-}$) or *E. multilocularis*- infected WT (AE-WT) mice; these cells were used for cytoplasmic RNA extraction. RNA yield and purification were performed using the RNeasy mini kit (Qiagen, Switzerland) according to the standard protocol suitable for freshly harvested cells. After removing contaminated DNA from the isolated RNA using DNaseI (Fermentas, Vilnius, Lithuania), the RNA samples were used for cDNA synthesis using the Omniscript® Reverse Transcription kit (Qiagen, Hilden, Germany). Briefly, 0.5 µg/µL of random Primer (Promega, Dübendorf, Switzerland) and 2µg of total RNA were used in a final volume of 20µL of reaction mixture and incubated at 37 °C overnight. cDNA was incubated at 95 °C for 3 min and frozen at -80 °C until use for qRT-PCR.

Quantitative real-time RT- PCR analysis

Quantitative real time RT-PCR (qRT-PCR) was run in a thermocycler (Qiagen, Hilden, Germany) with the SYBR Green PCR premix (Qiagen, Hilden, Germany) following the manufacturer's instructions. Thermocycling was performed in a final volume of 10 µL containing 2 µL cDNA and 10 pM of each primer (Table 1). To normalize for gene expression, mRNA expression of the housekeeping gene β-actin was measured. For every sample, both the housekeeping and the target genes were amplified in triplicate using the following cycle scheme: after initial denaturation of the samples at 95 °C for 15 min, 40 cycles of 95 °C for 15 s and 55 °C (or other) for 30 s were performed. Fluorescence was measured in every cycle, and a melting curve was analyzed after the PCR by increasing the temperature from 55 to 95 °C (0.5 °C

increments). A defined single peak was obtained for all amplicons, confirming the specificity of the amplification.

Suppression assay

In vitro suppression assays were carried out with cultures of 2×10^4 $CD4^+CD25^+$ T cells from WT mice as responder cells, together with 8×10^4 irradiated spleen cells as APC and titrated numbers of $CD4^+$ $CD25^+$ Treg cells from either *E.multilocularis*-infected AE-$fgl2^{-/-}$ or AE-WT mice as suppressor cells, compared with non-infected controls. Cultures were stimulated with Con A (1 μg/ml) for 48 h and BrdU was added for the last 16 h to measure proliferation of effector T cells. For antibody blockade studies, titrated concentrations of an MAb to FGL2 (no. H00010875-M01 monoclonal IgG2a Ab; Abnova, Luzern, Switzerland) were added to the cell cultures of $CD4^+$ effector T cells and $CD4^+$ $CD25^+$ Treg cells sorted from WT mice, at a 1:4 suppressor:responder cell ratio in the presence of APCs and ConA.

Sandwich Enzyme-Linked Immunosorbent Assay for FGL2

After washing of pre-coated plates 3 times with Tris-Tween buffered saline, serum samples (50 μL) were added to each well, and after a 2-hour incubation at room temperature and three washes with Tris-Tween buffered saline, the wells were incubated with mouse monoclonal FGL2 detection antibody for 1 hour at room temperature. The plates were washed again for 3 times, and polyclonal anti-FGL2 binding was detected with a secondary horseradish peroxidase-conjugated anti-rabbit antibody. Tetramethlybenzidine was then added and absorbance was measured at 450 nm using a Tecan Sunrise® plate reader.

Luminex for cytokine expression in the serum

Cytokine levels in mouse serum samples were assessed undiluted using microsphere-based multiplex assays (MILLIPLEX® MAP Mouse Cytokine/Chemokine Multiplex Assays MPXMCYTO-70K, Merck Millipore, Zug, Switzerland) that were performed according to the manufacturer's instructions. Serum concentrations of the following cytokines were measured: IL-1β, IL-4, IL-10, IL-17A, IFN-γ and TNF-α. A minimum of 50 beads per analyte was measured on a Bioplex-200 platform (Bio-Rad, Hercules, CA, USA). Calibration was performed using BioPlex Manager software version 4.1.1 by linear regression analysis using the four lowest standards provided by the manufacturer. When measured cytokine concentrations were below the detection limit, a value corresponding to the detection limit of the assay was used for statistical analysis.

Statistical analyses

All the data were analyzed by SPSS 17.0. The results were presented as means ± SD. One-way ANOVA and Student's *t*-test were used to compare the differences between groups, and Spearman's rho was used to analyze the correlation coefficient. $P<0.05$ was considered to indicate statistical significance.

Acknowledgements
We would like to thank Franziska Simon (Institute for Infectious Diseases, University of Bern) for her excellent technical assistance, and Prof. Christoph Müller (Institute of Pathology, University of Bern) for his suggestions concerning some experimental approaches carried out.

References

1. Vuitton DA (2003) The ambiguous role of immunity in echinococcosis: protection of the host or of the parasite? Acta Trop 85: 119-132.
2. Torgerson PR, Keller K, Magnotta M, Ragland N (2010) The global burden of alveolar echinococcosis. PLoS Negl Trop Dis 4: e722.
3. Vuitton DA, Zhang SL, Yang Y, Godot V, Beurton I, et al. (2006) Survival strategy of Echinococcus multilocularis in the human host. Parasitol Int 55 Suppl: S51-55.
4. Manfras BJ, Reuter S, Wendland T, Kern P (2002) Increased activation and oligoclonality of peripheral CD8(+) T cells in the chronic human helminth infection alveolar echinococcosis. Infect Immun 70: 1168-1174.
5. Manfras BJ, Reuter S, Wendland T, Boehm BO, Kern P (2004) Impeded Th1 CD4 memory T cell generation in chronic-persisting liver infection with Echinococcus multilocularis. Int Immunol 16: 43-50.
6. Bresson-Hadni S, Liance M, Meyer JP, Houin R, Bresson JL, et al. (1990) Cellular immunity in experimental Echinococcus multilocularis infection. II. Sequential and comparative phenotypic study of the periparasitic mononuclear cells in resistant and sensitive mice. Clin Exp Immunol 82: 378-383.
7. Tuxun T, Wang JH, Lin RY, Shan JY, Tai QW, et al. (2012) Th17/Treg imbalance in patients with liver cystic echinococcosis. Parasite Immunol 34: 520-527.
8. Gottstein B, Wittwer M, Schild M, Merli M, Leib SL, et al. (2011) Hepatic gene expression profile in mice perorally infected with Echinococcus multilocularis eggs. PLoS One 5: e9779.
9. Levy GA, Liu M, Ding J, Yuwaraj S, Leibowitz J, et al. (2000) Molecular and functional analysis of the human prothrombinase gene (HFGL2) and its role in viral hepatitis. Am J Pathol 156: 1217-1225.
10. Liu H, Shalev I, Manuel J, He W, Leung E, et al. (2008) The FGL2-FcgammaRIIB pathway: a novel mechanism leading to immunosuppression. Eur J Immunol 38: 3114-3126.
11. Ghanekar A, Mendicino M, Liu H, He W, Liu M, et al. (2004) Endothelial induction of fgl2 contributes to thrombosis during acute vascular xenograft rejection. J Immunol 172: 5693-5701.
12. Belyavsky M, Belyavskaya E, Levy GA, Leibowitz JL (1998) Coronavirus MHV-3-induced apoptosis in macrophages. Virology 250: 41-49.
13. Fingerote RJ, Abecassis M, Phillips MJ, Rao YS, Cole EH, et al. (1996) Loss of resistance to murine hepatitis virus strain 3 infection after treatment with corticosteroids is associated with induction of macrophage procoagulant activity. J Virol 70: 4275-4282.
14. Liu Y, Xu S, Xiao F, Xiong Y, Wang X, et al. (2010) The FGL2/fibroleukin prothrombinase is involved in alveolar macrophage activation in COPD through the MAPK pathway. Biochem Biophys Res Commun 396: 555-561.
15. McGilvray ID, Lu Z, Wei AC, Dackiw AP, Marshall JC, et al. (1998) Murine hepatitis virus strain 3 induces the macrophage prothrombinase fgl-2 through

p38 mitogen-activated protein kinase activation. J Biol Chem 273: 32222-32229.
16. Ning Q, Brown D, Parodo J, Cattral M, Gorczynski R, et al. (1998) Ribavirin inhibits viral-induced macrophage production of TNF, IL-1, the procoagulant fgl2 prothrombinase and preserves Th1 cytokine production but inhibits Th2 cytokine response. J Immunol 160: 3487-3493.
17. Mendicino M, Liu M, Ghanekar A, He W, Koscik C, et al. (2005) Targeted deletion of Fgl-2/fibroleukin in the donor modulates immunologic response and acute vascular rejection in cardiac xenografts. Circulation 112: 248-256.
18. Ning Q, Sun Y, Han M, Zhang L, Zhu C, et al. (2005) Role of fibrinogen-like protein 2 prothrombinase/fibroleukin in experimental and human allograft rejection. J Immunol 174: 7403-7411.
19. Wilczynski JR (2006) Immunological analogy between allograft rejection, recurrent abortion and pre-eclampsia - the same basic mechanism? Hum Immunol 67: 492-511.
20. Xie L, Ichimaru N, Morita M, Chen J, Zhu P, et al. (2011) Identification of a novel biomarker gene set with sensitivity and specificity to distinguish between allograft rejection and tolerance. Liver Transpl.
21. Zhang L, Ning Q, Guo H, Zhang WJ, Chen F, et al. (2004) [Expression of human fibrinogen-like protein 2/fibroleukin in renal acute allograft rejection and its potential clinical implication]. Zhonghua Yi Xue Za Zhi 84: 474-477.
22. Clark DA, Chaouat G, Gorczynski RM (2002) Thinking outside the box: mechanisms of environmental selective pressures on the outcome of the materno-fetal relationship. Am J Reprod Immunol 47: 275-282.
23. Fontenot JD, Rasmussen JP, Gavin MA, Rudensky AY (2005) A function for interleukin 2 in Foxp3-expressing regulatory T cells. Nat Immunol 6: 1142-1151.
24. Herman AE, Freeman GJ, Mathis D, Benoist C (2004) CD4+CD25+ T regulatory cells dependent on ICOS promote regulation of effector cells in the prediabetic lesion. J Exp Med 199: 1479-1489.
25. Fontenot JD, Rasmussen JP, Williams LM, Dooley JL, Farr AG, et al. (2005) Regulatory T cell lineage specification by the forkhead transcription factor foxp3. Immunity 22: 329-341.
26. Gavin MA, Rasmussen JP, Fontenot JD, Vasta V, Manganiello VC, et al. (2007) Foxp3-dependent programme of regulatory T-cell differentiation. Nature 445: 771-775.
27. Williams LM, Rudensky AY (2007) Maintenance of the Foxp3-dependent developmental program in mature regulatory T cells requires continued expression of Foxp3. Nat Immunol 8: 277-284.
28. Zheng Y, Josefowicz SZ, Kas A, Chu TT, Gavin MA, et al. (2007) Genome-wide analysis of Foxp3 target genes in developing and mature regulatory T cells. Nature 445: 936-940.

29. Zhang X, Chang Li X, Xiao X, Sun R, Tian Z, et al. (2013) CD4(+)CD62L(+) central memory T cells can be converted to Foxp3(+) T cells. PLoS One 8: e77322.
30. Harraga S, Godot V, Bresson-Hadni S, Mantion G, Vuitton DA (2003) Profile of cytokine production within the periparasitic granuloma in human alveolar echinococcosis. Acta Trop 85: 231-236.
31. Hancock WW, Szaba FM, Berggren KN, Parent MA, Mullarky IK, et al. (2004) Intact type 1 immunity and immune-associated coagulative responses in mice lacking IFN gamma-inducible fibrinogen-like protein 2. Proc Natl Acad Sci U S A 101: 3005-3010.
32. Vuitton DA, Bresson-Hadni S, Laroche L, Kaiserlian D, Guerret-Stocker S, et al. (1989) Cellular immune response in Echinococcus multilocularis infection in humans. II. Natural killer cell activity and cell subpopulations in the blood and in the periparasitic granuloma of patients with alveolar echinococcosis. Clin Exp Immunol 78: 67-74.
33. Playford MC, Kamiya M (1992) Immune response to Echinococcus multilocularis infection in the mouse model: a review. Jpn J Vet Res 40: 113-130.
34. Dai WJ, Waldvogel A, Siles-Lucas M, Gottstein B (2004) Echinococcus multilocularis proliferation in mice and respective parasite 14-3-3 gene expression is mainly controlled by an alphabeta CD4 T-cell-mediated immune response. Immunology 112: 481-488.
35. Mejri N, Muller N, Hemphill A, Gottstein B (2011) Intraperitoneal Echinococcus multilocularis infection in mice modulates peritoneal CD4+ and CD8+ regulatory T cell development. Parasitol Int 60: 45-53.
36. Mejri N, Hemphill A, Gottstein B (2009) Triggering and modulation of the host-parasite interplay by Echinococcus multilocularis: a review. Parasitology 137: 557-568.
37. Sailer M, Soelder B, Allerberger F, Zaknun D, Feichtinger H, et al. (1997) Alveolar echinococcosis of the liver in a six-year-old girl with acquired immunodeficiency syndrome. J Pediatr 130: 320-323.
38. Zingg W, Renner-Schneiter EC, Pauli-Magnus C, Renner EL, van Overbeck J, et al. (2004) Alveolar echinococcosis of the liver in an adult with human immunodeficiency virus type-1 infection. Infection 32: 299-302.
39. Kern P, Gruner B, Wahlers K (2011) Diagnosis and course of echinococcocal diseases in the transplant setting. Transpl Infect Dis 13: 217-221.
40. Geyer M, Wilpert J, Wiech T, Theilacker C, Stubanus M, et al. (2010) Rapidly progressive hepatic alveolar echinococcosis in an ABO-incompatible renal transplant recipient. Transpl Infect Dis 13: 278-284.
41. Sauer A, Rochet E, Lahmar I, Brunet J, Sabou M, et al. (2013) The local immune response to intraocular Toxoplasma re-challenge: less pathology and better parasite control through Treg/Th1/Th2 induction. Int J Parasitol 43: 721-728.
42. Hubner MP, Manfras BJ, Margos MC, Eiffler D, Hoffmann WH, et al. (2006) Echinococcus multilocularis metacestodes modulate cellular cytokine and

chemokine release by peripheral blood mononuclear cells in alveolar echinococcosis patients. Clin Exp Immunol 145: 243-251.
43. Zhao H, Bai X, Nie XH, Wang JT, Wang XX, et al. (2012) [Dynamic change of IL-10 and TGF-beta1 in the liver of Echinococcus multilocularis-infected mice]. Zhongguo Ji Sheng Chong Xue Yu Ji Sheng Chong Bing Za Zhi 30: 32-35.
44. Miyara M, Sakaguchi S (2007) Natural regulatory T cells: mechanisms of suppression. Trends Mol Med 13: 108-116.
45. McGeachy MJ, Bak-Jensen KS, Chen Y, Tato CM, Blumenschein W, et al. (2007) TGF-beta and IL-6 drive the production of IL-17 and IL-10 by T cells and restrain T(H)-17 cell-mediated pathology. Nat Immunol 8: 1390-1397.
46. Michel ML, Leite-de-Moraes MC (2013) Comment on "Induced IL-17-producing invariant NKT cells require activation in presence of TGF-beta and IL-1beta". J Immunol 190: 5909-5910.
47. Shalev I, Wong KM, Foerster K, Zhu Y, Chan C, et al. (2009) The novel CD4+CD25+ regulatory T cell effector molecule fibrinogen-like protein 2 contributes to the outcome of murine fulminant viral hepatitis. Hepatology 49: 387-397.
48. Chan CW, Kay LS, Khadaroo RG, Chan MW, Lakatoo S, et al. (2003) Soluble fibrinogen-like protein 2/fibroleukin exhibits immunosuppressive properties: suppressing T cell proliferation and inhibiting maturation of bone marrow-derived dendritic cells. J Immunol 170: 4036-4044.
49. Henriques-Pons A, Olivieri BP, Oliveira GM, Daeron M, de Araujo-Jorge TC (2005) Experimental infection with Trypanosoma cruzi increases the population of CD8(+), but not CD4(+), immunoglobulin G Fc receptor-positive T lymphocytes. Infect Immun 73: 5048-5052.
50. Wang J, Lin R, Zhang W, Li L, Gottstein B, et al. (2014) Transcriptional profiles of cytokine/chemokine factors of immune cell-homing to the parasitic lesions: a comprehensive one-year course study in the liver of E. multilocularis-infected mice. PLOS ONE (in press)
51. Malbec O, Attal JP, Fridman WH, Daeron M (2002) Negative regulation of mast cell proliferation by FcgammaRIIB. Mol Immunol 38: 1295-1299.
52. Marsden PA, Ning Q, Fung LS, Luo X, Chen Y, et al. (2003) The Fgl2/fibroleukin prothrombinase contributes to immunologically mediated thrombosis in experimental and human viral hepatitis. J Clin Invest 112: 58-66.
53. Dai WJ, Gottstein B (1999) Nitric oxide-mediated immunosuppression following murine Echinococcus multilocularis infection. Immunology 97: 107-116.
54. Gottstein B (1992) Echinococcus multilocularis infection: immunology and immunodiagnosis. Adv Parasitol 31: 321-380.

Main conclusions and remarks:

1) FGL2 contributes to the outcome of infection by the metacestode.
2) FGL2 partly contributes to Treg functions.
3) FGL2 can down-regulate the maturation of DCs, suppress Th1 and Th17 immune responses, and support Th2 and Treg immune responses.
4) FGL2 contributes to the induction of B cell death.
5) IL-17A contributes to FGL2 secretion.

8. General discussion

8.1 Does *Echinococcus multilocularis* influence the surrounding liver parenchyma?

8.1.1 Influence on hepatocyte proliferation and anti-apoptosis, growth arrest and apoptosis

Changes in the metabolic pathways involved in the regulation of hepatic cell proliferation and growth arrest, and especially in the MAPKs system, have been extensively studied in infectious/ inflammatory conditions, especially of viral origin (Alexia *et al.* 2004; Wu *et al.* 2008; Ko *et al.* 2010). Before the initiation of our work, very little was known of the influence of helminth parasites which develop in the liver on the proliferation/growth arrest of the hepatocytes in the infected liver. Until recently, no study had ever specifically addressed the issue of liver proliferation/regeneration and growth arrest/apoptosis after *E. multilocularis* infection. In this longitudinal study using the murine experimental model of intra-hepatic secondary *E. multilocularis* infection, we could show that, opposite to those involved in cell proliferation and anti-apoptosis which were activated in the first half of the infection course, metabolic pathways involved in growth arrest and apoptosis were significantly activated in the liver of the infected mice in the second half of the infection course. It was shown that activation of the metabolic pathways which govern growth arrest and apoptosis also paralleled the previously described decrease of lymphocyte proliferation and of cytokine production observed at the late stage of experimental infection (Emery *et al.* 1996, 1997; Gottstein *et al.* 1994).

Hepatocytes suffering sublethal injury have the capacity to activate an internally-triggered cell regeneration mechanism and our previous studies of our team as well as this one have brought evidence that, as it also occurs during viral infection or toxic injury (Viebahn *et al.* 2008), this regeneration mechanism was also operating in *E. multilocularis* infection (Lin *et al.* 2011; Jin *et al.* 2002). It was especially prominent at the first stages of infection, as was shown in our experimental mice until day180 after infection. Liver regeneration is controlled by a wide array of signaling factors and plays a key role in recovery after acute and chronic liver injury. Hepatic cell proliferation is essential to enhance or restore hepatic function (Taub *et al.* 2004; Fausto *et al.* 2006). Although hepatocyte proliferation is often mediated by the injury/regeneration response, however, in other circumstances it is part of an adaptive response to stress stimuli which do not lead to cell death (a process called ‘direct hyperplasia’). This proliferative response is regulated by cell cycle regulated proteins (Svegliati-Baroni *et al.* 2003). In AE, influence of the parasite on hepatocyte proliferation (and/or anti-apoptosis) is supported by the up-regulation of Cyclins A,

B1, D1 and Gadd45b. Until day180, i.e. in the early and middle stages of infection, gene expression level of CyclinA was increased in a time-dependent manner, while gene expression levels of Cyclin B1 and CyclinD1 were increased up to day30 and then returned to the control level after day60. On the other hand, no significant change in the expression of Cyclin E was observed at any time during the period of observation. Up-regulation of PCNA, Cyclin D1, A and B1 is related to the regulation of the G1/S and G2/M phases (Masaki *et al.* 2003; Neuwirt *et al.* 2009), which were previously reported to increase biphasically after partial hepatectomy and other parasitic infection (Spiewak *et al.* 1997; Bouzahzah *et al.* 2006). The ‘‘late stage’’ of infection, i.e. after day180 after infection, has rarely been studied in the murine model of secondary (or primary) *E. multilocularis* infection. In the most susceptible mice, impairment of vital functions due to *E. multilocularis* progression and metastases is fast and occurs between day180 and 270, which makes studies difficult to interpret. In addition, most of the studies addressed immunological mechanisms of immune tolerance; since they were just failing at that late stage (Emery *et al.* 1996, 1997; Gottstein *et al.* 1994), it was thus considered of less interest for that purpose. As the experimental mice we are working with, albeit quite susceptible to *E. multilocularis*, have a prolonged survival until day360, and because we observed activation of both proliferation and apoptosis pathways at day180, we decided to measure the expression and/or activation of the components of these pathways until day360. We were thus able to show the mirror image of growth arrest/apoptosis versus proliferation/anti-apoptosis during the natural course of metacestode progression in the liver. These results might suggest that the proliferative capability of hepatocytes was exhausted during continuously lasting hepatic damage, due to direct toxicity of parasitic components and/or cytotoxic attacks by the immune system. This exhaustion might also be due to the profound malnutrition (wasting disease/cachexia) observed in *E. multilocularis*-infected mice in the advanced stage of the disease, and the altered ability of liver cells to synthesize proteins, as suggested by the changes in the expression of many genes found at this stage using microarray analysis we recently performed (Lin *et al.* 2011). However, during the early and middle stage of infection, despite the presence of the metacestode and its growth, very little necrosis is observed on the liver pathological sections in the experimental model; we could confirm such observations (Liance *et al.* 1984). Necrosis of the liver lesion is not observed in all patients with AE: it has only been observed in more advanced/severe cases, and was associated with susceptibility markers and/or with expression of TNF-α by the periparasitic macrophages (Bresson-Hadni *et al.* 1994). On the other hand, the immune tolerance generated by the presence of *E. multilocularis* metacestode in the liver is associated with a poor development of NK cytotoxicity and an inhibition of T-lymphocyte-dependent cytotoxicity, despite the high proliferation potential of T-

lymphocytes, the presence of numerous CD8 T-lymphocytes in the liver within the parasitic lesion, and the expression of the appropriate ligands, such as MICA/B (Bresson-Hadni *et al.* 1989, 1991; Nicod *et al.* 1994). Such an inhibition is possibly due to the combined influence of IL-10 and TGF-β production, as discussed below (Bresson-Hadni *et al.* 1990; Vuitton *et al.* 1989; Zhang *et al.* 2008).

8.1.2 Influence on the development of liver fibrosis

Fibrosis is a hallmark of AE, leading to a complete disappearance of the liver parenchyma in the periparasitic area, and to fibrosis in portal spaces. Fibrosis protects the host against the parasitic growth, but at the same time it distorts the liver parenchyma, contributes to bile duct and vessel obstruction and can lead to secondary biliary cirrhosis (Ricard-Blum *et al.* 1996; Vuitton *et al.* 1986). The irreversible acellular keloid scar-like fibrosis observed in AE is the ultimate result of cytotoxic and fibrogenetic events related to the immune response of the host which are taking place initially in the granulomatous area surrounding the young parasite larvae (Vuitton *et al.* 2003). Previous observations in experimental models of AE have suggested that progression of fibrosis in AE involves an early deposition of type III collagen pro-peptide and type III collagen at the periphery of the granulomas, and a subsequent remodeling of fibrosis with bundles of type I collagen in the periparasitic central area (Vuitton *et al.* 1986; Guerret *et al.* 1998). Stellate cell–derived myofibroblasts have been observed in AE liver, both in humans (Vuitton *et al.* 1986) and in the experimental mouse model (Guerret *et al.* 1998). It was noted that in some regions of the liver where the parenchyma was totally replaced with dead parasitic lesions and fibrosis, HSC were the only cellular remnants present (Vuitton *et al.* 1986). We confirmed that á-SMA, a specific cell marker for MFB, as well as type I and III collagens, were highly expressed in tissues surrounding AE lesions; the expression of collagen I increased steadily through the course of the infection, whereas collagen III rapidly reached its maximum level of expression at day 8; this sequence of events, which is usual in fibrotic processes (collagen III being produced quickly by fibroblasts before collagen I is synthesized) was already noticed in the first studies on AE fibrosis in the experimental model; in humans, as well as in mice at later stages, location of collagen III in areas of recent larval development supported this sequence (Vuitton *et al.* 1986; Guerret *et al.* 1998).

8.2 Factors of the influence of E. multilocularis components on the host liver

8.2.1 Innate immunity- and pro-inflammatory cytokines

The role of pro-inflammatory cytokines, and especially tumor necrosis factor (TNF-α), in the protection of the host against *E. multilocularis* has been demonstrated, and it is likely that they act at least in part through the development of fibrosis (Amiot *et al.* 1999). TNF-$\alpha^{-/-}$ mice showed faster growth and invasion of the metacestode, but also disrupted and late fibrosis, compared to the WT mice in which fibrosis appeared early and was well organized (the usual concentric bundles around the parasite vesicles) (Amiot *et al.* 1999). Indeed, dead parasites were cordoned by granulomas containing numerous macrophages and lymphocytes leading to focal liver fibrosis at an early stage of infection. In contrast, most of LT-α TNF-$\alpha^{-/-}$ mice harboured metacestodes interspersed with leucocytes, realising purulent abscesses with secondary extensive irregular fibrosis at a late stage of infection (Amiot *et al.* 1999). In human livers with hepatic AE, the mRNAs of pro-inflammatory cytokines, interleukin (IL)-1β, IL-6, and TNF-α have been found in macrophages located at the periphery of granulomas, in those areas which were shown to be at the initiation of fibrogenesis (Bresson-Hadni *et al.* 1994). IL-12, which inhibits the development of the parasitic vesicles after *E. multilocularis* infection, was also shown to induce a fast development of peri-vesicle fibrosis (Emery *et al.* 1996). Pretreatment of mice with IL-12 is extremely efficient in preventing the development of lesions and leads to abortive parasitic vesicles surrounded by fully efficient periparasitic immune cell infiltration and fibrosis (Emery *et al.* 1996). In the present study, we found that IL-12α and TNF-α were developing in parallel during the different stages of *E. multilocularis* infection. After an initial increase, IL-12α and TNF-α expression decreased dramatically after the 30th day of infection of mice. This fits well to previous findings, which had indicated a protective role against *E. multilocularis* by *in vivo* treatment with recombinant IL-12 in C57BL/6J mice (Emery *et al.* 1998). An important role of these cytokines of innate immunity in the early expression of IFN-γ is likely. Our observations also fit with the outcome of *E. multilocularis* infection in mice KO for TNF-α (Amiot *et al.* 1999); as mentioned above, such mice revealed to be extremely susceptible to the development of AE lesions. Observations in patients with AE treated with a TNF-α inhibitor (Weiner *et al.* 2011), have also shown that they had a faster and more severe course of disease, and radiological images in these patients strongly evoked liver abscesses (i.e. cell-rich lesions) rather than typical AE lesions (usually characterized by the US and CT imaging features of dense fibrosis) (Weiner *et al.* 2011). In the mouse model, IL-1β and IL-6 were then showing up, presumably to sustain the inflammatory response, with a ‘mirror’ image of their

respective increase all along infection. The initial peak of IL-6 as early as 2 days post-infection may be related to the early activation of the acute phase protein genes in the hepatocytes, disclosed by previous microarray studies (Gottstein *et al.* 2011; Lin *et al.* 2011). Conversely, the absence of a significant increase of IL-6 at day 270 probably explains why, despite increased levels of haptoglobin, α-1 acid glycoprotein, C3 and C4, and ceruloplasmin in patients with AE, no increase of C-reactive protein (CRP) levels, typically associated with IL-6 stimulation, is usually observed, except in cases complicated by bacterial infection (Vuitton, 2009). Secretion of the pro-inflammatory cytokines IL-1β and IL-18 by PBMC of AE patients had been shown to be reduced in response to *E. multilocularis* metacestode vesicles, compared to controls (Eger *et al.* 2003). In our study in mice, although IL-1β was highly expressed at the early and middle stage, it subsequently decreased at the late stage and was not significantly different from control mice at day 180 post-infection and later, a time point which may approximately represent the disease stage of most patients at diagnosis of AE. Such selective dynamics of pro-inflammatory cytokine release may both install and maintain the periparasitic immune infiltrate from the very early stage of infection on, and also limit its activation and thus participate in the tolerance process. Such a profile would characterize the "susceptible" status of an intermediate host. It may be anticipated from our results and other observations in the mouse models (especially those made after host's treatment with recombinant IL-12) that a very early and sustained expression of all cytokines of innate immunity, and especially IL-12, TNF-α and very likely IFN-α (Godot *et al*, 2003), could prevent a sustained expression of IL-4 as well as regulatory cytokines, and reinforce Th1 pathways, and would thus characterize a "resistant" profile of intermediate hosts (i.e. most of the human beings contaminated by *E. multilocularis* eggs). A significant modulation of cytokine secretion, with a significant decrease in IL-13 and increase in IFN-γ by peritoneal macrophages and spleen cells, was observed in mice treated with IFN-α from the very beginning of infection (Godot et al. 2003). This cytokine modulation was actually associated with protection against metacestode growth.

8.2.2 T helper (Th)-related cytokines and chemokines

In the periparasitic granuloma. In most previous studies, secretion and expression of cytokines, chemokines, and related factors that govern immune cell-homing to *E. multilocularis* infection site were studied in the peripheral blood of human AE patients (Aumuller *et al.* 2004), and in lymph node or spleen cells of experimentally infected mice (Dai *et al.* 2004; Bresson-Hadni *et al.* 1990; Dai & Gottstein, 1999). Attempts at enhancing Th1-related immune responses have resulted in increased resistance to *E. multilocularis* infection in experimental mice. Treatment

with IFN-γ either before or after experimental infection has been shown to be only partially effective in reducing larval growth, although it was able to moderately increase the periparasitic fibrotic process (Liance *et al.* 1998). Isolated attempts of treatment with IFN-γ in patients at a late stage of AE were no more successful than those performed in experimental mice and they could not modify host's cytokine profile significantly (Jenne *et al.* 1998). Early expression of IFN-γ, as previously shown in studies on peripheral lymphocytes, was also confirmed in our longitudinal study of the periparasitic infiltrate; we hypothesize that it was very likely induced by the early expression of IL-12. The apparent decrease in IFN-γ at day 8 may be due either to a technical artefact or, more probably, to a temporary inhibition by IL-4, also markedly expressed at days 2 and 8 p.i.. Sustained IFN-γ expression together with the permanent expression of Th1 chemokines, and its negative correlation with TGF-β1 in the parasitic lesions all along the course of infection, although Th2 and Treg cytokines are also permanently expressed, suggests that IFN-γ is very important for the persistence of the periparasitic infiltrate by permanent homing of immune cells and/or inhibition of their emigration (Vuitton *et al.* 1989; Mejri *et al.* 2006, 2011).

In the experimental model of secondary infection in mice, the levels of Th1 cytokines as well as pro-inflammatory cytokines was initially elevated, and then progressively decreased while Th2 cytokines and IL-10 increased (Emery *et al.* 1996). However, little was known on the involvement of Th17, IL-17 secreting T cells, and of IL-21, -22 and -23 in the development of immune cell infiltration around the parasitic vesicles and their relationship with immuno-regulatory cells in echinococcosis. The recruitment and presence of all potential actors of Th17-driven immune reaction in the lesions highly suggests that the IL-23/IL-21/IL-22/IL-17 pathway is actually operating in echinococcosis. In our study, IL-17, as detected by a monoclonal antibody directed against the common epitopes of the protein, was present in cells of the periparasitic infiltrate all along the course of infection; however, as far as the expression of mRNA isotypes of the cytokines is concerned, both IL-17A and IL-17F were increased at the early stage of *E. multilocularis* infection, and then decreased at the late stage; they were both positively correlated with CCL12 and CCL17; however, IL-17A exhibited a positive correlation with TNF-α, and appeared lower than even in controls, at the late stage of infection, while IL-17F was also expressed at low levels, but still higher than controls. This may indicate that IL-17A was rather protective but quickly inhibited, while IL-17F was less suppressed with time and may contribute to both protection and pathogenesis, as reported in human AE patients (Lechner *et al.* 2012).

In the distant liver. The involvement of the adjacent, not directly affected liver tissue in the immune process of *E. multilocularis*/host interaction has received little attention. Recent studies have provided evidence that the adjacent liver was fully

involved in the relationship between the parasite and its host. Our study confirms that certain mediators of the immune reaction and their receptors may also be expressed in the liver tissue, thus also in areas not directly affected by the parasite and the periparasitic granuloma. In the adjacent liver tissue, the expression of the various cytokines/chemokines was selective: not all cytokines/chemokines were expressed in the surrounding liver; some seemed to be specific for the immune cells of the periparasitic infiltrate, e.g. TNF-α, IL-17F and CCL8, which were not expressed at all in the liver. The contribution of the surrounding liver tissue, however, was quite significant for other ones, e.g. IL-12, IFN-γ, IL-4 and IL-17A, at the early stage of infection; CXCL9, IL-4, IL-5, CCL17, at the middle stage; and IL-10 and TGF-β at the late stage of infection. TGF-β receptors were also expressed in the liver parenchyma from early to late stage post *E. multilocularis* infection, suggested that the markedly elevated levels of TGF-β1 present in *E. multilocularis*-infected liver, were functional to regulate the activities of immune cells as well as hepatocytes and cells involved in fibrosis. From our study, which was performed on liver samples without cell identification, it is difficult to know if such expression was restricted to cells of the immune response present in the sinusoids/portal spaces after their homing to the liver, or was also present in autochthonous liver cells such as Kupffer cells, stellate cells, or hepatocytes. Precise identification and respective location will require appropriate further studies.

8.2.3 T regulatory cytokines

Most of the studies in AE as well as in the experimental models have first focused onto IL-10. The anti-inflammatory properties of IL-10 are well known, especially through the inhibition of macrophage activation and cytotoxic functions (Emery *et al.* 1996).

Spontaneous secretion of IL-10 by the PBMCs is the immunological hallmark of patients with progressing lesions of AE (Godot *et al.* 1997). Conversely, IL-10 is significantly lower in patients with abortive lesions (Godot *et al.* 2000). IL-10 is measurable in the serum of the patients with AE at higher concentrations than in control subjects (Wellinghausen *et al.* 1999). A variety of cell types are involved in the secretion of IL-10 by resting and stimulated PBMC in patients with AE, especially CD4 and CD8 T-cells, but also non-T non-B cells (Godot *et al.* 1997) “Suppressor” CD8 T-cells, induced by parasite products, were reported to be involved in tolerance to *E. multilocularis* (Kizaki *et al.* 1991,1993). However, the relationship between the capacity of these cells to secrete IL-10 and their “suppressor” activity is unknown. A preliminary report has confirmed that locally, in the periparasitic granuloma, T-cells secreted IL-10 and the data suggest that IL-10 production is highest closer to the

parasitic vesicles (Harraga *et al.* 2003). We could also confirm the expression of IL-10 in the periparasitic granuloma, in an experimental model and studied all along the course of infection. After experimental infection with *E. multilocularis*, IL-10 secretion by spleen cells is slightly delayed and is part of the cytokine profile observed in the second phase of *E. multilocularis* growth (Emery *et al.* 1996). Similar changes were also observed when measuring IL-10 levels in the serum of infected mice: they remained low before 80 days post-infection and then increased sharply at 100 days post-infection when they reached a peak (Wei *et al.* 2004).

The presence of TGF-β secreting cells in the periparasitic granuloma surrounding *E. multilocularis* vesicles in the liver of patients with AE has been recognised only very recently (Zhang *et al.* 2008) and exploring TGF-β in its multiple functions in *E. multilocularis* infection was still an open field of research at the initiation of our work. In the liver, chronic injury causes continuous hepatocyte destruction and TGF-β1 stimulates quiescent HSCs into activated myofibroblast-like cells, which produce extracellular matrix to retrieve lost space made by destruction of hepatic parenchymal tissue. TGF-β is a cytokine that alters many functions in nearly all higher eukaryotic cells (Derynck & Zhang, 2003; Gordon & Blobe, 2008). The nature of the TGF-β action depends on many parameters, including type and state of differentiation of the cell targets, growth conditions, and presence of other growth factors. TGF-β controls extracellular matrix production, regulation of myogenesis, immune response, angiogenesis, and embryogenesis. Hepatic stellate cells are the primary cell type responsible for matrix deposition in liver fibrosis, undergoing a process of transdifferentiation into fibrogenic myofibroblasts. These cells, which undergo a similar transdifferentiation process when cultured in vitro, are a major target of the profibrogenic agent transforming growth factor-β (TGF-β) (Liu *et al.* 2003). The multifunctional feature of TGF-β suggests that it may be an important target of viruses to influence host cell fate in favor of virus replication and proliferation.

The positive correlation we found between their expression and expression of TGF-β1, both in the experimental model and in human livers, is an indirect argument for a significant role of this cytokine in AE fibrosis. The major peak of TGF-β1 at the middle stage of infection in experimental animals, and its expression in AE patients who are diagnosed at a similar stage, suggest that although lower levels may initiate immune tolerance as early as the early stage, the cytokine becomes prominent later, when both maintenance of the tolerance state and development of fibrosis are at stake.

The Smad family of proteins mediates signaling from the TGF-β R to the nucleus. In the current study, there was an increased expression of TGF-β R, Smad3 mRNA, and especially of Smad4 which is a central mediator in TGF-β superfamily signaling

(Heldin *et al.* 1997). Our study showed that expression of Smad4 was higher in areas surrounding lesions than in distant liver in the patients with AE. Smad7, which is induced by TGF-β itself, is responsible for the fine-tuning of TGF-β signals (Itoh *et al.* 2007). It prevents the phosphorylation of Smad proteins, associates with ubiquitin ligases involved in TGF-β R-degradation, and acts as a transcriptional repressor inhibiting Smad-dependent promoter activation (Schmierer *et al.* 2007). In physiological situations, its increase decreases the phosphorylation of Smad2/3, and thus decreases TGF-β functions. In chronic hepatic injury, the expression of Smad7 is paradoxically decreased (Del Pilar Alatorre-Carranza *et al.* 2009); as a result, TGF-β signal transduction cannot be effectively inhibited, and TGF-β functions are enhanced. An aberrant expression of Smad7 may thus disrupt the balanced activity of TGF-β under pathophysiological conditions. The low expression of Smad7 in the areas surrounding the lesions and its negative correlation with α-SMA and Collagen III highly suggest that in AE too the normal feed-back loop might not work properly, and that fibrosis might be permanently activated through that mechanism. As TGF-β is likely to be crucial to maintain the immune tolerance state and Treg generation/function essential to the parasite, *E. multilocularis* could be responsible for the paradoxical decrease of Smad7 in the periparasitic granuloma and nearby liver; this might be one of the mechanisms for the early induction of immune tolerance and for the progression from chronic hepatic injury to hepatic fibrosis during *E. multilocularis* infection.

E. multilocularis metacestode is sensitive to TGF-β signaling (Brehm, 2010; Vuitton & Gottstein, 2010; Zavala-Gongora *et al.*, 2008) and the metacestode ERK-like kinase, EmMPK1, phosphorylates EmSmadD, a metacestode analogue of the Co-Smads of the TGF-beta signaling cascade (Brehm, 2010). Our preliminary investigations of TGF-β in the host liver confirm the pivotal role that this cytokine might play in the proliferation process but also in the development of liver fibrosis, while ensuring parasite tolerance by the host. It will be of great interest to determine the mechanism used by *E.multilocularis* to trigger TGF-β signaling, whether that is the pathway that leads to G1 arrest, the pathway that initiates extracellular matrix deposition, or both. Ascertaining these problems are not just of academic interest, for an *E.multilocularis*-specified activation of the TGF-β pathway might underlie responses such as immunosuppression (Dai *et al.*, 2003; Emery *et al.*, 1996; Gottstein *et al.*, 2006) and abnormal extracellular matrix deposition (Bresson-Hadni *et al.*, 1998; Grenard *et al.*, 2001; Guerret *et al.*, 1998), each of them a dominant feature in human and animal intermediate hosts.

8.2.4 Cytokine and chemokine receptors

Expression of any stimulating/inhibiting factor is necessary but not sufficient to give evidence of their role/influence on cells. Giving evidence for the expression of the appropriate receptors is also important, albeit rarely done. Among cytokine receptors, only those for IL-1 (IL-R1 like), IL-7, IL-13 (IL-13 Rα1) and IL-17 (IL-17 R) were up-regulated when we studied them by using microarray; those for TGF-β (TGF-β RI and RII) were also up-regulated when studied by both qRT-PCR and immunohistochemisty. This indirectly suggests that the liver was affected by at least one pro-inflammatory cytokine (IL-1) and one growth factor (IL-7), by two types of Th-cytokines (Th2 and Th17), and by TGF-β. Such up-regulation of several cytokine and chemokine genes, in both models of AE, in the liver itself and not only within the periparasitic granuloma, confirms that the surrounding liver is fully involved in a process which was long considered to be a localized "tumor-like" event. However, absence of expression of the IL-6 receptor on hepatocytes is somehow puzzling, since IL-6 is directly related to the stimulation of acute phase protein synthesis by the hepatocytes, and using the microarray technique, genes for such proteins were among those most hyper-expressed in the liver. Additional studies using qRT-PCR should help us determine if this was or not due to technical or bio-informatics issues.

8.2.5. Direct influence by **E. multilocularis** *metacestode components?*

Metacestode surface molecules as well as excretory/secretory (E/S) metabolic products are considered to function as important key players to influence host immune response (Gottstein & Hemphill, 2008). The *E. multilocularis* metacestode actively secretes or expresses molecules that putatively have potent effects on the immune system of the murine host, including DCs and other immunologically relevant populations such as macrophages (M Ø), lymphocytes and other (inflammatory) cells that play a significant role in the putative control of (or respective failure to control) metacestode proliferation, and thus triggering of disease development. Carbohydrate components of the laminated layer, such as Em2 (G11) and Em492, as well as other parasite metabolites yield immunomodulatory effects that allow the parasite to survive in the host. The IgG response to the Em2 (G11)-antigen takes place independently of alpha-beta$^+$ CD4$^+$ T cells, and in the absence of interactions between CD40 and CD40 ligand (Dai *et al.* 2001). Such parasite molecules also interfere with antigen presentation and cell activation, leading to a mixed Th1/Th2-type response, not only at the late stage of infection, as was anticipated in the past, but from the very beginning of infection as we could show in our studies. Furthermore, Em492 (*Walker*

et al. 2004) as a purified parasite metabolite suppresses ConA and antigen-stimulated spleen cell proliferation.

Interesting insights into immunomodulation by the parasite were obtained with regard to human AE. *E. multilocularis* antigens (metacestode culture supernatant) depressed the release of the proinflammatory cytokine IL-12 by PBMC in response to lipopolysaccharide (LPS). This was accompanied by an increased number of $CD4^+CD25^+$ cells and a reduced release of the Th2 type chemokine CCL17 (thymus and activation regulated chemokine, TARC), suggesting an anti-inflammatory response to the metacestode in human AE patients (Hübner et al. 2006). Instead, the production of IFN-γ and the expression of CD28 on $CD4^+$ T cells were increased in PBMC from AE patients when compared to controls. This was accompanied by a higher release of the Th2-type chemokine CCL22 (macrophage derived chemokine, MDC) supporting that *E. multilocularis* also generates proinflammatory immune responses. These results indicate that *E. multilocularis* antigens modulated both, regulatory and inflammatory, Th1 and Th2 cytokines and chemokines. In a previous study by our team, a significant influence of *E. multilocularis* metacestode on the activation of MAPKs signalling pathways was found in the liver cells both *in vivo* in infected patients and *in vitro* in cultured rat hepatocytes (Lin *et al.* 2009). In preliminary *in vitro* studies (unpublished data) we observed a secretion of TGF-β1 and an activation of the TGF-β pathway in rat hepatocyte cultures incubated with vesicle fluid of parasitic origin, in the absence of inflammatory cells, thus of immune cell-related cytokines. A recent study has also provided evidence for the induction of apoptosis in host DC through E/S-products of early infectious stages of *E. multilocularis* (Nono *et al.* 2012). The parasite might thus influence signaling mechanisms of host cells through the secretion of various molecules which might bind to host cell surface receptors or to the temporary storage of host-derived molecules in the vesicle fluid. Such interactions could contribute to immunomodulatory activities of *E. multilocularis*, to pathological consequences on the host's tissues, and/or be involved in mechanisms of organotropism (Zhang *et al.* 2008). These observations suggest that parasitic components, and not only factors from host origin, are actually acting on the host.

It has also been shown, conversely, that the metacestode development in the murine liver is triggered by cell signaling originating from the intermediate host (Brehm *et al.* 2006). The phosphorylation of EmMPK1, a parasitic orthologue of the extracellular signal-regulated kinase (ERK) MAPK, is specifically induced in *in vitro* cultured *E. multilocularis* metacestode vesicles, in response to exogenous host serum, hepatic cells and/or human epidermal growth factor (EGF). The fact the intrahepatic

metacestode expresses signaling systems with significant homologies to those of the host raises the interesting question whether cross-communication between cytokines and corresponding receptors of host and parasite can occur during an infection, i.e. whether the parasite may also influence signaling mechanisms of host cells through the secretion of various molecules that might bind to host cell surface receptors. Such interactions could contribute to immunomodulatory activities of *E. multilocularis* or be involved in mechanisms of organotropism and/or in host tissue destruction or regeneration during parasitic development. This reinforces the hypothesis of a ‘‘cross-talk’’ between the parasitic larva and its host. The larval development of *E. multilocularis* might be triggered by cell signaling originating from the intermediate host (Spiliotis *et al.* 2006; Gelmedin *et al.* 2008), *E. multilocularis* metacestode being able to ‘‘sense’’ host factors, which may result in an activation of the parasite metabolic pathway cascades (Brehm *et al.* 2006).

8.3 FGL2 : a new and key-actor of the tolerance against *E. multilocularis* ?

Various molecular and cellular events have been proposed to explain the mechanism by which Tregs suppress immune responses. These include cell-to-cell contact-dependent suppression, cytotoxicity, and immunosuppressive cytokine secretion (Miyara *et al.* 2007). It is generally considered that anti-inflammatory cytokines, such as IL-10 and TGF-β, are important co-mediators of Treg activity *in vivo* (Miyara *et al.* 2007). However, the importance of these cytokines remains controversial, as several reports have demonstrated that antibodies against IL-10 and TGF-β fail to block Treg suppressive function. Also, Tregs from TGF-β–deficient mice have normal suppressive activity *in vitro* and can prevent development of autoimmune disease (Miyara *et al.* 2007). In addition, the ambiguous role of TGF-β, which is both a strong inducer of immune tolerance and an activator of the pro-inflammatory IL-17 cytokine system, remains puzzling (McGeachy *et al.* 2007; Michel *et al.* 2013).

Recently, it was reported that Tregs had increased expression of FGL2 encoding mRNA, and it was suggested that FGL2 might be an important Treg effector molecule (Shalev *et al.* 2009). In a previous explorative study, *fgl2* gene expression was found significantly increased in the periparasitic liver tissue of mice perorally infected with *E.multilocularis* eggs (Gottstein *et al.* 2011). Our resulting working hypothesis was thus that FGL2, with important roles in both innate and adaptive immunity, similar to other members of the fibrinogen-like family of proteins which include tenascin and angiopoietin, could be another key-actor in *E. multilocularis*-host interactions, unknown until now. In this study, we demonstrated experimentally that recombinant FGL2 suppressed T cell proliferation in response to Con A and to *E. multilocularis*

components present in the VF. FGL2 also inhibited maturation of dendritic cells (DCs), suppressed Th1 and Th17 immune responses, and polarized an allogeneic immune response toward a Th2-oriented cytokine profile, both *in vivo* and *in vitro*. Conversely, in $fgl2^{-/-}$ mice, Th1 cytokine levels and activity of DCs, B- and T cells were all increased. FGL2 serum levels correlated with IL-4 expression in wild type mice before and after *E.multilocularis* infection, suggesting a close relationship between FGL2 and Th2-related immune response. The development of a Th2 immune response in wild type mice after *E.multilocularis* infection fitted with the demonstrated effect of FGL2 to promote Th2 cytokine production with a subsequent inhibition of Th1 and Th17 immunity. Furthermore, serum levels of IL-17A showed a positive correlation with FGL2 serum expression, suggesting for the first time that IL-17A could contribute to FGL2 secretion. This was confirmed *in vitro*, in that recombinant IL-17A promoted the production of FGL2 in spleen cells, while anti-IL-17A blocked respective FGL2 secretion.

The mechanism by which FGL2 mediates its immunosuppressive activity is currently under intense investigation. Recent data have demonstrated that FGL2 binds to the inhibitory FcγRIIB receptor (CD32) expressed primarily on APCs. This FGL2-FcγRIIB interaction was shown to induce B cell apoptosis and inhibit DC maturation (Liu *et al.* 2008). In *E. multilocularis* infection, several cell types may express the inhibitory FcγRIIB, such as macrophages (including the 'epithelioid cells' that line the 'immuno-modulating' laminated layer), and also the numerous CD8 T cells present in the periparasitic infiltrate; CD8 T cells have actually been shown to express this receptor in a murine model of *Trypanosoma cruzi* (Henriques-Pons *et al.* 2005). Combined with the course of cytokine expression by the periparasitic immune infiltrate in *E.multilocularis* infection, our data suggest that, under the influence of *E. multilocularis* components (a) IL-6, TNF-α, IFN-γ and IL-17 are released; (b) these, especially IFN-γ as demonstrated previously (Hancock *et al.* 2004), but also IL-17A as we showed in this study, contribute to FGL2 secretion by Tregs and other cells;(c) once FGL2 is released, it can bind to FcγRIIB receptor, down-regulate the maturation of DCs, decrease co-stimulation of effector T cells, suppress Th1 and Th17 immune response, accelerate Th2 immune responses, induce apoptosis of B cells, and thus overall lead to an immune suppressed status that favours the continuous "tumour-like" progression of the parasitic metacestode tissue. Direct inhibition of macrophage and/or mast cell functions could also be induced by such a binding (Malbec *et al.* 2002).

8.4 Conclusion and perspectives

Taken together, the results obtained from our various experimental models and designs confirmed that *E. multilocularis* metacestode definitely exerts a deep influence on liver homeostasis through the immune response/immune tolerance. Our data support the concept, which was part of our working hypothesis, of a sequential activation of metabolic pathways which would first favor parasitic, liver and immune cell proliferation and survival, and thus promote metacestode fertility and tolerance by the host; and would then favor liver damage/apoptosis, impairment in protein synthesis and xenobiotic metabolism, as well as immune deficiency, and thus contribute to the dissemination of the protoscoleces after metacestode fertility has been acquired. The periparasitic infiltration by inflammatory cells is a key-player in cytokine/chemokine secretion and functional activities within the host-parasite interactions. However, the surrounding liver is also involved in the cross-talk between the parasite and its host. TGF-β and FGL2 and their fine turning by the various isotypes of IL-17 could determine the overall balance between tolerance towards the parasite and protection of the host and thus contribute to the outcome of *E. multilocularis* infection. Our study confirm stage-related homing and functions of immune cells around the metacestode which may explain the observed relationship between metacestode viability and uptake of tracers such as FDG by the periparasitic infiltrate. The next step of our work is thus more focused on applications for patients with AE. To further study the relationship between FDG-PET imaging and the course of the periparasitic granuloma, and between the metabolic activity of the granuloma and the viability of the metacestode, we are developing the use of micro-PET in infected mice, as well as pre-clinical models including various imaging techniques and immunological follow-up in rats and pigs. In addition, as preliminary results highly suggest that FGL2 could be a serum marker of progression in the patients with AE, our aim is now to check if there is any correlation between FGL2 serum levels and the metabolic activity of the periparasitic cells, i.e. with their FDG uptake at PET imaging in the patients with AE. Such studies and the results obtained in this thesis may also contribute to identify new targets for possible immune therapy to minimize *E. multilocularis*-related pathology and to complement the ‘parasitostatic-only’ effect of benzimidazoles in AE.

References

Abbas AK, Murphy KM, Sher A (1996) Functional diversity of helper T lymphocytes. Nature 383: 787-793.

Acharya SS, Dimichele DM (2008) Rare inherited disorders of fibrinogen. Haemophilia 14: 1151-1158.

Aleffi S, Petrai I, Bertolani C, Parola M, Colombatto S, et al. (2005) Upregulation of proinflammatory and proangiogenic cytokines by leptin in human hepatic stellate cells. Hepatology 42: 1339-1348.

Ali-Khan Z, Siboo R (1981) Echinococcus multilocularis: distribution and persistence of specific host immunoglobulins on cysts membranes. Exp Parasitol 51: 159-168.

Allen JT, Spiteri MA (2002) Growth factors in idiopathic pulmonary fibrosis: relative roles. Respir Res 3: 13

Allred DR (1995) Immune evasion by Babesia bovis and Plasmodium falciparum: cliff-dwellers of the parasite world. Parasitol Today 11: 100-1057.

Altieri P, Caridi G, Ghiggeri GM, Garberi A, Ginevri F, et al. (1995) Regulation by TGF-beta and bFGF of ECM expression by PKD cells 'in culture'. Contrib Nephrol 115: 122-126.

Amiot F, Vuong P, Defontaines M, Pater C, Dautry F, et al. (1999) Secondary alveolar echinococcosis in lymphotoxin-alpha and tumour necrosis factor-alpha deficient mice: exacerbation of Echinococcus multilocularis larval growth is associated with cellular changes in the periparasitic granuloma. Parasite Immunol 21: 475-483.

Amri M, Mezioug D, Touil-Boukoffa C (2009) Involvement of IL-10 and IL-4 in evasion strategies of Echinococcus granulosus to host immune response. Eur Cytokine Netw 20: 63-68.

Anscher MS, Peters WP, Reisenbichler H, Petros WP, Jirtle RL (1993) Transforming growth factor beta as a predictor of liver and lung fibrosis after autologous bone marrow transplantation for advanced breast cancer. N Engl J Med 328: 1592-1598

Anthony B, Mathieson W, de Castro-Borges W, Allen J (2010) Schistosoma mansoni: egg-induced downregulation of hepatic stellate cell activation and fibrogenesis. Exp Parasitol 124: 409-420.

Aoyama Y, Urushiyama S, Yamada M, Kato C, Ide H, et al. (2004) MFB-1, an F-box-type ubiquitin ligase, regulates TGF-beta signalling. Genes Cells 9: 1093-1101.

Aumuller E, Schramm G, Gronow A, Brehm K, Gibbs BF, et al. (2004) Echinococcus multilocularis metacestode extract triggers human basophils to release interleukin-4. Parasite Immunol 26: 387-395.

Bakkebo M, Huse K, Hilden VI, Smeland EB, Oksvold MP (2010) TGF-beta-induced growth inhibition in B-cell lymphoma correlates with Smad1/5 signalling and constitutively active p38 MAPK. BMC Immunol 11: 57.

Balko JM, Schwarz LJ, Bhola NE, Kurupi R, Owens P, et al. (2013) Activation of MAPK pathways due to DUSP4 loss promotes cancer stem cell-like phenotypes in basal-like breast cancer. Cancer Res.

Banas MC, Parks WT, Hudkins KL, Banas B, Holdren M, et al. (2007) Localization of TGF-beta signaling intermediates Smad2, 3, 4, and 7 in developing and mature human and mouse kidney. J Histochem Cytochem 55: 275-285.

Bartram U, Speer CP (2004) The role of transforming growth factor beta in lung development and disease. Chest 125: 754-765.

Beeson JG, Reeder JC, Rogerson SJ, Brown GV (2001) Parasite adhesion and immune evasion in placental malaria. Trends Parasitol 17: 331-337.

Belkaid Y, Sun CM, Bouladoux N (2006) Parasites and immunoregulatory T cells. Curr Opin Immunol 18: 406-412.

Bhargava R, Janssen W, Altmann C, Andres-Hernando A, Okamura K, et al. (2013) Intratracheal IL-6 protects against lung inflammation in direct, but not indirect, causes of acute lung injury in mice. PLoS One 8: e61405.

Blader IJ, Saeij JP (2009) Communication between Toxoplasma gondii and its host: impact on parasite growth, development, immune evasion, and virulence. APMIS 117: 458-476.

Bogdan C, Rollinghoff M (1998) The immune response to Leishmania: mechanisms of parasite control and evasion. Int J Parasitol 28: 121-134.

Bohm E, Sturm GJ, Weiglhofer I, Sandig H, Shichijo M, et al. (2004) 11-Dehydro-thromboxane B2, a stable thromboxane metabolite, is a full agonist of chemoattractant receptor-homologous molecule expressed on TH2 cells (CRTH2) in human eosinophils and basophils. J Biol Chem 279: 7663-7670.

Brehm K (2010) The role of evolutionarily conserved signalling systems in Echinococcus multilocularis development and host-parasite interaction. Med Microbiol Immunol 199: 247-259.

Brehm K (2010) Echinococcus multilocularis as an experimental model in stem cell research and molecular host-parasite interaction. Parasitology 137: 537-555.

Brehm K, Spiliotis M, Zavala-Gongora R, Konrad C, Frosch M (2006) The molecular mechanisms of larval cestode development: first steps into an unknown world. Parasitol Int 55 Suppl: S15-21.

Bresson-Hadni S, Liance M, Meyer JP, Houin R, Bresson JL, et al. (1990) Cellular immunity in experimental Echinococcus multilocularis infection. II. Sequential and comparative phenotypic study of the periparasitic mononuclear cells in resistant and sensitive mice. Clin Exp Immunol 82: 378-383.

Bresson-Hadni S, Petitjean O, Monnot-Jacquard B, Heyd B, Kantelip B, et al. (1994) Cellular localisations of interleukin-1 beta, interleukin-6 and tumor necrosis factor-alpha mRNA in a parasitic granulomatous disease of the liver, alveolar echinococcosis. Eur Cytokine Netw 5: 461-468.

Brumlik MJ, Wei S, Finstad K, Nesbit J, Hyman LE, et al. (2004) Identification of a novel mitogen-activated protein kinase in Toxoplasma gondii. Int J Parasitol 34: 1245-1254.

Brumlik MJ, Wei S, Finstad K, Nesbit J, Hyman LE, et al. (2004) Identification of a novel mitogen-activated protein kinase in Toxoplasma gondii. Int J Parasitol 34: 1245-1254.

Brunet LR, Kopf MA, Pearce EJ (1999) Schistosoma mansoni: IL-4 is necessary for concomitant immunity in mice. J Parasitol 85: 734-736.

Caoduro C, Porot C, Vuitton DA, Bresson-Hadni S, Grenouillet F, et al. (2013) The role of delayed 18F-FDG PET imaging in the follow-up of patients with alveolar echinococcosis. J Nucl Med 54: 358-363.

Chang NS (2000) TGF-beta-induced matrix proteins inhibit p42/44 MAPK and JNK activation and suppress TNF-mediated IkappaBalpha degradation and NF-kappaB nuclear translocation in L929 fibroblasts. Biochem Biophys Res Commun 267: 194-200.

Chen HY, Huang XR, Wang W, Li JH, Heuchel RL, et al. (2010) The protective role of Smad7 in diabetic kidney disease: mechanism and therapeutic potential. Diabetes 60: 590-601.

Chen M, Wang GJ, Diao Y, Xu RA, Xie HT, et al. (2005) Adeno-associated virus mediated interferon-gamma inhibits the progression of hepatic fibrosis in vitro and in vivo. World J Gastroenterol 11: 4045-4051.

Chen MM, Bird MD, Zahs A, Deburghgraeve C, Posnik B, et al. (2013) Pulmonary inflammation after ethanol exposure and burn injury is attenuated in the absence of IL-6. Alcohol 47: 223-229.

Cheng RJ, Deng WG, Niu CB, Li YY, Fu Y (2011) Expression of macrophage migration inhibitory factor and CD74 in cervical squamous cell carcinoma. Int J Gynecol Cancer 21: 1004-1012.

Cheng X, Gao W, Dang Y, Liu X, Li Y, et al. (2013) Both ERK/MAPK and TGF-Beta/Smad Signaling Pathways Play a Role in the Kidney Fibrosis of Diabetic Mice Accelerated by Blood Glucose Fluctuation. J Diabetes Res 2013: 463740.

Chung AC, Dong Y, Yang W, Zhong X, Li R, et al. (2012) Smad7 suppresses renal fibrosis via altering expression of TGF-beta/Smad3-regulated microRNAs. Mol Ther 21: 388-398.

Corchero J, Martin-Partido G, Dallas SL, Fernandez-Salguero PM (2004) Liver portal fibrosis in dioxin receptor-null mice that overexpress the latent transforming growth factor-beta-binding protein-1. Int J Exp Pathol 85: 295-302.

Correa-Oliveira R, Malaquias LC, Falcao PL, Viana IR, Bahia-Oliveira LM, et al. (1998) Cytokines as determinants of resistance and pathology in human Schistosoma mansoni infection. Braz J Med Biol Res 31: 171-177.

Cowan J, Pandey S, Filion LG, Angel JB, Kumar A, et al. (2012) Comparison of interferon-gamma-, interleukin (IL)-17- and IL-22-expressing CD4 T cells, IL-22-expressing granulocytes and proinflammatory cytokines during latent and active tuberculosis infection. Clin Exp Immunol 167: 317-329.

Crispin JC, Martinez A, Alcocer-Varela J (2003) Quantification of regulatory T cells in patients with systemic lupus erythematosus. J Autoimmun 21: 273-276.

Dai WJ, Gottstein B (1999) Nitric oxide-mediated immunosuppression following murine Echinococcus multilocularis infection. Immunology 97: 107-116.
Dai WJ, Waldvogel A, Siles-Lucas M, Gottstein B (2004) Echinococcus multilocularis proliferation in mice and respective parasite 14-3-3 gene expression is mainly controlled by an alphabeta CD4 T-cell-mediated immune response. Immunology 112: 481-488.
Damian RT (1997) Parasite immune evasion and exploitation: reflections and projections. Parasitology 115 Suppl: S169-175.
Daroqui MC, Vazquez P, Bal de Kier Joffe E, Bakin AV, Puricelli LI (2012) TGF-beta autocrine pathway and MAPK signaling promote cell invasiveness and in vivo mammary adenocarcinoma tumor progression. Oncol Rep 28: 567-575.
Del Pilar Alatorre-Carranza M, Miranda-Diaz A, Yanez-Sanchez I, Pizano-Martinez O, Hermosillo-Sandoval JM, et al. (2009) Liver fibrosis secondary to bile duct injury: correlation of Smad7 with TGF-beta and extracellular matrix proteins. BMC Gastroenterol 9: 81.
Delisle JS, Giroux M, Boucher G, Landry JR, Hardy MP, et al. (2013) The TGF-beta-Smad3 pathway inhibits CD28-dependent cell growth and proliferation of CD4 T cells. Genes Immun 14: 115-126.
Dreweck CM, Soboslay PT, Schulz-Key H, Gottstein B, Kern P (1999) Cytokine and chemokine secretion by human peripheral blood cells in response to viable Echinococcus multilocularis metacestode vesicles. Parasite Immunol 21: 433-438.
Eger A, Kirch A, Manfras B, Kern P, Schulz-Key H, et al. (2003) Pro-inflammatory (IL-1beta, IL-18) cytokines and IL-8 chemokine release by PBMC in response to Echinococcus multilocularis metacestode vesicles. Parasite Immunol 25: 103-105.
Eiermann TH, Bettens F, Tiberghien P, Schmitz K, Beurton I, et al. (1998) HLA and alveolar echinococcosis. Tissue Antigens 52(2):124-9.
Emery I, Liance M, Deriaud E, Vuitton DA, Houin R, et al. (1996) Characterization of T-cell immune responses of Echinococcus multilocularis-infected C57BL/6J mice. Parasite Immunol 18: 463-472.
Emery I, Leclerc C, Sengphommachanh K, Vuitton DA, Liance M (1998) In vivo treatment with recombinant IL-12 protects C57BL/6J mice against secondary alveolar echinococcosis. Parasite Immunol 20: 81-91.
Epping K, Brehm K (2011) Echinococcus multilocularis: molecular characterization of EmSmadE, a novel BR-Smad involved in TGF-beta and BMP signaling. Exp Parasitol 129: 85-94.
Falk P, Angenete E, Bergstrom M, Ivarsson ML (2013) TGF-beta1 promotes transition of mesothelial cells into fibroblast phenotype in response to peritoneal injury in a cell culture model. Int J Surg.
Faure-Andre G, Vargas P, Yuseff MI, Heuze M, Diaz J, et al. (2008) Regulation of dendritic cell migration by CD74, the MHC class II-associated invariant chain. Science 322: 1705-1710.

Feng M, Wang Q, Zhang F, Lu L (2011) Ex vivo induced regulatory T cells regulate inflammatory response of Kupffer cells by TGF-beta and attenuate liver ischemia reperfusion injury. Int Immunopharmacol 12: 189-196.

Feng XH, Lin X, Derynck R (2000) Smad2, Smad3 and Smad4 cooperate with Sp1 to induce p15(Ink4B) transcription in response to TGF-beta. EMBO J 19: 5178-5193.

Fink SP, Mikkola D, Willson JK, Markowitz S (2003) TGF-beta-induced nuclear localization of Smad2 and Smad3 in Smad4 null cancer cell lines. Oncogene 22: 1317-1323.

Fraser D (2007) SMAD7: at the interface of TGF-beta and proinflammatory signaling. Perit Dial Int 27: 523-525.

Friedman SL (2000) Molecular regulation of hepatic fibrosis, an integrated cellular response to tissue injury. J Biol Chem 275: 2247-2250.

Fujino S, Andoh A, Bamba S, Ogawa A, Hata K, et al. (2003) Increased expression of interleukin 17 in inflammatory bowel disease. Gut 52: 65-70.

Fujisawa T, Kato Y, Atsuta J, Terada A, Iguchi K, et al. (2000) Chemokine production by the BEAS-2B human bronchial epithelial cells: differential regulation of eotaxin, IL-8, and RANTES by TH2- and TH1-derived cytokines. J Allergy Clin Immunol 105: 126-133.

Ganeshan K, Johnston LK, Bryce PJ (2013) TGF-beta1 limits the onset of innate lung inflammation by promoting mast cell-derived IL-6. J Immunol 190: 5731-5738.

Gasperini S, Marchi M, Calzetti F, Laudanna C, Vicentini L, et al. (1999) Gene expression and production of the monokine induced by IFN-gamma (MIG), IFN-inducible T cell alpha chemoattractant (I-TAC), and IFN-gamma-inducible protein-10 (IP-10) chemokines by human neutrophils. J Immunol 162: 4928-4937.

Gelmedin V, Caballero-Gamiz R, Brehm K (2008) Characterization and inhibition of a p38-like mitogen-activated protein kinase (MAPK) from Echinococcus multilocularis: antiparasitic activities of p38 MAPK inhibitors. Biochem Pharmacol 76: 1068-1081.

Godot V, Harraga S, Beurton I, Deschaseaux M, Sarciron E, et al. (2000) Resistance/susceptibility to Echinococcus multilocularis infection and cytokine profile in humans. I. Comparison of patients with progressive and abortive lesions. Clin Exp Immunol 121: 484-490.

Godot V, Harraga S, Beurton I, Tiberghien P, Sarciron E, et al. (2000) Resistance/susceptibility to Echinococcus multilocularis infection and cytokine profile in humans. II. Influence of the HLA B8, DR3, DQ2 haplotype. Clin Exp Immunol 121(3):491-8.

Godot V, Harraga S, Podoprigora G, Liance M, Bardonnet K, et al. (2003) IFN alpha-2a protects mice against a helminth infection of the liver and modulates immune responses. Gastroenterology 124: 1441-1450.

Godot V, Arock M, Garcia G, Capel F, Flys C, et al. (2007) H4 histamine receptor mediates optimal migration of mast cell precursors to CXCL12. J Allergy Clin Immunol 120: 827-834.

Gottstein B, Wittwer M, Schild M, Merli M, Leib SL, et al. (2011) Hepatic gene expression profile in mice perorally infected with Echinococcus multilocularis eggs. PLoS One 5: e9779.

Grenard P, Bresson-Hadni S, El Alaoui S, Chevallier M, Vuitton DA, et al. (2001) Transglutaminase-mediated cross-linking is involved in the stabilization of extracellular matrix in human liver fibrosis. J Hepatol 35: 367-375.

Guerret S, Vuitton DA, Liance M, Pater C, Carbillet JP (1998) Echinococcus multilocularis: relationship between susceptibility/resistance and liver fibrogenesis in experimental mice. Parasitol Res 84: 657-667.

Guilmot A, Bosse J, Carlier Y, Truyens C (2013) Monocytes play an IL-12-dependent crucial role in driving cord blood NK cells to produce IFN-g in response to Trypanosoma cruzi. PLoS Negl Trop Dis 7: e2291.

Harraga S, Godot V, Bresson-Hadni S, Pater C, Beurton I, et al. (1999) Clinical efficacy of and switch from T helper 2 to T helper 1 cytokine profile after interferon alpha2a monotherapy for human echinococcosis. Clin Infect Dis 29: 205-206.

Harraga S, Godot V, Bresson-Hadni S, Mantion G, Vuitton DA (2003) Profile of cytokine production within the periparasitic granuloma in human alveolar echinococcosis. Acta Trop 85: 231-236.

Heldin CH, Miyazono K, ten Dijke P (1997) TGF-beta signalling from cell membrane to nucleus through SMAD proteins. Nature 390: 465-471.

Herrera B, Fernandez M, Benito M, Fabregat I (2002) cIAP-1, but not XIAP, is cleaved by caspases during the apoptosis induced by TGF-beta in fetal rat hepatocytes. FEBS Lett 520: 93-96.

Hicks DJ, Nunez A, Banyard AC, Williams A, Ortiz-Pelaez A, et al. (2013) Differential Chemokine Responses in the Murine Brain Following Lyssavirus Infection. J Comp Pathol.

Hubner MP, Manfras BJ, Margos MC, Eiffler D, Hoffmann WH, et al. (2006) Echinococcus multilocularis metacestodes modulate cellular cytokine and chemokine release by peripheral blood mononuclear cells in alveolar echinococcosis patients. Clin Exp Immunol 145: 243-251.

Issa R, Williams E, Trim N, Kendall T, Arthur MJ, et al. (2001) Apoptosis of hepatic stellate cells: involvement in resolution of biliary fibrosis and regulation by soluble growth factors. Gut 48: 548-557.

Ito Y, Sarkar P, Mi Q, Wu N, Bringas P, Jr., et al. (2001) Overexpression of Smad2 reveals its concerted action with Smad4 in regulating TGF-beta-mediated epidermal homeostasis. Dev Biol 236: 181-194.

Jenne L, Kilwinski J, Scheffold W, Kern P (1997) IL-5 expressed by CD4+ lymphocytes from Echinococcus multilocularis-infected patients. Clin Exp Immunol 109: 90-97.

Jenne L, Kilwinski J, Radloff P, Flick W, Kern P (1998) Clinical efficacy of and immunologic alterations caused by interferon gamma therapy for alveolar echinococcosis. Clin Infect Dis 26: 492-494.

Ji X, Li J, Xu L, Wang W, Luo M, et al. (2013) IL4 and IL-17A provide a Th2/Th17-polarized inflammatory milieu in favor of TGF-beta1 to induce bronchial epithelial-mesenchymal transition (EMT). Int J Clin Exp Pathol 6: 1481-1492.

Johnson A, Dipietro LA (2013) Apoptosis and angiogenesis: an evolving mechanism for fibrosis. FASEB J.

Kamiya Y, Miyazono K, Miyazawa K (2010) Smad7 inhibits transforming growth factor-beta family type i receptors through two distinct modes of interaction. J Biol Chem 285: 30804-30813.

Karam MC, Merckbawi R, El-Kouba JE, Bazzi SI, Bodman-Smith KB (2013) In Leishmania major-induced inflammation, interleukin-13 reduces hyperalgesia, down-regulates IL-1beta and up-regulates IL-6 in an IL-4 independent mechanism. Exp Parasitol 134: 200-205.

Kassis AI, Tanner CE (1977) Host serum proteins in Echinococcus multilocularis: complement activation via the classical pathway. Immunology 33: 1-9.

Kern P. (2010) Clinical features and treatment of alveolar echinococcosis. Curr Opin Infect Dis 23(5):505-12.

Kim SI, Kwak JH, Zachariah M, He Y, Wang L, et al. (2007) TGF-beta-activated kinase 1 and TAK1-binding protein 1 cooperate to mediate TGF-beta1-induced MKK3-p38 MAPK activation and stimulation of type I collagen. Am J Physiol Renal Physiol 292: F1471-1478.

Kocherscheidt L, Flakowski AK, Gruner B, Hamm DM, Dietz K, et al. (2008) Echinococcus multilocularis: inflammatory and regulatory chemokine responses in patients with progressive, stable and cured alveolar echinococcosis. Exp Parasitol 119: 467-474.

Kroetz DN, Deepe GS (2011) The role of cytokines and chemokines in Histoplasma capsulatum infection. Cytokine.

Ladero JM, Fernandez-Arquero M, Tudela JI, Agundez JA, Diaz-Rubio M, et al. (2002) Single nucleotide polymorphisms and microsatellite alleles of tumor necrosis factor alpha and interleukin-10 genes and the risk of advanced chronic alcoholic liver disease. Liver 22: 245-251.

Lechner CJ, Gruner B, Huang X, Hoffmann WH, Kern P, et al. (2012) Parasite-specific IL-17-type cytokine responses and soluble IL-17 receptor levels in Alveolar Echinococcosis patients. Clin Dev Immunol 2012: 735342.

Liance M, Ricard-Blum S, Emery I, Houin R, Vuitton DA (1998) Echinococcus multilocularis infection in mice: in vivo treatment with a low dose of IFN-gamma decreases metacestode growth and liver fibrogenesis. Parasite 5: 231-237.

Lin RY, Wang JH, Lu XM, Zhou XT, Mantion G, et al. (2009) Components of the mitogen-activated protein kinase cascade are activated in hepatic cells by

Echinococcus multilocularis metacestode. World J Gastroenterol 15: 2116-2124.
Lin R, Lu G, Wang J, Zhang C, Xie W, et al. (2011) Time course of gene expression profiling in the liver of experimental mice infected with Echinococcus multilocularis. PLoS One 6: e14557.
Maille E, Trinh NT, Prive A, Bilodeau C, Bissonnette E, et al. (2011) Regulation of normal and cystic fibrosis airway epithelial repair processes by TNF{alpha} after injury. Am J Physiol Lung Cell Mol Physiol.
Maille E, Trinh NT, Prive A, Bilodeau C, Bissonnette E, et al. (2011) Regulation of normal and cystic fibrosis airway epithelial repair processes by TNF{alpha} after injury. Am J Physiol Lung Cell Mol Physiol.
Manfras BJ, Reuter S, Wendland T, Kern P (2002) Increased activation and oligoclonality of peripheral CD8 (+) T cells in the chronic human helminth infection alveolar echinococcosis. Infect Immun 70: 1168-1174.
Manfras BJ, Reuter S, Wendland T, Boehm BO, Kern P (2004) Impeded Th1 CD4 memory T cell generation in chronic-persisting liver infection with Echinococcus multilocularis. Int Immunol 16: 43-50.
Mantion GA, Vuitton DA (2011) Auto-versus allo-transplantation of the liver for end-stage alveolar echinococcosis? Chin Med J (Engl) 124: 2803-2805.
Matowicka-Karna J, Kemona H, Panasiuk A (2004) [The evaluation of concentrations IL-5 and IL-6 in echinococcosis]. Wiad Parazytol 50: 435-438.
Mejri N, Hemphill A, Gottstein B (2009) Triggering and modulation of the host-parasite interplay by Echinococcus multilocularis: a review. Parasitology 137: 557-568.
Mejri N, Muller J, Gottstein B (2011) Intraperitoneal murine Echinococcus multilocularis infection induces differentiation of TGF-beta-expressing DCs that remain immature. Parasite Immunol 33: 471-482.
Mejri N, Muller N, Hemphill A, Gottstein B (2011) Intraperitoneal Echinococcus multilocularis infection in mice modulates peritoneal CD4+ and CD8+ regulatory T cell development. Parasitol Int 60: 45-53.
Meyer C, Liu Y, Kaul A, Peipe I, Dooley S (2013) Caveolin-1 abrogates TGF-beta mediated hepatocyte apoptosis. Cell Death Dis 4: e466.
Mondragon-de-la-Pena C, Ramos-Solis S, Barbosa-Cisneros O, Rodriguez-Padilla C, Tavizon-Garcia P, et al. (2002) Echinococcus granulosus down regulates the hepatic expression of inflammatory cytokines IL-6 and TNF alpha in BALB/c mice. Parasite 9: 351-356.
Mourglia-Ettlin G, Marques JM, Chabalgoity JA, Dematteis S (2011) Early peritoneal immune response during Echinococcus granulosus establishment displays a biphasic behavior. PLoS Negl Trop Dis 5: e1293.
Nakamura T, Ueno T, Sakamoto M, Sakata R, Torimura T, et al. (2004) Suppression of transforming growth factor-beta results in upregulation of transcription of regeneration factors after chronic liver injury. J Hepatol 41: 974-982.

Nakatsukasa H, Evarts RP, Hsia CC, Thorgeirsson SS (1990) Transforming growth factor-beta 1 and type I procollagen transcripts during regeneration and early fibrosis of rat liver. Lab Invest 63: 171-180.

Nono JK, Pletinckx K, Lutz MB, Brehm K (2012) Excretory/secretory-products of Echinococcus multilocularis larvae induce apoptosis and tolerogenic properties in dendritic cells in vitro. PLoS Negl Trop Dis 6: e1516.

Pahlavan PS, Feldmann RE, Jr., Zavos C, Kountouras J (2006) Prometheus' challenge: molecular, cellular and systemic aspects of liver regeneration. J Surg Res 134: 238-251.

Pak-Wittel MA, Yang L, Sojka DK, Rivenbark JG, Yokoyama WM (2012) Interferon-gamma mediates chemokine-dependent recruitment of natural killer cells during viral infection. Proc Natl Acad Sci U S A 110: E50-59.

Park JW, Li Z, Choi JS, Oh HJ, Park SH, et al. (2012) Expression of CXCL9, -10, and -11 in the Aqueous Humor of Patients With Herpetic Endotheliitis. Cornea.

Playford MC, Kamiya M (1992) Immune response to Echinococcus multilocularis infection in the mouse model: a review. Jpn J Vet Res 40: 113-130.

Playford MC, Kamiya M (1992) Immune response to Echinococcus multilocularis infection in the mouse model: a review. Jpn J Vet Res 40: 113-130.

Playford MC, Ooi HK, Oku Y, Kamiya M (1992) Secondary Echinococcus multilocularis infection in severe combined immunodeficient (scid) mice: biphasic growth of the larval cyst mass. Int J Parasitol 22: 975-982.

Prosser CC, Yen RD, Wu J (2006) Molecular therapy for hepatic injury and fibrosis: where are we? World J Gastroenterol 12: 509-515.

Przybyszewska M, Miloszewska J, Rzonca S, Trembacz H, Pysniak K, et al. (2011) Soluble TNF-alpha receptor I encoded on plasmid vector and its application in experimental gene therapy of radiation-induced lung fibrosis. Arch Immunol Ther Exp (Warsz) 59: 315-326.

Purps O, Lahme B, Gressner AM, Meindl-Beinker NM, Dooley S (2007) Loss of TGF-beta dependent growth control during HSC transdifferentiation. Biochem Biophys Res Commun 353: 841-847.

Qiu B, Frait KA, Reich F, Komuniecki E, Chensue SW (2001) Chemokine expression dynamics in mycobacterial (type-1) and schistosomal (type-2) antigen-elicited pulmonary granuloma formation. Am J Pathol 158: 1503-1515.

Ricard-Blum S, Bresson-Hadni S, Vuitton DA, Ville G, Grimaud JA (1992) Hydroxypyridinium collagen cross-links in human liver fibrosis: study of alveolar echinococcosis. Hepatology 15: 599-602.

Ricard-Blum S, Bresson-Hadni S, Guerret S, Grenard P, Volle PJ, et al. (1996) Mechanism of collagen network stabilization in human irreversible granulomatous liver fibrosis. Gastroenterology 111: 172-182.

Rigano R, Profumo E, Teggi A, Siracusano A (1996) Production of IL-5 and IL-6 by peripheral blood mononuclear cells (PBMC) from patients with Echinococcus granulosus infection. Clin Exp Immunol 105: 456-459.

Rutitzky LI, Lopes da Rosa JR, Stadecker MJ (2005) Severe CD4 T cell-mediated immunopathology in murine schistosomiasis is dependent on IL-12p40 and correlates with high levels of IL-17. J Immunol 175: 3920-3926.

Sabin EA, Pearce EJ (1995) Early IL-4 production by non-CD4+ cells at the site of antigen deposition predicts the development of a T helper 2 cell response to Schistosoma mansoni eggs. J Immunol 155: 4844-4853.

Sailer M, Soelder B, Allerberger F, Zaknun D, Feichtinger H, et al. (1997) Alveolar echinococcosis of the liver in a six-year-old girl with acquired immunodeficiency syndrome. J Pediatr 130: 320-323.

Samarakoon R, Overstreet JM, Higgins PJ (2012) TGF-beta signaling in tissue fibrosis: redox controls, target genes and therapeutic opportunities. Cell Signal 25: 264-268.

Scales HE, Ierna MX, Lawrence CE (2007) The role of IL-4, IL-13 and IL-4Ralpha in the development of protective and pathological responses to Trichinella spiralis. Parasite Immunol 29: 81-91.

Schmid-Hempel P (2008) Parasite immune evasion: a momentous molecular war. Trends Ecol Evol 23: 318-326.

Schmid-Hempel P (2009) Immune defence, parasite evasion strategies and their relevance for 'macroscopic phenomena' such as virulence. Philos Trans R Soc Lond B Biol Sci 364: 85-98.

Schneiderbauer MM, Dutton CM, Scully SP (2004) Signaling "cross-talk" between TGF-beta1 and ECM signals in chondrocytic cells. Cell Signal 16: 1133-1140.

Schoemaker MH, Moshage H (2004) Defying death: the hepatocyte's survival kit. Clin Sci (Lond) 107: 13-25.

Schopf LR, Hoffmann KF, Cheever AW, Urban JF, Jr., Wynn TA (2002) IL-10 is critical for host resistance and survival during gastrointestinal helminth infection. J Immunol 168: 2383-2392.

Shek FW, Benyon RC (2004) How can transforming growth factor beta be targeted usefully to combat liver fibrosis? Eur J Gastroenterol Hepatol 16: 123-126.

Shi DZ, Li FR, Bartholomot B, Vuitton DA, Craig PS (2004) Serum sIL-2R, TNF-alpha and IFN-gamma in alveolar echinococcosis. World J Gastroenterol 10: 3674-3676.

Shi DZ, Li FR, Bartholomot B, Vuitton DA, Craig PS (2004) Serum sIL-2R, TNF-alpha and IFN-gamma in alveolar echinococcosis. World J Gastroenterol 10: 3674-3676.

201. Shi MN, Zheng WD, Zhang LJ, Chen ZX, Wang XZ (2005) Effect of IL-10 on the expression of HSC growth factors in hepatic fibrosis rat. World J Gastroenterol 11: 4788-4793.

Spiliotis M, Konrad C, Gelmedin V, Tappe D, Bruckner S, et al. (2006) Characterisation of EmMPK1, an ERK-like MAP kinase from Echinococcus multilocularis which is activated in response to human epidermal growth factor. Int J Parasitol 36: 1097-1112.

Tangkijvanich P, Yee HF, Jr. (2002) Cirrhosis--can we reverse hepatic fibrosis? Eur J Surg Suppl: 100-112.

Teran LM, Mochizuki M, Bartels J, Valencia EL, Nakajima T, et al. (1999) Th1- and Th2-type cytokines regulate the expression and production of eotaxin and RANTES by human lung fibroblasts. Am J Respir Cell Mol Biol 20: 777-786.

Tomita K, Tamiya G, Ando S, Ohsumi K, Chiyo T, et al. (2006) Tumour necrosis factor alpha signalling through activation of Kupffer cells plays an essential role in liver fibrosis of non-alcoholic steatohepatitis in mice. Gut 55: 415-424.

Torgerson PR, Keller K, Magnotta M, Ragland N (2010) The global burden of alveolar echinococcosis. PLoS Negl Trop Dis 4: e722.

Vuitton DA (2003) The ambiguous role of immunity in echinococcosis: protection of the host or of the parasite? Acta Trop 85: 119-132.

Vuitton & Gottstein (2010) Echinococcus multilocularis and its intermediate host: a model of parasite-host interplay. J Biomed Biotechnol :923193.

Vuitton DA, Guerret-Stocker S, Carbillet JP, Mantion G, Miguet JP, et al. (1986) Collagen immunotyping of the hepatic fibrosis in human alveolar echinococcosis. Z Parasitenkd 72: 97-104.

Vuitton DA, Bresson-Hadni S, Laroche L, Kaiserlian D, Guerret-Stocker S, et al. (1989) Cellular immune response in Echinococcus multilocularis infection in humans. II. Natural killer cell activity and cell subpopulations in the blood and in the periparasitic granuloma of patients with alveolar echinococcosis. Clin Exp Immunol 78: 67-74.

Vuitton DA, Zhou H, Bresson-Hadni S, Wang Q, Piarroux M, et al. (2003) Epidemiology of alveolar echinococcosis with particular reference to China and Europe. Parasitology 127 Suppl: S87-107.

Vuitton DA, Zhang SL, Yang Y, Godot V, Beurton I, et al. (2006) Survival strategy of *Echinococcus multilocularis* in the human host. Parasitol Int 55 Suppl: S51-55.

Wallace K, Burt AD, Wright MC (2008) Liver fibrosis. Biochem J 411: 1-18.

Wang J, Zhang C, Wei X, Blagosklonov O, Lv G, et al. (2013) TGF-beta and TGF-beta/Smad signaling in the interactions between *Echinococcus multilocularis* and its hosts. PLoS One 8: e55379.

Wang JM, Shi L, Ma CJ, Ji XJ, Ying RS, et al. (2013) Differential regulation of interleukin-12 (IL-12)/IL-23 by Tim-3 drives T(H)17 cell development during hepatitis C virus infection. J Virol 87: 4372-4383.

Wang K, Lin B, Brems JJ, Gamelli RL (2013) Hepatic apoptosis can modulate liver fibrosis through TIMP1 pathway. Apoptosis 18: 566-577.

Weiner SM, Krenn V, Koelbel C, Hoffmann HG, Hinkeldey K, et al. (2010) Echinococcus multilocularis infection and TNF inhibitor treatment in a patient with rheumatoid arthritis. Rheumatol Int 31: 1399-1400.

Wenzel UA, Bank E, Florian C, Forster S, Zimara N, et al. (2011) Leishmania major parasite stage-dependent host cell invasion and immune evasion. FASEB J 26: 29-39.

Wu XW, Chen XL, Zhang SJ, Zhang X, Sun H, et al. (2011) Pericyst may be a new pharmacological and therapeutic target for hydatid disease. Chin Med J (Engl) 124: 2857-2862.

Wu XW, Peng XY, Zhang SJ, Niu JH, Sun H, et al. (2004) [Formation mechanisms of the fibrous capsule around hepatic and splenic hydatid cyst]. Zhongguo Ji Sheng Chong Xue Yu Ji Sheng Chong Bing Za Zhi 22: 1-4.

Xiong W, Frasch SC, Thomas SM, Bratton DL, Henson PM (2013) Induction of TGF-beta1 Synthesis by Macrophages in Response to Apoptotic Cells Requires Activation of the Scavenger Receptor CD36. PLoS One 8: e72772.

Xu GJ, Gan TY, Tang BP, Chen ZH, Mahemuti A, et al. (2013) Accelerated fibrosis and apoptosis with ageing and in atrial fibrillation: Adaptive responses with maladaptive consequences. Exp Ther Med 5: 723-729.

Zhang C, Wang J, Lu G, Li J, Lu X, et al. (2012) Hepatocyte proliferation/growth arrest balance in the liver of mice during E. multilocularis infection: a coordinated 3-stage course. PLoS One 7: e30127.

Zhang LH, Wu JG, Yao HP (2001) [Experimental study of inhibitory effect of kangxian recipe on TGF-beta 1 induced hepatocyte apoptosis]. Zhongguo Zhong Xi Yi Jie He Za Zhi 21: 37-39.

Zhang LJ, Wang XZ (2006) Interleukin-10 and chronic liver disease. World J Gastroenterol 12: 1681-1685.

Zhang LJ, Yu JP, Li D, Huang YH, Chen ZX, et al. (2004) Effects of cytokines on carbon tetrachloride-induced hepatic fibrogenesis in rats. World J Gastroenterol 10: 77-81.

Zhang S, Hue S, Sene D, Penfornis A, Bresson-Hadni S, et al. (2008) Expression of major histocompatibility complex class I chain-related molecule A, NKG2D, and transforming growth factor-beta in the liver of humans with alveolar echinococcosis: new actors in the tolerance to parasites? J Infect Dis 197: 1341-1349.

Zhao H, Bai X, Nie XH, Wang JT, Wang XX, et al. (2012) [Dynamic change of IL-10 and TGF-beta1 in the liver of Echinococcus multilocularis-infected mice]. Zhongguo Ji Sheng Chong Xue Yu Ji Sheng Chong Bing Za Zhi 30: 32-35.

Zingg W, Renner-Schneiter EC, Pauli-Magnus C, Renner EL, van Overbeck J, et al. (2004) Alveolar echinococcosis of the liver in an adult with human immunodeficiency virus type-1 infection. Infection 32: 299-302.